

DETERMINATION OF PLASMA DENSITY
PROFILE AND OTHER PARAMETERS
WITH AN ELECTROACOUSTIC PROBE

Thesis for the Degree of Ph. D.
MICHIGAN STATE UNIVERSITY
JACK G. OLIN
1974



This is to certify that the

thesis entitled

DETERMINATION OF PLASMA DENSITY PROFILE AND
OTHER PARAMETERS WITH AN ELECTROACOUSTIC PROBE

presented by

Jack G. Olin

has been accepted towards fulfillment
of the requirements for

Ph.D. degree in Electr. Engineering

Major professor

Date April 28, 1974



DET
OTHER

The electri
cylindrical warm-
thermal resonance
field from the pr
resonances as the

For each d
three T-D resonan
measure the relat
resonances occur
plasma parameters

In the det
resonances are use
solution of Poiss
conditions for the
and the total phas
WB approximation
average electron
numerical values

ABSTRACT

DETERMINATION OF PLASMA DENSITY PROFILE AND OTHER PARAMETERS WITH AN ELECTROACOUSTIC PROBE

By

Jack G. Olin

The electron density profile and other plasma parameters of a cylindrical warm-plasma column are studied through the excitation of thermal resonances using an electroacoustic probe. The electromagnetic field from the probe excites a series of thermal (Tonks-Dattner) resonances as the current density is varied.

For each driving frequency, the dipole resonance and the first three T-D resonances are recorded. In this study, it is sufficient to measure the relative magnitudes of the plasma densities at which these resonances occur in order to determine the density profile and other plasma parameters such as the temperature and the number density.

In the determination of the plasma density, the thermal resonances are used to determine the unknown parameters appearing in the solution of Poisson's Equation in the plasma column. The boundary conditions for the thermal resonances in the plasma column are derived and the total phase for the thermal resonances is determined using the WKB approximation. The dipole resonance is used to determine the average electron density in the plasma column. The analysis leads to numerical values for the electron density profile parameters.

DE
OTH

in

DETERMINATION OF PLASMA DENSITY PROFILE AND
OTHER PARAMETERS WITH AN ELECTROACOUSTIC PROBE

By

Jack G. Olin

A THESIS

Submitted to
Michigan State University
in partial fulfillment of the requirements
for the degree of

DOCTOR OF PHILOSOPHY

Department of Electrical Engineering

1974

1/2/5

To my family
Sigrid, Peter and Leslie

The au
guidance and e
Gen.

He also
Myquist, J. As
project.

The aut
great effort pu
Green. Her hel
invaluable. He
and infinite pat

ACKNOWLEDGMENTS

The author expresses his sincere appreciation and thanks for the guidance and encouragement given him by his major professor, Dr. K. M. Chen.

He also wishes to thank the committee members, Drs. P. D. Nyquist, J. Asmussen, B. Ho, and G. Pollack for their interest in this project.

The author furthermore wishes to express his gratitude for the great effort put into the final typing of this thesis by Mrs. Roberta Green. Her help in producing the final version of this thesis was invaluable. He also thanks his wife, Sigrid, for the preliminary typing and infinite patience.

ACKNOWLEDGEMENT

LIST OF FIGURES

1. INTRODUCTION

2. BASIC THEORY

2.1 Introduction

2.2 General

2.3 Determination

2.4 Determination

Resonance

2.5 Development

Frequency

Column

3. DETERMINATION

PLASMA COLUMN

SHEATH REGION

3.1 Introduction

3.2 Experiment

3.3 Development

Density

3.4 Determination

Cylindrical

Approximation

3.5 Determination

Plasma Column

the Form

4. NUMERICAL RESULTS

CYLINDRICAL PLASMA

4.1 Introduction

4.2 Numerical

Profile

4.3 Numerical

Approximation

Profile

4.4 Graphical

the WKB

TABLE OF CONTENTS

	Page
ACKNOWLEDGMENTS	iii
LIST OF FIGURES	vi
1. INTRODUCTION	1
2. BASIC THEORY OF TEMPERATURE RESONANCES IN PLASMA SHEATHS . .	3
2.1 Introduction	3
2.2 General Theory	8
2.3 Determination of the Boundary Condition at the Wall . .	18
2.4 Determination of the Total Phase for the Thermal Resonances	19
2.5 Development of Relationships Between Dipole Resonance Frequency and Plasma Frequency in a Cylindrical Plasma Column	31
3. DETERMINATION OF ELECTRON DENSITY PROFILE IN CYLINDRICAL PLASMA COLUMN BASED ON THERMAL RESONANCE DATA IN THE SHEATH REGION	41
3.1 Introduction	41
3.2 Experimental Procedure	43
3.3 Development of Functional Form for the Electron- Density Profile	46
3.4 Determination of Electron-Density Profile in a Cylindrical Warm Plasma Column Based on a Parabolic Approximation	56
3.5 Determination of the Electron-Density in a Warm Plasma Cylinder Assuming Potential Distribution of the Form $(1 - I_0(\gamma r))$	66
4. NUMERICAL RESULTS FOR THE ELECTRON DENSITY PROFILE IN A CYLINDRICAL PLASMA COLUMN	80
4.1 Introduction	80
4.2 Numerical Results Based on Parabolic Electron-Density Profile Approximation	80
4.3 Numerical Results Based on the Bessel Function Approximation for the Static Electron-Density Profile	87
4.4 Graphical Presentation of Thermal Resonances Using the WKB Approximation	126

APPENDIX A

APPENDIX B

REFERENCES

	Page
APPENDIX A NUMERICAL COMPUTER READOUTS AND ADDITIONAL COMPUTER GRAPHS	133
APPENDIX B FORTRAN COMPUTER PROGRAMS WRITTEN SPECIFICALLY FOR THE NUMERICAL ANALYSIS IN THIS RESEARCH PROJECT	186
REFERENCES	203

Figure

2.1.1

1.1.2

2.1.3

2.2.1

2.3.1

2.4.1

2.4.2

2.4.3

2.5.1

t
A
i
s

T
(
f
p
r
w
ne

Ge
th
wa
po
is
mu
a

Ph
n

The
ma
an
co

Sk
A

Ty
re
po
go

Ge
con
wa
out

LIST OF FIGURES AND TABLES

Figure		Page
2.1.1	Typical electron, ion and potential profiles in the sheath region of a semiinfinite plasma in the vicinity of a solid boundary. With the assumption of ion drift towards the wall, the ion density is not significantly changed in the sheath region . . .	4
2.1.2	Typical electron and ion density profiles in the sheath region of a cylindrical plasma column. Assuming ion drift towards the solid boundary, the ion density does not significantly change in the sheath region	6
2.1.3	Typical sketches of the first three thermal resonances ($m = 1,2,3$) occurring at a given frequency of the incident EM field at three discharge current levels producing density profiles n_{e1} , n_{e2} , and n_{e3} . The resonances occur when $\omega^2 = \omega_p^2$ at any current level which corresponds to $n_{e1}(t_1) = n_{e2}(t_2) = n_{e3}(t_3) = \frac{m \epsilon_0 \omega^2}{e^2} \dots \dots \dots$	7
2.2.1	Geometric arrangement used in the region where thermal resonances occur. n_1 represents a typical waveform of a thermal resonance; t_1 is the critical point where $\omega = \omega_p$. The one-dimensional approach is justified in this region because t_1 is typically much smaller than the radius of the plasma column, a	17
2.3.1	Phase relation between electron density perturbation n_1 and associated electron velocity perturbation v_1 .	20
2.4.1	The under-dense region in which thermal resonances may occur if the phase conditions are satisfied and an appropriate EM field illuminates the plasma column	21
2.4.2	Sketch of Airy function, $Ai(z) = \frac{1}{\pi} \cos(s^3/3 + s z) dz \dots \dots \dots$	29
2.4.3	Typical waveforms of the first three thermal resonances. x_{p1} , x_{p2} , and x_{p3} are the critical points at which k_{p1} , k_{p2} , and k_{p3} respectively go to zero	32
2.5.1	Geometric arrangement of cylindrical plasma column contained in a cylindrical glass discharge tube of wall thickness b . The inside radius is a while the outside radius is c	38

Figure

3.1.1

A
a
l
r

3.2.1

Es
re
Ar
th
cc
sc
of

3.2.2

Ex
th
pl
cu
EM
cur
fir
occ

3.2.3

Exp
the
plas
f 1
1,
the
reso

3.2.4

Expe
the
plas
f 1
1,
the
reso

3.2.5

Expe
the
plas
f 1
1,
the
reso

Figure		Page
3.1.1	A cylindrical plasma column illuminated by TM field as shown. E_{0t} and E_{0l} represent the transverse and longitudinal components of electric field respectively	42
3.2.1	Experimental arrangement for obtaining plasma resonance data in a cylindrical plasma column. An electroacoustic (E.A.) probe is used to excite the dipole and thermal resonances in the plasma column. The E.A. probe also picks up the scattered field whose peaks indicate the presence of resonances in the plasma	44
3.2.2	Experimental results (data sets #1 and #2) for the back scattered EM field from a cylindrical plasma column as a function of discharge current. f is the frequency of the incident EM field. i_d , i_1 , i_2 , and i_3 are the discharge currents at which the dipole resonance and the first three thermal resonances respectively occur	47
3.2.3	Experimental results (data sets #3 and #4) for the back scattered EM field from a cylindrical plasma column as a function of discharge current. f is the frequency of the incident EM field. i_d , i_1 , i_2 , and i_3 are the discharge currents at which the dipole resonance and the first three thermal resonances respectively occur	48
3.2.4	Experimental results (data sets #5 and #6) for the back scattered EM field from a cylindrical plasma column as a function of discharge current. f is the frequency of the incident EM field. i_d , i_1 , i_2 , and i_3 are the discharge currents at which the dipole resonance and the first three thermal resonances respectively occur	49
3.2.5	Experimental results (data sets #7 and #8) for the back scattered EM field from a cylindrical plasma column as a function of discharge current. f is the frequency of the incident EM field. i_d , i_1 , i_2 , and i_3 are the discharge currents at which the dipole resonance and the first three thermal resonances respectively occur	50

Figure

- 4.2.1
1
1
1
1
- 4.2.2
N
a
A
B
1
- 4.2.3
No
a
Al
Ba
1
- 4.2.4
No
a
Al
Ba
1
- 4.2.5
Nor
a f
Als
Bas
1
- 4.2.6
Nor
a f
Als
Bas
1
- 4.2.7
Nor
a f
Als
Bas
1
- 4.2.8
Nor
a f
Als
Bas
1

Figure		Page
4.2.1	Normalized parabolic electron density profile as a function of r/a , $n_{e1}(r/a)/n_{o1} = 1 - .83(r/a)^2$. Also the normalized potential profile $\eta_1(r/a)/\eta_w$. Based on data set #1 ($f = 2.016$ GHz, $i_d = 270$ ma, $i_1 = 185$ ma, $i_2 = 150$ ma, $i_3 = 125$ ma)	88
4.2.2	Normalized parabolic electron density profile as a function of r/a , $n_{e1}(r/a)/n_{o1} = 1 - .82(r/a)^2$. Also the normalized potential profile $\eta_1(r/a)/\eta_w$. Based on data set #2 ($f = 2.10$ GHz, $i_d = 290$ ma, $i_1 = 190$ ma, $i_2 = 150$ ma, $i_3 = 120$ ma)	89
4.2.3	Normalized parabolic electron density profile as a function of r/a , $n_{e1}(r/a)/n_{o1} = 1 - .83(r/a)^2$. Also the normalized potential profile $\eta_1(r/a)/\eta_w$. Based on data set #3 ($f = 2.23$ GHz, $i_d = 340$ ma, $i_1 = 235$ ma, $i_2 = 185$ ma, $i_3 = 160$ ma)	90
4.2.4	Normalized parabolic electron density profile as a function of r/a , $n_{e1}(r/a)/n_{o1} = 1 - .80(r/a)^2$. Also the normalized potential profile $\eta_1(r/a)/\eta_w$. Based on data set #4 ($f = 2.32$ GHz, $i_d = 355$ ma, $i_1 = 245$ ma, $i_2 = 200$ ma, $i_3 = 175$ ma)	91
4.2.5	Normalized parabolic electron density profile as a function of r/a , $n_{e1}(r/a)/n_{o1} = 1 - .86(r/a)^2$. Also the normalized potential profile $\eta_1(r/a)/\eta_w$. Based on data set #5 ($f = 1.917$ GHz, $i_d = 270$ ma, $i_1 = 180$ ma, $i_2 = 135$ ma, $i_3 = 110$ ma)	92
4.2.6	Normalized parabolic electron density profile as a function of r/a , $n_{e1}(r/a)/n_{o1} = 1 - .83(r/a)^2$. Also the normalized potential profile $\eta_1(r/a)/\eta_w$. Based on data set #6 ($f = 2.017$ GHz, $i_d = 285$ ma, $i_1 = 190$ ma, $i_2 = 150$ ma, $i_3 = 120$ ma)	93
4.2.7	Normalized parabolic electron density profile as a function of r/a , $n_{e1}(r/a)/n_{o1} = 1 - .84(r/a)^2$. Also the normalized potential profile $\eta_1(r/a)/\eta_w$. Based on data set #7 ($f = 2.275$ GHz, $i_d = 290$ ma, $i_1 = 195$ ma, $i_2 = 150$ ma, $i_3 = 120$ ma)	94
4.2.8	Normalized parabolic electron density profile as a function of r/a , $n_{e1}(r/a)/n_{o1} = 1 - .85(r/a)^2$. Also the normalized potential profile $\eta_1(r/a)/\eta_w$. Based on data set #8 ($f = 2.322$ GHz, $i_d = 320$ ma, $i_1 = 210$ ma, $i_2 = 160$ ma, $i_3 = 135$ ma)	95

Figure

4.3.1 Nor
as
nel
nor
on
il

4.3.2 Nor
as
nel
nor
on
il

4.3.3 Nor
as
nel
nor
data
il

4.3.4 Norm
as a
nel
norm
data
il

4.3.5 Norm
as a
nel
norm
data
il

4.3.6 Norm
as a
nel
norm
data
il

4.3.7 Norm
as a
nel
norm
data
il

Figure	Page	
4.3.1	Normalized Bessel series electron density profile as a function of z/a , $n_{e1}(z/a)/n_{o1} = \exp(1 - I_0(327(1 - z/a)))$. Also the normalized potential profile $\eta_1(z/a)/\eta_w$. Based on data set #1 ($f = 2.016$ GHz, $i_d = 270$ ma, $i_1 = 185$ ma, $i_2 = 150$ ma, $i_3 = 125$ ma)	102
4.3.2	Normalized Bessel series electron density profile as a function of z/a , $n_{e1}(z/a)/n_{o1} = \exp(1 - I_0(326(1 - z/a)))$. Also the normalized potential profile $\eta_1(z/a)/\eta_w$. Based on data set #2 ($f = 2.10$ GHz, $i_d = 290$ ma, $i_1 = 190$ ma, $i_2 = 150$ ma, $i_3 = 120$ ma)	103
4.3.3	Normalized Bessel series electron density profile as a function of z/a , $n_{e1}(z/a)/n_{o1} = \exp(1 - I_0(323(1 - z/a)))$. Also the normalized potential profile $\eta_1(z/a)/\eta_w$. Based on data set #3 ($f = 2.23$ GHz, $i_d = 340$ ma, $i_1 = 235$ ma, $i_2 = 185$ ma, $i_3 = 160$ ma)	104
4.3.4	Normalized Bessel series electron density profile as a function z/a , $n_{e1}(z/a)/n_{o1} = \exp(1 - I_0(330(1 - z/a)))$. Also the normalized potential profile $\eta_1(z/a)/\eta_w$. Based on data set #4 ($f = 2.32$ GHz, $i_d = 355$ ma, $i_1 = 245$ ma, $i_2 = 200$ ma, $i_3 = 175$ ma)	105
4.3.5	Normalized Bessel series electron density profile as a function of z/a , $n_{e1}(z/a)/n_{o1} = \exp(1 - I_0(327(1 - z/a)))$. Also the normalized potential profile $\eta_1(z/a)/\eta_w$. Based on data set #5 ($f = 1.917$ GHz, $i_d = 270$ ma, $i_1 = 180$ ma, $i_2 = 135$ ma, $i_3 = 110$ ma)	106
4.3.6	Normalized Bessel series electron density profile as a function of z/a , $n_{e1}(z/a)/n_{o1} = \exp(1 - I_0(327(1 - z/a)))$. Also the normalized potential profile $\eta_1(z/a)/\eta_w$. Based on data set #6 ($f = 2.017$ GHz, $i_d = 285$ ma, $i_1 = 190$ ma, $i_2 = 150$ ma, $i_3 = 120$ ma)	107
4.3.7	Normalized Bessel series electron density profile as a function of z/a , $n_{e1}(z/a)/n_{o1} = \exp(1 - I_0(328(1 - z/a)))$. Also the normalized potential profile $\eta_1(z/a)/\eta_w$. Based on data set #7 ($f = 2.275$ GHz, $i_d = 290$ ma, $i_1 = 195$ ma, $i_2 = 150$ ma, $i_3 = 120$ ma)	108

Figure

4.3.8 Norm
as a
nel
norm
data
 $i_2 =$

4.3.9 Norm
at r
the
 k_{p1}
data
 $i_2 =$

4.3.10 Norm
at r
the
 k_{p1}
data
 $i_2 =$

4.3.11 Norma
at re
the c
 k_{p1} a
data
 $i_2 =$

4.3.12 Norma
at re
the c
 k_{p1} a
data
 $i_2 =$

4.3.13 Norma
at re
the c
 k_{p1} a
data
 $i_2 =$

4.3.14 Norma
at re
the c
 k_{p1} a
data
 $i_2 =$

Figure		Page
4.3.8	Normalized Bessel series electron density profile as a function of z/a , $n_{e1}(z/a)/n_{o1} = \exp(1 - I_0(331(1 - z/a)))$. Also the normalized potential profile $\eta_1(z/a)/\eta_w$. Based on data set #8 ($f = 2.322$ GHz, $i_d = 320$ ma, $i_1 = 210$ ma, $i_2 = 160$ ma, $i_3 = 135$ ma)	109
4.3.9	Normalized Bessel series electron density profiles at resonances 1 and 2. Points t_1 and t_2 represent the critical points in the plasma sheath at which k_{p1} and k_{p2} respectively go to zero. Based on data set #1 ($f = 2.016$ GHz, $i_d = 270$ ma, $i_1 = 185$ ma, $i_2 = 150$ ma, $i_3 = 125$ ma)	110
4.3.10	Normalized Bessel series electron density profiles at resonances 1 and 2. Points t_1 and t_2 represent the critical points in the plasma sheath at which k_{p1} and k_{p2} respectively go to zero. Based on data set #2 ($f = 2.10$ GHz, $i_d = 290$ ma, $i_1 = 190$ ma, $i_2 = 150$ ma, $i_3 = 120$ ma)	111
4.3.11	Normalized Bessel series electron density profiles at resonances 1 and 2. Points t_1 and t_2 represent the critical points in the plasma sheath at which k_{p1} and k_{p2} respectively go to zero. Based on data set #3 ($f = 2.23$ GHz, $i_d = 340$ ma, $i_1 = 235$ ma, $i_2 = 185$ ma, $i_3 = 160$ ma)	112
4.3.12	Normalized Bessel series electron density profiles at resonances 1 and 2. Points t_1 and t_2 represent the critical points in the plasma sheath at which k_{p1} and k_{p2} respectively go to zero. Based on data set #4 ($f = 2.32$ GHz, $i_d = 355$ ma, $i_1 = 245$ ma, $i_2 = 200$ ma, $i_3 = 175$ ma)	113
4.3.13	Normalized Bessel series electron density profiles at resonances 1 and 2. Points t_1 and t_2 represent the critical points in the plasma sheath at which k_{p1} and k_{p2} respectively go to zero. Based on data set #5 ($f = 1.917$ GHz, $i_d = 270$ ma, $i_1 = 180$ ma, $i_2 = 135$ ma, $i_3 = 110$ ma)	114
4.3.14	Normalized Bessel series electron density profiles at resonances 1 and 2. Points t_1 and t_2 represent the critical points in the plasma sheath at which k_{p1} and k_{p2} respectively go to zero. Based on data set #6 ($f = 2.017$ GHz, $i_d = 285$ ma, $i_1 = 190$ ma, $i_2 = 150$ ma, $i_3 = 120$ ma)	115

Figure

4.3.15 Norm
at r
the
kpl
data
12

4.3.16 Norm
at r
the
kpl
data
12

4.3.17 Norm
at r
the
kpl
data
12

4.3.18 Norm
at r
the
kpl
data
12

4.3.19 Norm
at r
the
kpl
data
12

4.3.20 Norm
at r
the
kpl
data
12

4.3.21 Norm
at r
the
kpl
data
12

Figure		Page
4.3.15	Normalized Bessel series electron density profiles at resonances 1 and 2. Points t_1 and t_2 represent the critical points in the plasma sheath at which k_{p1} and k_{p2} respectively go to zero. Based on data set #7 ($f = 2.275$ GHz, $i_d = 290$ ma, $i_1 = 195$ ma, $i_2 = 150$ ma, $i_3 = 120$ ma)	116
4.3.16	Normalized Bessel series electron density profiles at resonances 1 and 2. Points t_1 and t_2 represent the critical points in the plasma sheath at which k_{p1} and k_{p2} respectively go to zero. Based on data set #8 ($f = 2.322$ GHz, $i_d = 320$ ma, $i_1 = 210$ ma, $i_2 = 160$ ma, $i_3 = 135$ ma)	117
4.3.17	Normalized Bessel series electron density profiles at resonances 1 and 3. Points t_1 and t_3 represent the critical points in the plasma sheath at which k_{p1} and k_{p3} respectively go to zero. Based on data set #1 ($f = 2.016$ GHz, $i_d = 270$ ma, $i_1 = 185$ ma, $i_2 = 150$ ma, $i_3 = 125$ ma)	118
4.3.18	Normalized Bessel series electron density profiles at resonances 1 and 3. Points t_1 and t_3 represent the critical points in the plasma sheath at which k_{p1} and k_{p3} respectively go to zero. Based on data set #2 ($f = 2.10$ GHz, $i_d = 290$ ma, $i_1 = 190$ ma, $i_2 = 150$ ma, $i_3 = 120$ ma)	119
4.3.19	Normalized Bessel series electron density profiles at resonances 1 and 3. Points t_1 and t_3 represent the critical points in the plasma sheath at which k_{p1} and k_{p3} respectively go to zero. Based on data set #3 ($f = 2.23$ GHz, $i_d = 340$ ma, $i_1 = 235$ ma, $i_2 = 185$ ma, $i_3 = 160$ ma)	120
4.3.20	Normalized Bessel series electron density profiles at resonances 1 and 3. Points t_1 and t_3 represent the critical points in the plasma sheath at which k_{p1} and k_{p3} respectively go to zero. Based on data set #4 ($f = 2.32$ GHz, $i_d = 355$ ma, $i_1 = 245$ ma, $i_2 = 200$ ma, $i_3 = 175$ ma)	121
4.3.21	Normalized Bessel series electron density profiles at resonances 1 and 3. Points t_1 and t_3 represent the critical points in the plasma sheath at which k_{p1} and k_{p3} respectively go to zero. Based on data set #5 ($f = 1.917$ GHz, $i_d = 270$ ma, $i_1 = 180$ ma, $i_2 = 135$ ma, $i_3 = 110$ ma)	122

Figure

4.3.22 Norm
at r
the
kp1
data
i2 =

4.3.23 Norm
at r
the
kp1
data
i2 =

4.3.24 Norm
at r
the
kp1
data
i2 =

4.4.1 Firs
WB
prof

4.4.2 Seco
a WB
dens

4.4.3 Firs
a WB
dens

4.4.4 Seco
a WB
dens

Table

1.2.1 Expe
frec
char
dipo
resc

Figure		Page
4.3.22	Normalized Bessel series electron density profiles at resonances 1 and 3. Points t_1 and t_3 represent the critical points in the plasma sheath at which k_{p1} and k_{p3} respectively go to zero. Based on data set #6 ($f = 2.017$ GHz, $i_d = 285$ ma, $i_1 = 190$ ma, $i_2 = 150$ ma, $i_3 = 120$ ma)	123
4.3.23	Normalized Bessel series electron density profiles at resonances 1 and 3. Points t_1 and t_3 represent the critical points in the plasma sheath at which k_{p1} and k_{p3} respectively go to zero. Based on data set #7 ($f = 2.275$ GHz, $i_d = 290$ ma, $i_1 = 195$ ma, $i_2 = 150$ ma, $i_3 = 120$ ma)	124
4.3.24	Normalized Bessel series electron density profiles at resonances 1 and 3. Points t_1 and t_3 represent the critical points in the plasma sheath at which k_{p1} and k_{p3} respectively go to zero. Based on data set #8 ($f = 2.322$ GHz, $i_d = 320$ ma, $i_1 = 210$ ma, $i_2 = 160$ ma, $i_3 = 135$ ma)	125
4.4.1	First thermal resonance for data set #1 based on a WKB formulation using the parabolic electron density profile	128
4.4.2	Second thermal resonance for data set #1 based on a WKB formulation using the parabolic electron density profile	129
4.4.3	First thermal resonance for data set #1 based on a WKB formulation using the Bessel series electron density profile	130
4.4.4	Second thermal resonance for data set #1 based on a WKB formulation using the Bessel series electron density profile	131
 Table		 Page
3.2.1	Experimental data set 1 through 8. Given are the frequency of the incident EM field and the discharge currents i_d , i_1 , i_2 and i_3 at which the dipole resonance and the first three thermal resonances respectively occur	51

Table

4.2.1 Num
l t
and
from
(j =

4.2.2 Num
elec
for

4.2.3 Num
r; t
thro

4.2.4 Num
tan
res
rat
thro

4.2.5 Num
wal
T f
ide
num
of d
1,3

4.3.1 Num
sets
j =
for
res
rest

4.3.2 Num
aver
no2

4.3.3 Num
dist
plas
a at

4.3.4 Num
rw =
for
ide
num
tion
res

Table	Page	
4.2.1	Numerical results for the factor α for data sets 1 through 8. The columns identified by $j = 2$ and $j = 3$ represent numerical values for α obtained from the use of combinations of resonances 1,2 ($j = 2$) and 1,3 ($j = 3$) respectively	81
4.2.2	Numerical results for the ratio of peak to average electron density $n_{01}/\langle n_{e1}(r) \rangle$ and $n_{02}/\langle n_{e2}(r) \rangle$ for data sets 1 through 8	82
4.2.3	Numerical values for the ratio of critical radius r_j to the total radius a , r_j/a , for data sets 1 through 8	83
4.2.4	Numerical values for the ratio of critical distance z_j measured from the wall for the j^{th} resonance to the total radius a as well as the ratios z_2/z_1 and z_3/z_1 for the data sets 1 through 8	84
4.2.5	Numerical values of relative potential at the wall, $\eta_w = eV(a)/kT$ and electron temperature T for data sets 1 through 8. The columns identified by $j = 2$ and $j = 3$ represent the numerical values for η_w and T based on the use of combinations of resonances 1,2 ($j = 2$) and 1,3 ($j = 3$) respectively	85
4.3.1	Numerical results for the factor γ for data sets 1 through 8. The columns identified by $j = 2$ and $j = 3$ represent the numerical values for γ obtained from use of combinations of resonances 1,2 ($j = 2$) and 1,3 ($j = 3$) respectively	96
4.3.2	Numerical results for the ratio of peak to average electron density $n_{01}/\langle n_{e1}(r) \rangle$ and $n_{02}/\langle n_{e1}(r) \rangle$ for data sets 1 through 8	97
4.3.3	Numerical values for the ratio of the critical distance z_j measured from the wall into the plasma for the j^{th} resonance to the total radius a and also the ratios z_2/z_1 and z_3/z_1	98
4.3.4	Numerical values of the relative potential $\eta_w = eV(a)/kT$ and the electron temperature T for the data sets 1 through 8. The columns identified by $j = 2$ and $j = 3$ represent the numerical results based on the use of combinations of resonances 1,2 ($j = 2$) and 1,3 ($j = 3$) respectively	99

Knowledge
in the so-called
analytical work
region has been
approximate the
ing the static
boundaries has a
knowledge of the
cylindrical plas
columns, a para

is frequently er

This rese
density profile
data for the dip
probe which illu
the backscatter
with experiment
plasma column at
frequency ω .

The theore
functional expres
tical plasma col
plasma column. T

CHAPTER 1

INTRODUCTION

Knowledge of the static electron density profile of warm plasmas in the so-called sheath region near solid boundaries is significant in analytical work involving the plasma electron density. The sheath region has been analyzed in plane geometries by researchers based on approximate theoretical models.¹ The more complex problems of determining the static electron density profile in warm plasmas with cylindrical boundaries has also been treated theoretically by researchers.²⁻⁹ When knowledge of the functional form of the electron density profile in a cylindrical plasma column is needed for work involving such plasma columns, a parabolic electron density profile of the form

$$n_e(r) = n_o \left(1 - \alpha \left(\frac{r}{a}\right)^2\right)$$

is frequently employed using some typical value for the parameter α .^{4,10}

This research deals with the determination of the static electron density profile in warm cylindrical plasma columns based on experimental data for the dipole and thermal resonances induced by an electroacoustic probe which illuminates the plasma column with an EM field and receives the backscattered field. The experimental part of the research deals with experimental determination of the discharge current levels in the plasma column at which thermal resonances occur for a given excitation frequency ω .

The theoretical part of the research considers possible functional expressions for the static electron density in warm cylindrical plasma columns based on a study of Poisson's Equation in the plasma column. The phase conditions for thermal resonances are studied

and the relation
exciting frequency
approximation is
solution to Poisson
to the Poisson

The numerical
solution of simple
thermal resonance
Graphs on the effect
different approximations
appropriate Bessel
well represent
the actual profile

Chapter 2
sheath region of
studied using WKB
and the ratio of
column to the external

Chapter 3
cylindrical plasma
possible solutions
assumed functional
of all parameters

Chapter 4
electron density
functional forms

and the relationship between the average plasma frequency and the exciting frequency is developed. The commonly used parabolic profile approximation is considered as an approximation to a Bessel function solution to Poisson's Equation. Next, a Bessel function approximation to the Poisson Equation is considered.

The numerical work done as part of this research deals with the solution of simultaneous equations based on the phase condition for the thermal resonances and the electron density profiles proposed above. Graphs on the electron densities obtained on the basis of these different approaches are presented and compared. It is found that an appropriate Bessel function approximation of the profile density may well represent a functional form considerably more representative of the actual profile than the conventional parabolic profile.

Chapter 2 presents the basic theory of thermal resonances in the sheath region of cylindrical plasma columns. Phase conditions are studied using WKB approximations of the electron density perturbations and the ratio of the average plasma frequency $\langle \omega_p(r) \rangle$ in the plasma column to the exciting frequency ω is developed.

Chapter 3 deals with the formulation of Poisson's Equation in a cylindrical plasma column and considers various functional forms as possible solutions. Simultaneous equations are presented for each assumed functional form whose numerical solution permits determination of all parameters appearing in the proposed profile functions.

Chapter 4 presents the numerical results and shows graphs of the electron density profiles obtained. The profiles based on different functional forms are compared.

BASIC THE

1.1 Introduction

The
plasma bou
well known
electron d
associated
sheath phen
of the prof
ment of the
phenomenolo

Elec
positively
profile in
which decre
a typical p
solid bounda
is shown whe

The p
 $x = 0$ to a r
model assume
an approxima
Typical valu
potential n
shown to be

CHAPTER 2

BASIC THEORY OF TEMPERATURE RESONANCES IN PLASMA SHEATHS

2.1 Introduction

The occurrence of a plasma sheath in the vicinity of a plasma boundary such as a solid wall, metallic or nonmetallic, is well known. The plasma sheath represents a region of reduced electron density due to the loss of electrons hitting the wall associated with a negative potential region near the wall. The sheath phenomenon is briefly discussed to establish the geometry of the problem at hand. The well documented mathematical treatment of the sheath problem is not presented here but a brief phenomenological discussion appears in order.

Electrons hitting a nonmetallic wall mostly recombine with positively charged ions. This leads to an electron density profile in the vicinity of the wall, the so-called sheath region, which decreases monotonically towards the wall. Figure 2.1.1 shows a typical plasma sheath for a semi-infinite plasma slab with a solid boundary at $x = 0$. The relative electron density $n_e(x)/n_0$ is shown where n_0 is the electron density as x approaches infinity.

The potential $V(x)$ also goes monotonically from zero at $x = \infty$ to a negative wall potential. The commonly accepted sheath model assumes an ion drift in the sheath region which results in an approximately constant ion density also shown in Figure 2.1.1. Typical values determined for the ratio of the relative wall potential $\eta_w = \frac{eV_w}{kT}$ are in the neighborhood of 2. This value is shown to be independent of electron density profile parameters.

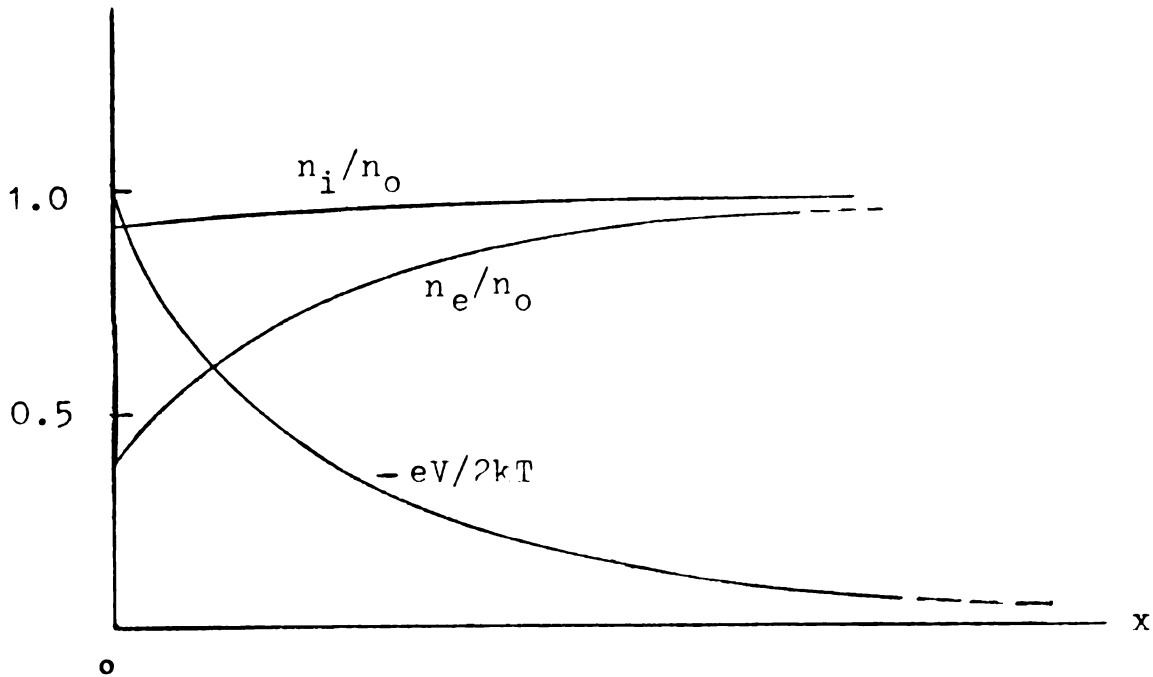


Fig. 2.1.1 Typical electron, ion and potential profiles in the sheath region of a semiinfinite plasma in the vicinity of a solid boundary. With the assumption of ion drift towards the wall, the ion density is not significantly changed in the sheath region.

Even though
should never

The
complex in

Figure 2.1.

assumed when

goal of this

the electro

with other

this study

resonances

section 3.2

resonances

dical plas

the sheath

magnetic wa

the plasma i

frequency w

shown in Fig

a typical sk

thermal reso

this report

established.

Based

phenomenon,

sheaths is p

thermal reso

Even though it may vary somewhat in a cylindrical plasma sheath it should nevertheless be approximately the same.

The electron density and potential distributions are more complex in a cylindrical geometry as typically represented in Figure 2.1.2. A parabolic electron density profile is frequently assumed when cylindrical plasma columns are studied. The main goal of this thesis is, in fact, the experimental determination of the electron density profile assuming a parabolic profile, along with other functional forms of the profile. The tool employed in this study is an electroacoustic probe used to excite thermal resonances in the plasma sheath region as discussed below in section 3.2. Figure 2.1.3 shows typical sketches of thermal resonances that may be excited in the sheath region of a cylindrical plasma column. The cylindrical column of warm plasma with the sheath region as shown is illuminated by an incident electromagnetic wave of frequency ω . The incident wave interacts with the plasma in the sheath region near the wall where the plasma frequency $\omega_p(r)$ is less than ω to excite electroacoustic waves as shown in Figure 2.1.3. Figure 2.1.3 is only intended to represent a typical sketch of such resonances. The total phase of the m^{th} thermal resonance is assumed to be $m\pi$. In subsequent sections of this report a more refined value for this total phase value is established.

Based on this introductory discussion of the sheath phenomenon, the basic theory of thermal resonances in plasma sheaths is presented in this chapter. Boundary conditions for the thermal resonances at the wall are examined. The phase condition

nor
ele

r=0
Center
Plasma

Fig. 2.1.2

Pr
a
As
br
Si
re

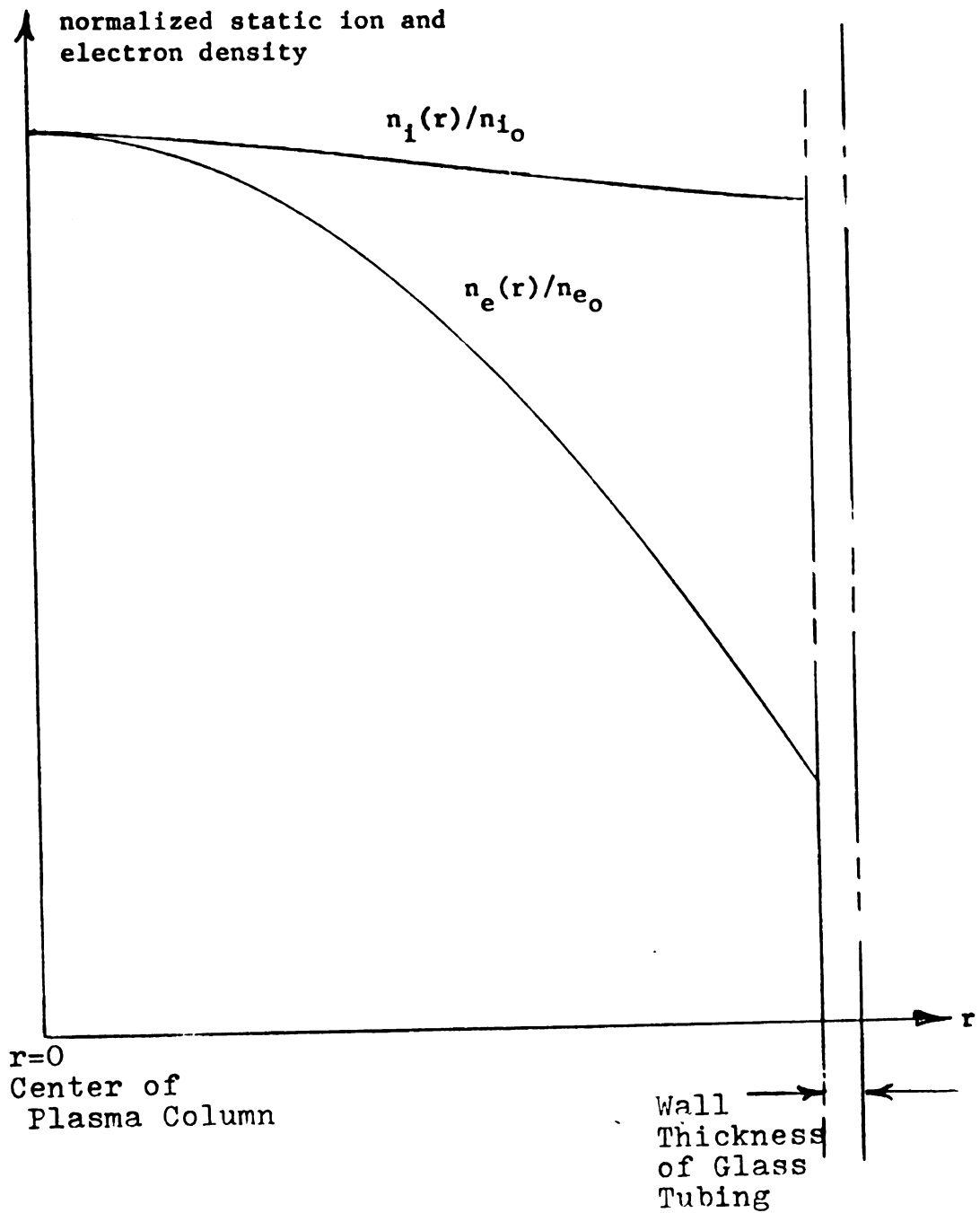


Fig. 2.1.2 Typical electron and ion density profiles in the sheath region of a cylindrical plasma column. Assuming ion drift towards the solid boundary, the ion density does not significantly change in the sheath region.

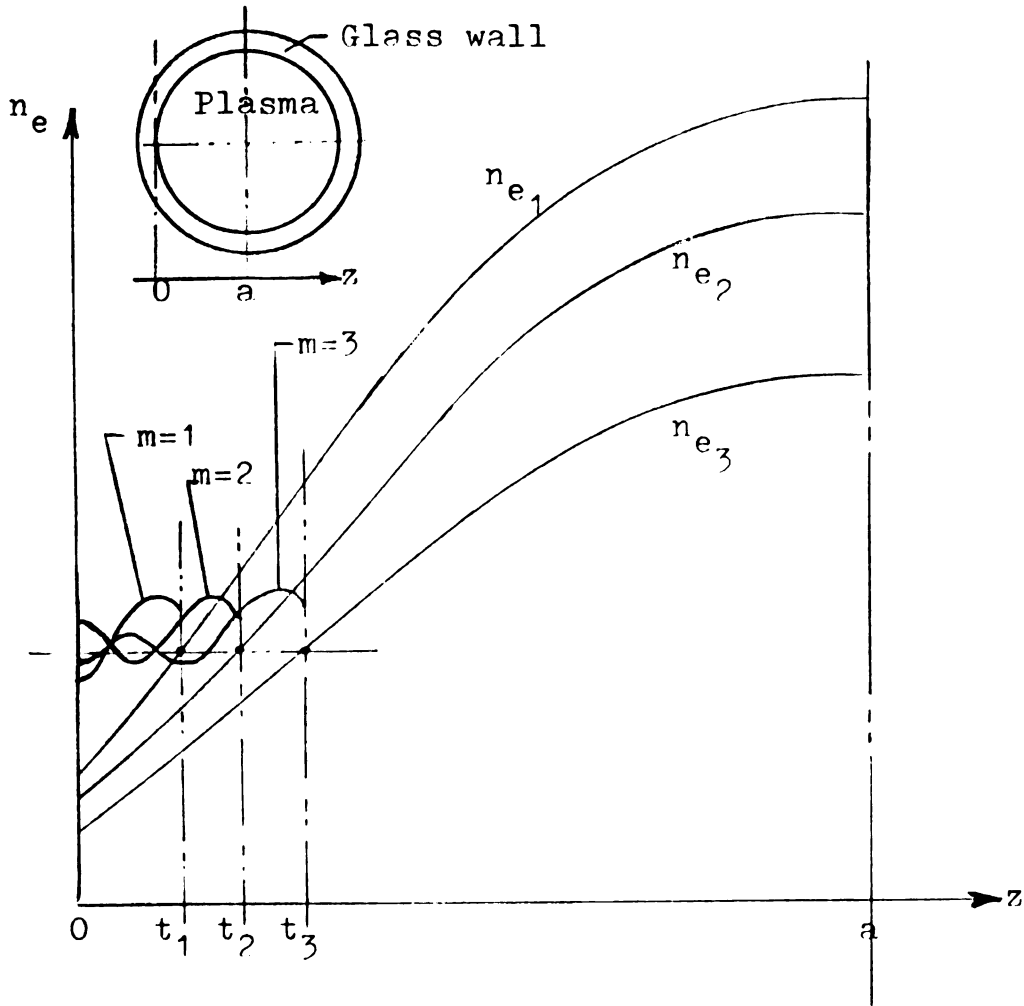


Fig. 2.1.3 Typical sketches of the first three thermal resonances ($m=1,2,3$) occurring at a given frequency of the incident EM field at three discharge current levels producing density profiles n_{e1} , n_{e2} , and n_{e3} .

The resonances occur when $\omega^2 = \omega_p^2$ at any current level which corresponds to

$$n_{e1}(t_1) = n_{e2}(t_2) = n_{e3}(t_3) = \frac{m \epsilon_0 \omega^2}{e^2}$$

for the pr
the sheath
and finally
the experi
for the pr
frequency

3.3 General The

The
region are

and

where \bar{E} and
intensity a
represents
which is no
represents
leading ter
tion is ba
negligible
analysis th
 $n_e(\bar{x}, t)$ will
perturbatio

for the possible occurrence of electroacoustic thermal resonances in the sheath region is examined using a WKB approximation technique, and finally dipole resonances in the cylindrical plasma used in the experiment are studied for the purpose of obtaining a value for the proportionality constant C_p relating the average plasma frequency $\langle \omega_p(r) \rangle$ to the exciting frequency ω by

$$C_p = \left(\frac{\langle \omega_p(r) \rangle^2}{\omega^2} \right).$$

2.2 General Theory

The Maxwell and moment equations applicable to the plasma region are

$$\nabla \times \bar{E} = - \frac{\partial}{\partial t} \mu_0 \bar{H} \quad (2.1)$$

and

$$\nabla \times \bar{H} = - e n_{e_0} \bar{v} + \frac{\partial}{\partial t} \epsilon_0 \bar{E} \quad (2.2)$$

where \bar{E} and \bar{H} respectively represent the total electric field intensity and total magnetic field intensity in the plasma; n_{e_0} represents the static electron density distribution in the plasma which is non-uniform in the plasma sheath near a boundary; \bar{v} represents the mean ac electron velocity so that $-en_{e_0}\bar{v}$ is the leading term of the mean induced electron current. This formulation is based on the assumption that the positive ion motion is negligible in comparison to the electron motion. In the subsequent analysis the total instantaneous electron density distribution $n_e(\bar{x}, t)$ will represent the dc component $n_{e_0}(\bar{x})$ plus the ac perturbation term $n_1(\bar{x}, t)$. All other quantities associated with

these two

field, and

dc and per

In

moment equ

interest f

Since $n_e(x)$

Since $n_e \bar{v}$

terms and

equation (

From the v

equation (

The second

given by

these two components of electron density such as the electric field, and the velocity are also represented by a superposition of dc and perturbation terms.

In order to study perturbations in the plasma sheath, two moment equations must be used. The first moment equation of interest is the continuity equation

$$\frac{\partial n_e}{\partial t} + \nabla \cdot (n_e \bar{v}) = 0 . \quad (2.3)$$

Since $n_e(x,t) = n_{e_0}(x) + n_1(x,t)$, the continuity equation becomes

$$\frac{\partial n_1(\bar{x},t)}{\partial t} + \nabla \cdot n_e \bar{v} = 0 . \quad (2.4)$$

Since $n_e \bar{v} = n_{e_0} \bar{v} + n_1 \bar{v}$, where $n_1 \bar{v}$ is a product of two perturbation terms and therefore represents a negligible second order effect, equation (2.4) becomes

$$\frac{\partial n_1}{\partial t} + \nabla \cdot n_{e_0} \bar{v} = 0 . \quad (2.5)$$

From the vector identity

$$\nabla \cdot \phi \bar{A} = \phi \nabla \cdot \bar{A} + \nabla \phi \cdot \bar{A} \quad (2.6)$$

equation (2.5) can be rewritten as follows

$$\frac{\partial n_1}{\partial t} + n_{e_0} \nabla \cdot \bar{v} + \bar{v} \cdot \nabla n_{e_0} = 0 . \quad (2.7)$$

The second moment equation based on the summation of momenta is given by

$$\frac{\partial \bar{v}}{\partial t} + v \bar{v} = - \frac{e}{m} \bar{E}_{\text{total}} - \frac{\gamma k T}{m n_{e_0}} \nabla n_e . \quad (2.8)$$

Here the
gradient

and

For the c
harmonic

In the pr
law

must be u
region of
of specif
of freedo
acoustic

Se
the follo

Here the density gradient ∇n_e is associated with the pressure gradient ∇p . For an isothermal process,

$$p = nkT$$

and

$$\nabla p = kT \nabla n_e .$$

For the case of an ac perturbation, $n_1(\bar{x}, t)$, due to an external harmonic force, the total electron density is

$$n_e(\bar{x}, t) = n_{e_0}(\bar{x}) + n_1(\bar{x}, t) .$$

In the presence of ac perturbation at high frequency the adiabatic law

$$p n^{-\gamma} = \text{constant}$$

must be used because the temperature is not equalized in the region of high frequency electron perturbations. γ is the ration of specific heats and is given by $(m + 2)/m$ where m is the degree of freedom of the gas. For high frequency longitudinal electro-acoustic plasma oscillations, $m = 1$, so that for these oscillations

$$\gamma = 3 \tag{2.9}$$

Separating equation (2.8) into its dc and ac components, the following equations result. The dc equation is given by

$$0 = - \frac{e}{m} \bar{E}_{dc} - \frac{kT}{m n_{e_0}} \nabla n_{e_0}(\bar{x}) . \tag{2.10}$$

The ac equ

Solution o

$\phi_{dc}(\bar{x})$ in

A one-dime

K, K' , and

the electr

The ac equation is given by

$$\frac{\partial \bar{v}}{\partial t} + \bar{v} \bar{v} = - \frac{e}{m} \bar{E}_{ac} - \frac{3kT}{n_{e_0} m} \nabla n_1(\bar{x}, t). \quad (2.11)$$

Solution of the dc equation for n_{e_0} in terms of the potential $\phi_{dc}(\bar{x})$ in the plasma proceeds as follows:

$$\bar{E}_{dc}(\bar{x}) = - \nabla \phi_{dc}(\bar{x}) \quad (2.12)$$

$$\nabla \phi_{dc}(\bar{x}) = \frac{kT}{n_{e_0} e} \nabla n_{e_0}(\bar{x}) \quad (2.13)$$

A one-dimensional component of equation (2.13) becomes

$$\frac{d}{dx} \phi(x) = \frac{kT}{en_{e_0}} \frac{d}{dx} n_{e_0}(x) \quad (2.14)$$

$$\int d\phi(x) = \frac{kT}{e} \int \frac{1}{n_{e_0}} dn_{e_0}(x) + K$$

$$\phi(x) = \frac{kT}{e} \ln n_{e_0}(x) + K$$

$$\ln n_{e_0}(x) = \frac{e\phi(x)}{kT} + K'$$

$$n_{e_0}(x) = K'' e^{\frac{e\phi(x)}{kT}}$$

K , K' , and K'' are related arbitrary constants. Defining n_0 to be the electron density where $\phi(x) = 0$, $K'' = n_0$; therefore

which rept

which is u

In

necessary

here for r

Con

Ac

Sin

is excited

of the for

into the c

and

In equation

dropped for

$$n_{e_0}(\mathbf{x}) = n_0 e^{\frac{e\phi(\mathbf{x})}{kT}} \quad (2.15)$$

which represents a Maxwellian dc electron density distribution which is used in the subsequent plasma column analysis.

In order to analyze the ac behavior of the plasma it is necessary to combine equations (2.5) and (2.11) which are repeated here for reference:

Continuity Equation:

$$\frac{\partial n_1(\bar{\mathbf{x}}, t)}{\partial t} + \nabla \cdot n_{e_0} \bar{\mathbf{v}} = 0 \quad (2.16)$$

Ac Momentum Transfer Equation:

$$\frac{\partial \bar{\mathbf{v}}}{\partial t} + \mathbf{v} \bar{\mathbf{v}} = -\frac{e}{m} \bar{\mathbf{E}}_{ac} - \frac{3kT}{n_{e_0} m} \nabla n_1(\bar{\mathbf{x}}, t) \quad (2.17)$$

Since the ac perturbation of the electron density $n_1(\bar{\mathbf{x}}, t)$ is excited by a time harmonic incident EM wave with time dependence of the form $\text{Re } e^{j\omega t}$, the system of equations may be transformed into the complex phasor domain:

$$j\omega n_1 + \nabla \cdot n_{e_0} \bar{\mathbf{v}} = 0 \quad (2.18)$$

and

$$j\omega \bar{\mathbf{v}} + \mathbf{v} \bar{\mathbf{v}} = -\frac{e}{m} \bar{\mathbf{E}} - \frac{3kT}{n_{e_0} m} \nabla n_1 \quad (2.19)$$

In equations (2.18) and (2.19), the functional notation has been dropped for simplicity with the understanding that

(1) n_1 rep

of \bar{x} o

(2) \bar{v} repr

of \bar{x} o

(3) \bar{E} is t

only.

Max

only, becc

and

To obtain

derived ta

Therefore

From equat

Equation (

- (1) n_1 represents the phasor transform of $n_1(\bar{x}, t)$ and is a function of \bar{x} only.
- (2) \bar{v} represents the phasor transform of $v(\bar{x}, t)$ and is a function of \bar{x} only.
- (3) \bar{E} is the phasor transform of $E(\bar{x}, t)$ and is a function of x only.

Maxwell's equations (2.1) and (2.2), for ac variations only, become (after phasor transformation)

$$\nabla \times \bar{E} = -j\omega\mu_0 \bar{H} \quad (2.20)$$

and

$$\nabla \times \bar{H} = -en_0 \bar{v} + j\omega\epsilon_0 \bar{E} \quad (2.21)$$

To obtain a solution for n_1 , a differential equation for n_1 is derived taking the divergence of equation (2.21), relating \bar{E} to \bar{v} :

$$\nabla \cdot \nabla \times \bar{H} = -e\nabla \cdot (n_0 \bar{v}) + j\omega\epsilon_0 \nabla \cdot \bar{E}$$

Therefore

$$\nabla \cdot \bar{E} = \frac{e}{\epsilon_0 j\omega} \nabla \cdot (n_0 \bar{v}) \quad (2.22)$$

From equation (2.18)

$$\nabla \cdot n_0 \bar{v} = -j\omega n_1 \quad (2.23)$$

Equation (2.22) becomes

$$\nabla \cdot \bar{E} = -\frac{en_1}{\epsilon_0} \quad (2.24)$$

In order

(2.19):

Combining

From equa:

and using

It follows

Substituti

-(j)

After rear

7² n

In order to eliminate \bar{E} , the divergence is taken of equation (2.19):

$$(j\omega + \nu)\nabla \cdot \bar{v} = -\frac{e}{m}\nabla \cdot E - \frac{3kT}{n_{e_0}m}\nabla^2 n_1 \quad (2.25)$$

Combining equations (2.25) and (2.24) yields

$$(j\omega + \nu)\nabla \cdot \bar{v} = +\frac{e^2 n_1}{m\epsilon_0} - \frac{3kT}{n_{e_0}m}\nabla^2 n_1 \quad (2.26)$$

From equation (2.23)

$$\nabla \cdot n_{e_0} \bar{v} = -j\omega n_1 \quad (2.27)$$

and using vector identity equation (2.6),

$$\nabla \cdot n_{e_0} \bar{v} = n_{e_0} \nabla \cdot \bar{v} + \bar{v} \cdot \nabla n_{e_0} = -j\omega n_1 \quad (2.28)$$

It follows that

$$\nabla \cdot \bar{v} = -\frac{j\omega n_1}{n_{e_0}} - \frac{\bar{v} \cdot \nabla n_{e_0}}{n_{e_0}} \quad (2.29)$$

Substituting equation (2.29) into equation (2.26) yields

$$\frac{-(j\omega + \nu)j\omega n_1}{n_{e_0}} - \frac{+(j\omega + \nu)\bar{v} \cdot \nabla n_{e_0}}{n_{e_0}} = \frac{e^2 n_1}{m\epsilon_0} - \frac{3kT}{n_{e_0}m}\nabla^2 n_1 \quad (2.30)$$

After rearranging, a differential equation for n_1 is obtained:

$$\nabla^2 n_1 + \frac{\omega^2 - \omega_p^2 - j\omega\nu}{\left(\frac{3kT}{m}\right)} n_1 = \frac{j\omega + \nu}{(3kT/m)} \bar{v} \cdot \nabla n_{e_0} \quad (2.31)$$

If as a f

zero, equ

where ω_p^2

inhomogen

$(j\omega/V^2)(\bar{v}$

force for

driving fo

satisfied:

(1) There

density

(2) there

density

The first

cylindrica

in the rad

electron v

by an elec

radial dir

represents

incident E

the radial

driving fo

If as a first approximation the collision frequency is set to zero, equation (2.31) becomes (with $v_o^2 = 3kT/m$)

$$\nabla^2 n_1 + \frac{\omega^2 - \omega_p^2}{v^2} n_1 = \frac{j\omega}{v^2} \bar{v} \cdot \nabla n_{e_o} \quad (2.32)$$

where ω_p^2 is the plasma frequency $(e^2 n_e)/(m_e \epsilon_o)$. This is an inhomogeneous Helmholtz equation in n_1 with a forcing function $(j\omega/v^2)(\bar{v} \cdot \nabla n_{e_o})$. This forcing function represents the driving force for the perturbation in n_1 . Careful examination of this driving force shows that it is nonzero only if two conditions are satisfied:

- (1) There must exist a nonzero gradient of the static electron density n_{e_o} in the region of interest, and
- (2) there must exist a component of \bar{v} parallel to the electron density gradient ∇n_{e_o} .

The first condition is satisfied in the sheath region of a cylindrical plasma column where an electron density gradient exists in the radial direction. The second condition is satisfied if an electron velocity perturbation in the radial direction is set up by an electric field component in the incident EM field in the radial direction. Thus the velocity \bar{v} in the driving function represents the coupling term between the radial component of the incident EM field and the electron density perturbation n_1 . Here the radial component of the EM field represents physically the driving force exciting the electron density perturbation.

In
cylinder
the vari
wall ($x =$
character
compared
to treat
planar g
region a

$$\frac{d^2 n_1}{dx^2} + \frac{\omega^2}{c^2} n_1 = 0$$

The corre

Equation

of x in w

the wall

$$\omega = \omega_p$$

ω_p^2 , the

oscillato

subject to

of $\omega_p(x)$,

In the sub

wall is ex

In the region of interest near the wall of the plasma cylinder the geometry of interest is shown in Figure 2.2.1. Here the variable x is introduced representing the distance from the wall ($x = 0$) into the plasma normal to the wall. Since the characteristic dimension of the sheath region is relatively small compared to the radius of the plasma cylinder, it is justifiable to treat the section of the sheath region shown in Figure 2.2.1 in planar geometry. Thus equation (2.32) may be rewritten for that region as a one-dimensional equation in x as

$$\frac{d^2 n_1}{dx^2} + \frac{\omega^2 - \omega_p^2(x)}{v^2} n_1 = ((j\omega)/v^2) (v_x \frac{dn_{e_0}}{dx}) \quad (2.33)$$

The corresponding homogeneous equation is

$$\frac{d^2 n_1}{dx^2} + \frac{\omega^2 - \omega_p^2(x)}{v^2} n_1 = 0 \quad (2.34)$$

Equation (2.34) has a natural oscillatory solution in the region of x in which ω^2 is larger than $\omega_p^2(x)$. This is the region between the wall ($x = 0$) and the so-called critical point ($x = x_p$) where $\omega = \omega_p$. For values of x larger than x_p , where ω^2 is less than ω_p^2 , the solution represents an evanescent wave. The natural oscillatory solution for n_1 in the sheath region is of course subject to boundary conditions at the wall and the functional form of $\omega_p(x)$, where

$$\omega_p^2(x) = \frac{e^2 n_{e_0}(x)}{m_e \epsilon_0} \quad (2.35)$$

In the subsequent sections the boundary condition for n_1 at the wall is examined, followed by a study of the total phase require-

→ 31a
→ 31b
→ 31c



Fig. 2.2.1

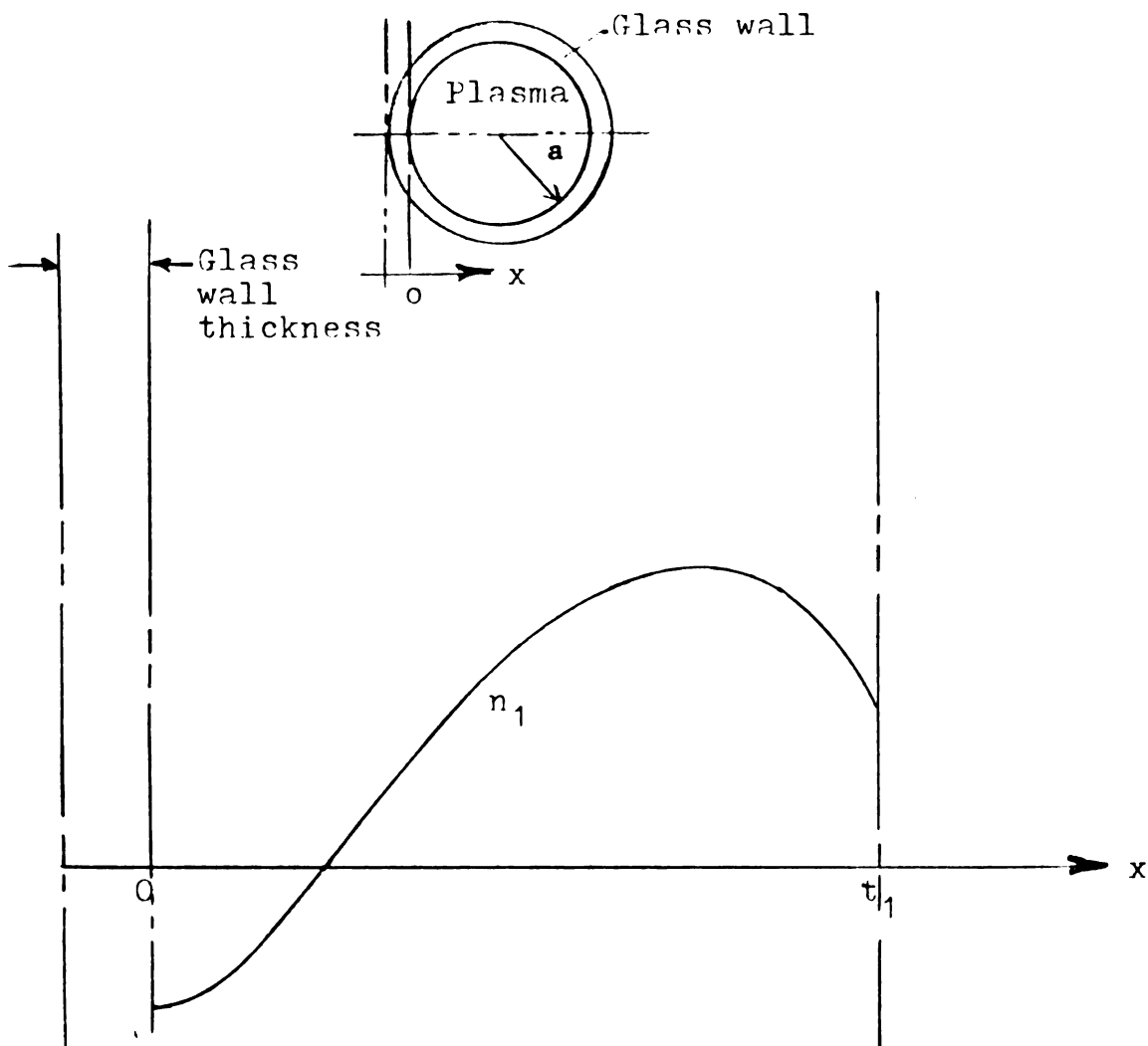


Fig. 2.2.1 Geometric arrangement used in the region where thermal resonances occur. n_1 represents a typical waveform of n_1 a thermal resonance; t_1 is the critical point where $\omega = \omega_p$. The one-dimensional approach is justified in this region because t_1 is typically much smaller than the radius of the plasma column, a .

ment betw

of natura

1.3 Determina

T.

on phenom

velocity

zero in t

standing

(n_{e_0} inde

$v_{wall} = 0$

maximum a

From equa

and using

and lettin

in one-dir

Since we a

dependence

where A an

ment between the wall and the critical point x_p for the existence of natural resonances.

2.3 Determination of the Boundary Condition at the Wall

The boundary conditions at the wall can only be established on phenomenological grounds. It is reasonable to assume that the velocity v associated with the electroacoustic wave motion goes to zero in the immediate vicinity of the wall. For electroacoustic standing wave perturbations in a uniform dc electron density (n_{e_0} independent of x) it can be shown that the boundary condition $v_{\text{wall}} = 0$ corresponds to the boundary condition that n_1 is a maximum at the wall as follows:

From equation (2.18)

$$j\omega n_1 + \nabla \cdot n_{e_0} \bar{v} = 0 \quad (2.36)$$

and using vector identity equation (2.6)

$$j\omega n_1 = -n_{e_0} \nabla \cdot \bar{v} + \nabla n_{e_0} \cdot \bar{v} \quad (2.37)$$

and letting $\nabla n_{e_0} \doteq 0$ near the wall the following equation results in one-dimensional form in x :

$$j\omega n_1 = -n_{e_0} \frac{d}{dx} v \quad (2.38)$$

Since we are assuming a standing wave in n_1 and v , the functional dependence of v on x is of the form

$$v(x) = A \sin(k_p x + \theta) \quad (2.39)$$

where A and θ are the arbitrary magnitude and phase constants

respectiv

wall and

Substitut

Therefore

It is imp

of the ord

$(-\frac{1}{j\omega})$ sho

n_1 and v_1

$n_1(x)$ lead

$(x = 0)$, n

at the wal

It

Figure 2.3

wall. It

phase cons

represente

2.4 Determinat

Fig

expected f

The

warm plas

respectively. For the assumed condition that v goes to zero at the wall and letting $x = 0$ at the wall, equation (2.39) becomes:

$$v(x) = A \sin(k_p x) \quad (2.40)$$

Substituting equation (2.40) into equation (2.38) yields

$$j\omega n_1 = -n_{e_0} \frac{d}{dx} A \sin(k_p x) \quad (2.41)$$

Therefore

$$n_1 = -n_{e_0} \left(\frac{Ak}{j\omega} \right) \cos(k_p x) . \quad (2.42)$$

It is important to recall that n_1 represents the phasor transform of the original time harmonic function $n_1(x,t)$. The phase term $(-\frac{1}{j\omega})$ shows that a $\pi/2$ radian time phase difference exists between n_1 and v . In addition, a spatial phase difference exists with $n_1(x)$ leading $v(x)$ by $\pi/2$ radians. This means that at the wall ($x = 0$), n_1 should have a maximum corresponding to the zero of v at the wall. This phenomenon is shown graphically in Figure 2.3.1.

It should be understood that the sketches for v and n_1 in Figure 2.3.1 are only intended to show the relative phase at the wall. It is clear that the actual thermal resonances have varying phase constant and magnitude away from the wall which is not represented here.

2.4 Determination of the Total Phase for the Thermal Resonances

Figure 2.4.1 shows the typical electron-density contour expected in a cylindrical plasma column.

The propagation constant for electroacoustic waves in a warm plasma, $k_p(x)$, is given by:



Fig. 2.2.1

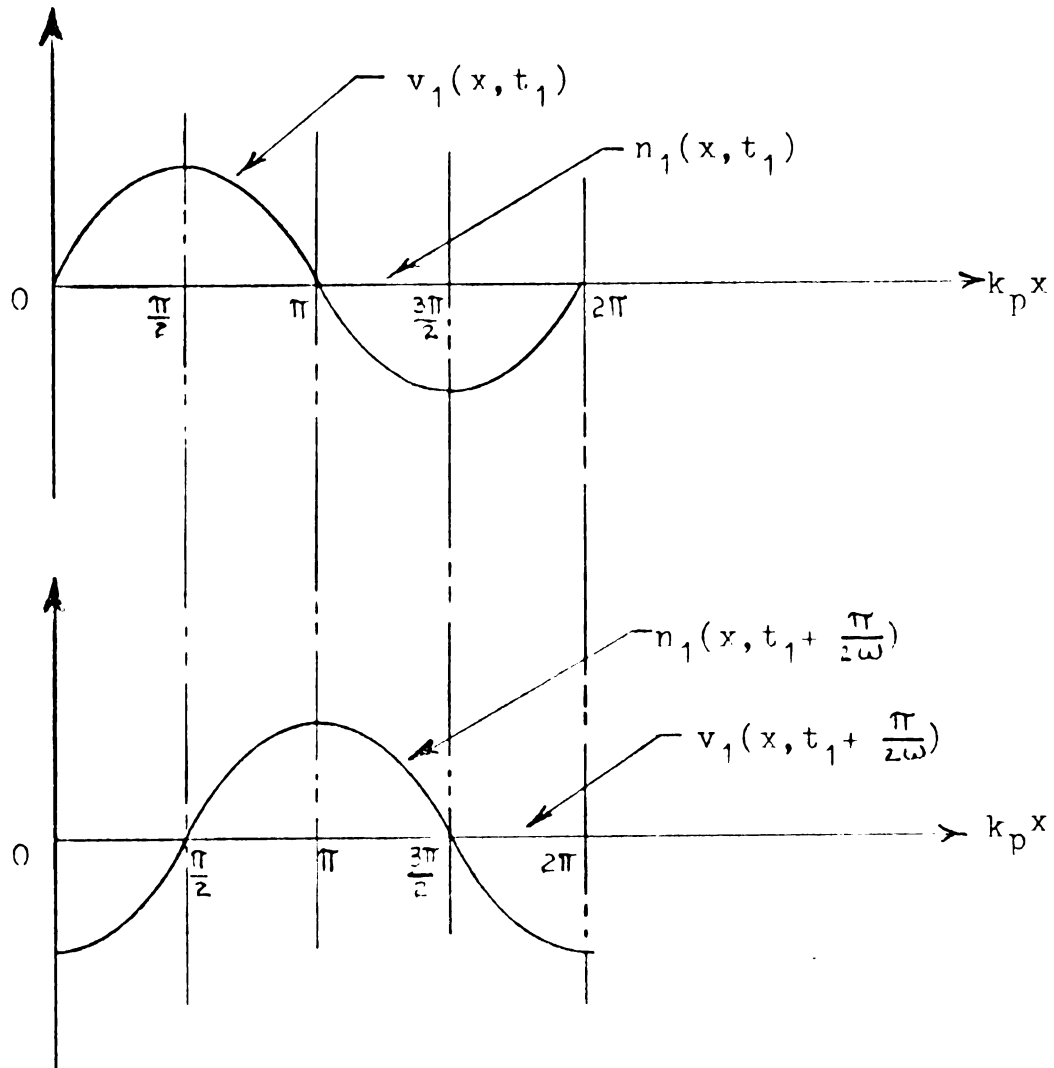


Fig. 2.3.1 Phase relation between electron density perturbation n_1 and associated electron velocity perturbation v_1 .

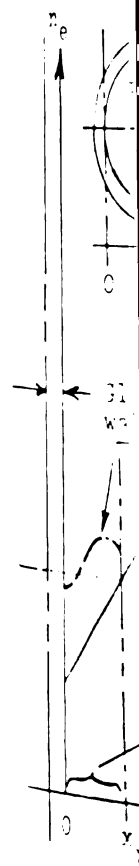


Fig. 2.4.1

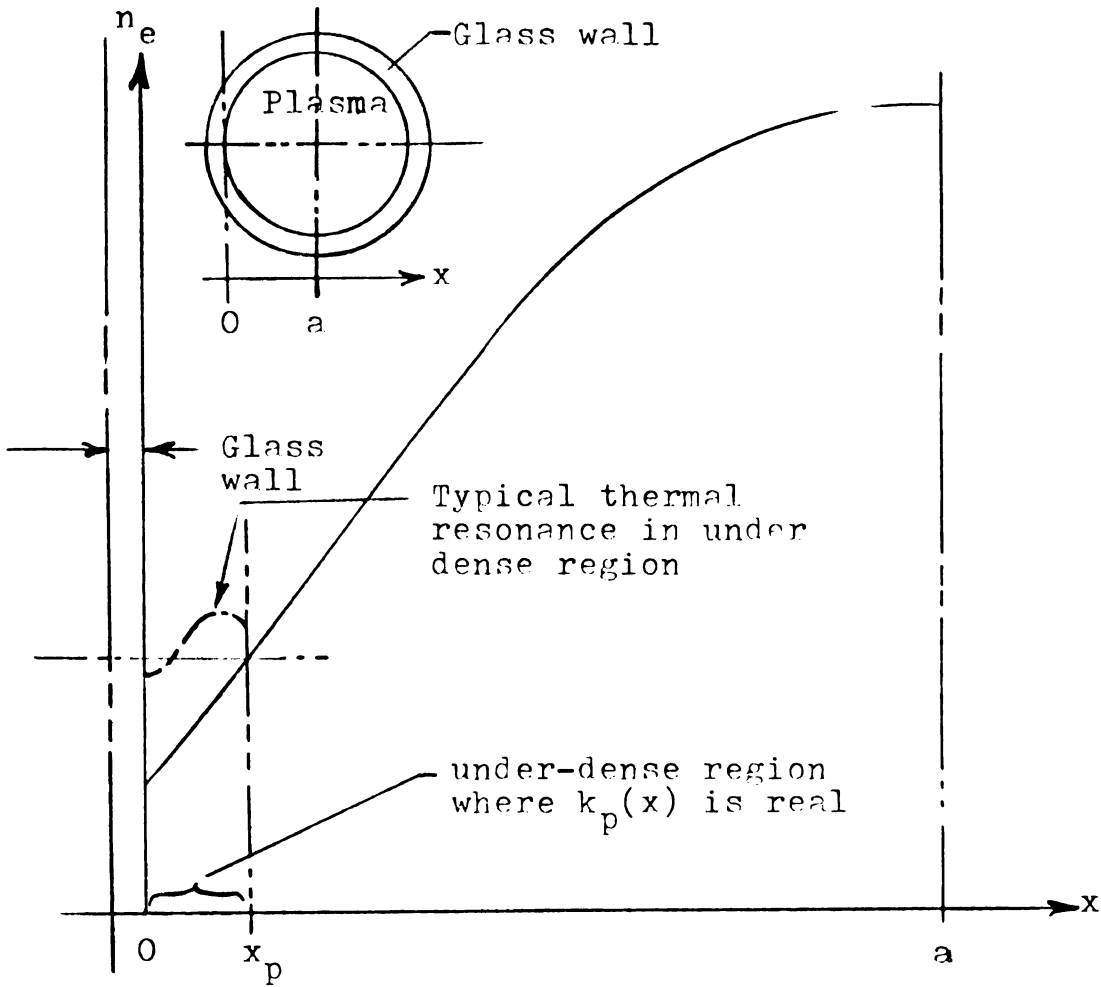


Fig. 2.4.1 The under-dense region in which thermal resonances may occur if the phase conditions are satisfied and an appropriate EM field illuminates the plasma column.

where: $\omega_p(x)$

$\omega_p(x)$

v_c

k

T

n_e

The propa

$\omega_p(x)^2 / \omega^2$

$0 < x < x$

$x = 0$ and

a given f

$x = 0$ and

satisfies

condition

necessar

$x = x_p$

T

for elec

referenc

$$k_p(x) = \frac{\omega}{v_o} \left(1 - \frac{\omega_p(x)^2}{\omega^2}\right)^{1/2} \quad (2.43)$$

where: ω = radian frequency of the electroacoustic wave

$\omega_p(x)$ = plasma frequency as a function of x

$$v_o = \sqrt{\frac{3kT}{m_e}} = \text{thermal electron velocity}$$

k = Boltzman constant

T = electron temperature

m_e = electron mass.

The propagation constant $k_p(x)$ is real only in regions in which $\omega_p(x)^2/\omega^2 \leq 1$. In Figure 2.4.1, $k_p(x)$ is real in the region $0 < x < x_p$, so that an electroacoustic wave can propagate between $x = 0$ and $x = x_p$. This permits electroacoustic standing waves of a given frequency ω to be excited in the sheath region between $x = 0$ and $x = x_p$ as long as the total phase of the standing wave satisfies the phase conditions to be derived. The boundary condition at $x = 0$ was established in section 2.2. It is now necessary to determine the total phase condition between $x = 0$ and $x = x_p$.

The standard time-independent wave equation in one dimension for electroacoustic waves, equation (2.34) is repeated here for reference:

$$\frac{dn_1^2}{dx^2} + k_p^2(x) n_1 = 0 \quad (2.44)$$

where n_1

function

the WKB

x-depend

$$\int^x k_p(x)$$

where the

correspo

directio

in $\phi(x)$

by subst

into the

$$\frac{dn_1}{dx} = \frac{dz}{dx}$$

$$\frac{d^2 n_1}{dx^2} = \frac{d^2 z}{dx^2}$$

$$\frac{d^2 n_1}{dx^2} = ($$

*

where n_1 represents the phasor transform of $n_1(x,t)$ and is a function of x only. In order to establish the total phase of n_1 , the WKB approximation is used; $n_1(x)$ is expressed in terms of an x -dependent magnitude function $\phi(x)$ and an x dependent phase term $\int^x k_p(x') dx$ as follows:¹¹

$$n_1(x) = \phi(x) e^{\pm i \int^x k_p(x') dx'} \quad (2.45)$$

where the plus and minus signs in front of the phase term correspond to waves propagating in the negative and positive x directions respectively. It is now necessary to find an equation in $\phi(x)$ from which $\phi(x)$ can be determined. This is accomplished by substituting the assumed solution for $n_1(x)$, equation (2.45), into the wave equation (2.44),

$$\begin{aligned} \frac{dn_1}{dx} &= \frac{d\phi}{dx} e^{\pm i \int^x k_p(x') dx'} + \pm i k_p(x) \phi e^{\pm i \int^x k_p(x') dx'} \\ \frac{d^2 n_1}{dx^2} &= \frac{d^2 \phi}{dx^2} e^{\pm i \int^x k_p(x') dx'} + \frac{d\phi}{dx} e^{\pm i \int^x k_p(x') dx'} (\pm i k_p(x)) \\ &\quad + \frac{d\phi}{dx} e^{\pm i \int^x k_p(x') dx'} (\pm i k_p(x)) + \phi e^{\pm i \int^x k_p(x') dx'} \\ &\quad \cdot (\pm i k_p(x))^2 + \phi e^{\pm i \int^x k_p(x') dx'} \left(\pm i \frac{dk_p(x)}{dx} \right) \\ \frac{d^2 n_1}{dx^2} &= \left(\frac{d^2 \phi}{dx^2} \pm 2i k_p(x) \frac{d\phi}{dx} + \phi \left(-k_p^2(x) \pm i \frac{dk_p(x)}{dx} \right) \right) \\ &\quad * e^{\pm i \int^x k_p(x') dx'} \end{aligned}$$

Therefore

$$\frac{d^2 \phi}{dx^2} \pm 2i$$

$$\frac{d^2 \phi}{dx^2} \pm 2i$$

$$\frac{1}{ik(x)}$$

If, in the

function

compared

waves at

are consi-

of electri-

Therefore

vicinity

derivativ

in $\phi(x)$ i

Therefore

Therefore equation (2.44) becomes

$$\frac{d^2\phi}{dx^2} \pm 2ik_p(x) \frac{d\phi}{dx} - k_p^2(x)\phi \pm i \frac{dk_p(x)}{dx} \phi + k_p^2(x)\phi = 0 \quad (2.46)$$

$$\frac{d^2\phi}{dx^2} \pm 2ik_p(x) \frac{d\phi}{dx} \pm i \frac{dk_p(x)}{dx} \phi = 0$$

$$\frac{1}{ik_p(x)} \frac{d^2\phi}{dx^2} \pm \left(2 \frac{d\phi}{dx} + \frac{1}{k_p(x)} \frac{dk_p(x)}{dx} \phi \right) = 0 \quad (2.47)$$

If, in the region of interest, $\phi(x)$ does not change rapidly as a function of x , the first term in equation (2.47) is negligible compared with the other terms. In the electroacoustic standing waves at hand, the first two, or in some cases, three resonances are considered, so that approximately one to three half-wavelengths of electroacoustic standing wave are expected in the sheath region. Therefore the variation of the peak magnitude of n_1 , $\phi(x)$, in the vicinity of the turning point is quite small and the second derivative term, $\frac{d^2\phi}{dx^2}$, may be neglected. The resulting equation in $\phi(x)$ is given by

$$\frac{2}{\phi} \frac{d\phi}{dx} + \frac{1}{k_p(x)} \frac{dk_p(x)}{dx} = 0 \quad (2.48)$$

Therefore

$$\frac{2d\phi}{\phi} + \frac{dk_p(x)}{k_p(x)} = 0$$

Integrat

where K_3
expressio

where $k_p(x)$

In

imaginary

$x_p < x$ is

Since only

positive t

Integration leads to the following solution:

$$2 \int \frac{d\phi}{\phi} = - \int \frac{dk_p(x)}{k_p(x)} + K_1$$

$$\ln(\phi^2) = - \ln(k_p(x)) + \ln(K_2)$$

$$\ln(\phi^2) = \ln\left(\frac{K_2}{k_p(x)}\right)$$

$$\phi(x) = \frac{K_3}{\sqrt{k_p(x)}} \quad (2.49)$$

where K_3 is an arbitrary integration constant. Thus, the expression for $n_1(x)$ postulated in equation (2.45) takes the form:

$$n_1(x) = K \frac{1}{\sqrt{k_p(x)}} e^{\pm i \int_{x_p}^x k_p(x') dx'} \quad (2.50)$$

where $k_p(x)$ is real for $x \leq x_p$.

In the region where x is larger than x_p , $k_p(x)$ is imaginary and may be written as $i|k_p(x)|$ so that $n_1(x)$ for $x_p < x$ is most conveniently written as

$$n_1(x) = K \frac{1}{\sqrt{|k_p(x)|}} e^{\pm i \int_{x_p}^x |k_p(x')| dx'} \quad (2.51)$$

Since only an attenuated wave is expected in this region, the positive term in the exponential is not applicable so that:

Thus the

n

Since the

represent

convenient

where θ re

breaks do

unbounded.

vicinity of

$u_p(x)$ is a

$k_p^2(x)$ can

This is a

$$n_1(x) = K \frac{1}{\sqrt{|k_p(x)|}} e^{-\int_{x_p}^x |k_p(x')| dx'} \quad (2.52)$$

Thus the expressions for $n_1(x)$ are summarized as follows:

$$n_1(x) = \left\{ \begin{array}{l} \frac{K_1}{\sqrt{k_p(x)}} e^{\pm i \int_{x_p}^x k_p(x') dx'} \quad \text{for } 0 < x < x_p \\ \frac{K_2}{\sqrt{|k_p(x)|}} e^{-\int_{x_p}^x |k_p(x')| dx'} \quad \text{for } x > x_p \end{array} \right\} \quad (2.53)$$

Since the electroacoustic waves between $x = 0$ and $x = x_p$ represent standing waves, equation (2.53) for that region may be conveniently written as

$$n_1(x) = \frac{K_1}{\sqrt{k_p(x)}} \sin\left(\int_x^{x_p} k_p(x') dx' + \theta\right) \quad (2.54)$$

where θ represents an arbitrary phase constant. This expression breaks down in the limit as x goes to x_p where $K_1/\sqrt{k_p(x)}$ becomes unbounded. Therefore another formulation is required for the vicinity of $x = x_p$: Since $k_p^2(x) = \frac{1}{v_o^2} (\omega^2 - \omega_p^2(x))$, where $\omega_p(x)$ is a slowly changing function of x , the expression for $k_p^2(x)$ can be linearized near $x = x_p$ as follows:

$$k_p^2(x) = \frac{-\alpha}{v_o^2} (x - x_p) \quad (2.55)$$

This is a linear function with a value of zero at $x = x_p$ as

required

De

leads to:

transform

The wave e

Now:

and

$$\frac{d^2 n}{dx^2}$$

required and a slope equal to $(-\frac{\alpha}{v_o^2})$.

Defining a new variable

$$z = +(\frac{\alpha}{v_o^2})^{1/3} (x - x_p) \quad (2.56)$$

leads to:

$$k_p^2(z) = -(\frac{\alpha}{v_o^2})^{2/3} z \quad (2.57)$$

Transformation of the original wave equation proceeds as follows:

The wave equation (2.34) from section 2.2 was

$$\frac{d^2 n_1}{dx^2} + k_p^2(x) n_1 = 0$$

Now:

$$\frac{dn_1}{dx} = \frac{dn_1}{dz} \frac{dz}{dx} = -\frac{dn_1}{dz} (\frac{\alpha}{v_o^2})^{1/3}$$

and

$$\begin{aligned} \frac{d^2 n_1}{dx^2} &= \frac{d}{dx} \left(\frac{dn_1}{dx} \right) = \frac{d}{dz} \left(\frac{dn_1}{dx} \right) \frac{dz}{dx} = -\frac{d}{dz} \frac{dn_1}{dz} \left(\frac{\alpha}{v_o^2} \right)^{1/3} \left(\frac{\alpha}{v_o^2} \right)^{1/3} \\ &= -\frac{d^2 n_1}{dz^2} \left(\frac{\alpha}{v_o^2} \right)^{2/3} \end{aligned}$$

Thus the w

$x = x_p$ be

The soluti

function

where N_0 f

equation (

for $z > 0$

and for z

See Figure

in the vic

(2.67) and

the linear

may be cor

(in terms

Thus the wave equation in z applicable to the vicinity of $x = x_p$ becomes:

$$\frac{d^2 n_1}{dz^2} - zn = 0 \quad (2.58)$$

The solution to equation (2.58) is given in terms of the Airy function as follows:

$$n_1(z) = \frac{N_0}{\pi} \int_0^{\infty} \cos\left(\frac{s^2}{3} + sz\right) ds \quad (2.59)$$

where N_0 is an arbitrary constant. For large values of $|z|$, equation (2.59) has the following asymptotic approximation: for $z > 0$ which is equivalent to $x > x_p$

$$n_1(z) = \frac{N_0}{2\sqrt{\pi} z^{1/4}} e^{-2/3z^{3/2}} \quad (2.60)$$

and for $z < 0$ which is equivalent to $x < x_p$

$$n_1(z) = \frac{N_0}{\sqrt{\pi} (-z)^{1/4}} \sin\left(\frac{2}{3} (-z)^{3/2} + \pi/4\right) \quad (2.61)$$

See Figure 2.4.2 for a typical graph of the Airy function in the vicinity of $z = 0$. Since equations (2.53) and equations (2.60) and (2.61) should agree at some distance from $x = x_p$, where the linear approximation for $k_p^2(x)$ still holds, the two solutions may be compared. In the region $x < x_p$, equation (2.53) gives (in terms of the variable z , using equation (2.54))

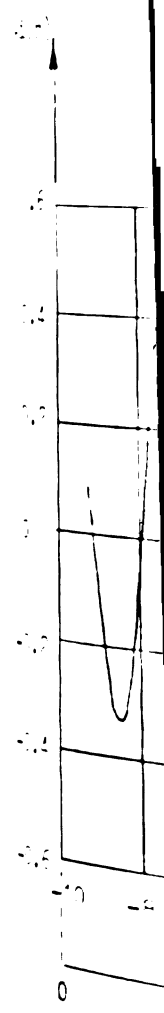


Fig. 2.4.2

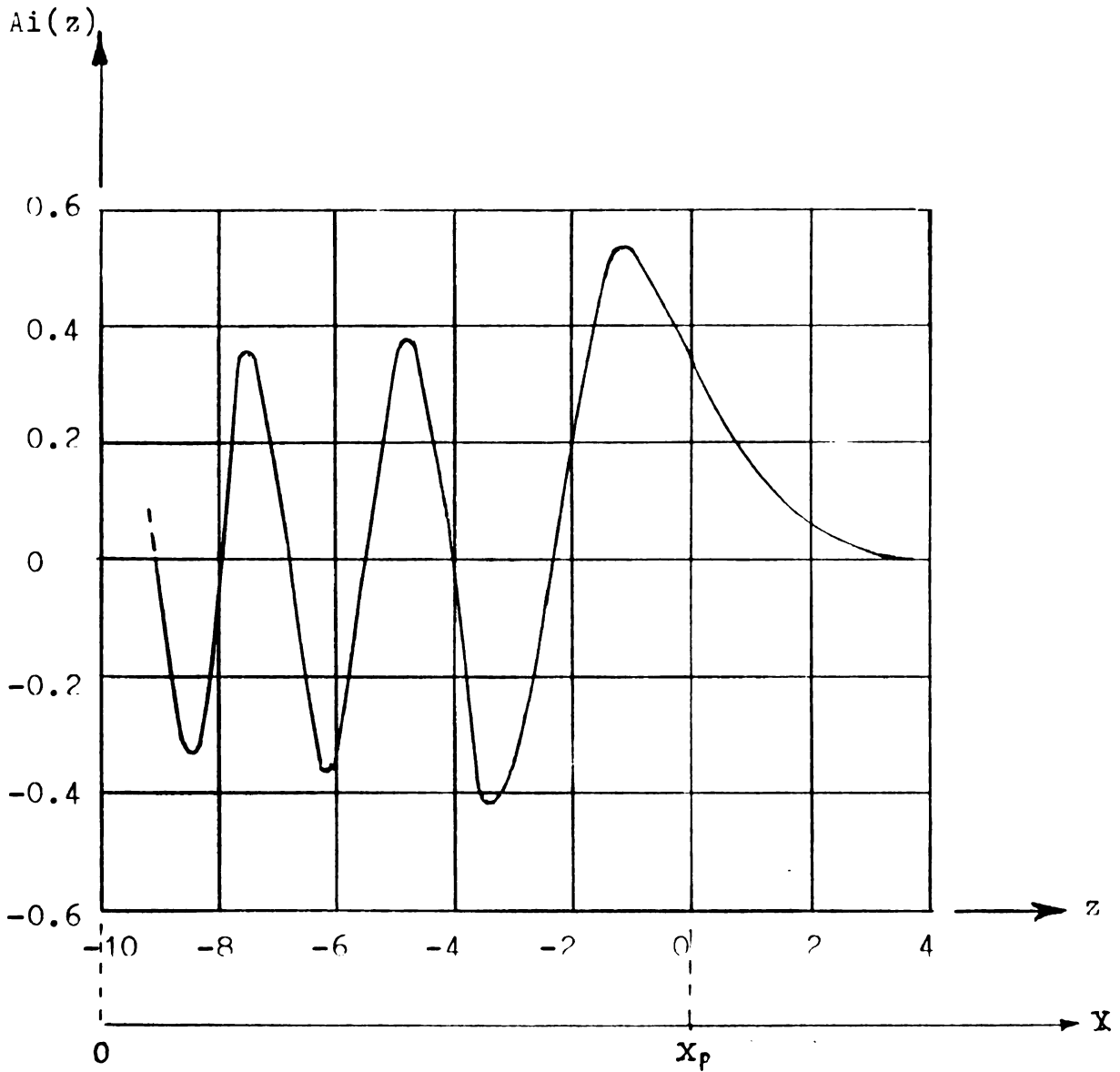


Fig. 2.4.2 Sketch of Airy function,¹¹

$$\text{Ai}(z) = \frac{1}{\pi} \int_0^{\infty} \cos(s^3/3 + s z) dz$$

$$n_1(z) = -$$

and after

n

The phas

phase to

Thus the

$$n_1(x) = \left\{ \begin{array}{l} \sqrt{\dots} \\ \sqrt{\dots} \end{array} \right.$$

The sign

determin

resonanc

thermal

phase ex

(2.54) a

n

must rep

that

(

$$n_1(z) = \frac{K_1}{\sqrt{(\alpha/V_0^2)^{2/3}(-z)^{1/2}}} \sin\left(\int_z^0 (-z')^{1/2} dz' + \theta\right) \quad (2.62)$$

and after performing the integration in the phase term,

$$n_1(z) = \frac{K_1}{\sqrt{(\alpha/V_0^2)^{2/3}(-z)^{1/2}}} \sin\left(\frac{2}{3}(-z)^{3/2} + \theta\right) \quad (2.63)$$

The phase term in the argument of equation (2.63) agrees with the phase term in equation (2.61) if

$$\theta = \pi/4 \quad (2.64)$$

Thus the WKB formulations for $n_1(x)$ in the two regions become

$$n_1(x) = \left\{ \begin{array}{l} \frac{F_1}{\sqrt{k_p(x)}} \exp\left(-\int_{x_p}^x k_p(x') dx'\right) \text{ for } x > x_p \\ \frac{K_2}{\sqrt{k_p(x)}} \sin\left(\int_x^{x_p} k_p(x') dx' + \pi/4\right) \text{ for } 0 < x < x_p \end{array} \right\} \quad (2.65)$$

The significant result from this section needed in the subsequent determination of the electron density profile from the thermal resonance data is an expression for the total phase of these thermal resonances between the wall and the critical point. This phase expression is now obtainable as follows. From equation (2.54) and (2.65) it is seen that at the wall where $x = 0$,

$$n_1(0) = \frac{K_1}{\sqrt{k_p(x)}} \sin\left(\int_0^{x_p} k_p(x') dx' + \pi/4\right) \quad (2.66)$$

must represent a maximum of $n_1(x)$. This leads to the condition that

$$\left(\int_0^{x_p} k_p(x') dx' + \pi/4\right) = (2m + 1) (\pi/2) \quad (2.67)$$

where μ

becomes

or

Figure 2.

to be ex

in Figure

conjuncti

represent

The

analytical

of the e

The

thermal re

thermal re

plasma co

density pr

2.5 Development

and Plasma

In

cylindrica

necessary

where m is a positive integer. Therefore the total phase integral becomes

$$\int_0^{x_p} k_p(x') dx' = (2m + 1)(\pi/2) - \pi/4$$

or

$$\int_0^{x_p} k_p(x') dx' = (m + 1/4)\pi \quad (2.68)$$

Figure 2.4.3 shows typical wave forms of the thermal resonances to be expected in the plasma sheath region. Only the phase shown in Figure 2.4.3 for the various resonances is significant in conjunction with this discussion; the magnitudes are merely representative of typical waveforms.

The phase integral in equation (2.68) is used in the analytical techniques developed in section 3 for the determination of the electron density profiles in cylindrical plasma columns.

The WKB approximation developed in this section for the thermal resonances is also used subsequently to graph examples of thermal resonances with normalized magnitude for actual cylindrical plasma columns based on the numerical results for the electron density profile $n_e(r)$ presented in Chapter 4.

2.5 Development of Relationships between Dipole Resonance Frequency and Plasma Frequency in a Cylindrical Plasma Column

In the determination of the electron density profile in a cylindrical plasma column based on thermal resonance data, it is necessary to know the relationship between the exciting EM wave

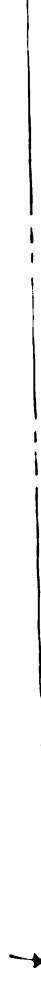


Fig. 2.4.

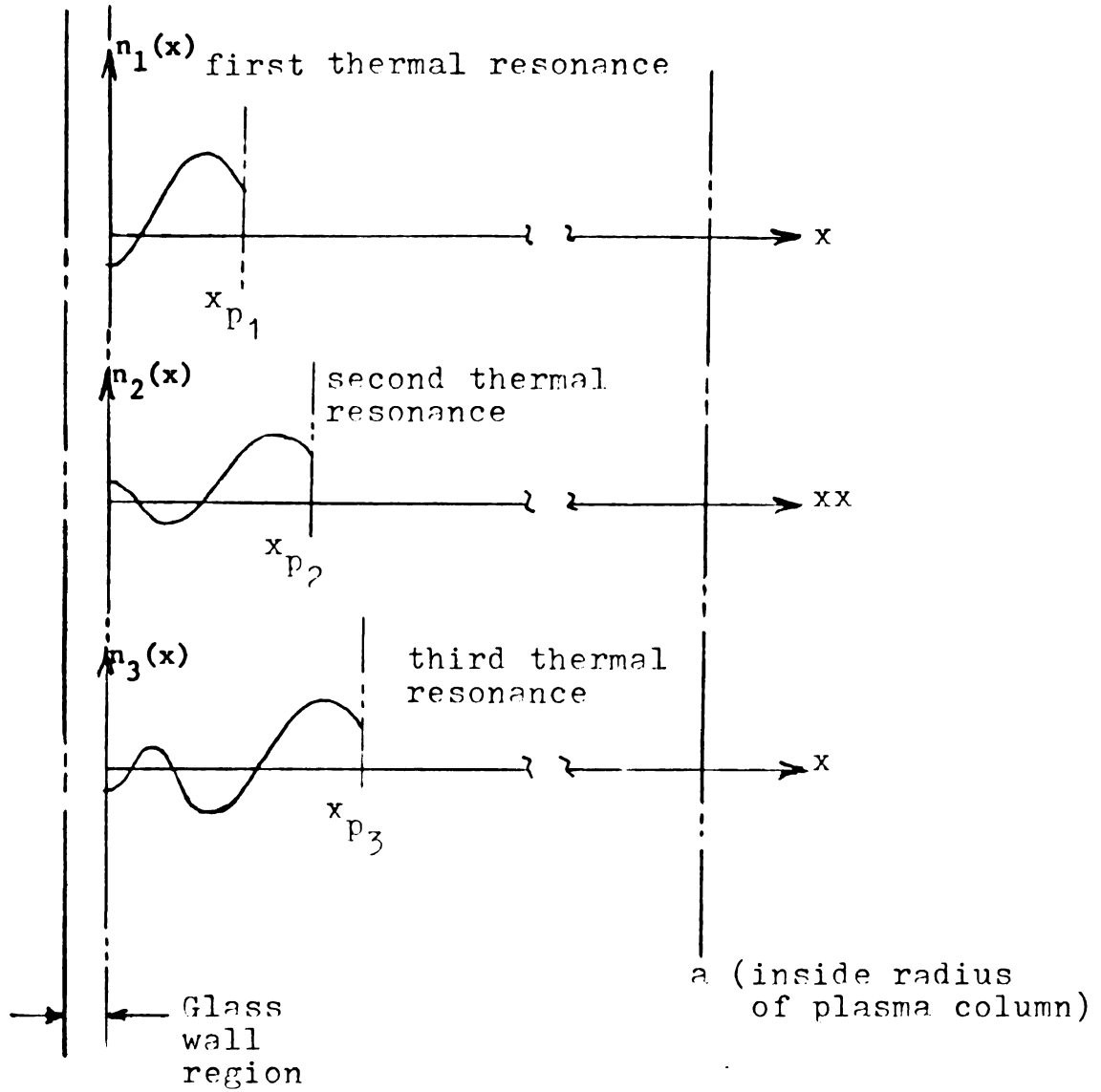


Fig. 2.4.3 Typical waveforms of the first three thermal resonances. x_{p1} , x_{p2} , and x_{p3} are the critical points at which k_{p1} , k_{p2} , and k_{p3} respectively go to zero.

frequen

column.

where C

exact so

of the e

Such exa

paraboli

cylindri

equation

between t

Si

electron

inapprox

an approx

It is, th

uniform p

average <

ω_p of the

It

appropria

quasi-sta

tion of M

of a unif

region ar

frequency ω and the average plasma frequency $\langle \omega_p(r) \rangle$ in the plasma column.

$$\langle \omega_p^2(r) \rangle = C_p \omega^2 \quad (2.69)$$

where C_p is a proportionality constant to be determined. An exact solution for $\langle \omega_p(r) \rangle$ as a function of ω requires knowledge of the electron density profile in the cylindrical plasma column. Such exact analyses have been performed based on an assumed parabolic electron density profile subdividing the plasma into cylindrical sublayers and performing a numerical analysis on the equations resulting from the boundary conditions at the walls and between the strata.¹²

Since it is the objective of this research to determine the electron density profile in the plasma cylinder, it would be inappropriate to presume any specific profile a priori. However, an approximate value to C_p is sufficient for a profile analysis. It is, therefore, appropriate to base the determination on a uniform plasma with a uniform plasma density ω_{p_u} so that the average $\langle \omega_p(r) \rangle$ in the actual plasma cylinder corresponds to ω_{p_u} of the assumed uniform plasma.

It has been shown that a quasi-static approximation is appropriate in many cases.¹³ The test for the validity of the quasi-static approach in any specific case is based on an examination of Maxwell's Equations for the plasma region in the absence of a uniform magnetic field. Maxwell's Equations in the plasma region are:

Taking the
results

Letting

Now in the
of Laola

Expressi
of equat

In compa
the homo
quasi-st
small.
of the tw

$$\nabla \times \bar{B} = +j\omega\mu_o\epsilon_p\bar{E} \quad (2.70)$$

$$\nabla \times \bar{E} = -j\omega\bar{B} \quad (2.71)$$

$$\nabla \cdot \bar{B} = 0 \quad (2.72)$$

$$\nabla \cdot \bar{E} = 0 \quad (2.73)$$

Taking the curl of equation (2.70) and (2.71) and combining the results leads to the homogeneous Helmholtz Equation

$$(\nabla^2 + \epsilon_p\mu_o\omega^2)\bar{E} = 0 \quad (2.74)$$

Letting $k_e^2 = \omega^2\mu_o\epsilon_p$, equation (2.74) becomes

$$(\nabla^2 + k_e^2)\bar{E} = 0 \quad (2.75)$$

Now in the quasi-static approach the system may be solved by use of Laplace's Equation

$$\nabla^2\phi = 0 \quad (2.76)$$

Expressing equation (2.76) in terms of \bar{E} by taking the gradient of equation (2.76) leads to

$$\nabla^2\bar{E} = 0 \quad (2.77)$$

In comparing equation (2.77) for the quasi-static approximation to the homogeneous Helmholtz equation (2.75) it appears that the quasi-static approximation is justified if k_e^2 is negligibly small. Studying, for example, a one-dimensional application in x of the two equations, equation (2.75) becomes

The solut

Given the

can be de

$\left(\frac{\partial}{\partial x}\right)$

so that

Thus the

On the ot

is

where from

$$\frac{d^2}{dx^2} E(x) + k_e^2 E(x) = 0 \quad (2.78)$$

The solution to equation (2.78) is

$$E(x) = K_1 \cos(k_e x) + K_2 \sin(k_e x) \quad (2.79)$$

Given the boundary conditions E_0 and $(\frac{\partial E}{\partial x})_0$ at $x = 0$, K_1 and K_2 can be determined as follows:

$$K_1 = E_0 \quad (2.80)$$

$$(\frac{\partial E}{\partial x})_0 = (K_1 k_e \sin(k_e x) + K_2 k_e \cos k_e x)_0 \quad (2.81)$$

so that

$$K_2 = (\frac{\partial E}{\partial x})_0 (\frac{1}{k_e})$$

Thus the solution of equation (2.78) becomes

$$E(x) = E_0 \cos(k_e x) + (\frac{\partial E}{\partial x})_0 \frac{\sin(k_e x)}{k_e} \quad (2.82)$$

On the other hand, the solution to

$$\frac{\partial^2}{\partial x^2} E(x) = 0 \quad (2.83)$$

is

$$E(x) = K_1 x + K_2 \quad (2.84)$$

where from the boundary conditions E_0 and $(\frac{\partial E}{\partial x})_0$ at $x = 0$:

$$K_2 = E_0 \quad (2.85)$$

and

It follows

For values

equation

(2.87),

is in fact

(2.82)

Thus the

In terms

where d is

w is the

permeabil

and

$$\left(\frac{\partial E}{\partial x}\right)_0 = K_1 \quad (2.86)$$

It follows that

$$E(x) = E_0 + \left(\frac{\partial E}{\partial x}\right)_0 x \quad (2.87)$$

For values $|k_e x|^2 \ll 1$, the solution to the Helmholtz Equation, equation (2.82), approaches the solution to Laplace's Equation (2.87), because equation (2.87)

$$E(x) = E_0 + \left(\frac{\partial E}{\partial x}\right)_0 x$$

is in fact the first order Taylor series approximation of equation (2.82)

$$E(x) = E_0 \cos(k_e x) + \left(\frac{\partial E}{\partial x}\right)_0 \frac{\sin k_e x}{k_e}$$

Thus the condition for using a quasi-static approximation is:

$$|k_e x|^2 \ll 1 \quad (2.88)$$

In terms of the cylindrical plasma column this means that

$$|\epsilon_p \mu_0 \omega^2 d_c^2| \ll 1 \quad (2.89)$$

where d_c represents the characteristic dimension of the system; ω is the incident EM wave frequency, μ_0 is the free space permeability and

$$\epsilon_p = \epsilon_0 \left(1 - \frac{\omega_p^2}{\omega^2}\right)$$

if the

system

order c

m, and

Thus |e

that th

in Figu

in cyli

series

where n

indica

where a

Since f

excitin

dipolar

if the collision frequency ν is assumed zero. In the experimental system at hand, ω_p is in the order of 20×10^9 rad/sec, ω is in the order of 10×10^9 rad/sec, d_c may be taken as the radius $a = .007$ m, and ϵ_0 is the free space permittivity all taken in mks units. Thus $|\epsilon_0 (1 - \frac{\omega_p^2}{\omega^2})^{1/2} \mu_0 \omega^2 d_c^2|$ is in the order of 1×10^{-2} so that the quasi-static approximation is justified in this analysis.

Consider the geometry of a cylindrical plasma column shown in Figure 2.5.1. The solution of Laplace's Equation

$$\nabla^2 \phi = 0 \quad (2.90)$$

in cylindrical coordinates with z-independence can be expressed as series solution

$$\phi = (K_{1n} r^n + K_{2n} r^{-n}) e^{in\theta} \quad (2.91)$$

where n is an integer unequal zero. In regions 1 through 3 as indicated in Figure 2.5.1, the solutions become:

$$\phi_1 = A_n r^n \cos(n\theta) \quad (2.92)$$

$$\phi_2 = B_n r^n \cos(n\theta) + C_n r^{-n} \cos(n\theta) \quad (2.93)$$

$$\phi_3 = D_n r^{-n} \cos(n\theta) + r^n \cos(n\theta) \quad (2.94)$$

where an exciting field of the form $r^n \cos(n\theta)$ is considered. Since in the system at hand the free space wavelength of the exciting EM wave is much larger than the radial dimension, the dipolar contribution ($n = 1$) is most significant so that the



Fig. 2.5.1

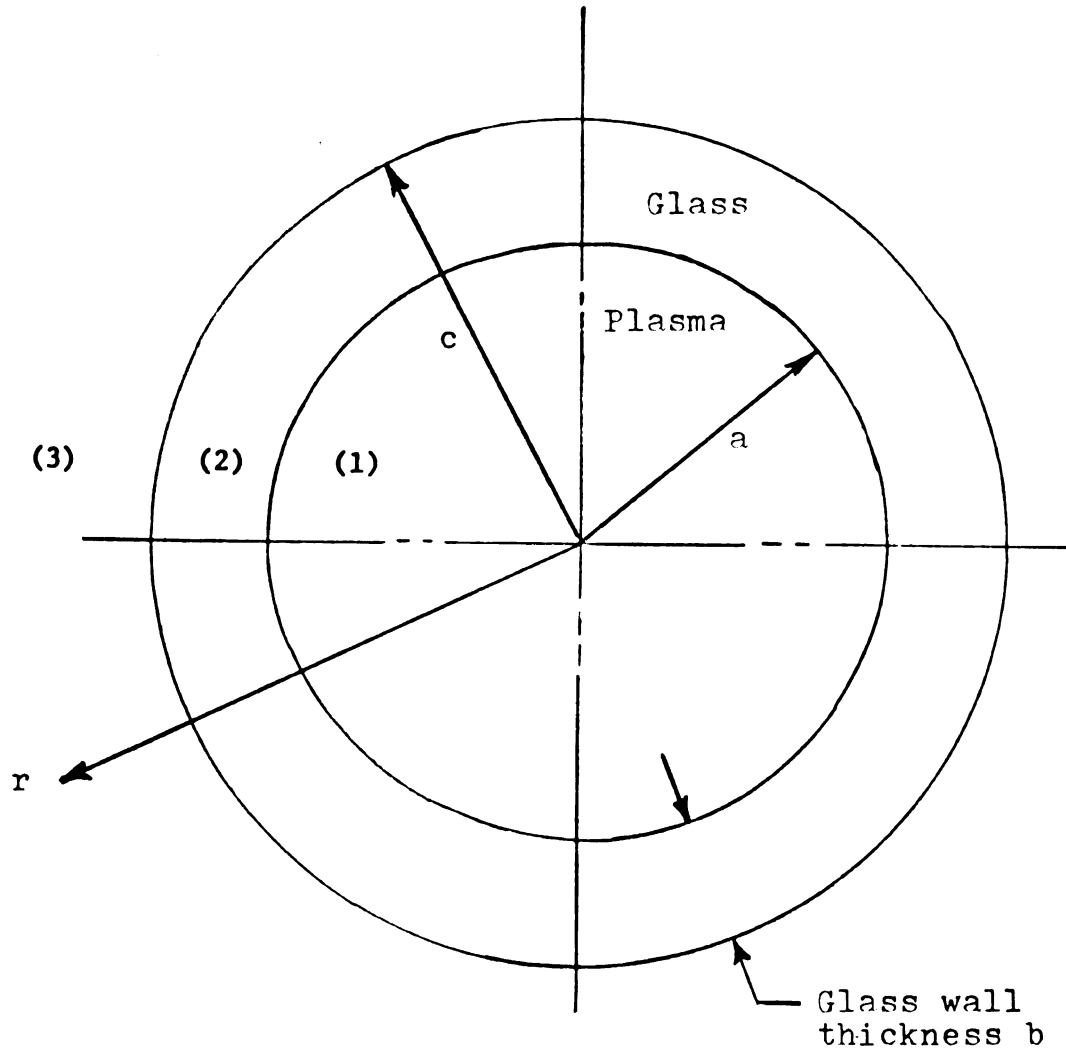


Fig. 2.5.1 Geometric arrangement of cylindrical plasma column contained in a cylindrical glass discharge tube of wall thickness b . The inside radius is a while the outside radius is c .

probl

(2.92)

Conti

elect

solut

becaus

resona

$$\begin{bmatrix} a \\ 0 \\ \epsilon \\ p \\ 0 \end{bmatrix}$$

The val

dipole

Rule, i

the det

to zero.

problem can be simplified significantly by rewriting equations (2.92) through (2.94) for $n = 1$:

$$\phi_1 = Ar \cos(\theta) \quad (2.95)$$

$$\phi_2 = Br \cos(\theta) + C \frac{1}{r} \cos(\theta) \quad (2.96)$$

$$\phi_3 = D \frac{1}{r} \cos n(\theta) + r \cos(\theta) \quad (2.97)$$

Continuity of the potential ϕ and the normal component of the electric displacement at the two boundaries $r = a$ and $r = c$ permit solution of the arbitrary constants. D is of primary interest because it is maximum at the value $\frac{\omega_p \mu}{\omega}$ at which the dipole resonance occurs.

The system of equations to be solved is:

$$\begin{bmatrix} a & -a & -1/a & 0 \\ 0 & c & 1/c & -1/c \\ \epsilon_p & -\epsilon_g & \frac{\epsilon_g}{a^2} & 0 \\ 0 & \epsilon_g & -\frac{\epsilon_g}{c^2} & \frac{\epsilon_o}{c^2} \end{bmatrix} \begin{bmatrix} A \\ B \\ C \\ D \end{bmatrix} = \begin{bmatrix} 0 \\ c \\ 0 \\ \epsilon_o \end{bmatrix} \quad (2.98)$$

The value of the arbitrary constant D must be maximum at the dipole resonance. Since D can be expressed in terms of Cramer's Rule, it is evident that its maximum value is obtained by setting the determinant of the coefficient matrix in equation (2.98) equal to zero,

a
0
 ϵ_p
0

Letting ϵ_{gr}

$$\epsilon_g = \epsilon_0 \epsilon_{gr}$$

plasma, ϵ_p

(1/a

Equation (2

the numeric

numerical v

permittivit

Since

This value

analysis.

for similar

$$\begin{vmatrix} a & -a & -1/a & 0 \\ 0 & c & 1/c & -1/c \\ \epsilon_p & -\epsilon_g & \epsilon_g/a^2 & 0 \\ 0 & \epsilon_g & -\epsilon_g/c^2 & \epsilon_o/c^2 \end{vmatrix} = 0 \quad (2.99)$$

Letting ϵ_{g_r} represent the relative permittivity of the glass, $\epsilon_g = \epsilon_o \epsilon_{g_r}$, and ϵ_{p_r} represent the relative permittivity of the plasma, $\epsilon_p = \epsilon_o \epsilon_{p_r}$, the expansion of equation (2.99) becomes

$$\begin{aligned} & (1/a^2 + 1/c^2)\epsilon_{g_r} (1 + \epsilon_{p_r}) + (1/a^2 - 1/c^2) \\ & (\epsilon_{p_r} - \epsilon_{g_r}^2) = 0 \end{aligned} \quad (2.100)$$

Equation (2.100) may be solved for ϵ_{p_r} which in turn is used in the numerical determination of ω_p^2/ω^2 as follows. Given numerical values for the radial dimensions and the relative permittivity of the glass, $\epsilon_{g_r} = 5$, $a = .007$ m, and $c = .008$ m:

$$\frac{\epsilon_p}{\epsilon_o} = -1.6$$

Since
$$\frac{\epsilon_p}{\epsilon_o} = 1 - \frac{\omega_p^2}{\omega^2} = 1 - C_p,$$

$$C_p = 2.6$$

This value for $C_p = \frac{\omega_p^2}{\omega^2}$ is used in the subsequent numerical analysis. The value for C_p agrees well with values obtained by Lee¹² for similar discharge columns.

3.1 Introdu

plasma

a frequ

the pla

sheath

and dis

electro

wall in

center.

towards

from th

electro

r in th

Here w
P

where n

is the

space p

CHAPTER 3

DETERMINATION OF ELECTRON DENSITY PROFILE IN CYLINDRICAL PLASMA COLUMN BASED ON THERMAL RESONANCE DATA IN THE SHEATH REGION

3.1 Introduction

When an electromagnetic wave is incident on a cylindrical plasma as shown in Figure 3.1.1, a dipole resonance is excited at a frequency ω depending on the average plasma frequency $\omega_p(r)$ in the plasma. Furthermore, thermal resonances may be excited in the sheath region near the wall at certain combinations of frequency and discharge current levels. These thermal resonances represent electroacoustic waves. The sheath region is the region near the wall in which the electron density is reduced from its value at the center. It is well known that the electron density decreases towards the wall along with an increase in negative potential away from the center.¹ The propagation constant associated with the electroacoustic wave, $k_p(r)$, is a function of the radial distance r in the plasma column and is given by:

$$k_p(r) = \frac{\omega}{v_o} \left(1 - \frac{\omega_p^2(r)}{\omega^2}\right)^{1/2} \quad (3.1)$$

Here $\omega_p(r)$ is the plasma frequency as a function of r defined as:

$$\omega_p^2(r) = \frac{e^2 n_e(r)}{m_e \epsilon_o} \quad (3.2)$$

where $n_e(r)$ is the static electron density as a function of r , e is the electron charge, m_e is the electron mass and ϵ_o is the free space permittivity; ω is the frequency of the incident electro-

11.11.11



11.11.11

11.11.11

11.11.11

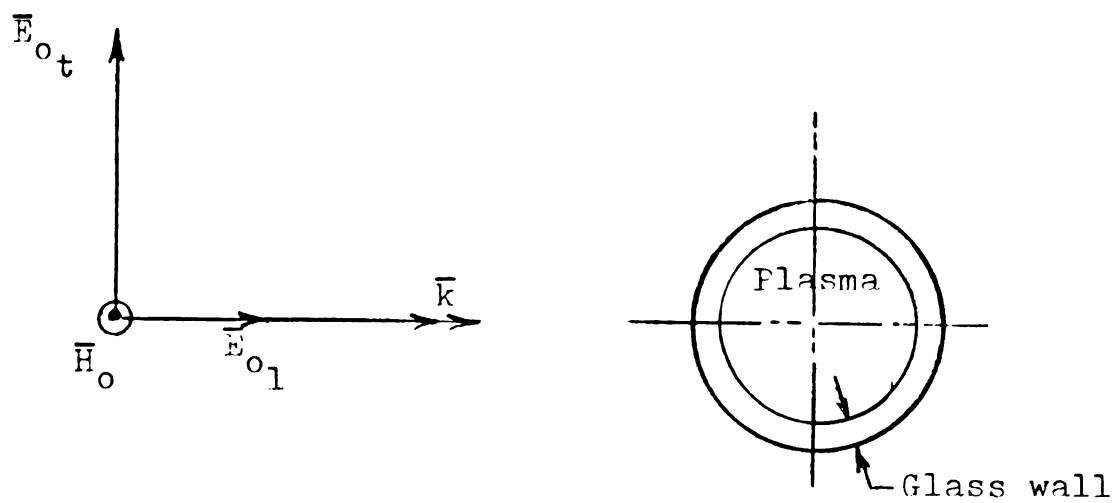


Fig. 3.1.1 A cylindrical plasma column illuminated by TM field as shown. \vec{E}_{0t} and \vec{E}_{0l} represent the transverse and longitudinal components of electric field respectively.

magne

sheat

$\omega_p(r)$

fact

the w

frequ

say r

and k

reson

frequ

satis

shown

$(m +$

elect

appea

data

the e

reson

of th

1.2 Exper

data

The e

reson

regio

use o

an op

magnetic field. Thermal resonances can exist, if in the so-called sheath region near the wall, the electron density, and therefore $\omega_p(r)$ is small enough to yield a real value for $k_p(r)$. Since in fact $n_e(r)$ and therefore $\omega_p(r)$ increase monotonically away from the wall as discussed in Chapter 2, there may exist for a given frequency ω of an incident EM wave a point in the plasma column, say $r = r_p$, at which $\omega = \omega_p(r)$, so that $k_p(r)$ is real for $r > r_p$ and $k_p(r)$ is imaginary for $r < r_p$. Under these conditions thermal resonances may exist between $r = r_p$ and the wall where $r = a$ for frequencies ω for which the total phase of such resonances satisfies the total phase condition derived in Chapter 2. It was shown there that the total phase for the m^{th} resonance must be $(m + 1/4)\pi$. If an appropriate functional description of the electron density profile can be formulated, the unknown parameters appearing in such a formulation can be determined from pertinent data regarding the thermal resonances. In the following section, the experimental procedure is presented for collecting thermal resonance data followed by a formulation of useful functional forms of the electron density profile $n_e(r)$ and their analysis.

3.2 Experimental Procedure

The experimental arrangement for obtaining plasma resonance data in a cylindrical plasma column is illustrated in Figure 3.2.1. The experimental technique is based on the excitation of the dipole resonance along with excitation of thermal resonances in the sheath region in a bounded cylindrical plasma column in glass tubing by use of an electroacoustic probe. The probe consists essentially of an open-ended coaxial line fed by an RF generator through a direc-



Cross-section
 of plasma
 cylinder
 inner radius
 $a = 7.0 \text{ cm}$

Fig. 3.2.1

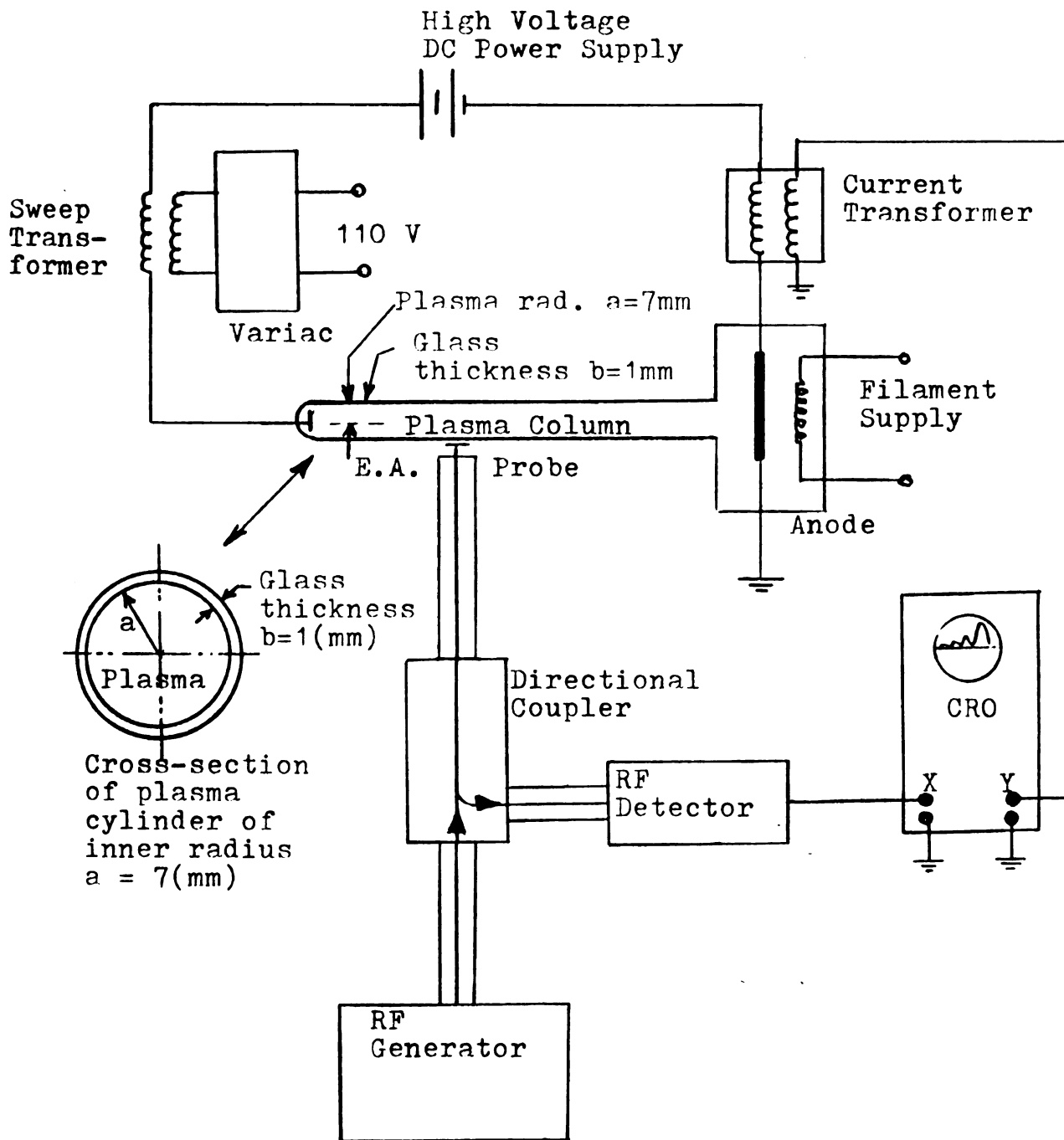


Fig. 3.2.1 Experimental arrangement for obtaining plasma resonance data in a cylindrical plasma column. An electroacoustic (E.A.) probe is used to excite the dipole and thermal resonances in the plasma column. The E.A. probe also picks up the scattered field whose peaks indicate the presence of resonances in the plasma.

tiona

the p

glass

the c

of th

neces

longi

Refle

are d

conne

densi

produ

catho

has a

The a

curre

Whene

the r

at an

observ

resona

The d

few ti

analy

tional coupler. In order to excite electroacoustic resonances in the plasma column, the open end of the probe is placed near the glass wall containing the plasma column. The inner conductor of the coaxial line is extended a small distance beyond the open end of the outer conductor so that the RF radiation contains the necessary longitudinal component of \bar{E} field to excite the desired longitudinal electroacoustic resonances in the sheath region. Reflections from the plasma cylinder are received by the probe and are directionally coupled to an RF detector whose output is connected to the vertical input of an oscilloscope. The electron density in the plasma column is adjusted by a discharge current produced by a high voltage source connected to the anode and cathode of the plasma tube as shown in Figure 3.2.1. The current has a low frequency (60 Hz) ac variation superposed on its dc level. The ac component produces a variation in the plasma discharge current and also produces the horizontal sweep on the oscilloscope. Whenever the current level passes through a value which satisfies the resonance condition

$$\int_{r_m}^a \frac{1}{V_0} (\omega^2 - \omega_p^2(r_m))^{1/2} dr = (m + 1/4)\pi$$

at an excitation frequency ω for the m^{th} resonance, a peak is observed in the reflected power level. In addition, the dipole resonance is observed as the strongest resonance in the column. The discharge current levels at the dipole resonance and the first few thermal resonances are observed. In the subsequent numerical analysis only the ratios of the discharge current levels are used.

shown

charg

frenu

3.3 Devel

the e

poten

where

assum

the v

imate

Since

neces

where

plasm

form

Poiss

funct

the s

Eight sets of data obtained in the experimentation are shown in Figures 3.2.2 through 3.2.5. Table 3.2.1 shows the discharge currents i_d , i_1 , i_2 , and i_3 along with the excitation frequency for each of the eight data sets.

3.3 Development of Functional Form for the Electron-Density Profile

If a Maxwellian electron density distribution is assumed, the electron density profile $n_e(r)$ is expressed in terms of the potential profile, $V(r)$, by equation (2.15) in section 2.2,

$$n_e(r) = n_o e^{\frac{eV(r)}{kT}} \quad (3.3)$$

where n_o is the electron density at $V(r) = 0$. It is reasonable to assume that in the plasma cylinder used in the experimentation, the voltage at $r = 0$, $V(0)$, is negligibly small and may be approximated as zero,

$$V(0) \doteq 0 \quad (3.4)$$

Since the actual value of $V(0)$ is not known, this approximation is necessary to obtain a solution for the problem. Thus

$$n_o = n_e(0) \quad (3.5)$$

where n_o represents the electron density at the center of the plasma column. The problem then is the formulation of a functional form for $V(r)$. This might best be arrived at by considering Poisson's Equation in the region of interest and choosing a functional relationship for $V(r)$ which at least in form agrees with the solution to Poisson's Equation. A complete solution of

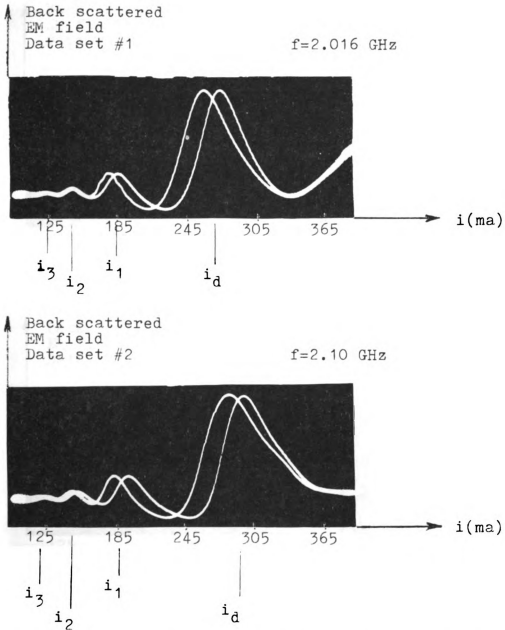


Fig. 3.2.2 Experimental results (data sets #1 and 2) for the back scattered EM field from a cylindrical plasma column as a function of discharge current. f is the frequency of the incident EM field. i_d , i_1 , i_2 , and i_3 are the discharge currents at which the dipole resonance and the first three thermal resonances respectively occur.

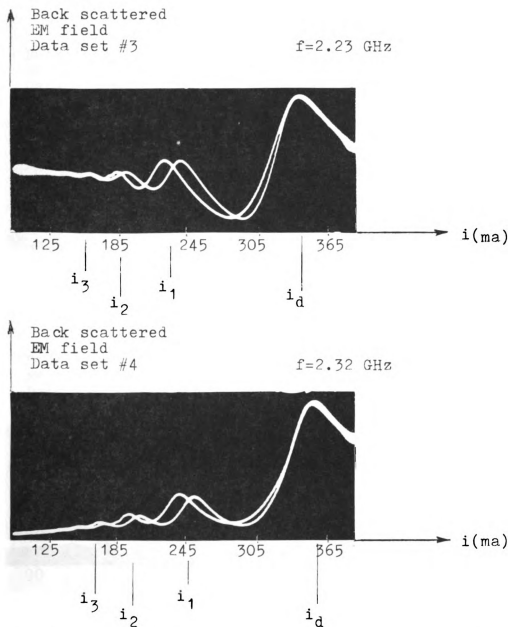


Fig. 3.2.3 Experimental results (data sets #3 and 4) for the back scattered EM field from a cylindrical plasma column as a function of discharge current. f is the frequency of the incident EM field. i_d , i_1 , i_2 , and i_3 are the discharge currents at which the dipole resonance and the first three thermal resonances respectively occur.

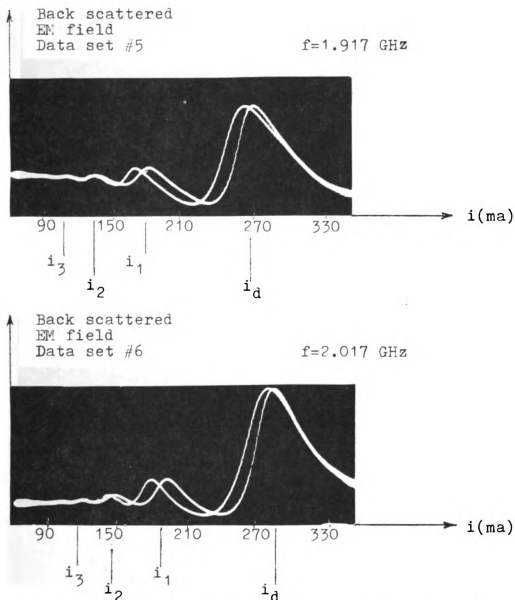


Fig. 3.2.4 Experimental results (data sets #5 and 6) for the back scattered EM field from a cylindrical plasma column as a function of discharge current. f is the frequency of the incident EM field. i_d , i_1 , i_2 , and i_3 are the discharge currents at which the dipole resonance and the first three thermal resonances respectively occur.

3.2.5

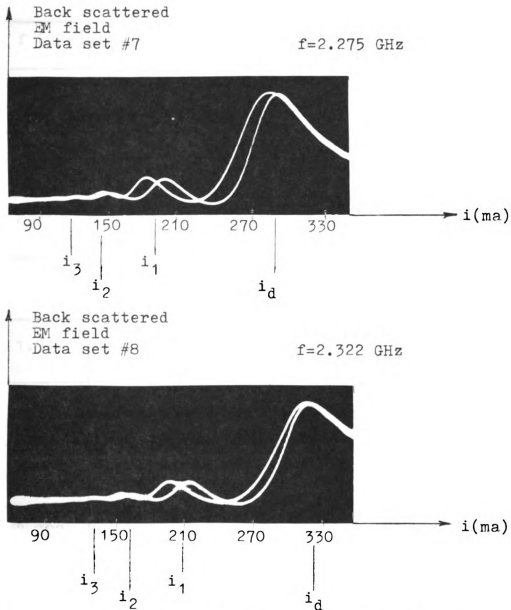


Fig. 3.2.5 Experimental results (data sets #7 and 8) for the back scattered EM field from a cylindrical plasma column as a function of discharge current. f is the frequency of the incident EM field. i_d , i_1 , i_2 , and i_3 are the discharge currents at which the dipole resonance and the first three thermal resonances respectively occur.

Data set #	f (GHz)	i_d (ma)	i_1 (ma)	i_2 (ma)	i_3 (ma)
1	2.016	270	185	150	125
2	2.100	290	190	150	120
3	2.230	340	235	185	160
4	2.320	355	245	200	175
5	1.917	270	180	135	110
6	2.017	285	190	150	120
7	2.275	290	195	150	120
8	2.322	320	210	160	135

Table 3.2.1 Experimental data set 1 through 8. Given are the frequency of the incident EM field and the discharge currents i_d , i_1 , i_2 and i_3 at which the dipole resonance and the first three thermal resonance respectively occur.

Pois

the

exp

Her

and

D(r

is

to:

int

In

app

so

This

zero

Poisson's Equation in the plasma column is not possible because the boundary condition for $V(0)$ is not known and the available experimental data are insufficient to determine it.

Poisson's Equation in cylindrical coordinates is given by:

$$\frac{d^2V(r)}{dr^2} + \frac{1}{r} \frac{dV(r)}{dr} = - \frac{\rho(r)}{\epsilon_0} \quad (3.6)$$

Here

$$\rho(r) = en_0 \left(1 - e^{\frac{eV(r)}{kT}} \right) \quad (3.7)$$

and T represents the electron temperature. This expression for $\rho(r)$ is based on the plasma sheath model in which the ion density is nearly constant throughout the plasma region due to ion drift towards the negative wall potential. Substituting equation (3.7) into equation (3.6) yields:

$$\frac{d^2V(r)}{dr^2} + \frac{1}{r} \frac{dV(r)}{dr} = - \frac{en_0}{\epsilon_0} \left(1 - e^{\frac{eV(r)}{kT}} \right) \quad (3.8)$$

In the region away from the wall where $eV(r) \ll kT$, the following approximation may be made:

$$\frac{d^2V(r)}{dr^2} + \frac{1}{r} \frac{dV(r)}{dr} = - \frac{en_0}{\epsilon_0} \left(1 - 1 - \frac{eV(r)}{kT} \right) \quad (3.9)$$

so that we have the following approximation of Poisson's Equation:

$$\frac{d^2V(r)}{dr^2} + \frac{1}{r} \frac{dV(r)}{dr} - \frac{e^2 n_0}{kT \epsilon_0} V(r) = 0 \quad (3.10)$$

This is a Bessel Equation and the solution is in the form of a zero order Bessel function with imaginary argument:

wh

and

use

$V(\rho)$

equ

app

pla

hol

$\frac{e^{\psi(\rho)}}{kT}$

form

$V(a)$

beco

Suff

$$V(r) = C_1 I_0(K_1 r) \quad (3.11)$$

where C_1 is an arbitrary constant and $K_1 = \frac{e^2 n_0}{kT \epsilon_0}$, containing n_0 and electron temperature as constants. If equation (3.11) were used throughout the plasma column, C_1 would represent the potential $V(0)$. As stated above, a value for $V(0)$ is not available so that equation (3.11) is merely used to show that a Bessel series is an appropriate form for the potential $V(r)$ near the center of the plasma column. The approximations made in equation (3.10) do not hold near the wall. The wall region is considered next.

In the sheath region near the wall, where the approximation $\frac{eV(r)}{kT} \ll 1$ does not hold, the following alternate approximate formulation may be used. Letting V_w be the wall potential, $V(a) = V_w$, Poisson's Equation may be written as follows:

$$\frac{d^2 V(r)}{dr^2} + \frac{1}{r} \frac{dV(r)}{dr} = - \frac{en_0}{\epsilon_0} \left(1 - e^{\frac{eV(r)}{kT}} - \frac{eV_w}{kT} \frac{eV_w}{e^{\frac{eV_w}{kT}}} \right) \quad (3.12)$$

Defining a new variable $v'(r) = V(r) - V_w$, equation (3.12)

becomes:

$$\frac{d^2 v'(r)}{dr^2} + \frac{1}{r} \frac{dv'(r)}{dr} = - \frac{en_0}{\epsilon_0} \left(1 - e^{\frac{eV_w}{kT}} \frac{e^{v'(r)}}{e^{\frac{eV_w}{kT}}} \right) \quad (3.13)$$

Sufficiently close to the wall, $v(r)$ is small enough to let

$$\frac{e^{v'(r)}}{e^{\frac{eV_w}{kT}}} \doteq 1 + \frac{ev'(r)}{kT} \quad . \quad \text{Therefore:}$$

This equa

$$\frac{d^2 v(r)}{dr^2} +$$

or

with K_2

electron

The solut

with imag

The fact

the form

available

of zero po

the expect

with a uni

(letting n

$z = \gamma r$):

$$\frac{d^2 v'(r)}{dr^2} + \frac{1}{r} \frac{dv'(r)}{dr} = - \frac{en_0}{\epsilon_0} \left(1 - e^{\frac{eV_w}{kT}} \left(1 + \frac{ev'(r)}{kT} \right) \right) \quad (3.14)$$

This equation becomes:

$$\frac{d^2 v'(r)}{dr^2} + \frac{1}{r} \frac{dv'(r)}{dr} - \frac{e^2 n_0}{kT \epsilon_0} e^{\left(\frac{eV_w}{kT}\right)} v(r) = - \frac{en_0}{\epsilon_0} \left(1 - e^{\frac{eV_w}{kT}} \right) \quad (3.15)$$

or

$$\frac{d^2 v'(r)}{dr^2} + \frac{1}{r} \frac{dv'(r)}{dr} - K_2 v'(r) = -K_3 \quad (3.16)$$

with K_2 and K_3 constants containing the wall potential, the electron density at $r = 0$, n_0 , and the electron temperature T . The solution is again in the form of a zero order Bessel function with imaginary argument in addition to a constant term:

$$v'(r) = C_2 I_0(K_2 r) + K_3/K_2 \quad (3.17)$$

The fact that the potential variation throughout the region is in the form of Bessel function $I_0(x)$ and recalling that the only available boundary condition for $V(r)$ is based on the assumption of zero potential at $r = 0$, a reasonable choice for curve fitting the expected potential distribution is a Bessel function $I_0(z)$ with a unity offset bringing it to zero at the origin as follows (letting $\eta(r) = \frac{eV(r)}{kT}$ for simplicity of notation and the argument $z = \gamma r$):

$$\eta(r) = 1 - I_0(\gamma r) \quad (3.18)$$

where γ
(3.18) i
negative
lends it
profile
correspo

n_0 and γ
the ti
for n_e (r
paraboli
drical r
does ind
(3.19) a

Letting
In the f
develope

where γ is an arbitrary constant to be determined. In equation (3.18) it is anticipated on phenomenological grounds that $V(r)$ is negative for all $0 < r < a$. The particular form of equation (3.18) lends itself well to the determination of the electron density profile from thermal resonance data as shown subsequently. The corresponding electron-density distribution $n_e(r)$ is given by:

$$n_e(r) = n_0 e^{(1 - I_0(\gamma r))} ; \quad (3.19)$$

n_0 and γ must now be determined from numerical analysis based on the thermal resonance data.

As an initial simplified approach, a parabolic approximation for $n_e(r)$ is used in the next section. This is done because the parabolic approximation for the electron density profile in cylindrical plasma columns has been used extensively in the past and it does indeed represent an approximation of $n_e(r)$ given in equation (3.19) as follows:

$$n_e(r) = n_0 e^{(1 - I_0(\gamma r))} \quad (3.20)$$

$$\doteq n_0 (1 + 1 - I_0(\gamma r))$$

$$\doteq n_0 (1 - (\frac{\gamma r}{2})^2) \quad (3.21)$$

Letting $(\frac{\gamma}{2})^2 = \alpha/a^2$ leads to the customarily used approximation:

$$n_e(r) = n_0 (1 - \alpha(\frac{r}{a})^2) \quad (3.22)$$

In the following section, a numerical solution technique is developed for n_0 and α as well as the electron temperature T , the

relative

resonance

R.

3.4 Determina

Plasma Co

In

appropria

The unkno

(1) $n_{O_1} =$

(2) $n_{O_2} =$

(3) $n_{O_1} =$

(4) $\langle n_e \rangle =$

(5) $r_1 =$

(6) $r_2 =$

(7) $\alpha = c$

(8) $T = e$

In

following

(1) $\frac{i_1}{i_d} = \frac{n}{n}$

(2) $\frac{i_2}{i_d} = \frac{n}{n}$

relative wall potential n_w , the turning points for the first m resonances r_m , and the ratio of peak to average electron density, R .

3.4 Determination of Electron Density Profile in a Cylindrical Warm Plasma Column Based on a Parabolic Approximation

In order to solve for the pertinent parameters, an appropriate system of simultaneous equations must be developed. The unknown quantities are

- (1) n_{o1} = center peak electron density for the first thermal resonance;
- (2) n_{o2} = center peak electron density for the second thermal resonance;
- (3) n_{o_d} = center peak electron density for the dipole resonance;
- (4) $\langle n_e(r) \rangle_{av}$ = average electron density for dipole resonance;
- (5) r_1 = value of r where $k_{p1}(r) = 0$ (critical turning point) for first thermal resonance;
- (6) r_2 = value of r where $k_{p2}(r) = 0$ (critical turning point) for second thermal resonance;
- (7) α = constant in $n_{e_m}(r) = n_{o_m} (1 - \alpha (\frac{r}{a})^2)$;
- (8) T = electron temperature.

In order to solve for these eight unknown parameters, the following eight independent simultaneous equations are necessary:

$$(1) \frac{i_1}{i_d} = \frac{n_{o1}}{n_{o_d}} \quad (3.23a)$$

$$(2) \frac{i_2}{i_d} = \frac{n_{o2}}{n_{o_d}} \quad (3.23b)$$

Equation

density

only rat

$$(3) \langle \omega_p^2 \rangle$$

Equation

resonance

section 2

constant

$$(4) \omega_{p1}(r)$$

$$(5) \omega_{p2}(r)$$

Equations

goes to z

$$(6) \int_{r_1}^a$$

$$(7) \int_{r_2}^a$$

Equations

the first

(2.68) in

$$(8) \langle n_{ed}(r) \rangle$$

Equations (3.23a) and (3.23b) are valid because the electron density is proportional to the plasma current level. In this study only ratios of currents are needed.

$$(3) \langle \omega_p^2(r) \rangle_{av} = \frac{e^2}{m_e \epsilon_0} \langle n_e(r) \rangle_{av} = C_p \omega^2 \quad (3.23c)$$

Equation (3.23c) is based on the relation between the dipole resonance frequency and the average electron density discussed in section 2.5 where a numerical value for the proportionality constant C_p was found.

$$(4) \omega_{p1}(r_1) = \omega \quad (3.23d)$$

$$(5) \omega_{p2}(r_2) = \omega \quad (3.23e)$$

Equations (3.23d) and (3.23e) are based on the fact that $k_p(r)$ goes to zero when $\omega_p(r) = \omega$.

$$(6) \int_{r_1}^a k_{p1}(r) dr = \frac{5}{4} \pi \quad (3.23f)$$

$$(7) \int_{r_2}^a k_{p2}(r) dr = \frac{9}{4} \pi \quad (3.23g)$$

Equations (3.23f) and (3.23g) represent the total phase spanned by the first two thermal resonances respectively based on equation (2.68) in section 2.4.

$$(8) \langle n_{ed}(r) \rangle_{av} = \frac{1}{\pi a^2} \int_0^a n_{od} (1 - \alpha \left(\frac{r}{a}\right)^2) 2\pi r dr \quad (3.23h)$$

In equat

average

ship hold

In

equations

a numeric

U

profile

the value

determine

experimen

electron

be develo

computer.

It

square of

occurs is

where C
p

The plasm

where $\omega < \omega_{pe}$

resonance.

In equation (3.23h), the peak electron density is related to the average electron density for the dipole resonance; this relationship holds equivalently for any thermal resonances.

In the following development, these eight simultaneous equations are discussed in greater detail and are used to develop a numerical solution for the desired parameters.

Using the parabolic approximation to the electron density profile

$$n_e(r) = n_o \left(1 - \alpha \left(\frac{r}{a}\right)^2\right), \quad (3.24)$$

the values of n_o and α must be determined. These values can be determined in terms of the thermal resonance data obtained in the experimentation. To obtain the desired numerical solution for the electron density profile, a system of simultaneous equations must be developed which lends itself to a numerical solution on the computer.

It was shown in section 2.5 that the average value of the square of the plasma frequency, $\langle \omega_{pd}^2(r) \rangle$ when the dipole resonance occurs is related to the resonance frequency ω by the relation:

$$\langle \omega_{pd}^2 \rangle = C_p \omega^2 \quad (3.25)$$

where C_p is a proportionality constant determined in section 2.5.

The plasma frequency ω_{pd} is by definition given by

$$\langle \omega_{pd}^2(r) \rangle = \frac{e^2}{m_e \epsilon_o} \langle n_{ed}(r) \rangle \quad (3.26)$$

where $\langle n_{ed}(r) \rangle$ is the average electron density at the dipole resonance. Letting n_{od} represent the peak density at the center

of the co

as follow

C

C

Therefore

The first

$(r = a)$ a

$k_{p_1}(r)$ go

Similarly,

zero at r_2

From basic

is given b

of the column at dipole resonance, $\langle n_{e_d}(r) \rangle$ can be related to ω as follows:

$$\langle n_{e_d}(r) \rangle = \frac{\langle \omega_{pd}^2(r) \rangle m_e \epsilon_0}{e^2}$$

$$\langle n_{e_d}(r) \rangle = \frac{m_e \epsilon_0 C_p \omega^2}{e^2}$$

$$\frac{C_p m_e \epsilon_0 \omega^2}{e^2} = \frac{n_{o_d}}{\pi a} \int_0^a (1 - \alpha (\frac{r}{a})^2) 2\pi r dr$$

$$\frac{C_p \epsilon_0 m_e \omega^2}{e^2 n_{o_d}} = (1 - \frac{\alpha}{2}) = \frac{\langle n_e(r) \rangle}{n_{o_d}} \quad (3.27)$$

Therefore

$$\omega^2 = \frac{(1 - \frac{\alpha}{2}) e^2 n_{o_d}}{C_p \epsilon_0 m_e} \quad (3.28)$$

The first thermal-resonance standing wave exists between the wall ($r = a$) and the point r_1 in the plasma, at which the phase term $k_{p1}(r)$ goes to zero:

$$k_{p1}(r_1) = 0 \quad (3.29)$$

Similarly, for the second resonance, the phase term $k_{p2}(r)$ goes to zero at r_2 :

$$k_{p2}(r_2) = 0 \quad (3.30)$$

From basic theory, the phase term $k_p(r)$ for an electroacoustic wave is given by

$$k_p(r) = \frac{\omega}{V_o} \left(1 - \frac{\omega_p^2(r)}{\omega^2}\right)^{1/2} \quad (3.31)$$

where V_o represents the thermal electron velocity $\sqrt{\frac{3kT}{m_e}}$.

Therefore

$$\frac{e^2 n_{o1} \left(1 - \alpha \left(\frac{r_1}{a}\right)^2\right)}{m_e \epsilon_o} = \omega^2 \quad (3.32)$$

and

$$\frac{e^2 n_{o2} \left(1 - \alpha \left(\frac{r_2}{a}\right)^2\right)}{m_e \epsilon_o} = \omega^2 \quad (3.33)$$

Combining equations (3.28) and (3.32) leads to

$$\left(1 - \alpha \left(\frac{r_1}{a}\right)^2\right) = \frac{1}{C_p} \left(1 - \frac{\alpha}{2}\right) \cdot \left(\frac{n_{od}}{n_{o1}}\right) \quad (3.34)$$

and combining equations (3.28) and (3.33) leads to

$$\left(1 - \alpha \left(\frac{r_2}{a}\right)^2\right) = \frac{1}{C_p} \left(1 - \alpha/2\right) \cdot \left(\frac{n_{od}}{n_{o2}}\right) \quad (3.35)$$

Since $\frac{n_{od}}{n_{o2}} = \frac{i_d}{i_1}$ and $\frac{n_{od}}{n_{o1}} = \frac{i_d}{i_2}$, where i_d , i_1 and i_2 are the currents at which the dipole and first two thermal resonances occur, equations (3.34) and (3.35) lead to the following expressions for r_1 and r_2 :

$$r_1 = a \left(\frac{1}{\alpha} - \frac{1}{C_p} \left(\frac{1}{\alpha} - \frac{1}{2}\right) \frac{i_d}{i_1}\right)^{1/2} \quad (3.36)$$

$$r_2 = a \left(\frac{1}{\alpha} - \frac{1}{C_p} \left(\frac{1}{\alpha} - \frac{1}{2}\right) \frac{i_d}{i_2}\right)^{1/2} \quad (3.37)$$

Since the total phase for the first two thermal resonances is $\frac{5}{4}\pi$ and $\frac{9}{4}\pi$ radius respectively, the following phase integrals result:

$$\int_{r_1}^a \frac{\omega}{v_o} \left(1 - \frac{\omega_p^2(r)}{\omega^2}\right)^{1/2} dr = (5/4)\pi \quad (3.38)$$

and

$$\int_{r_2}^a \frac{\omega}{v_o} \left(1 - \frac{\omega_p^2(r)}{\omega^2}\right)^{1/2} dr = (9/4)\pi \quad (3.39)$$

Since for the first two thermal resonances:

$$\omega_{p1}^2(r_1) = \frac{e^2 n_{o1} (1 - \alpha(\frac{r}{a})^2)}{m_e \epsilon_o},$$

and

$$\omega_{p2}^2(r_2) = \frac{e^2 n_{o2} (1 - (\frac{r}{a})^2)}{m_e \epsilon_o},$$

equation (3.38) and (3.39) become

$$\int_{r_1}^a \frac{\omega}{v_o} \left(1 - \frac{e^2 n_{o1} (1 - \alpha(\frac{r}{a})^2)}{\omega^2 m_e \epsilon_o}\right)^{1/2} dr = (5/4)\pi \quad (3.40)$$

and

$$\int_{r_2}^a \frac{\omega}{v_o} \left(1 - \frac{e^2 n_{o2} (1 - \alpha(\frac{r}{a})^2)}{\omega^2 m_e \epsilon_o}\right)^{1/2} dr = (9/4)\pi \quad (3.41)$$

Combining equations (3.40) and (3.41), and expressing n_{o1} and n_{o2} in terms of n_{od} from equation (3.28), recalling that $\frac{n_{o1}}{n_{od}} = \frac{i_1}{i_d}$ and

$\frac{n_{o2}}{n_{od}} = \frac{i_2}{i_d}$, the following equation results:

$$9/4 \int_1^{r_1/a} \left(1 - \left(\frac{i_1}{i_d}\right) \left(\frac{C_p}{(1 - .5\alpha)}\right) (1 - \alpha\left(\frac{r}{a}\right)^2)^{1/2} d\left(\frac{r}{a}\right) \right. \\ \left. - \int_1^{r_2/a} \left(1 - \left(\frac{i_2}{i_d}\right) \left(\frac{C_p}{(1 - .5\alpha)}\right) (1 - \alpha\left(\frac{r}{a}\right)^2)^{1/2} d\left(\frac{r}{a}\right) = 0 \right. \right. \quad (3.42)$$

Equation (3.42) contains the three unknowns α , r_1/a and r_2/a ; r_2/a can be expressed in terms of r_1/a based on equations (3.36) and (3.37) as follows:

$$\Delta\left(\frac{r}{a}\right) = \frac{r_2}{a} - \frac{r_1}{a} = \left(\frac{1}{\alpha} - \frac{1}{C_p} \left(\frac{1}{\alpha} - \frac{1}{2}\right) \cdot \frac{i_d}{i_2}\right)^{1/2} \\ - \left(\frac{1}{\alpha} - \frac{1}{C_p} \left(\frac{1}{\alpha} - \frac{1}{2}\right) \cdot \frac{i_d}{i_1}\right)^{1/2} \quad (3.43)$$

Therefore equation (3.42) becomes:

$$9/4 \int_1^{r_1/a} \left(1 - \left(\frac{i_1}{i_d}\right) \left(\frac{C_p}{(1 - .5\alpha)}\right) (1 - \alpha\left(\frac{r}{a}\right)^2)^{1/2} d\left(\frac{r}{a}\right) \right. \\ \left. - \int_1^{\frac{r_1}{a} + \Delta(r/a)} \left(1 - \left(\frac{i_2}{i_d}\right) \left(\frac{C_p}{(1 - .5\alpha)}\right) (1 - \alpha\left(\frac{r}{a}\right)^2)^{1/2} d\left(\frac{r}{a}\right) = 0 \right. \right. \quad (3.44)$$

Solving equation (3.36) for α in terms of r_1/a yields:

$$\alpha = \frac{(1 - \frac{i_d}{C_p i_1})}{(\frac{r_1}{a})^2 - \frac{i_d}{2i_1 C_p}} \quad (3.45)$$

Equations (3.44) and (3.45) represent two simultaneous equations in two unknowns which may be solved numerically. After r_1/a and α are available, equation (3.40) can be solved for V_o which in turn gives the electron temperature T from $V_o = \sqrt{\frac{3kT}{m_e}}$,

$$V_o = \frac{4\omega}{5\pi} \int_{r_1/a}^1 (1 - (\frac{i_1}{i_d}) (\frac{C_p}{1 - .5\alpha}) (1 - (\frac{r}{a})^2))^{1/2} d(\frac{r}{a}) \quad (3.46)$$

and:

$$T = \frac{m_e V_o^2}{3k} \quad (3.47)$$

The ratio of peak to average electron density $n_o / \langle n_e(r) \rangle$ is obtained from equation (3.27) as

$$R = \frac{n_o}{\langle n_e(r) \rangle} = \frac{1}{(1 - \alpha/2)}$$

The equations developed in this section for use in the computer analysis are summarized here in the form in which they are incorporated into the computer program for the numerical analysis.

$$(1) \quad \frac{9}{4} \int_1^{r_1/a} (1 - \frac{i_1}{i_d} \frac{C_p}{1 - \alpha/2} (1 - \alpha(\frac{r}{a})^2))^{1/2} d(\frac{r}{a}) - \int_1^{r_1/a} + \Delta(\frac{r}{a}) (1 - \frac{i_2}{i_d} \frac{C_p}{1 - \alpha/2} (1 - \alpha(\frac{r}{a})^2))^{1/2} d(\frac{r}{a}) = 0 \quad (3.48a)$$

$$(2) \quad \alpha = \frac{1 - \frac{i_d}{i_1 C_p}}{\left(\frac{r_1}{a}\right)^2 - \frac{i_d}{2i_1 C_p}} \quad (3.48b)$$

$$(3) \quad \Delta(r/a) = \left(\frac{1}{\alpha} - \frac{1}{C_p} \left(\frac{1}{\alpha} - \frac{1}{2}\right) \frac{i_d}{i_2}\right)^{1/2} \\ - \left(\frac{1}{\alpha} - \frac{1}{C_p} \left(\frac{1}{\alpha} - \frac{1}{2}\right) \frac{i_d}{i_1}\right)^{1/2} \quad (3.48c)$$

$$(4) \quad R = \frac{n_o}{\langle n_e(r) \rangle} = \left(\frac{1}{1 - \frac{\alpha}{2}}\right)$$

$$(5) \quad v_o = \frac{4\omega}{5\pi} \int_{r_1/a}^1 \left(1 - \frac{i_1}{i_d} \frac{C_p}{1 - \alpha/2} \left(1 - \alpha\left(\frac{r}{a}\right)^2\right)\right)^{1/2} d\left(\frac{r}{a}\right) \quad (3.48d)$$

and:

$$(6) \quad T = \frac{m_e v_o^2}{3k} \quad (3.48e)$$

The experimental procedure also yields values for i_3 , the discharge current level at which the third resonance occurs. These data are not as reliable as those for i_d , i_1 , and i_2 because the third thermal resonance is somewhat weak. It is nevertheless possible to check the results obtained from the numerical analysis of equations (3.48) by performing a similar analysis based on the use of the first and third resonance data. The corresponding equations differ from equations (3.48) only in that the subscript (2) must be replaced by the subscript (3) as shown.

$$(1) \quad 13/4 \int_1^{r_1/a} \left(1 - \frac{i_1}{i_d} \frac{C_p}{1 - \alpha/2} (1 - \alpha(\frac{r}{a})^2)\right)^{1/2} d(\frac{r}{a})$$

(3.49a)

$$- \int_1^{\frac{r_1}{a} + \Delta(\frac{r}{a})} \left(1 - \frac{i_3}{i_d} \frac{C_p}{1 - \alpha/2} (1 - \alpha(\frac{r}{a})^2)\right)^{1/2} d(\frac{r}{a}) = 0$$

$$(2) \quad \alpha = \frac{1 - \frac{i_d}{i_1 C_p}}{\left(\frac{r_1}{a}\right)^2 - \frac{i_d}{2i_1 C_p}} \quad (3.49b)$$

$$(3) \quad \Delta(r/a) = \left(\frac{1}{\alpha} - \frac{1}{C_p} \left(\frac{1}{\alpha} - \frac{1}{2}\right) \frac{i_d}{i_3}\right)^{1/2}$$

$$- \left(\frac{1}{\alpha} - \frac{1}{C_p} \left(\frac{1}{\alpha} - \frac{1}{2}\right) \frac{i_d}{i_1}\right)^{1/2} \quad (3.49c)$$

$$(4) \quad \frac{n_o}{\langle n_e(r) \rangle} = \left(\frac{1}{1 - \frac{\alpha}{2}}\right)$$

$$(5) \quad v_o = \frac{4\omega}{5\pi} \int_{r_1/a}^1 \left(1 - \frac{i_1}{i_d} \frac{C_p}{1 - \alpha/2} (1 - \alpha(\frac{r}{a})^2)\right)^{1/2} d(\frac{r}{a}) \quad (3.49d)$$

and:

$$(6) \quad T = \frac{m v_o^2}{3k} \quad (3.49e)$$

The numerical results obtained from the computer analysis of these sets of simultaneous equations, (3.48) and (3.49), are presented and discussed in Chapter 4.

3.5 Determination of the Electron Density in a Warm Plasma Cylinder

Assuming Potential Distribution of the Form $(1 - I_0(\gamma r))$

The assumption of the functional form:

$$\eta(r) = (1 - I_0(\gamma r)) \quad (3.18)$$

where $\eta(r) = eV(r)/kT$ is based on the solutions of Poisson's Equation in different regions of the cylinder in section 3.3. It was seen there that this solution cannot represent an exact solution for the potential distribution but it is of the correct form especially in the sheath region where an offset Bessel function was obtained as a solution. It furthermore satisfies the approximate condition that $V(0)$ and therefore $\eta(0) = 0$.

Although this approximation makes the necessary numerical analysis somewhat complex, it is still sufficiently manageable to be useful as a diagnostic technique which is the ultimate goal of this thesis.

The known quantities from the experimental work with the electroacoustic probe are:

ω = the frequency of the incident radiation:

i_d = the current level at which the dipole resonance is observed;

i_1 = the current level at which the first thermal resonance is observed;

i_2 = the current at which the second thermal resonance occurs.

The unknown quantities are:

(1) n_{01} = the peak electron density at the center of the plasma column for the first thermal resonance;

- (2) n_{o2} = the peak electron density at the center of the plasma column for the second thermal resonance;
- (3) n_{o_d} = the peak electron density at the dipole resonance;
- (4) $\langle n_e(r)_d \rangle$ = the average electron density at the dipole resonance;
- (5) r_1 = the critical phase point ($k_{p1}(r_1) = 0$) for the first thermal resonance;
- (6) r_2 = the critical phase point ($k_{p2}(r_2) = 0$) for the second thermal resonance;
- (7) γ = the constant appearing in the Bessel function approximation $(1 - I_0(\gamma r))$ for the potential profile;
- (8) T = electron temperature.

Since eight unknowns appear in the analysis, eight independent equations are needed; these equations are:

$$(1) \quad \frac{i_1}{i_d} = \frac{n_{o1}}{n_{o_d}} \quad (3.50a)$$

$$(2) \quad \frac{i_2}{i_d} = \frac{n_{o2}}{n_{o_d}} \quad (3.50b)$$

Equations (3.50a) and (3.50b) are based on the fact that the peak electron density in the plasma is proportional to the current level. These equations also show that only the ratio of the currents are used for the analysis.

$$(3) \quad \langle \omega_p^2(r) \rangle_{av} = \frac{e^2}{m_e \epsilon_0} \langle n_e(r)_d \rangle = C_p \omega^2 \quad (3.50c)$$

Equation (3.50c) states that at the dipole resonance at a given current level, and thus electron density level n_{o_d} , the average

of the square of the plasma frequency is proportional to the angular frequency ω^2 of the incident radiation. (The proportionality constant C_p was found in section 2.5.)

$$(4) \quad \omega_{p1}(r_1) = \omega \quad (3.50d)$$

$$(5) \quad \omega_{p2}(r_2) = \omega \quad (3.50e)$$

Equations (3.50d) and (3.50e) relate the critical points r_1 and r_2 for the first and second thermal resonances respectively to the incident radiation frequency ω ; here: $\omega_{p1}^2(r_1) = \frac{e^2}{m_e \epsilon_0} n_{o1} \exp(1 - I_o(\gamma r_1))$; and: $\omega_p^2(r_2) = \frac{e^2}{m_e \epsilon_0} n_{o2} \exp(1 - I_o(\gamma r_2))$.

$$(6) \quad \int_{r_1}^a k_{p1}(r) dr = (5/4)\pi \quad (3.50f)$$

$$(7) \quad \int_{r_2}^a k_{p2}(r) dr = (9/4)\pi \quad (3.50g)$$

Equations (3.50f) and (3.50g) are based on the fact that the total phase of the second thermal resonances span $(5/4)\pi$ and $(9/4)\pi$ respectively based on equation (2.68) in section 2.4. Here:

$$k_{p1}(r) = \frac{\omega}{v_o} \left(1 - \frac{\omega_{p1}^2(r)}{\omega^2}\right)^{1/2}$$

and

$$k_{p2}(r) = \frac{\omega}{v_o} \left(1 - \frac{\omega_{p2}^2(r)}{\omega^2}\right)^{1/2} .$$

$$(8) \quad \langle n_{e_d}(r) \rangle_{av} = \frac{1}{\pi a^2} \int_0^a n_{o_d} \exp(1 - I_0(\gamma r)) 2\pi r \, dr \quad (3.50h)$$

Equation (3.50h) relates the average electron density $\langle n_{e_d}(r) \rangle$ to the center peak electron density n_{o_d} at the dipole resonance. The ratio of peak to average electron density remains the same as the current level is changed so that equation (3.50h) may be formulated in terms of one of the thermal resonances. Equations (3.50) are now used to develop a system of simultaneous equations suitable for numerical analysis on the computer.

Since in this section the assumed functional relationship for the relative potential distribution as a function of r ,

$\eta(r) = \frac{eV(r)}{kT}$, is given by

$$\eta(r) = 1 - I_0(\gamma r), \quad (3.51)$$

the constant γ appearing in the Bessel function is the primary parameter of interest. The relative potential distribution appears in the Maxwellian electron density distribution as follows

$$n_e(r) = n_o \exp(1 - I_0(\gamma r)). \quad (3.52)$$

Here again n_o represents the electron density at the center of the cylindrical plasma column where the potential $V(o)$ is assumed zero and therefore the relative potential $\eta(0)$ is zero as a boundary condition. Since $I_0(0) = 1$, equation (3.52) shows that $n_e(o)$ is indeed n_o at the center of the column ($r = 0$). The formulation of $n_e(r)$ in equation (3.52) introduces n_o as an additional parameter that must be determined for any given electron density profile and

corresponding current level.

The relationship fundamental to this analysis is based on the phenomenological argument, that the total phases of the electroacoustic thermal resonances in the sheath region are separated by π radians and that furthermore the fundamental thermal resonance spans a total of one and one quarter π radians between the wall and the critical turning point r_1 where the propagation constant goes to zero. This argument is based on equation (2.68) in section 2.4. Now

$$\lim_{\substack{r \rightarrow r_1 \\ r > r_1}} \left[k_p(r) \right] = 0 \quad (3.53)$$

For the m^{th} resonance, the total phase can therefore be written as follows:

$$\int_{r_m}^a k_{p_m}(r) dr = (m + 1/4)\pi \quad (3.54)$$

Since:

$$k_{p_m}(r) = \frac{\omega}{V_o} \left(1 - \frac{\omega_{p_m}^2(r)}{\omega^2} \right)^{1/2}, \quad (3.55)$$

Equation (3.54) becomes

$$\int_{r_m}^a \left(1 - \frac{\omega_{p_m}^2(r)}{\omega^2} \right)^{1/2} dr = \frac{(m + 1/4)\pi V_o}{\omega} \quad (3.56)$$

From the definition of the plasma frequency $\omega_p(r)$

$$\omega_{p_m}^2(r) = \frac{e^2 n_e(r)}{m_e \epsilon_0} \quad (3.57)$$

and since from equation (3.52) repeated here for reference

$$n_e(r) = n_o \exp(1 - I_o(\gamma r)), \quad (3.58)$$

the total phase equation for the m^{th} electroacoustic thermal resonance becomes

$$\int_{r_m}^a \left(1 - \left(\frac{e^2 n_{o_m} \exp(1 - I_o(\gamma r))}{\omega^2 m_e \epsilon_0}\right)^{1/2} dr\right) = \frac{(m + 1/4)\pi V_o}{\omega} \quad (3.59)$$

Here the electron density at the center, $n_{e_m}(0) = n_{o_m}$ for the m^{th} thermal resonance, depends on the discharge current level maintained in the plasma column; the current level resulting in n_{o_m} is i_m which is available from the experimental data. There exists a direct proportionality between the current level i_m and the electron density n_{o_m} because the electron drift velocity may be considered constant in a cylindrical plasma discharge column.

The relationship between the current i_m and the corresponding dc electron density n_{o_m} is established experimentally through the dipole resonance frequency ω which is related to the corresponding plasma frequency $\omega_{p_d}(r)$ by

$$\langle \omega_{p_d}^2(r) \rangle = C_p \omega^2 \quad (3.60)$$

Here C_p is a proportionality constant; $\omega_{p_d}(r)$ is the plasma frequency as a function of r at which a dipole resonance is observed when the incident radiation frequency is ω ; $\langle \omega_{p_d}^2(r) \rangle$ represents the average of the square of the dipole resonance plasma frequency. The relationship between ω and $\langle \omega_{p_d}(r) \rangle$ in equation (3.60) was established in section 2.5, where a numerical value for C_p was obtained. Since

$$\omega_{p_d}^2(r) = \frac{e^2 n_{e_d}(r)}{m_e \epsilon_0} \quad (3.61)$$

it follows that

$$\langle n_{e_d}(r) \rangle = C_p \frac{\omega^2 m_e \epsilon_0}{e^2} \quad (3.62)$$

Similarly, because of the direct proportionality between the current levels and the electron densities, equations for $\langle n_{e_1}(r) \rangle$ and $\langle n_{e_2}(r) \rangle$ can be written as follows

$$\langle n_{e_1}(r) \rangle = \left(\frac{C_p \omega^2 m_e \epsilon_0}{e^2} \right) \left(\frac{i_1}{i_d} \right) \quad (3.63)$$

and

$$\langle n_{e_2}(r) \rangle = \left(\frac{C_p \omega^2 m_e \epsilon_0}{e^2} \right) \left(\frac{i_2}{i_d} \right) \quad (3.64)$$

and in general for the m^{th} resonance

$$\langle n_{e_m}(r) \rangle = \left(\frac{C_p \omega^2 m_e \epsilon_0}{e^2} \right) \left(\frac{i_m}{i_d} \right) \quad (3.65)$$

In order to work with equation (3.59), it is necessary to obtain an expression for n_{0m} ; this can be accomplished in terms of equation (3.65) by formulating $\langle n_{e_m}(r) \rangle$ in terms of n_{0m} as follows

$$\langle n_{e_m}(r) \rangle = \frac{1}{\pi a^2} \int_0^a n_{0m} \exp(1 - I_0(\gamma r)) 2\pi r \, dr \quad (3.66)$$

Defining R to be the ratio of the peak electron density n_{0m} to the average electron density $\langle n_e(r) \rangle$,

$$R = \frac{n_{0m}}{\langle n_e(r) \rangle} = \frac{\pi a^2}{\int_0^a \exp(1 - I_0(\gamma r)) 2\pi r \, dr} \quad (3.67)$$

n_{0m} can be expressed in terms of the frequency of the incident radiation ω and current ratios as follows:

$$n_{0m} = \left(\frac{C \omega^2 m_e \epsilon_0}{e^2} \right) (R) \left(\frac{i_m}{i_d} \right) \quad (3.68)$$

The phase integral in equation (3.59) furthermore contains r_m and V_0 as unknown parameters. There exists no independent relationship from which r_m and V_0 can be determined but it is possible to express r_m in terms of r_{m-1} , for example r_2 in terms of r_1 . The condition leading to a functional relationship between r_m and r_{m-1} is the following:

$$k_m(r_m) = 0 \quad (3.69)$$

where again r_m is the critical turning point for the m^{th} resonance.

Therefore:

$$\frac{\omega}{V_o} \left(1 - \frac{\omega_{p_m}^2(r_m)}{\omega^2} \right) = 0,$$

so that

$$\omega_{p_m}^2(r_m) = \omega^2 \quad (3.70)$$

Since

$$\omega_{p_m}^2(r_m) = \frac{e^2 n_{o_m} \exp(1 - I_o(\gamma r_m))}{m_e \epsilon_o}, \quad (3.71)$$

it follows that

$$\exp(1 - I_o(\gamma r_m)) = \frac{m_e \epsilon_o \omega^2}{e^2 n_{o_m}} \quad (3.72)$$

Defining

$$A_m = \frac{e^2 n_{o_m}}{\omega_m^2 \epsilon_o},$$

$$\exp(1 - I_o(\gamma r_m)) = \frac{1}{A_m} \quad (3.73)$$

The value of A_m can be determined numerically based on the value of n_{o_m} obtained through the solution of equations (3.65) through (3.68). Since equation (3.73) contains both r_m and the parameter of final interest, γ , r_m cannot be determined directly from equation (3.73). However it is possible to determine r_n in terms of r_m (n integer $\neq m$) by simultaneous solution of

$$(1) \quad \exp(1 - I_o(\gamma r_n)) = 1/A_n \quad (3.74)$$

and

$$(2) \quad \exp(1 - I_0(\gamma r_m)) = 1/A_m \quad (3.75)$$

Simultaneous solution of equations (3.74) and (3.75) leads to a value for $\Delta r_{m,n}$ defined by

$$\Delta r_{m,n} = r_n - r_m \quad (3.76)$$

In terms of r_m and $\Delta r_{m,n}$ it is possible to write two simultaneous phase integral equations in the form of equation (3.59) as follows:

$$\int_{r_m}^a (1 - A_m \exp(1 - I_0(\gamma r)))^{1/2} dr = \frac{(m + 1/4)\pi V_0}{\omega} \quad (3.77)$$

and

$$\int_{r_m + \Delta r_{m,n}}^a (1 - A_n \exp(1 - I_0(\gamma r)))^{1/2} dr = \frac{(n + 1/4)\pi V_0}{\omega} \quad (3.78)$$

Forming the ratio of equations (3.77) and (3.78) yields

$$\frac{\int_{r_m}^a (1 - A_m \exp(1 - I_0(\gamma r)))^{1/2} dr}{\int_{r_m + \Delta r_{m,n}}^a (1 - A_n \exp(1 - I_0(\gamma r)))^{1/2} dr} = \frac{(m + 1/4)}{(n + 1/4)} \quad (3.79)$$

For any combination of m and n , $m \neq n$ for which resonance data are available, equation (3.79) still contains two unknown parameters, r_m and γ . If equation (3.79) is combined with equation (3.73),

repeated here for reference:

$$\exp(1 - I_0(\gamma r_m)) = \frac{1}{A_m}, \quad (3.80)$$

equations (3.79) and (3.80) may be solved simultaneously for r_m and γ .

After obtaining values for r_m and γ , V_o can be calculated from equation (3.77) as follows:

$$V_o = \frac{\omega}{(m + 1/4)} \int_{r_m}^a (1 - A_m \exp(1 - I_0(\gamma r)))^{1/2} dr \quad (3.81)$$

Since:

$$V_o = \sqrt{\frac{3kT}{m_e}}, \quad (3.82)$$

the electron temperature T can be calculated as:

$$T = \frac{V_o^2 m_e}{3k} \quad (3.83)$$

where k is Boltzmann's constant.

In the numerical analysis at hand, the first two electro-acoustic thermal resonances are used so that $m = 1$ and $n = 2$. The equations used in the subsequent computer analysis formulation, written in terms of the first two thermal resonances, are summarized here in the form used in the numerical analysis:

$$(1) \quad \frac{\int_{r_1}^a (1 - A_1 \exp(1 - I_0(\gamma r)))^{1/2} dr}{\int_{r_1 + \Delta r_{1,2}}^a (1 - \Lambda_2 \exp(1 - I_0(\gamma r)))^{1/2} dr} = \frac{(1 + 1/4)}{(2 + 1/4)} \quad (3.84a)$$

$$(2) \quad \exp(1 - I_0(\gamma r_1)) = \frac{1}{A_1} \quad (3.84b)$$

$$(3) \quad \exp(1 - I_0(\gamma r_2)) = \frac{1}{\Lambda_2} \quad (3.84c)$$

$$(4) \quad A_1 = \frac{e^2 n_{01}}{\omega^2 m_e \epsilon_0} \quad (3.84d)$$

$$(5) \quad \Lambda_2 = \frac{e^2 n_{02}}{\omega^2 m_e \epsilon_0} \quad (3.84e)$$

$$(6) \quad n_{01} = \left(\frac{C \omega^2 m_e \epsilon_0}{p e^2} \right) (R) \left(\frac{i_1}{i_d} \right) \quad (3.84f)$$

$$(7) \quad n_{02} = \left(\frac{C \omega^2 m_e \epsilon_0}{p e^2} \right) (R) \left(\frac{i_2}{i_d} \right) \quad (3.84g)$$

$$(8) \quad R = \frac{\pi a^2}{\int_0^a \exp(1 - I_0(\gamma r)) 2\pi r dr} \quad (3.84h)$$

$$(9) \quad v_o = \frac{\omega}{(1 + 1/4)\pi} \int_{r_1}^a (1 - A_1 \exp(1 - I_o(\gamma r)))^{1/2} dr \quad (3.84i)$$

and

$$(10) \quad T = \frac{v_o^2 m_e}{3k} \quad (3.84j)$$

A numerical analysis based on these equations is also performed using a combination of the first and third resonance data. The results from this analysis are used as a check on the results obtained from the use of the first two resonances. In order to use equations (3.84) for the first and third thermal resonance combination, it is only necessary to replace the subscript (2) whenever it appears by the subscript (3). The corresponding set of equations are:

$$(1) \quad \frac{\int_{r_1}^a (1 - A_1 \exp(1 - I_o(\gamma r)))^{1/2} dr}{\int_{r_1 + \Delta r_{1,3}}^a (1 - A_3 \exp(1 - I_o(\gamma r)))^{1/2} dr} = \frac{(1 + 1/4)}{(3 + 1/4)} \quad (3.85a)$$

$$(2) \quad \exp(1 - I_o(\gamma r_1)) = \frac{1}{A_1} \quad (3.85b)$$

$$(3) \quad \exp(1 - I_o(\gamma r_3)) = \frac{1}{A_3} \quad (3.85c)$$

$$(4) \quad A_1 = \frac{e^2 n_{o1}}{\omega^2 m_e \epsilon_o} \quad (3.85d)$$

$$(5) \quad A_3 = \frac{e^2 n_{o3}}{\omega^2 m_e \epsilon_o} \quad (3.85e)$$

$$(6) \quad n_{o1} = \left(\frac{C_p \omega^2 m_e \epsilon_o}{e^2} \right) (R) \left(\frac{i_1}{i_d} \right) \quad (3.85f)$$

$$(7) \quad n_{o3} = \left(\frac{C_p \omega^2 m_e \epsilon_o}{e^2} \right) (R) \left(\frac{i_3}{i_d} \right) \quad (3.85g)$$

$$(8) \quad R = \frac{\pi a^2}{\int_0^a \exp(1 - I_o(\gamma r)) 2\pi r \, dr} \quad (3.85h)$$

$$(9) \quad V_o = \frac{\omega}{(1 + 1/4)\pi} \int_{r_1}^a (1 - A_1 \exp(1 - I_o(\gamma r)))^{1/2} dr \quad (3.85i)$$

and:

$$(10) \quad T = \frac{V_o^2 m_e}{3k} \quad (3.85j)$$

The numerical results obtained from the computer solution from equations (3.84) and (3.85) are presented and discussed in the following chapter.

CHAPTER 4

NUMERICAL RESULTS FOR THE ELECTRON DENSITY PROFILE IN A CYLINDRICAL PLASMA COLUMN

4.1 Introduction

The simultaneous equations presented in section 3.4 and section 3.5 are solved numerically using the data given in section 3.2. The solutions are presented in this chapter. The results obtained for the different approaches are presented.

4.2 Numerical Results Based on Parabolic Electron Density Profile Approximation

The numerical results obtained in the simultaneous computer solution of equations (3.48) and (3.49) are listed in Tables 4.2.1 through 4.2.5 for the eight sets of data analyzed. For ease of identification, the data sets are identified throughout by two numbers, i, j ; $i = 1$ to 8 represents the set number; $j = 2$ represents the use of the combination of the first and second resonance (equations (3.48)) while $j = 3$ represents the use of the combination of the first and third resonance (equations (3.49)).

The parameters listed in the Tables are:

(1) The factor α in the parabolic approximation

$$n_e(r) = n_{e_0} \left(1 - \alpha \left(\frac{r}{a}\right)^2\right).$$

(2) The calculated value of the ratio $R = n_e(r = 0) / \langle n_{e_1}(r) \rangle$.

(3) The critical points r_m/a for the m^{th} resonance.

(4) $z_m/a = (a - r_m)/a$.

Data set #	\mathcal{L} j = 2	\mathcal{L} j = 3
1	.83	.83
2	.82	.85
3	.83	.83
4	.80	.86
5	.86	.86
6	.83	.83
7	.84	.87
8	.85	.85

Table 4.2.1 Numerical results for the factor \mathcal{L} for data sets 1 through 8. The columns identified by j=2 and j=3 represent numerical values for \mathcal{L} obtained from the use of combinations of resonances 1,2 (j=2) and 1,3 (j=3) respectively.

Data set #	$n_{o_1}/\langle n_{e_1}(r) \rangle$	$n_{o_2}/\langle n_{e_2}(r) \rangle$
1	1.70	1.70
2	1.70	1.74
3	1.71	1.71
4	1.67	1.75
5	1.76	1.76
6	1.72	1.72
7	1.73	1.77
8	1.74	1.74

Table 4.2.2 Numerical results for the ratio of peak to average electron density $n_{o_1}/\langle n_{e_1}(r) \rangle$ and $n_{o_2}/\langle n_{e_2}(r) \rangle$ for data sets 1 through 8.

Data set #	r_1/a	r_2/a	r_3/a
1	.88	.83	.77
2	.87	.80	.71
3	.88	.81	.77
4	.89	.84	.74
5	.86	.79	.71
6	.87	.81	.73
7	.87	.80	.72
8	.86	.79	.71

Table 4.2.3 Numerical values for the ratio of critical radius r_j to the total radius a , r_j/a , for data sets 1 through 8.

Data set #	z_1/a	z_2/a	z_3/a	z_2/z_1	z_3/z_1
1	.12	.17	.23	1.44	1.95
2	.13	.19	.28	1.50	2.02
3	.12	.18	.23	1.51	1.90
4	.11	.16	.26	1.48	2.00
5	.14	.21	.29	1.53	2.07
6	.13	.19	.27	1.48	2.10
7	.13	.20	.28	1.53	2.02
8	.14	.21	.29	1.52	2.07

Table 4.2.4 Numerical values for the ratio of critical distance z_j measured from the wall for the j^{th} resonance to the total radius a as well as the ratios z_2/z_1 and z_3/z_1 for the data sets 1 through 8.

Data set #	η_w j = 2	η_w j = 3	T j = 2	T j = 3
1	-1.75	-1.75	14670	14670
2	-1.73	-1.90	19960	31630
3	-1.78	-1.78	18950	18950
4	-1.63	-1.96	11590	33070
5	-1.99	-1.99	29000	29000
6	-1.80	-1.80	20480	20480
7	-1.84	-2.00	27370	42820
8	-1.91	-1.91	39060	39060

Table 4.2.5 Numerical values of relative potential at the wall, $\eta_w = eV(a)/kT$ and electron temperature T for data sets 1 through 8. The columns identified by j=2 and j=3 represent the numerical values for η_w and T based on the use of combinations of resonances 1,2 (j=2) and 1,3 (j=3) respectively.

- (5) The ratios z_2/z_1 where $z_1 = a - r_1$ and $z_2 = a - r_2$.
- (6) The ratio z_3/z_1 , where $z_3 = a - r_3$.
- (7) $\eta_w = eV_w/kT$ evaluated at the wall where V_w is the potential, k is the Boltzman constant and T is the electron temperature.
- (8) T , the calculated electron temperature.

The most significant parameter in the parabolic electron density profile is the parameter α appearing in the functional formulation of equation (2.44)

$$n_e(r) = n_{o1} \left(1 - \alpha \left(\frac{r}{a}\right)^2\right)$$

The values for α obtained for any one data set using first the combination of the first and second resonance and then the combination of the first and third resonance are very close. Since these two values for any one data set represent a mutual check, it appears that the results obtained for α are correct. It must be kept in mind, of course, that any calculations employing the third resonance are only approximate, since the third resonances are difficult to interpret from the oscillographs.

The ratio of peak electron density at the center of the plasma column to the average static electron density in the column for the discharge current level i_1 was another of the parameters obtained from the solution of the simultaneous equations (3.48) and (3.49). Again this ratio is very close for data sets 1,2 and data sets 1,3, indicating that the results are reliable. Good correspondence for results using data sets 1,2 and 1,3 is also found for the relative wall potential η_w ($\eta_w = eV_w/kT$). The temperature T indicates some variation as seen in Table 4.2. The relative

variation is still insignificant considering how sensitive the temperature is to variations in other plasma column parameters. It should be recalled that the temperature is determined directly from the phase integral.

The graphical results are shown in Figures 4.2.1 through 4.2.8 for the parabolic electron density profiles and the relative potential distributions for the eight data sets 1,2 on a normalized scale.

In conclusion, it is observed that some of the values obtained in this analysis agree well with numerical values obtained from approximate theoretical treatments or independent experimental analyses. Theoretical analysis of a plasma sheath, for example,¹ leads to a relative wall potential η_w of approximately 2 which is in agreement with the values obtained in this numerical analysis. More significantly, the ratios of z_2/z_1 obtained in this analysis of approximately 1.5 agrees well with ratios of the distances from the wall observed for the electric field perturbation for the first and second thermal resonances in experimental work reported earlier.¹⁴

The appendix contains complete computer readouts of all the parameters for each data set.

4.3 Numerical Results Based on the Bessel Function Approximation for the Static Electron Density Profile

The numerical results obtained in the simultaneous computer analysis of equations (3.85) are listed in Tables 4.3.1 through 4.3.4 for the eight sets of data analyzed. For ease of identification, the data sets are identified throughout by two numbers

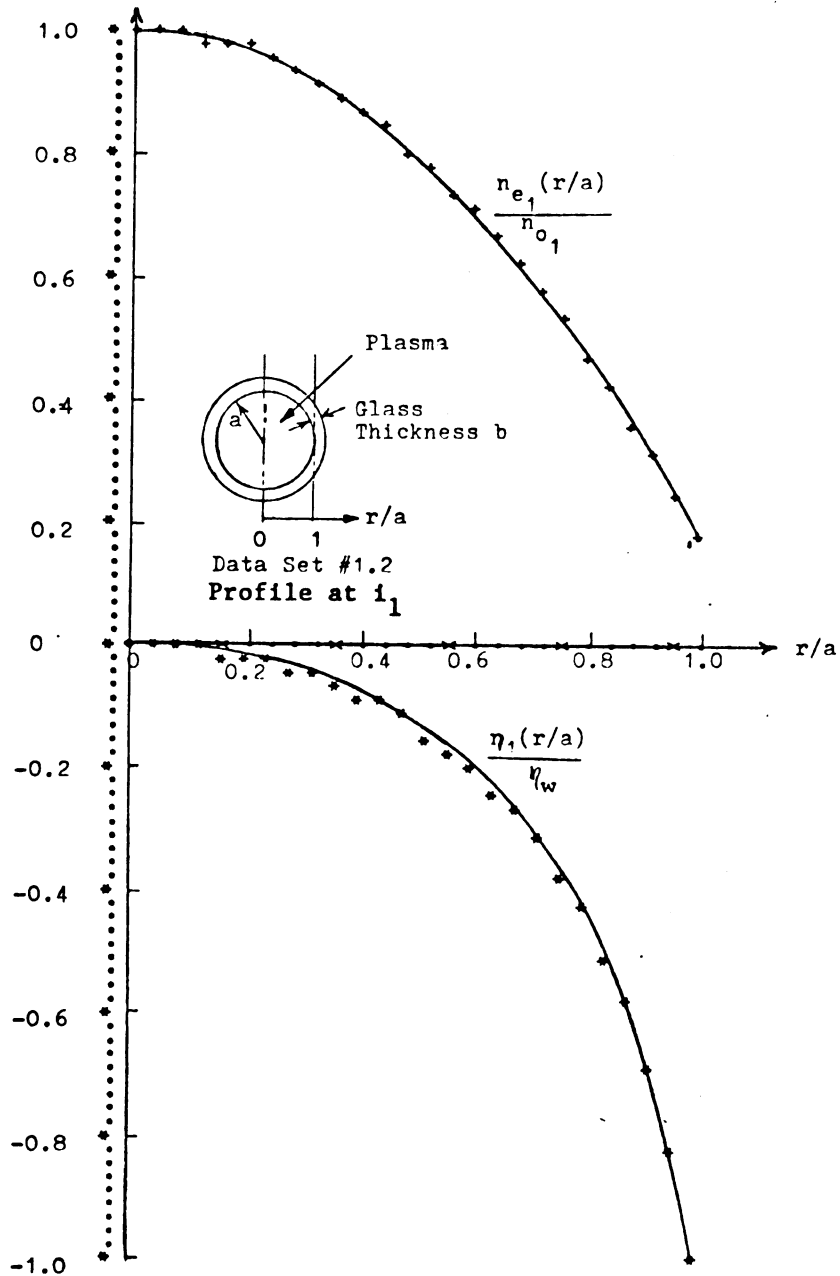


Fig. 4.2.1 Normalized parabolic electron density profile as a function of r/a ,

$$\frac{n_{e_1}(r/a)}{n_{o_1}} = 1 - .83(r/a)^2.$$

Also the normalized potential profile $\eta_1(r/a)/\eta_w$. Based on data set #1. ($f=2.016$ GHz, $i_d=270$ ma, $i_1=185$ ma, $i_2=150$ ma, $i_3=125$ ma).

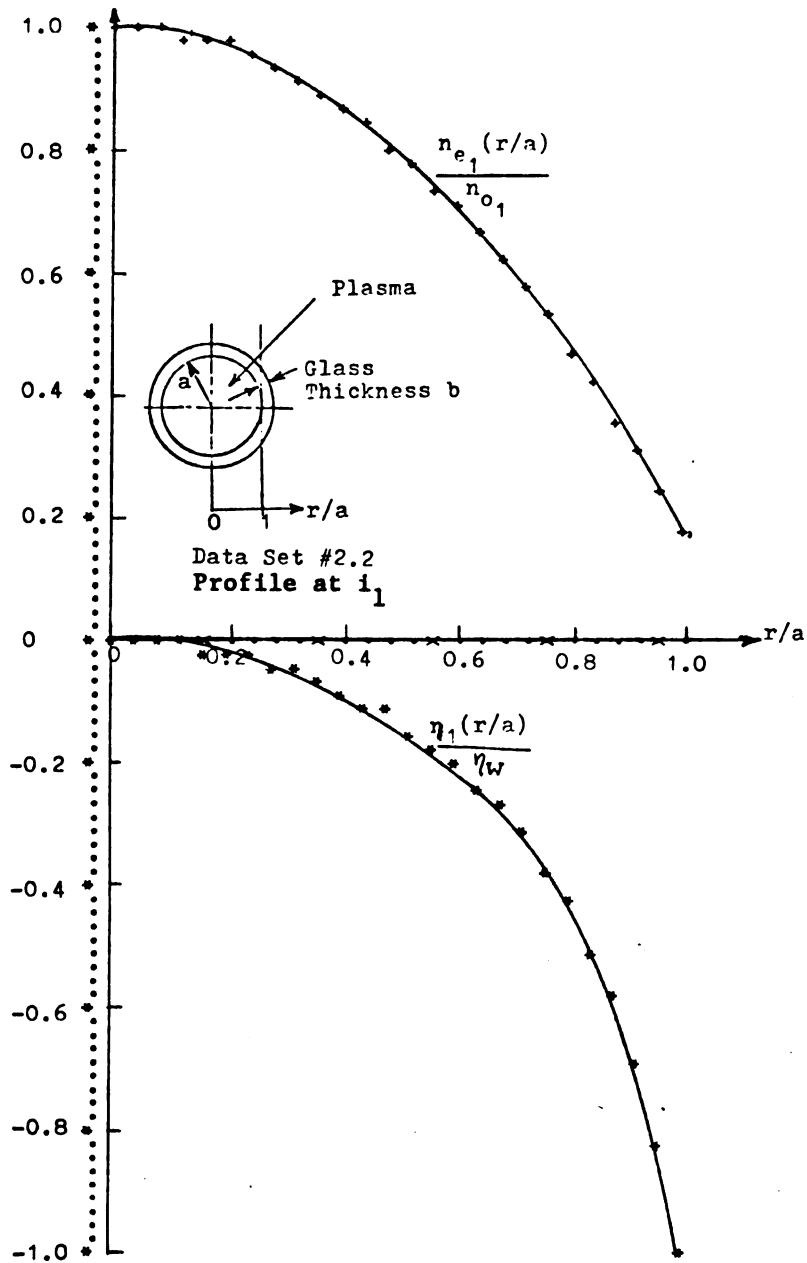


Fig. 4.2.2 Normalized parabolic electron density profile as a function of r/a ,

$$\frac{n_{e_1}(r/a)}{n_{o_1}} = 1 - .82(r/a)^2.$$

Also the normalized potential profile $\frac{\eta_1(r/a)}{\eta_w}$. Based on data set #2 ($f=2.10$ GHz, $i_d=290$ ma, $i_1=190$ ma, $i_2=150$ ma, $i_3=120$ ma).

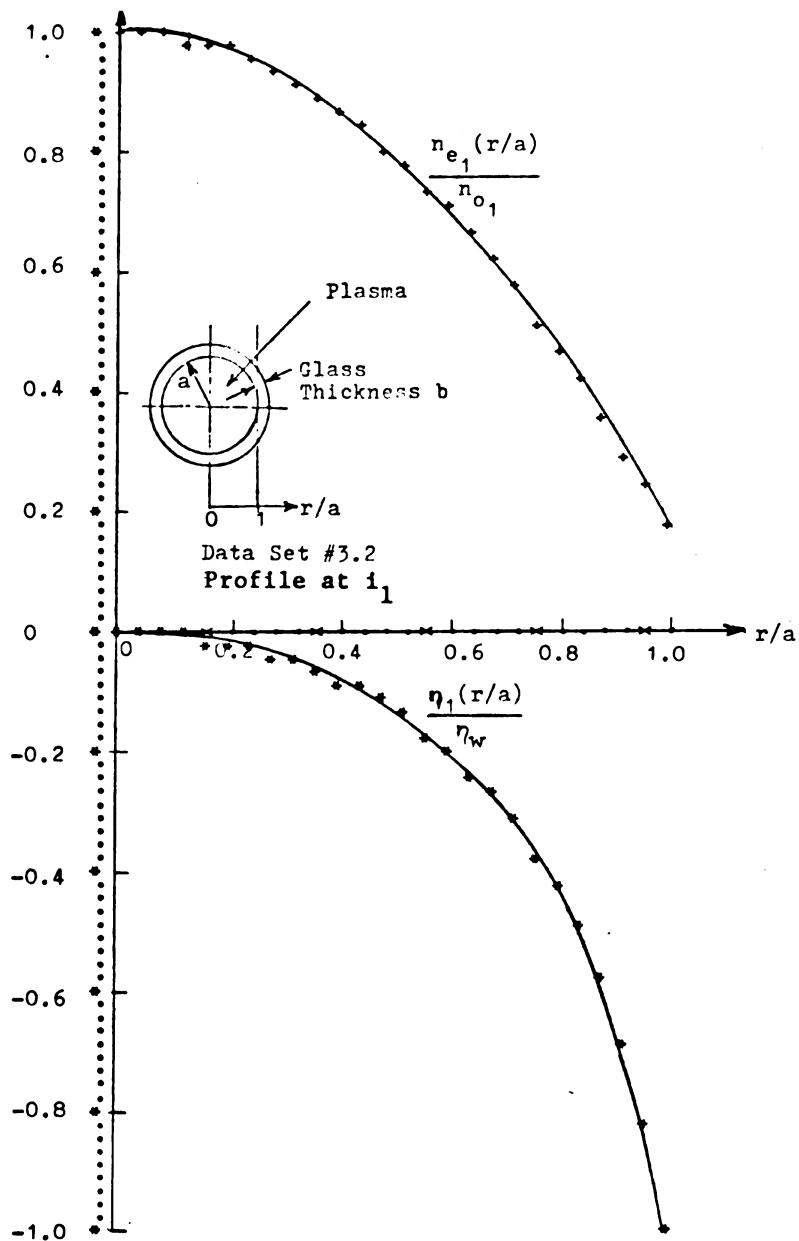


Fig. 4.2.3 Normalized parabolic electron density profile as a function of r/a ,

$$\frac{n_{e_1}(r/a)}{n_{o_1}} = 1 - .83(r/a)^2.$$

Also the normalized potential profile $\eta_1(r/a)/\eta_w$. Based on data set #3 ($f=2.23$ GHz, $i_d=340$ ma, $i_1=235$ ma, $i_2=185$ ma, $i_3=160$ ma).

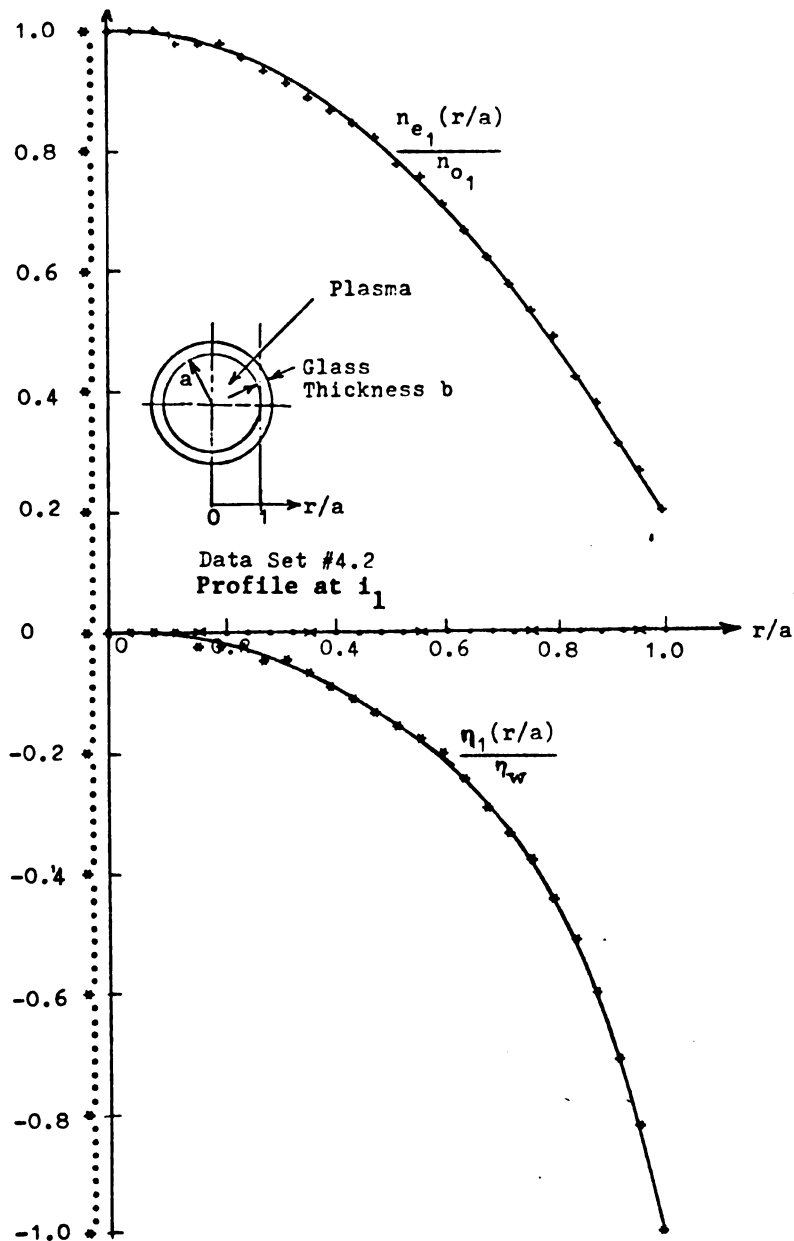


Fig. 4.2.4 Normalized parabolic electron density profile as a function of r/a ,

$$\frac{n_{e_1}(r/a)}{n_{o_1}} = 1 - .80(r/a)^2.$$

Also the normalized potential profile $\eta_1(r/a)/\eta_w$. Based on data set #4 ($f=2.32$ GHz, $i_d=355$ ma, $i_1=245$ ma, $i_2=200$ ma, $i_3=175$ ma).

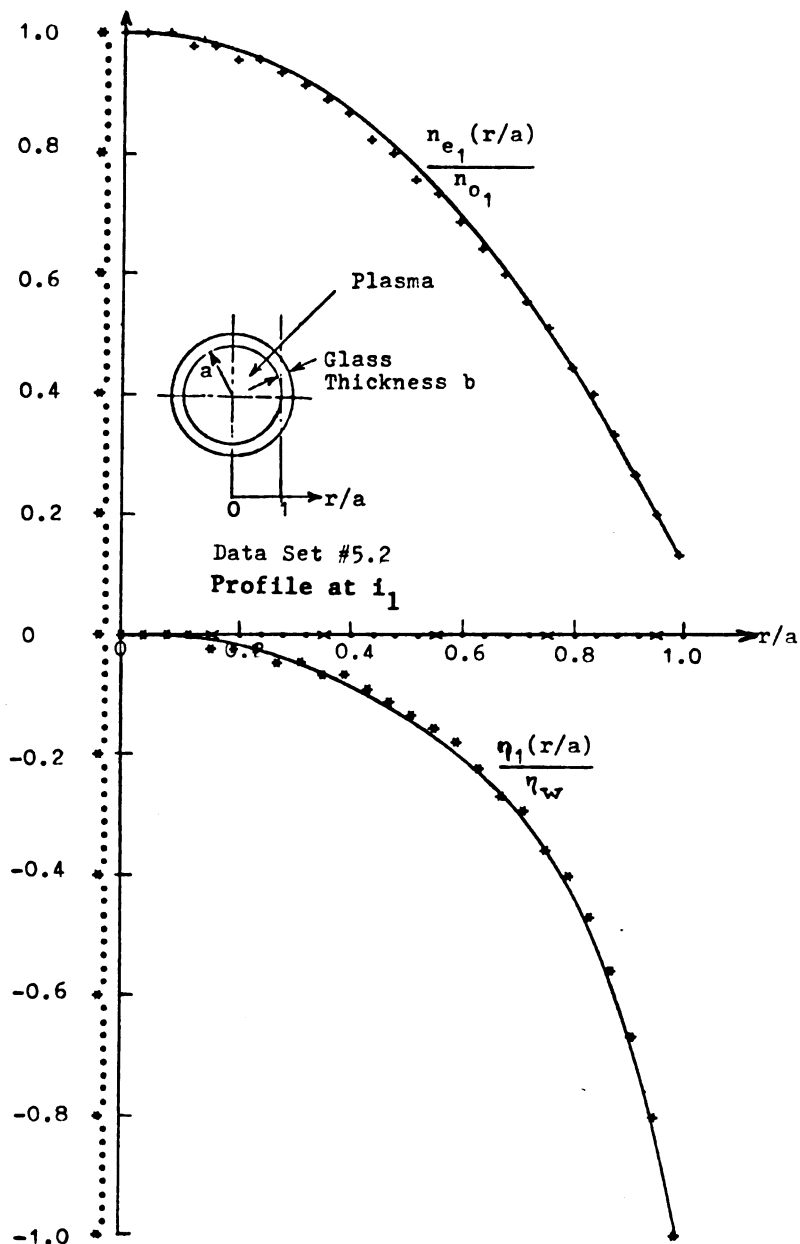


Fig. 4.2.5 Normalized parabolic electron density profile as a function of r/a ,

$$\frac{n_{e_1}(r/a)}{n_{0_1}} = 1 - .86(r/a)^2.$$

Also the normalized potential profile $\frac{\eta_1(r/a)}{\eta_w}$. Based on data set #5 ($f=1.917$ GHz, $i_d=270$ ma, $i_1=180$ ma, $i_2=135$ ma, $i_3=110$ ma).

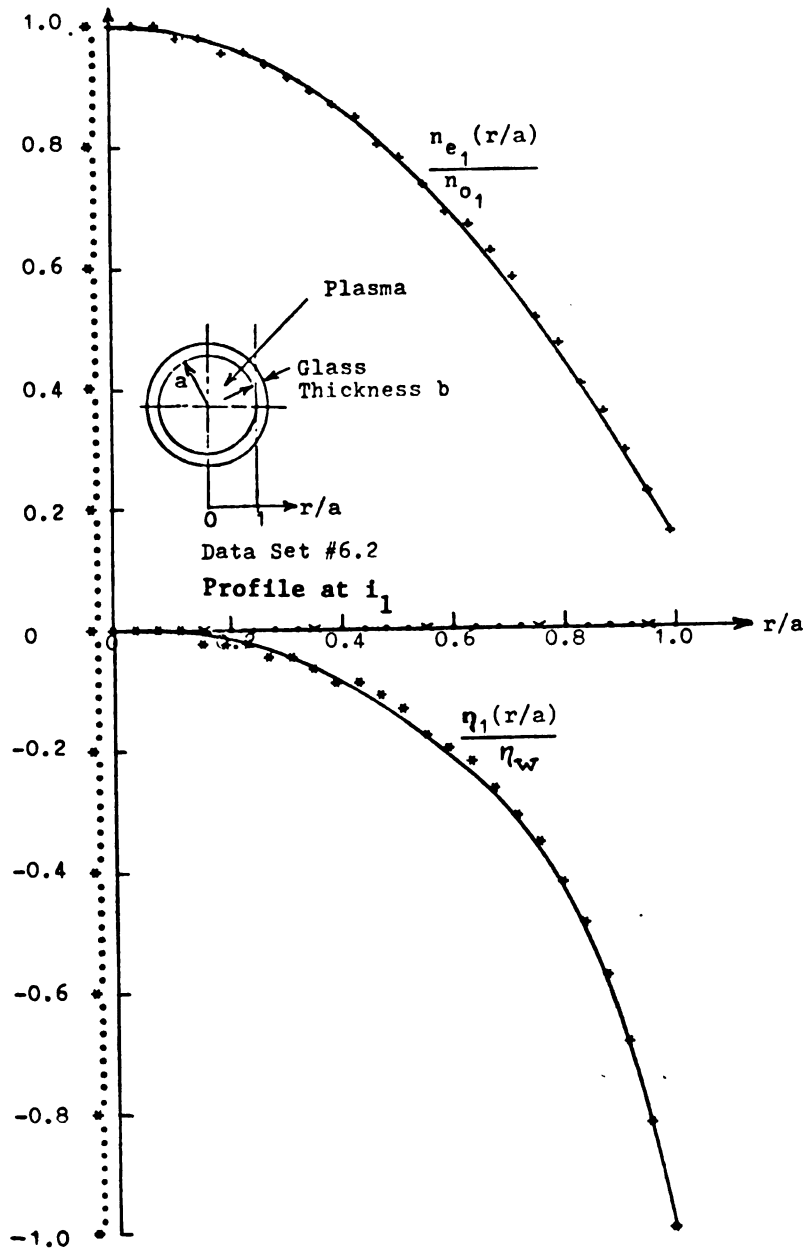


Fig. 4.2.6 Normalized parabolic electron density profile as a function of r/a ,

$$\frac{n_{e_1}(r/a)}{n_{o_1}} = 1 - .83(r/a)^2.$$

Also the normalized potential profile $\eta_1(r/a)/\eta_w$. Based on data set #6 ($f=2.017$ GHz, $i_d=285$ ma, $i_1=190$ ma, $i_2=150$ ma, $i_3=120$ ma).

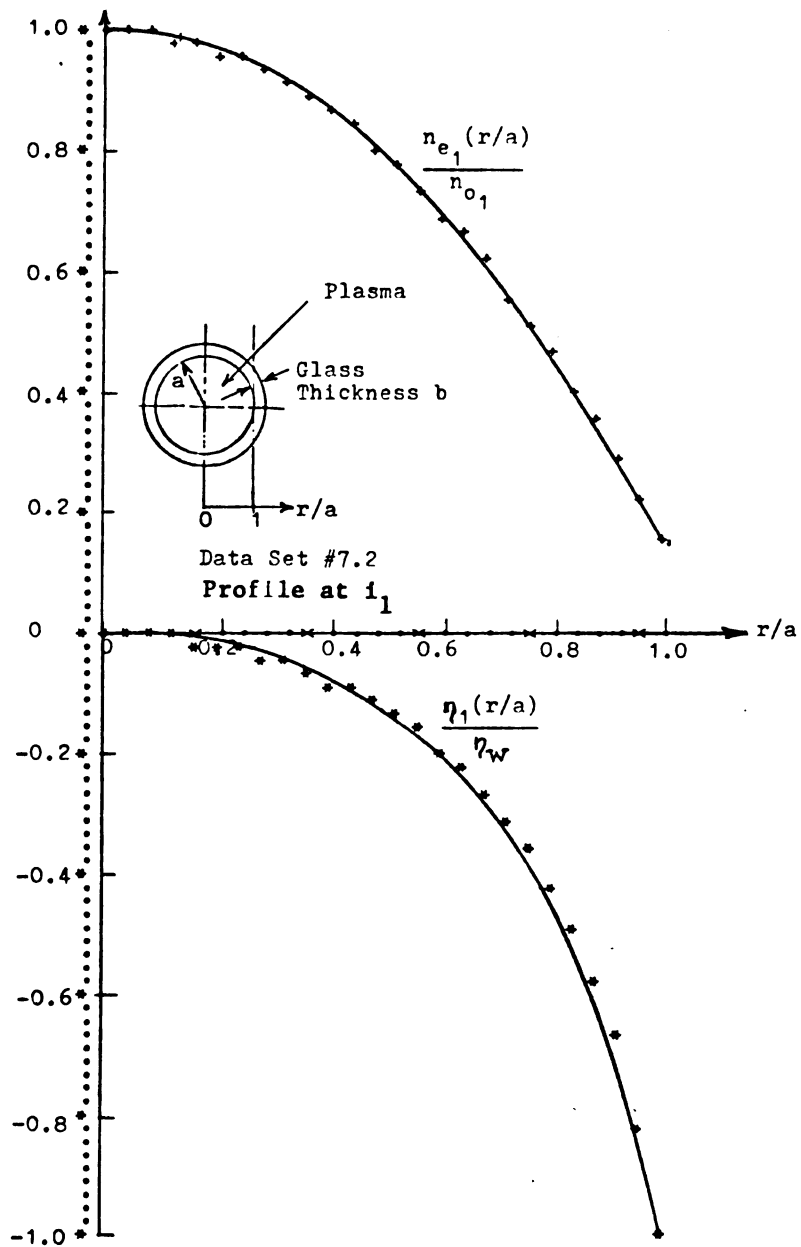


Fig. 4.2.7 Normalized parabolic electron density profile as a function of r/a ,

$$\frac{n_{e_1}(r/a)}{n_{o_1}} = 1 - .84(r/a)^2.$$

Also the normalized potential profile $\eta_1(r/a)/\eta_w$. Based on data set #7 ($f=2.275$ GHz, $i_d=290$ ma, $i_1=195$ ma, $i_2=150$ ma, $i_3=120$ ma).

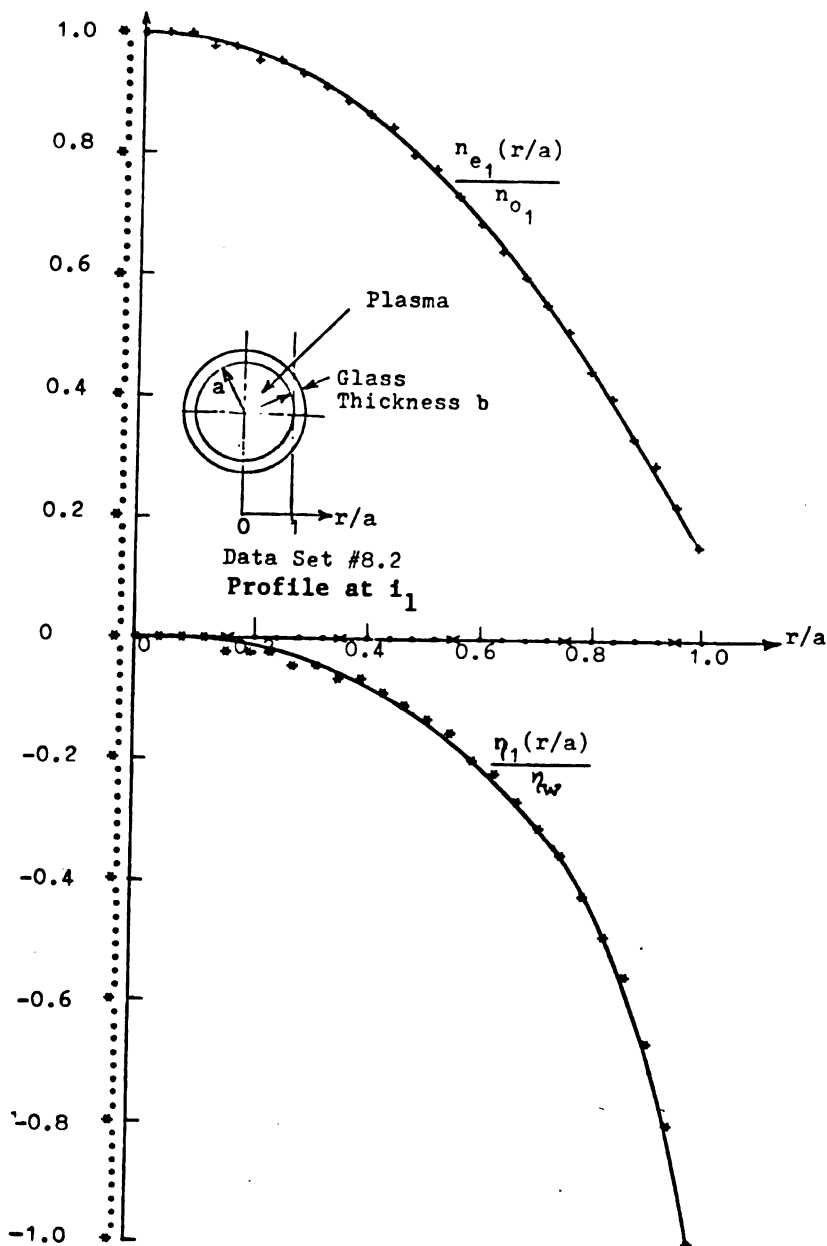


Fig. 4.2.8 Normalized parabolic electron density profile as a function of r/a ,

$$\frac{n_{e_1}(r/a)}{n_{o_1}} = 1 - .85(r/a)^2.$$

Also the normalized potential profile $\frac{\eta_1(r/a)}{\eta_w}$. Based on data set #8. ($f=2.322$ GHz, $i_d=320$ ma, $i_1=210$ ma, $i_2=160$ ma, $i_3=135$ ma).

Data set #	γ j = 2	γ j = 3
1	327	321
2	326	319
3	323	328
4	330	328
5	327	327
6	327	322
7	328	328
8	331	325

Table 4.3.1 Numerical results for the factor γ for data sets 1 through 8. The columns identified by j=2 and j=3 represent the numerical values for γ obtained from use of combinations of resonances 1,2 (j=2) and 1,3 (j=3) respectively.

Data set #	$n_{o_1}/\langle n_{e_1}(r) \rangle$	$n_{o_2}/\langle n_{e_2}(r) \rangle$
1	1.99	1.94
2	1.98	1.93
3	1.96	1.99
4	2.01	1.99
5	1.99	1.99
6	1.99	1.95
7	1.99	1.99
8	2.02	1.97

Table 4.3.2 Numerical results for the ratio of peak to average electron density $n_{o_1}/\langle n_{e_1}(r) \rangle$ and $n_{o_2}/\langle n_{e_2}(r) \rangle$ for data sets 1 through 8.

Data set #	z_1/a	z_2/a	z_3/a	z_2/z_1	z_3/z_1
1	.14	.20	.23	1.49	2.02
2	.14	.21	.27	1.53	2.22
3	.11	.18	.26	1.60	1.94
4	.13	.20	.26	1.47	2.15
5	.14	.22	.28	1.59	2.08
6	.14	.21	.27	1.53	2.19
7	.14	.21	.28	1.53	2.06
8	.15	.24	.29	1.57	2.17

Table 4.3.3 Numerical values for the ratio of the critical distance z_j measured from the wall into the plasma for the j^{th} resonance to the total radius a and also the ratios z_2/z_1 and z_3/z_1 .

Data set #	η_w j = 2	η_w j = 3	T j = 2	T j = 3
1	-1.8	-1.7	47380	30580
2	-1.8	-1.7	83690	74860
3	-1.8	-1.8	67470	57060
4	-1.9	-1.8	47950	77700
5	-1.8	-1.8	10350	10350
6	-1.8	-1.7	71630	66900
7	-1.8	-1.8	14400	14400
8	-1.9	-1.8	10200	10120

Table 4.3.4 Numerical values of the relative potential $\eta_w = eV(a)/kT$ and the electron temperature T for the data sets 1 through 8. The columns identified by j=2 and j=3 represent the numerical results based on the use of combinations of resonances 1,2 (j=2) and 1,3 (j=3) respectively.

i, j ; here $i = 1$ through 8 represents the set number; $j = 2$ represents the use of the combination of the first and second resonance while $j = 3$ represents the use of the combination of the first and third resonance.

The parameters listed in the Tables are:

- (1) The calculated value of the ratio $R = n_0(r = 0) / \langle n_{e1}(r) \rangle$.
- (2) The factor γ in the Bessel series formulation in equation (3.52)

$$n_e(r) = n_0 \exp(1 - I_0(\gamma r)) .$$

- (3) The ratios z_2/z_1 and z_3/z_1 .
- (4) The critical points z_m/a for the m^{th} resonance.
- (5) $n_w = eV_w/kT$ evaluated at the wall where V_w is the potential, k is the Boltzmann constant and T is the electron temperature.
- (6) T , the electron temperature.

The most important parameter in this analysis is γ . The values for γ obtained for data sets 1,2 and 1,3 compare well for the eight sets analyzed and since sets 1,2 and 1,3 represent a mutual check it appears that the functional form obtained is acceptable.

Good correspondence using data sets 1,1 and 1,2 is also obtained for the relative wall potential $n_w = eV_w/kT$ and to a satisfactory extent for the electron temperature T . Since T is very sensitive to other parameter variations, the difference observed in some data sets between sets 1,2 and 1,3 is not very significant.

The graphical results for the normalized electron density profiles $n_{e1}(z)/n_{01}$ (here $n_{e1}(z)$ is the static electron density at

discharge current i_1 where $z = a - r$) and the corresponding relative potential $\eta(r) = eV(r)/kT$ are shown for the eight data sets in Figures 4.3.1 through 4.3.8. Subsequently, Figures 4.3.9 through 4.3.16 show simultaneous plots for the normalized electron density profiles $n_{e1}(z)/n_{o1}$ and $n_{e2}(z)/n_{o1}$ for each data set. These Figures also show the location of the critical turning points z_1/a and z_2/a marked as t_1 and t_2 . These must, of course, occur at the same vertical magnitude on the graphs to be correct and indeed good agreement with this requirement is observed indicating that the numerical analysis is sufficiently accurate. Figures 4.3.17 through 4.3.24 show the corresponding simultaneous plots for $n_{e1}(z)/n_{o1}$ and $n_{e3}(z)/n_{o1}$. Again critical points z_1/a and z_3/a marked at t_1 and t_3 closely satisfy the condition that the vertical magnitudes are the same. It should be recalled from the theoretical development that t_1 , t_2 and t_3 occur at points at which

$$\omega_p^2(t_m) = \omega^2,$$

so that

$$\frac{n_{e_m}(t_m)}{n_{o_m}} = \frac{\omega_m^2 \epsilon_0}{e^2 n_{o_m}}$$

which depends only on the excitation frequency ω which is held constant in any one data set.

In conclusion it is observed that the value of η_w agrees with typical values predicted theoretically for plane plasma sheaths which should not behave too differently near the wall in

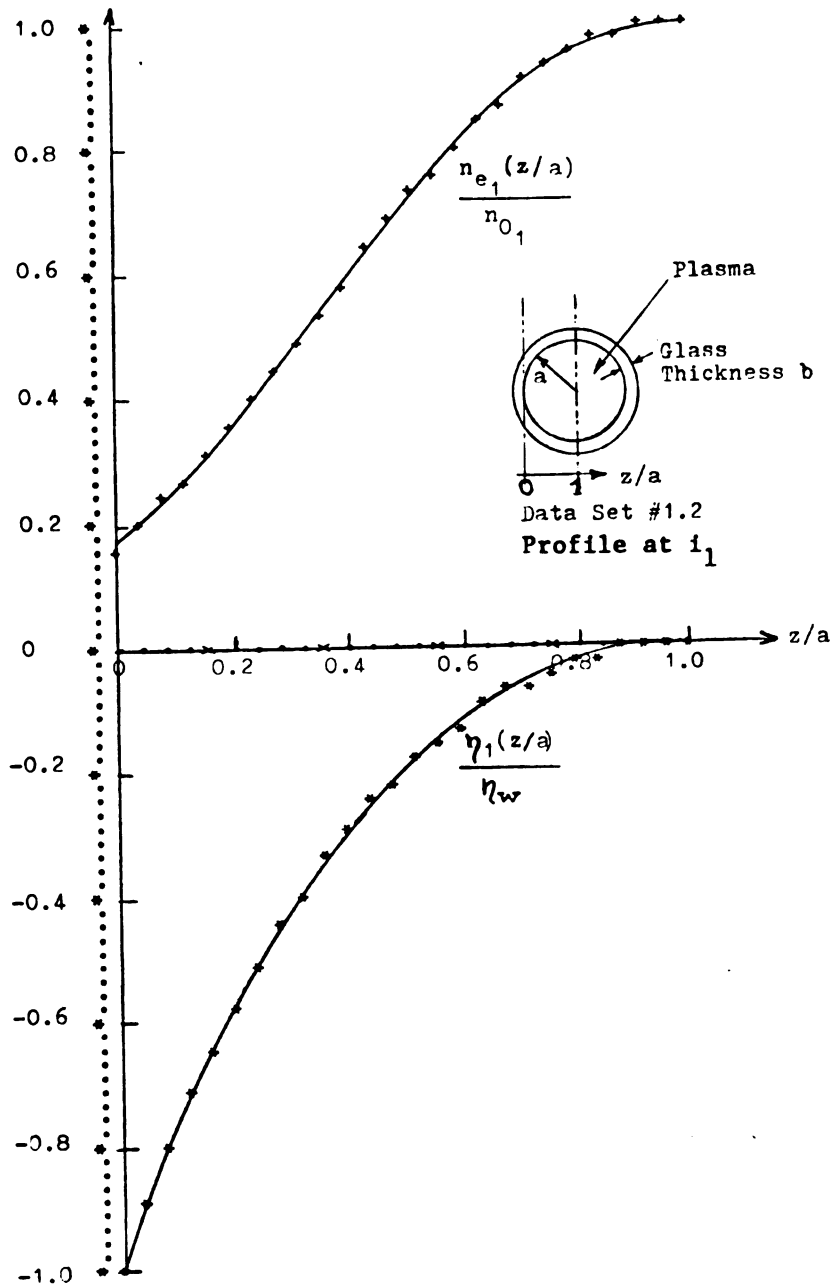


Fig.4.3.1 Normalized Bessel series electron density profile as a function of z/a ,

$$\frac{n_{e_1}(z/a)}{n_{0_1}} = \exp(1 - \hat{I}_0(327(1-z/a))).$$

Also the normalized potential profile
 $\frac{\eta_1(z/a)}{\eta_w}$. Based on data set #1 ($f=2.016$ GHz,
 $i_d=270$ ma, $i_1=185$ ma, $i_2=150$ ma, $i_3=125$ ma).

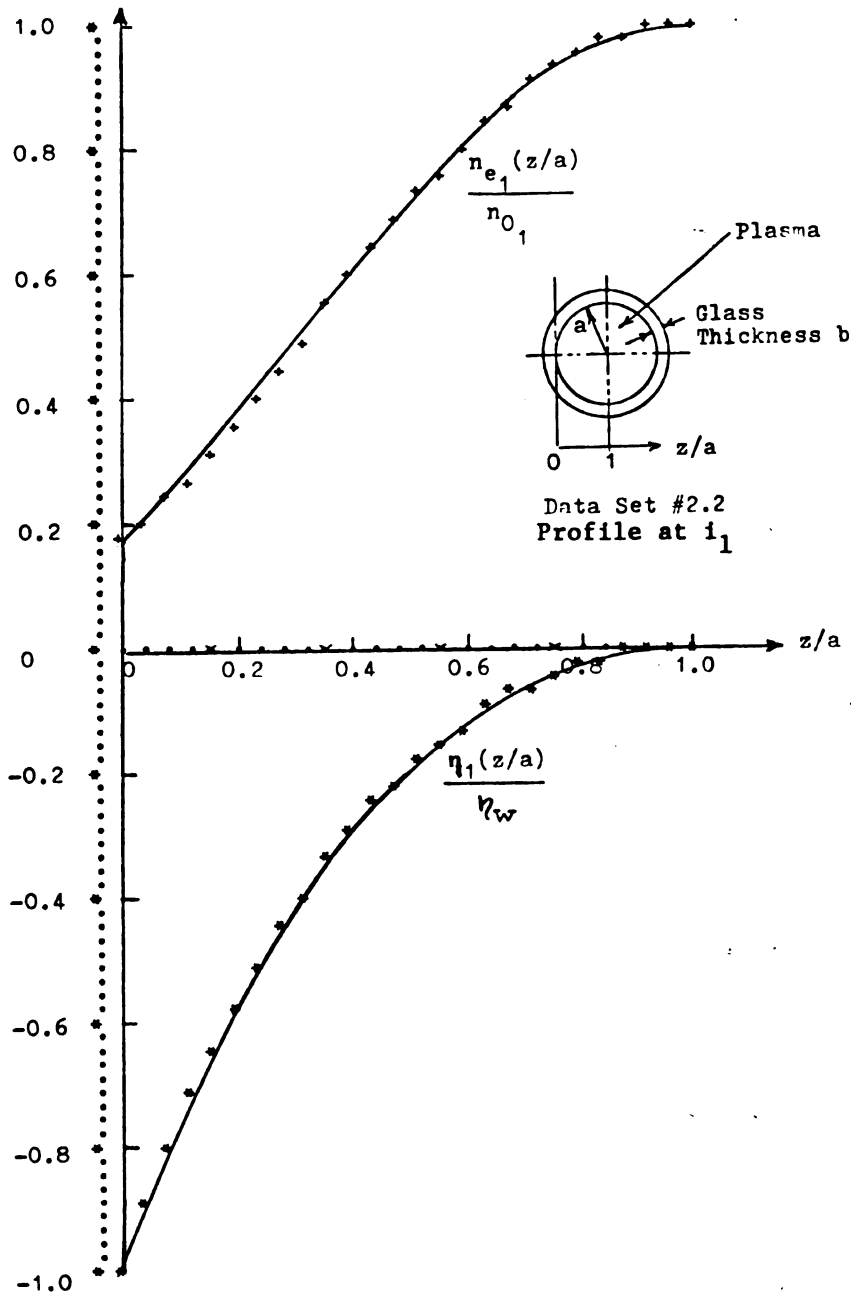


Fig. 4.3.2 Normalized Bessel series electron density profile as a function of z/a ,

$$\frac{n_{e_1}(z/a)}{n_{0_1}} = \exp(1 - I_0(326(1-z/a))).$$

Also the normalized potential profile $\eta_1(z/a)/\eta_w$. Based on data set #3 ($f=2.10$ GHz; $i_d=290$ ma, $i_1=190$ ma, $i_2=150$ ma, $i_3=120$ ma).

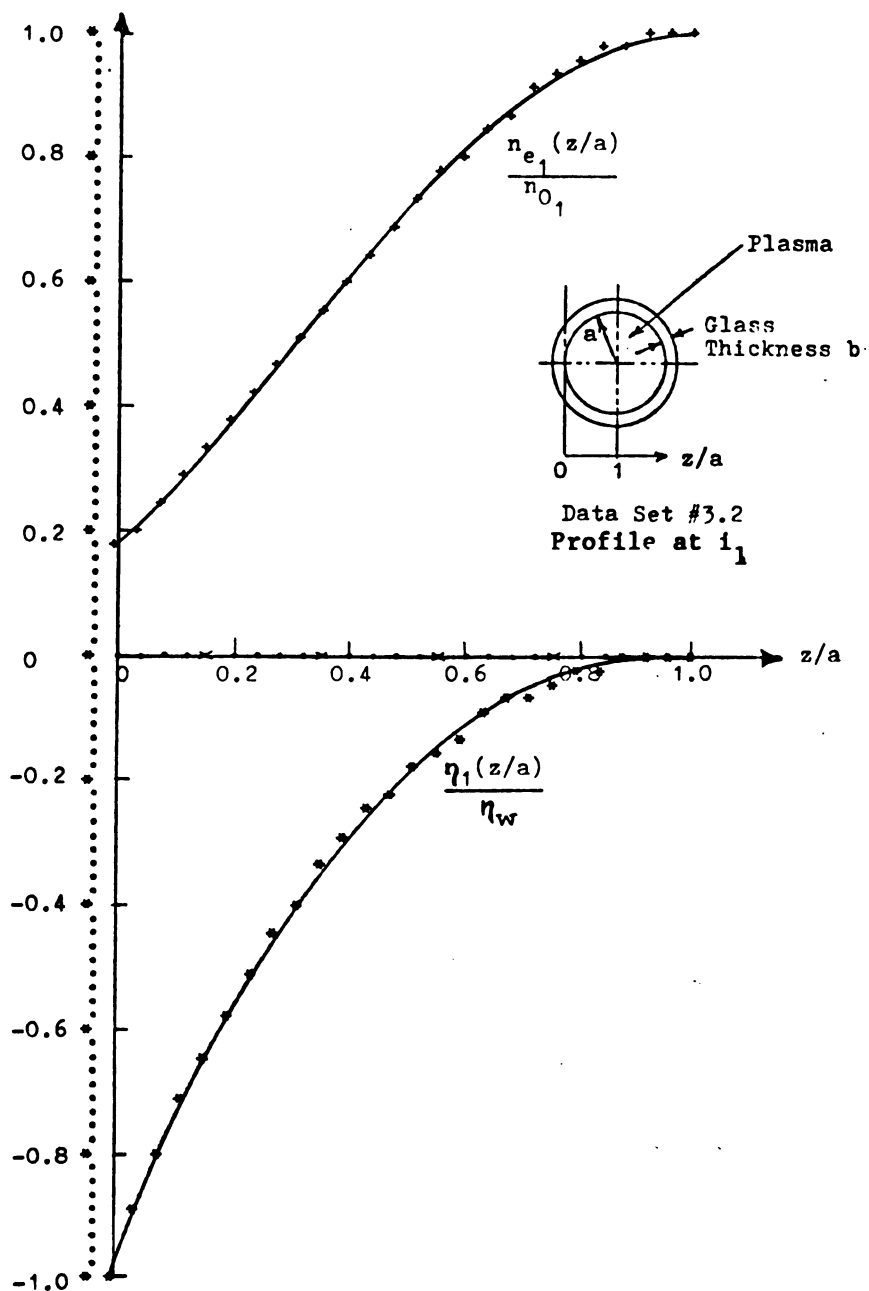


Fig. 4.3.3 Normalized Bessel series electron density profile as a function of z/a ,

$$\frac{n_e(z/a)}{n_{01}} = \exp(1 - I_0(323(1-z/a))).$$

Also the normalized potential profile $\eta_1(z/a)/\eta_w$. Based on data set #3 ($f=2.23$ GHz, $i_d=340$ ma, $i_1=235$ ma, $i_2=185$ ma, $i_3=160$ ma).

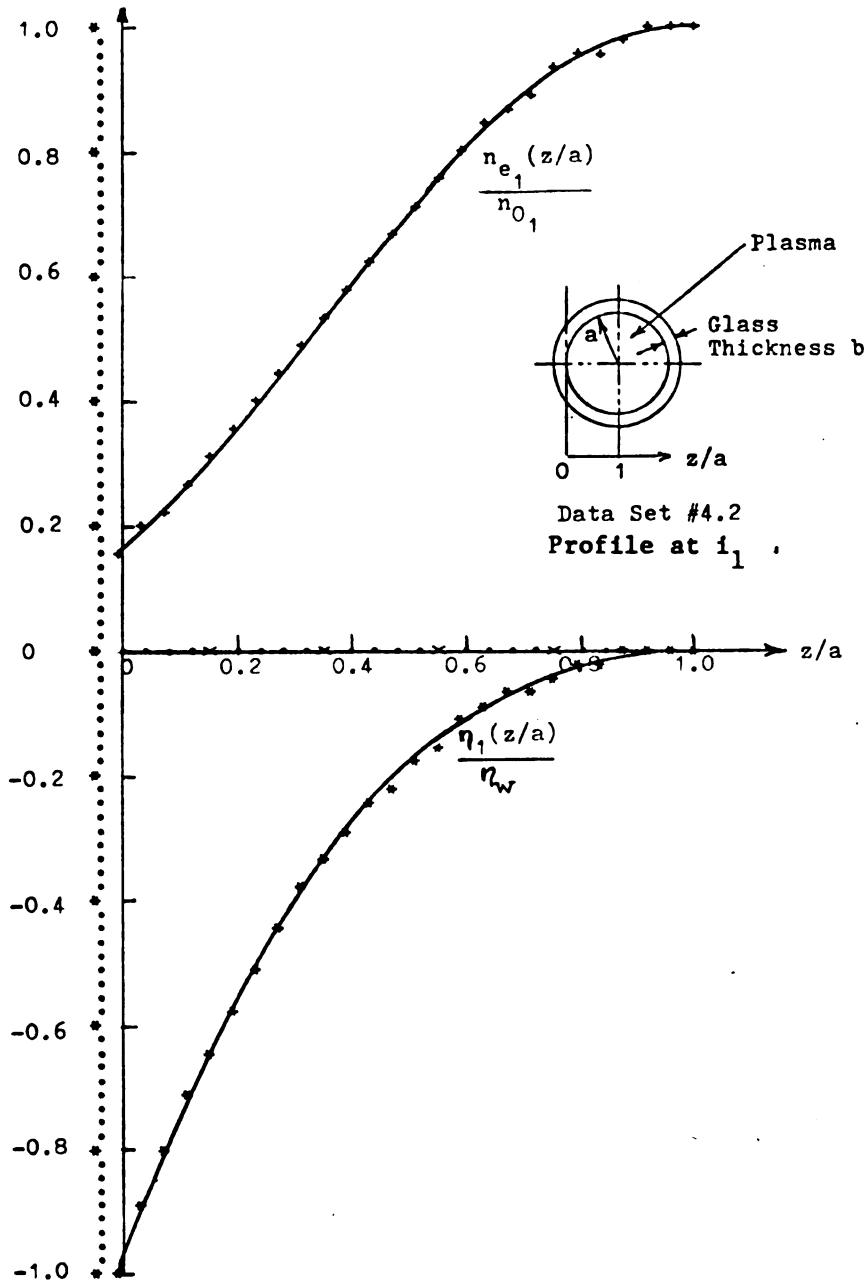


Fig. 4.3.4 Normalized Bessel series electron density profile as a function z/a ,

$$\frac{n_{e_1}(z/a)}{n_{0_1}} = \exp(1 - I_0(330(1-z/a))).$$

Also the normalized potential profile
 $\frac{\eta_1(z/a)}{\eta_w}$. Based on data set #4 ($f=2.32$ GHz,
 $i_d=355$ ma, $i_1=245$ ma, $i_2=200$ ma, $i_3=175$ ma).

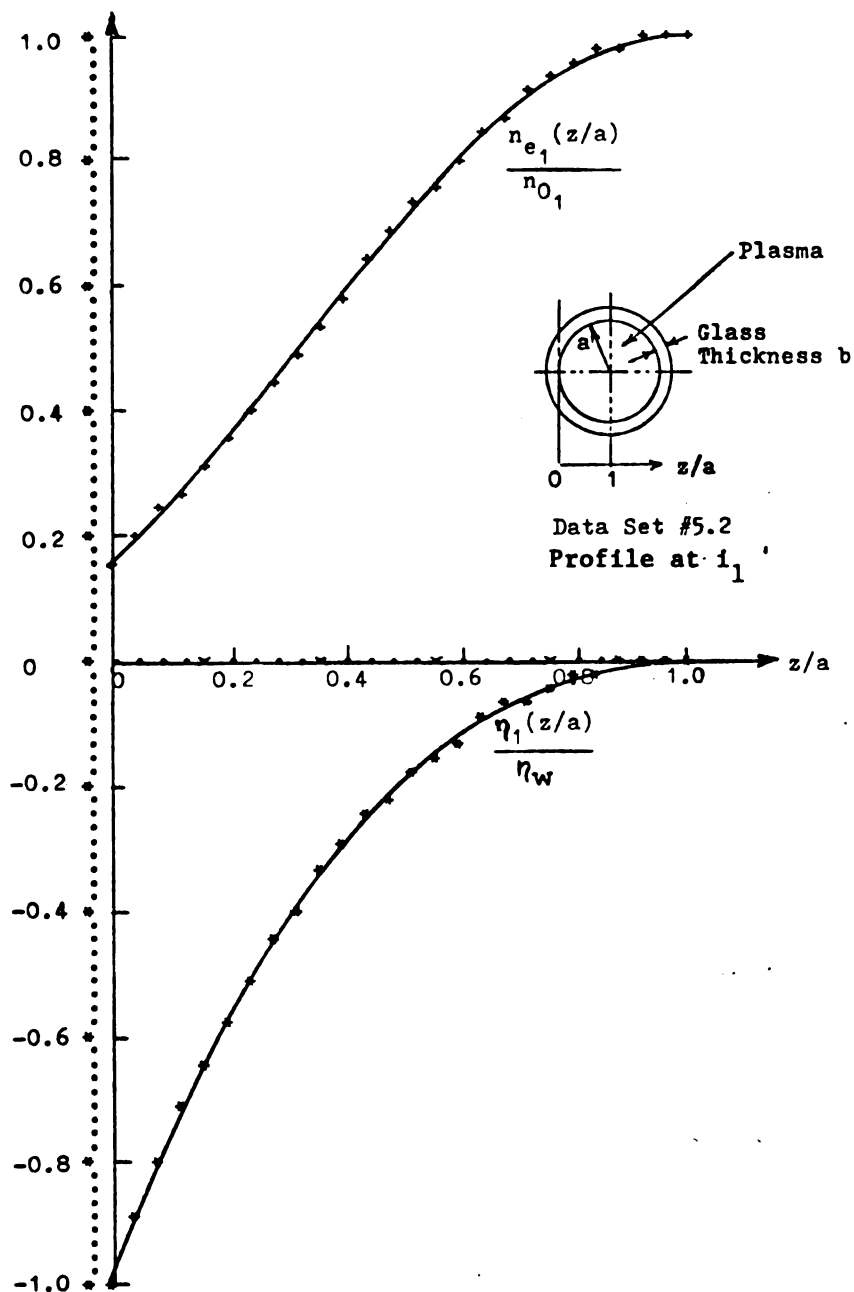


Fig. 4.3.5 Normalized Bessel series electron density profile as a function of z/a ,

$$\frac{n_{e_1}(z/a)}{n_{0_1}} = \exp(1 - I_0(327(1-z/a))).$$

Also the normalized potential profile
 $\eta_1(z/a)/\eta_w$. Based on data set #5 ($f=1.917$ GHz,
 $i_d=270$ ma, $i_1=180$ ma, $i_2=135$ ma, $i_3=110$ ma).

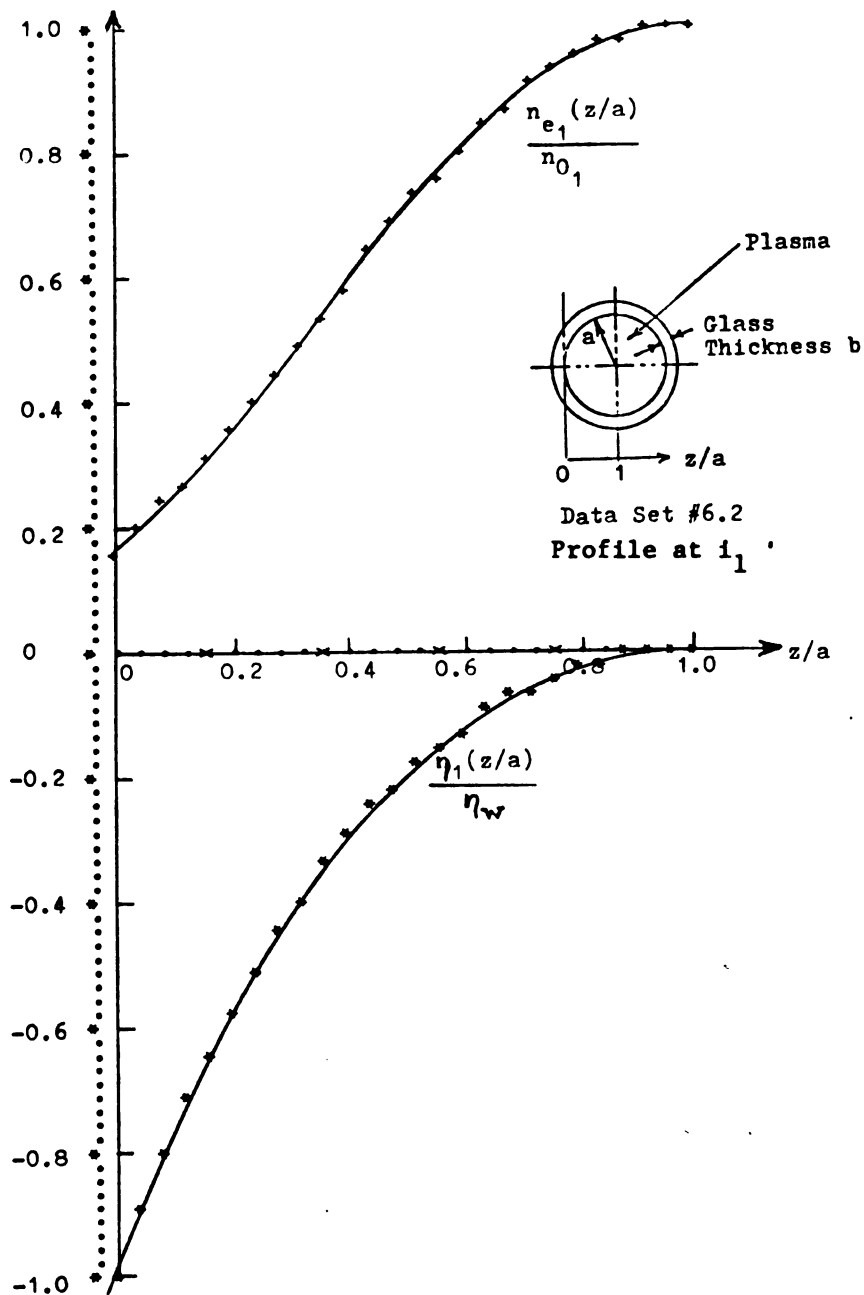


Fig. 4.3.6 Normalized Bessel series electron density profile as a function of z/a ,

$$\frac{n_{e_1}(z/a)}{n_{0_1}} = \exp(1 - I_0(327(1-z/a))).$$

Also the normalized potential profile $\frac{\eta_1(z/a)}{\eta_w}$. Based on data set #6 ($f=2.017$ GHz, $i_d=285$ mA, $i_1=190$ ma, $i_2=150$ ma, $i_3=120$ ma).

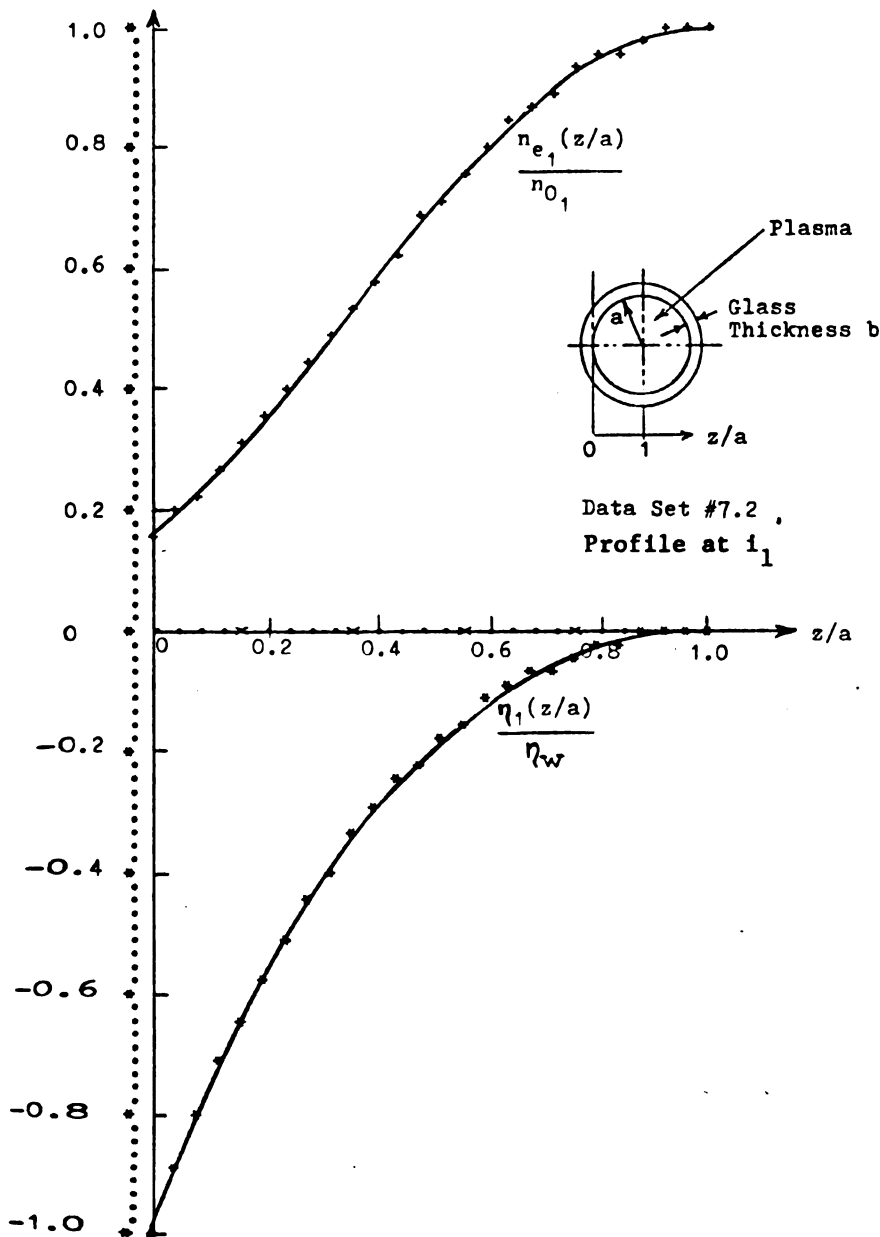


Fig. 4.3.7

Normalized Bessel series electron density profile as a function of z/a ,

$$n_{e_1}(z/a)/n_{0_1} = \exp(1 - I_0(328(1-z/a))).$$

Also the normalized potential profile $\eta_1(z/a)/\eta_w$. Based on data set #7 ($f=2.275$ GHz, $i_d=290$ ma, $i_1=195$ ma, $i_2=150$ ma, $i_3=120$ ma).

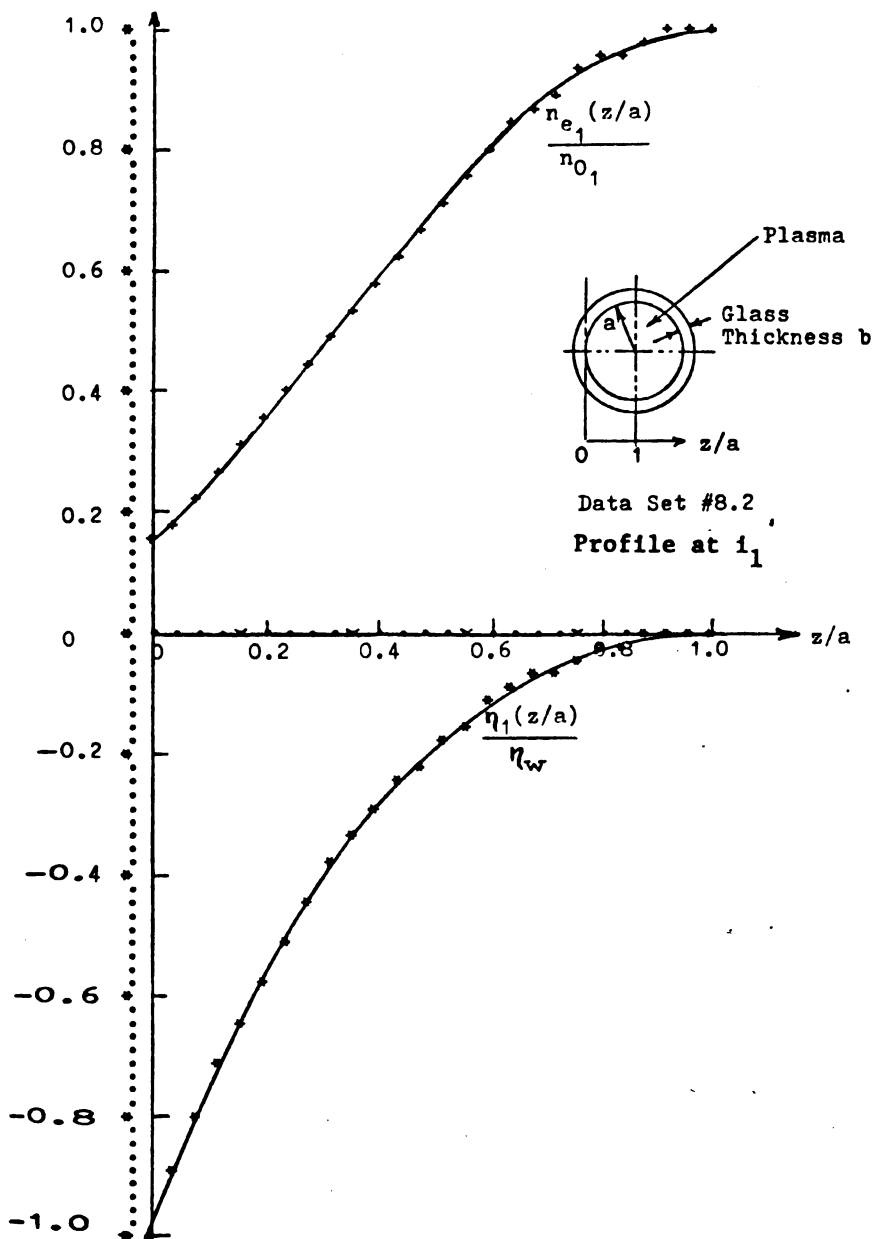


Fig. 4.3.8 Normalized Bessel series electron density profile as a function of z/a ,

$$\frac{n_{e_1}(z/a)}{n_{0_1}} = \exp(1 - I_0(331(1-z/a)))$$

Also the normalized potential profile
 $\frac{\eta_1(z/a)}{\eta_w}$. Based on data set #8 ($f=2.322$ GHz,
 $i_d=320$ ma, $i_1=210$ ma, $i_2=160$ ma, $i_3=135$ ma).

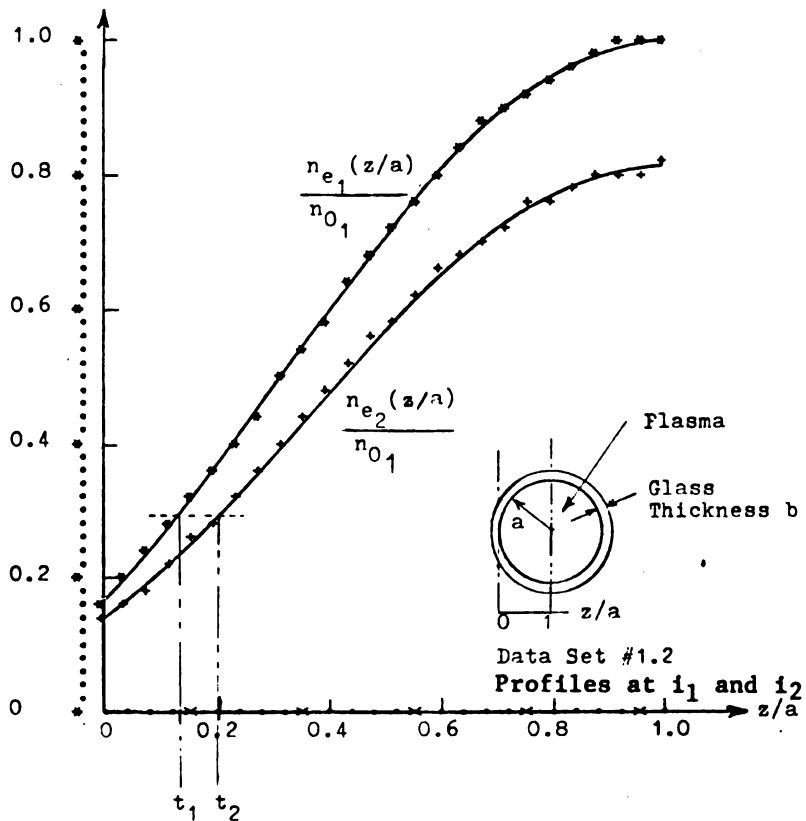


Fig. 4.3.9 Normalized Bessel series electron density profiles at resonances 1 and 2. Points t_1 and t_2 represent the critical points in the plasma sheath at which k_{p1} and k_{p2} respectively to zero. Based on data set #1. ($f=2.016$ GHz, $i_d=270$ ma, $i_1=185$ ma, $i_2=150$ ma, $i_3=125$ ma).

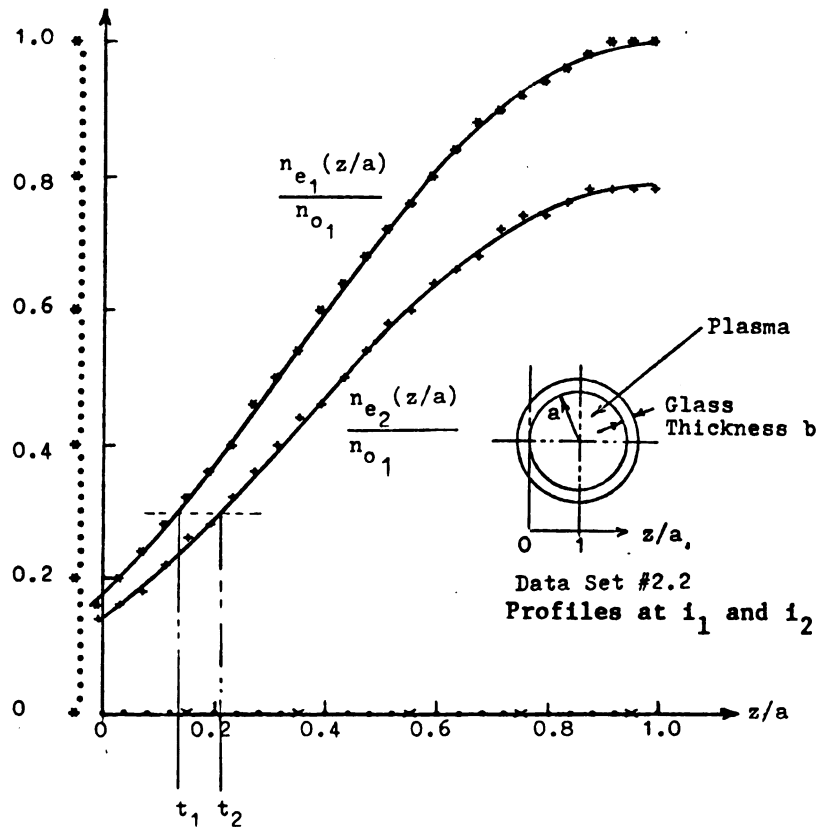


Fig. 4.3.10 Normalized Bessel series electron density profiles at resonances 1 and 2. Points t_1 and t_2 represent the critical points in the plasma sheath at which k_{p1} and k_{p2} respectively go to zero. Based on data set #2. ($f=2.10$ GHz, $i_d=290$ ma, $i_1=190$ ma, $i_2=150$ ma, $i_3=120$ ma).

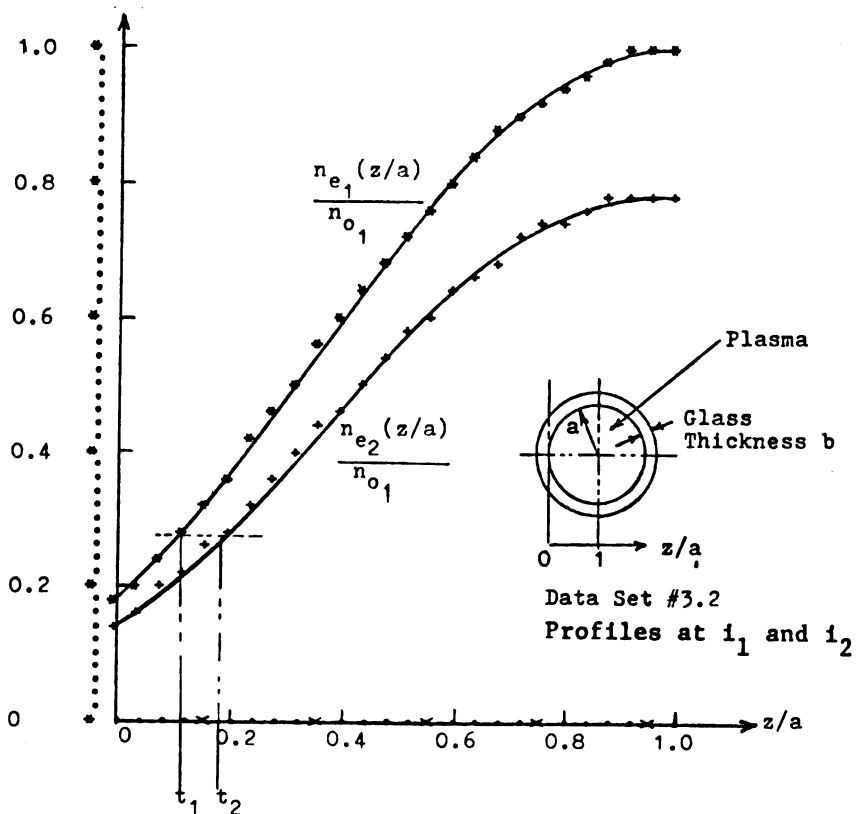


Fig. 4.3.11 Normalized Bessel series electron density profiles at resonances 1 and 2. Points t_1 and t_2 represent the critical points in the plasma sheath at which k_{p_1} and k_{p_2} respectively go to zero. Based on data set #3. ($f=2.23$ GHz, $i_d=340$ ma, $i_1=235$ ma, $i_2=185$ ma, $i_3=160$ ma).

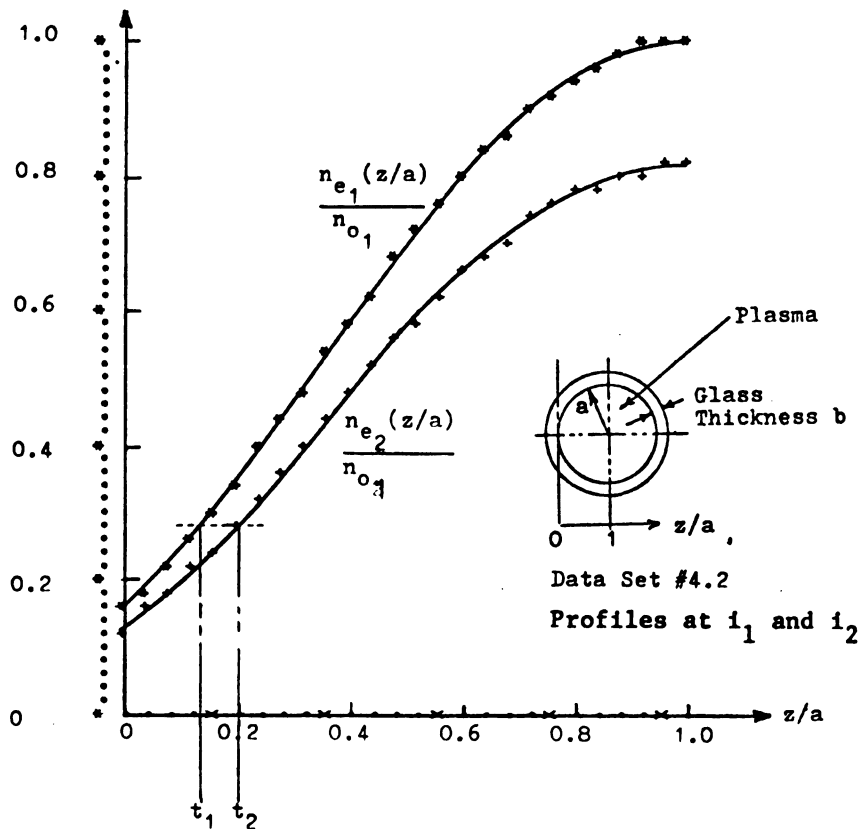


Fig. 4.3.12 Normalized Bessel series electron density profiles at resonances 1 and 2. Points t_1 and t_2 represent the critical points in the plasma sheath at which k_{p_1} and k_{p_2} respectively go to zero. Based on data set #4. ($f=2.32$ GHz, $i_d=355$ ma, $i_1=245$ ma, $i_2=200$ ma, $i_3=175$ ma).

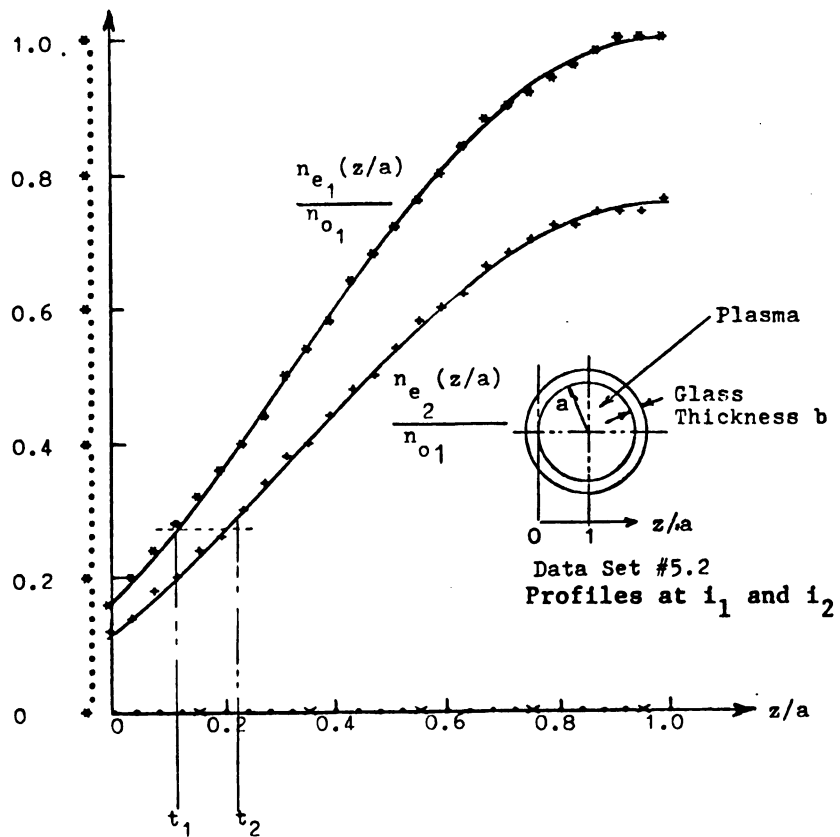
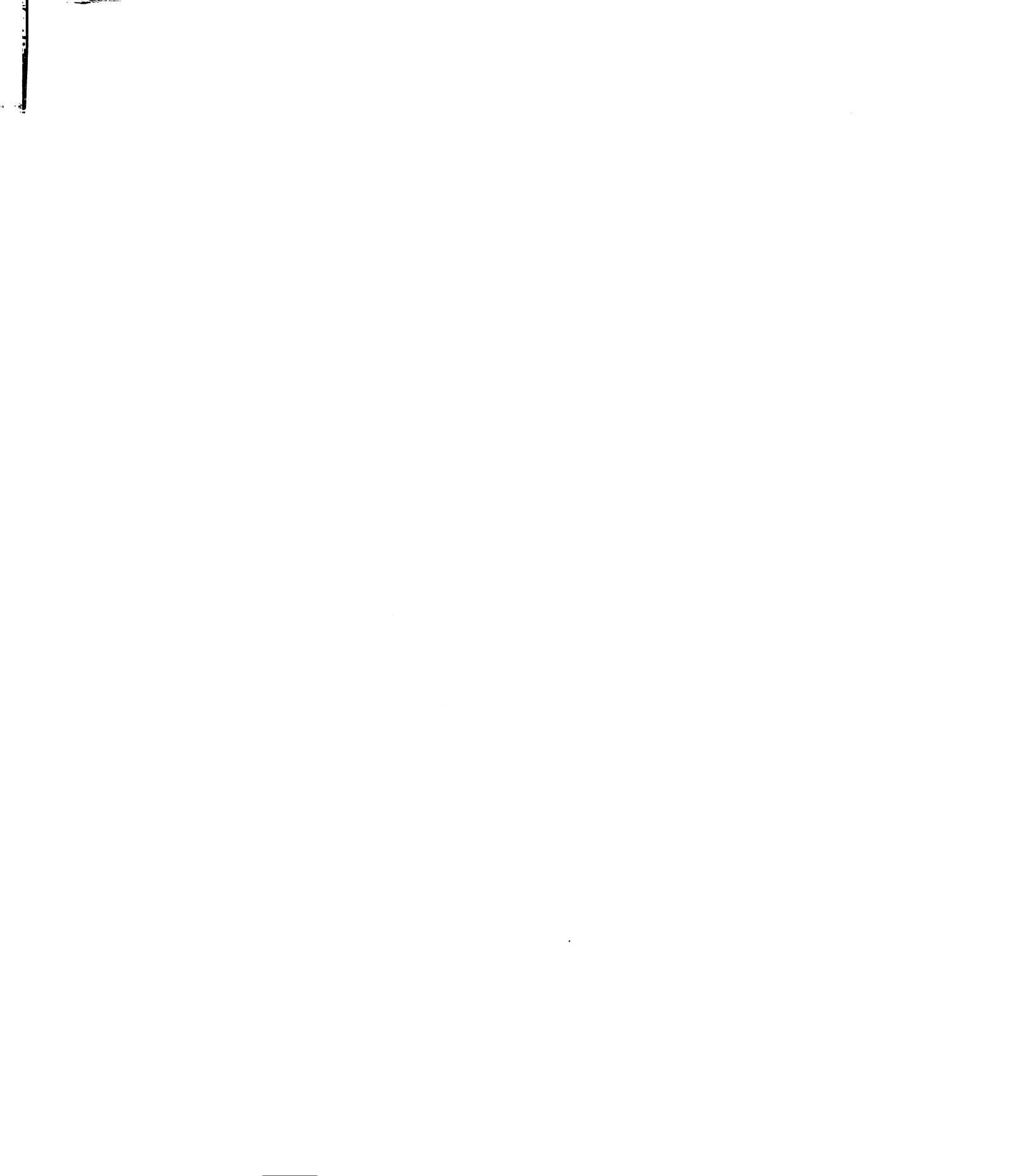


Fig. 4.3.13 Normalized Bessel series electron density profiles at resonances 1 and 2. Points t_1 and t_2 represent the critical points in the plasma sheath at which k_{p1} and k_{p2} respectively go to zero. Based on data set #5. ($f=1.917$ GHz, $i_d=270$ ma, $i_1=180$ ma, $i_2=135$ ma, $i_3=110$ ma).



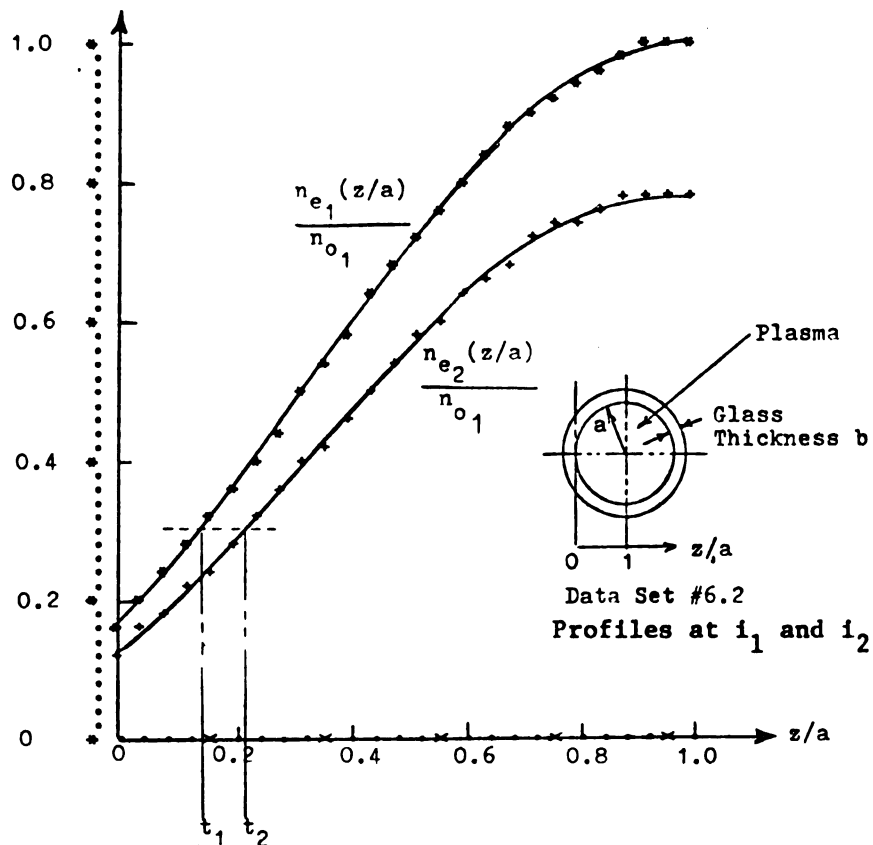


Fig. 4.3.14 Normalized Bessel series electron density profiles at resonances 1 and 2. Points t_1 and t_2 represent the critical points in the plasma sheath at which k_{p_1} and k_{p_2} respectively go to zero. Based on data set #6. ($f=2.017$ GHz, $i_d=285$ ma, $i_1=190$ ma, $i_2=150$ ma, $i_3=120$ ma).

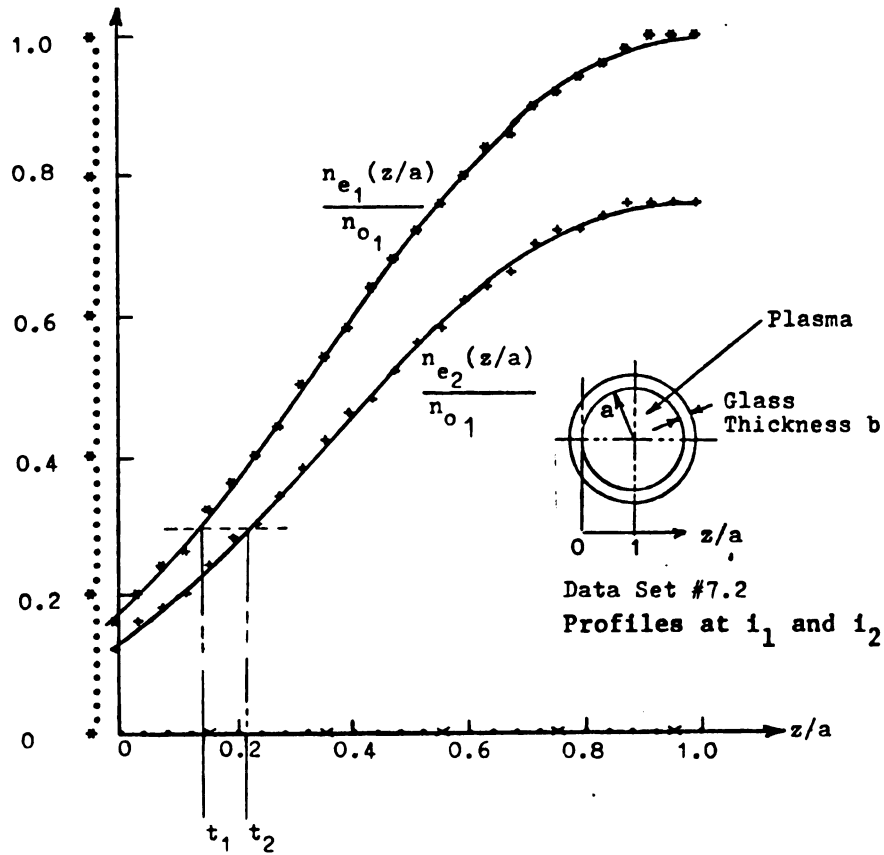


Fig. 4.3.15 Normalized Bessel series electron density profile at resonances 1 and 2. Points t_1 and t_2 represent the critical points in the plasma sheath at which k_{p1} and k_{p2} respectively go to zero. Based on data set #7. ($f=2.275$ GHz, $i_d=290$ ma, $i_1=195$ ma, $i_2=150$ ma, $i_3=120$ ma).

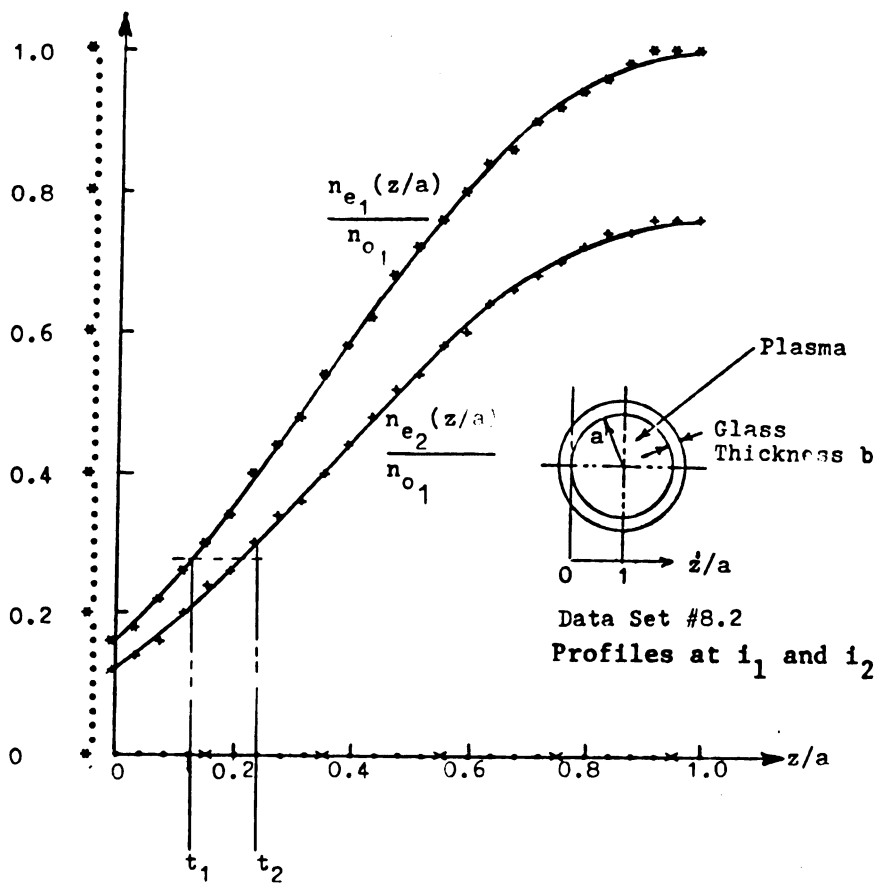


Fig. 4.3.16 Normalized Bessel series electron density profiles at resonances 1 and 2. Points t_1 and t_2 represent the critical points in the plasma sheath at which k_{p_1} and k_{p_2} respectively go to zero. Based on data set #8. ($f=2.322$ GHz, $i_d=320$ ma, $i_1=210$ ma, $i_2=160$ ma, $i_3=135$ ma).

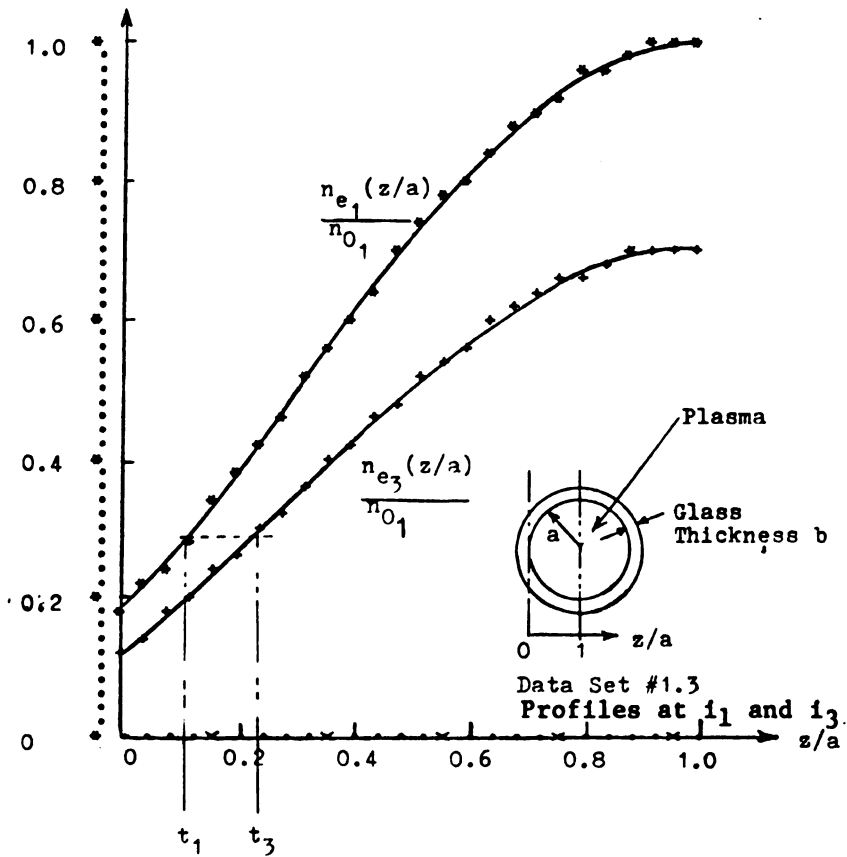


Fig. 4.3.17 Normalized Bessel series electron density profiles at resonances 1 and 3. Points t_1 and t_3 represent the critical points in the plasma sheath at which k_{p_1} and k_{p_3} respectively go to zero. Based on data set #1. ($f=2.016$ GHz, $i_d=270$ ma, $i_1=185$ ma, $i_2=150$ ma, $i_3=125$ ma).

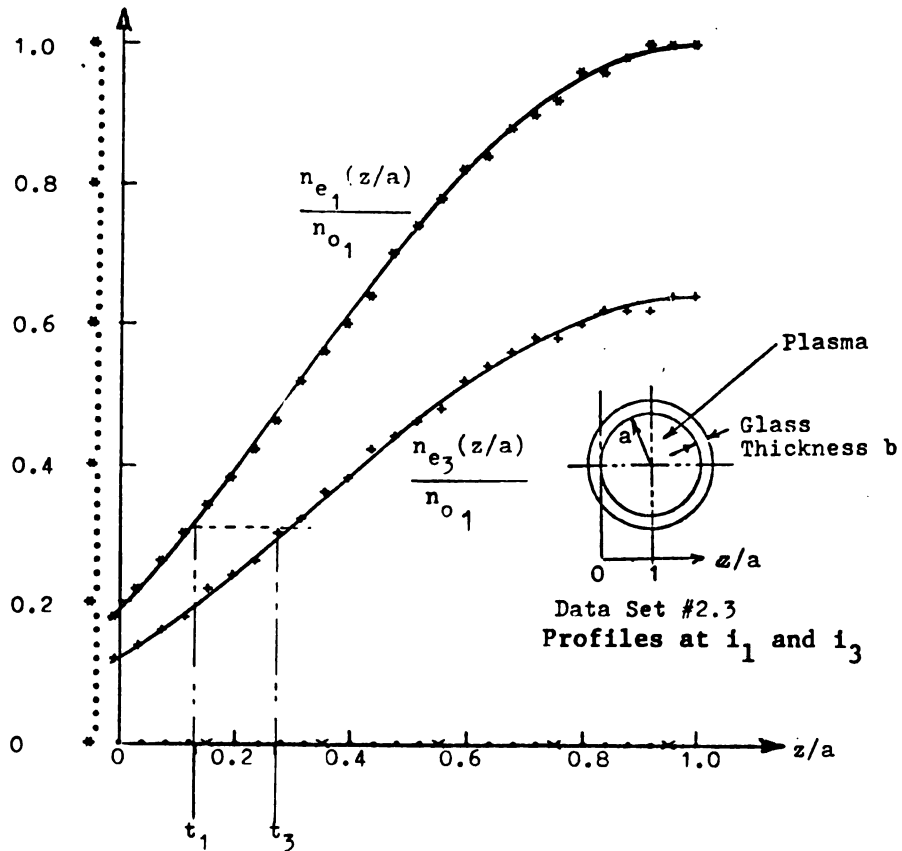


Fig. 4.3.18 Normalized Bessel series electron density profiles at resonances 1 and 3. Points t_1 and t_3 represent the critical points in the plasma sheath at which k_{p1} and k_{p3} respectively go to zero. Based on data set #2. ($f=2.10$ GHz, $i_d=290$ ma, $i_1=190$ ma, $i_2=150$ ma, $i_3=120$ ma).

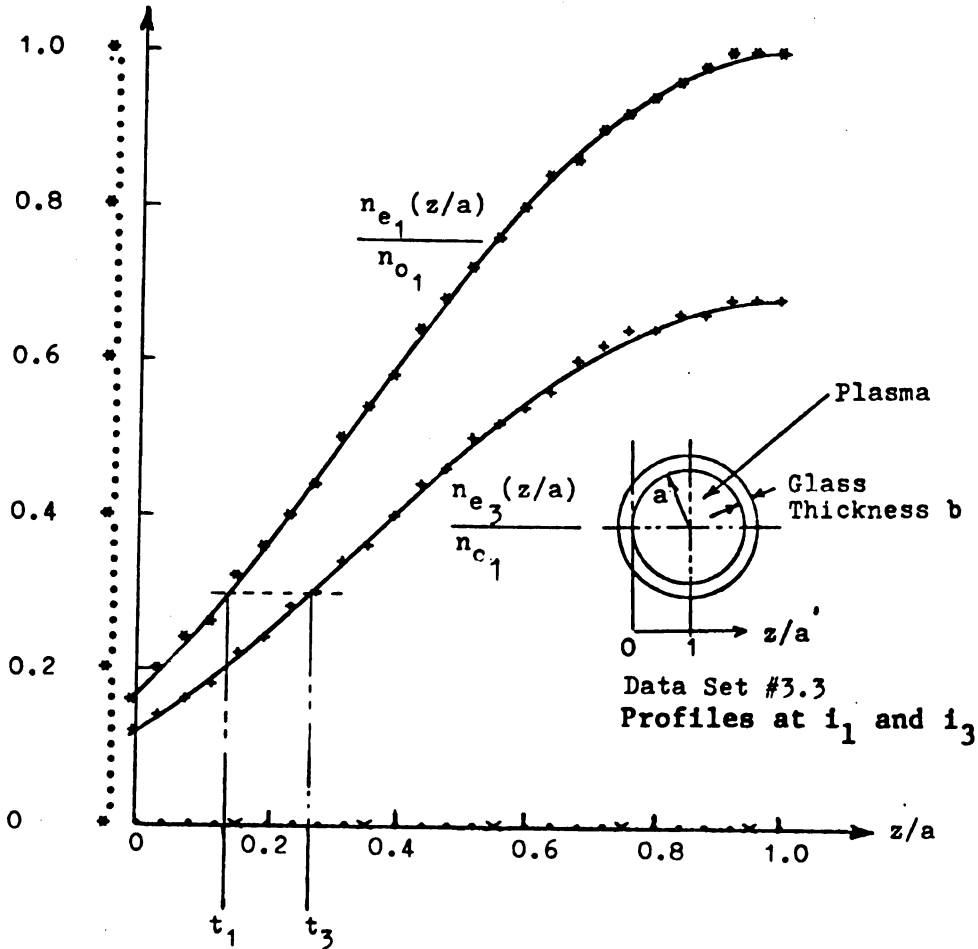


Fig. 4.3.19 Normalized Bessel series electron density profiles at resonances 1 and 3. Points t_1 and t_3 represent the critical points in the plasma sheath at which k_{p1} and k_{p3} respectively go to zero. Based on data set #3. ($f=2.23$ GHz, $i_d=340$ ma, $i_1=235$ ma, $i_2=185$ ma, $i_3=160$ ma).

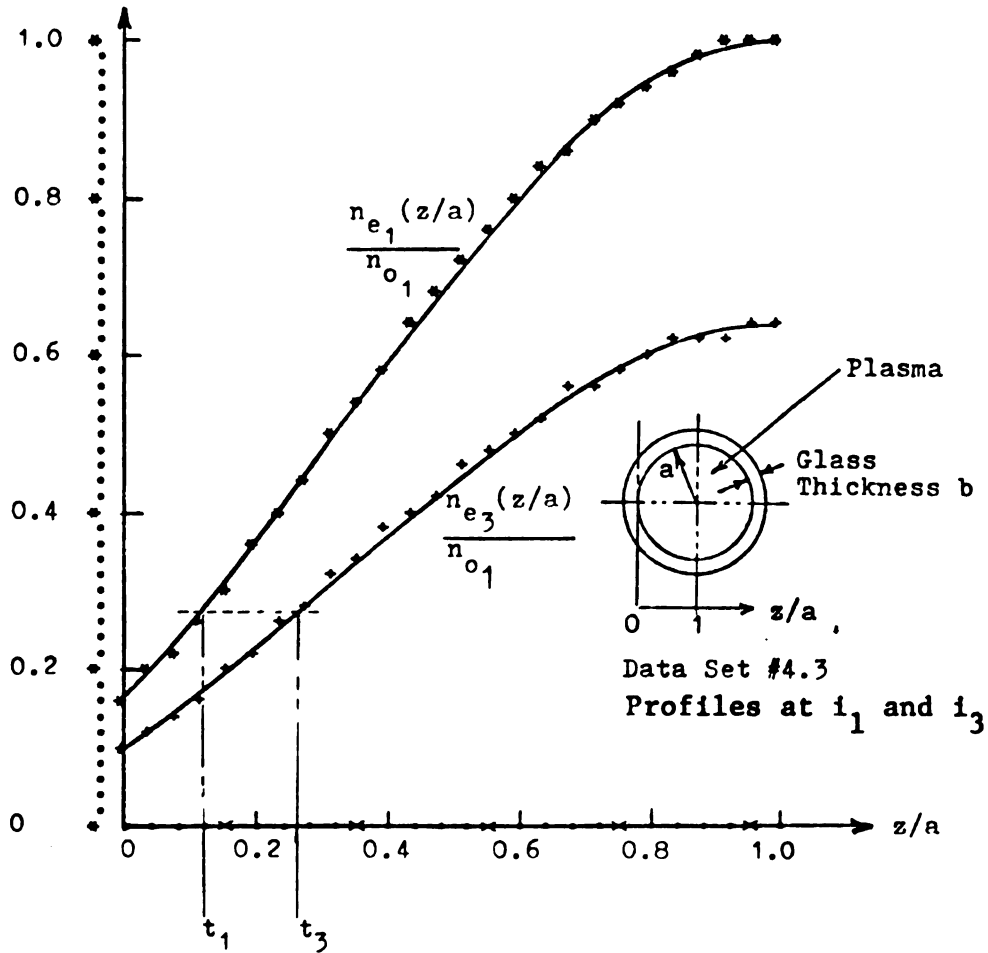


Fig. 4.3.20 Normalized Bessel series electron density profiles at resonances 1 and 3. Points t_1 and t_3 represent the critical points in the plasma sheath at which k_{p_1} and k_{p_3} respectively go to zero. Based on data set #4. ($f=2.32$ GHz, $i_d=355$ ma, $i_1=245$ ma, $i_2=200$ ma, $i_3=175$ ma).

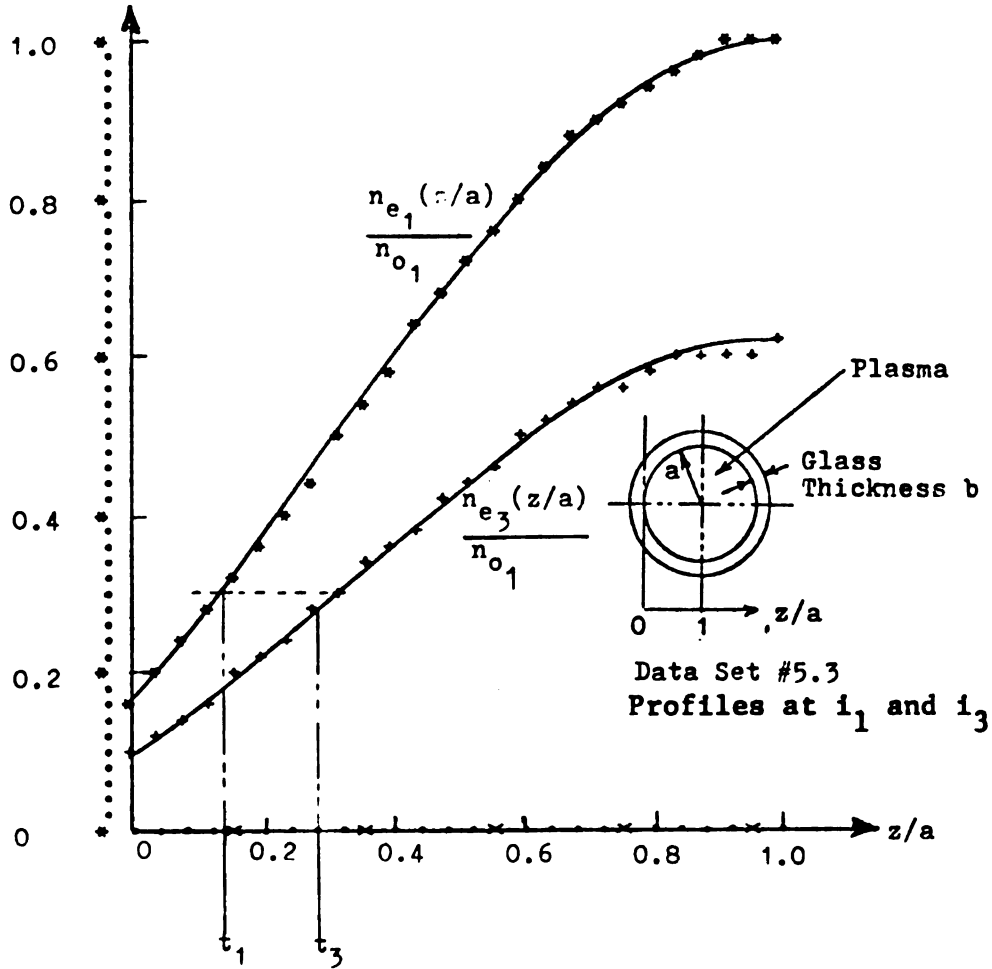


Fig. 4.3.21 Normalized Bessel series electron density profiles at resonances 1 and 3. Points t_1 and t_3 represent the critical points in the plasma sheath at which k_{p1} and k_{p3} respectively go to zero. Based on data set #5. ($f=1.917$ GHz, $i_d=270$ ma, $i_1=180$ ma, $i_2=135$ ma, $i_3=110$ ma).

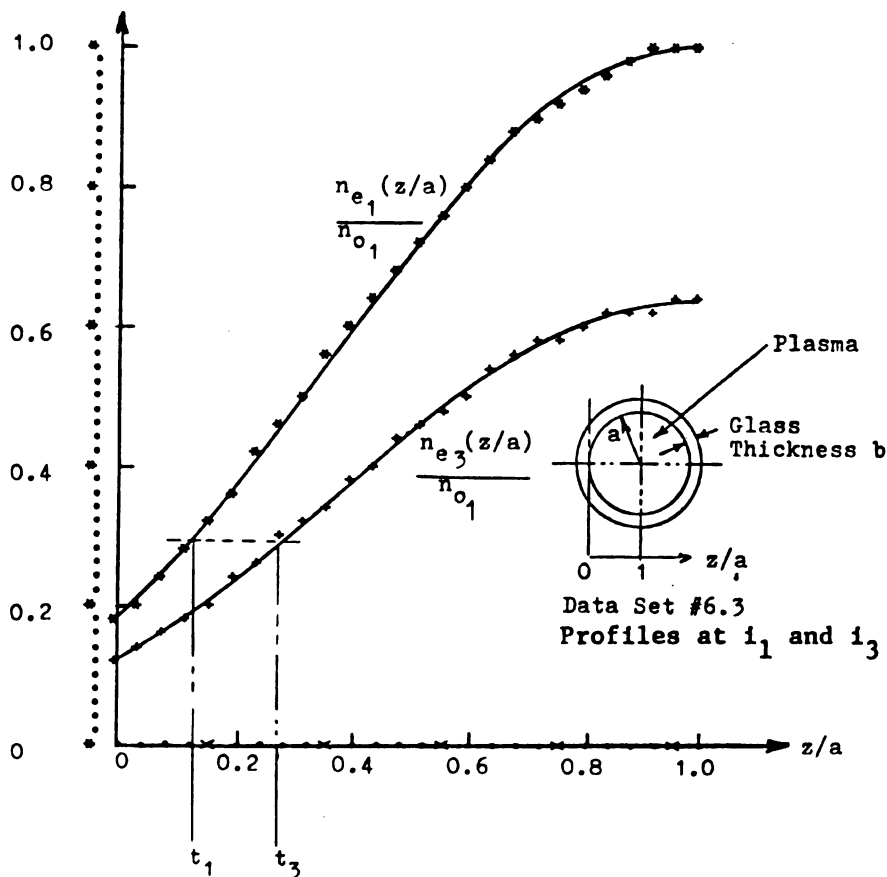


Fig. 4.3.22 Normalized Bessel series electron density profiles at resonances 1 and 3. Points t_1 and t_3 represent the critical points in the plasma sheath at which k_{p1} and k_{p3} respectively go to zero. Based on data set #6. ($f=2.017$ GHz, $i_d=285$ ma, $i_1=190$ ma, $i_2=150$ ma, $i_3=120$ ma).

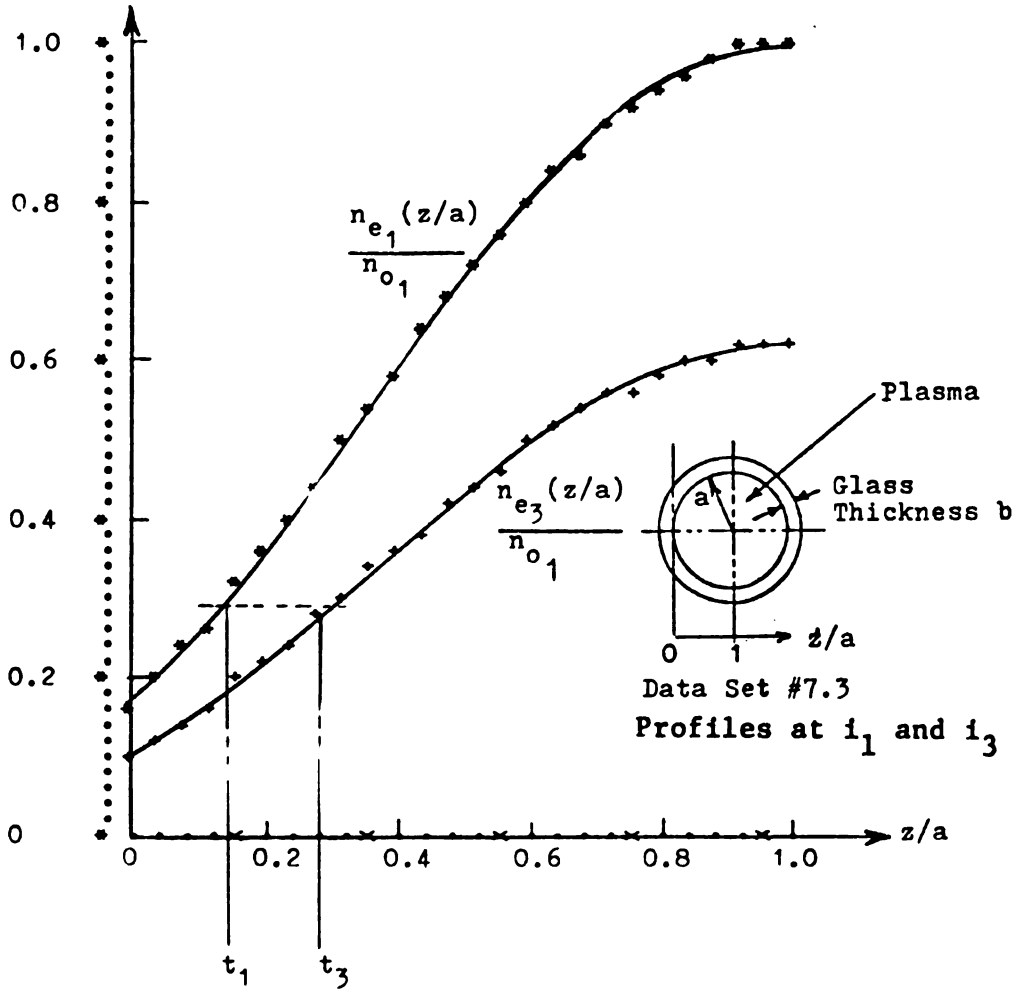


Fig. 4.3.23 Normalized Bessel series electron density profiles at resonances 1 and 3. Points t_1 and t_3 represent the critical points in the plasma sheath at which k_{p1} and k_{p3} respectively go to zero. Based on data set #7. ($f=2.275$ GHz, $i_d=290$ ma, $i_1=195$ ma, $i_2=150$ ma, $i_3=120$ ma).

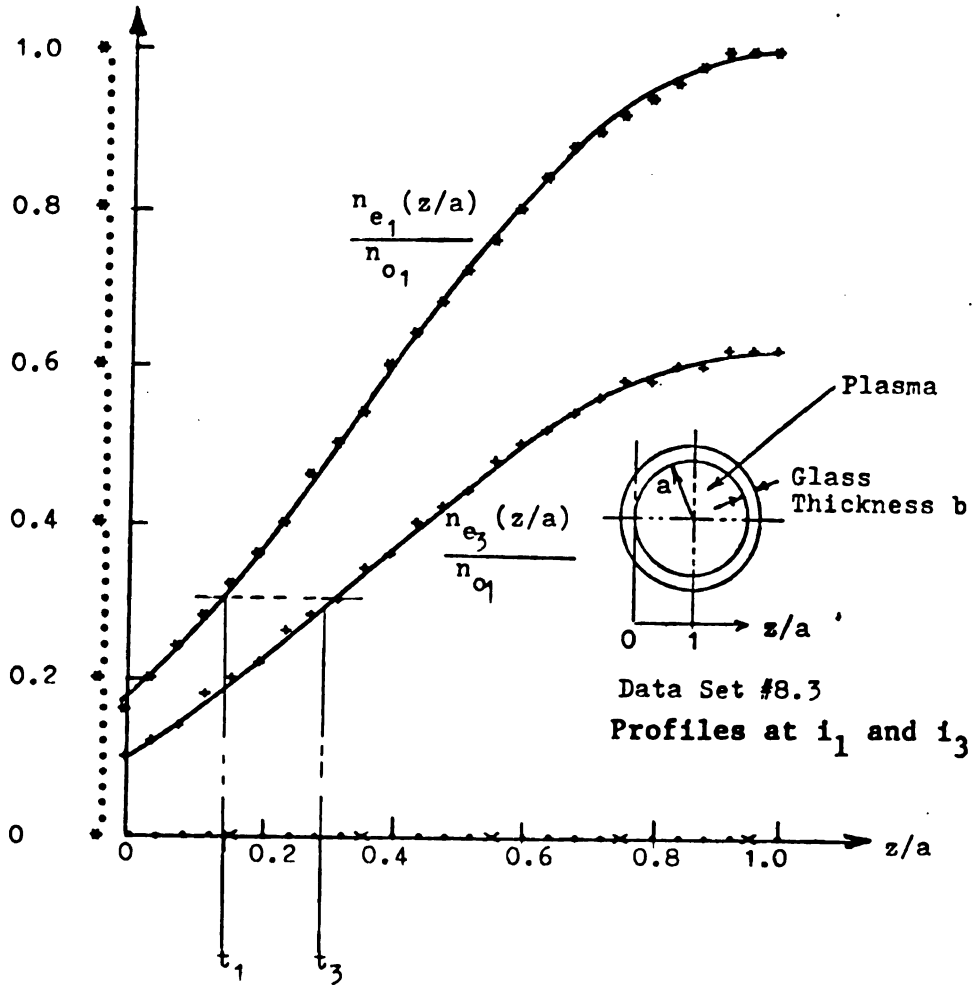


Fig. 4.3.24 Normalized Bessel series electron density profiles at resonances 1 and 3. Points t_1 and t_3 represent the critical points in the plasma sheath at which k_{p1} and k_{p3} respectively go to zero. Based on data set #8. ($f=2.322$ GHz, $i_d=320$ ma, $i_1=210$ ma, $i_2=160$ ma, $i_3=135$ ma).

the sheath region. More significantly, the ratio z_2/z_1 agrees well with observed values of approximately 1.5 from measurements of the corresponding E field peaks in the thermal resonances.¹⁴

4.4 Graphical Presentation of Thermal Resonances Using the WKB

Approximation

Since the static electron profile analysis was based on the phase integral in the underdense region, the WKB formulation for the m^{th} thermal resonance given in equation (2.65)

$$n_{1m}(x) = \frac{1}{k_{pm}(x)} \sin \left(\int_x^{x_m} k_{pm}(x') dx' + \pi/4 \right)$$

should yield the correct form of the m^{th} thermal resonance some distance away from the critical point. Here $x = 0$ at the wall and is positive into the plasma; $k_p(x)$ represents the phase constant as a function of x . The mathematical formulation of the phase integrals for the two profile formulations are, of course, different. For the parabolic profile it is based on equations (3.40) and (3.41) and is

$$\int_x^{x_m} k_p(x') dx' = \int_x^{x_m} \frac{\omega}{v_o} \left(1 - \frac{e^2 n_{om}}{\omega^2 m_e \epsilon_o} \left(1 - \alpha \left(\frac{r}{a} \right)^2 \right) \right)^{1/2} dx \quad (4.1)$$

For the Bessel function approximation the phase integral is based on equation (3.77) and is

$$\int_x^{x_m} k_p(x') dx' = \int_x^{x_m} \frac{\omega}{v_o} \left(1 - \frac{e^2 n_{o_m}}{\omega^2 \epsilon_o} \exp(1 - I_o(\gamma r))\right)^{1/2} dr \quad (4.2)$$

Based on these phase integrals, the WKB form

$$n_{1_m}(x) = \frac{1}{k_{p_m}(x)} \left(\int_x^{x_m} k_{p_m}(x) dx + \pi/4 \right) \quad (4.3)$$

is numerically evaluated and graphically presented in Figures 4.4.1 and 4.4.2 for the parabolic form and in Figures 4.4.3 and 4.4.4 for the Bessel function formulation for data set #1. The Figures show the first and second resonance. In the region near the critical point where the WKB approximation fails, the expected section is sketched in for completeness and does not represent a precise solution. The interesting point is the phase of the perturbation function $n_{1_m}(x)$. The basic theory suggested that $n_{1_m}(0)$ at the wall ($x = 0$) has a maximum so that a peak should be observed. In fact, for the Bessel function formulation $n_{1_1}(x)$ and $n_{1_2}(x)$ fall slightly short of reaching a peak, while the parabolic approximation is slightly over the expected peak. It should be recalled that the numerical analysis was based on the assumption that the total phase for $n_{1_m}(x)$ between $x = 0$ and x_m is $(m + 1/4)\pi$.

The deviation from the expected phase of $n_{1_m}(0)$ at the wall indicates a limitation in the accuracy of the numerical integration techniques. Greater precision would not yield significant improvement in the electron density profile in view of the approximate nature of the available resonance data. It would, however, require

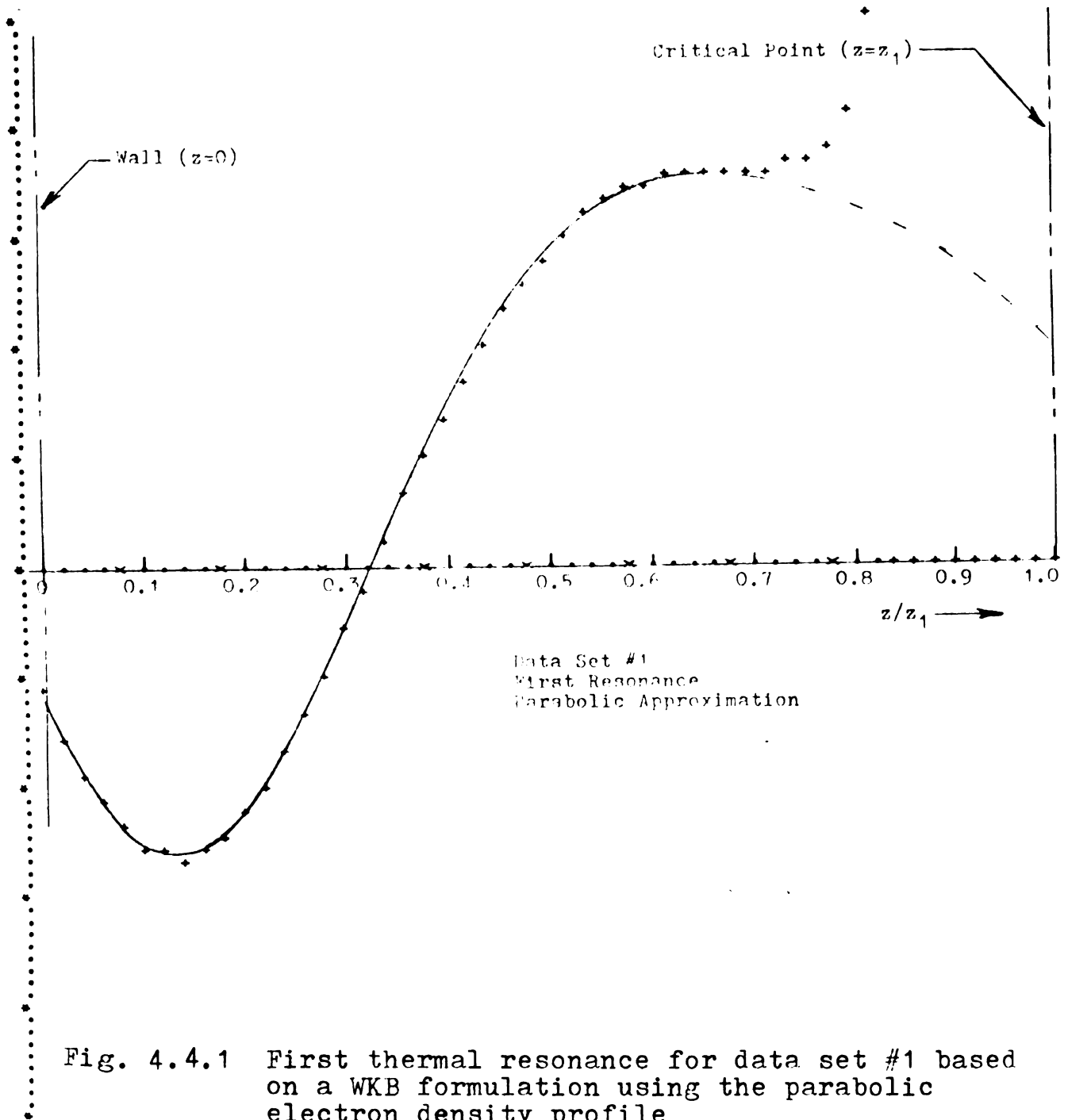


Fig. 4.4.1 First thermal resonance for data set #1 based on a WKB formulation using the parabolic electron density profile.

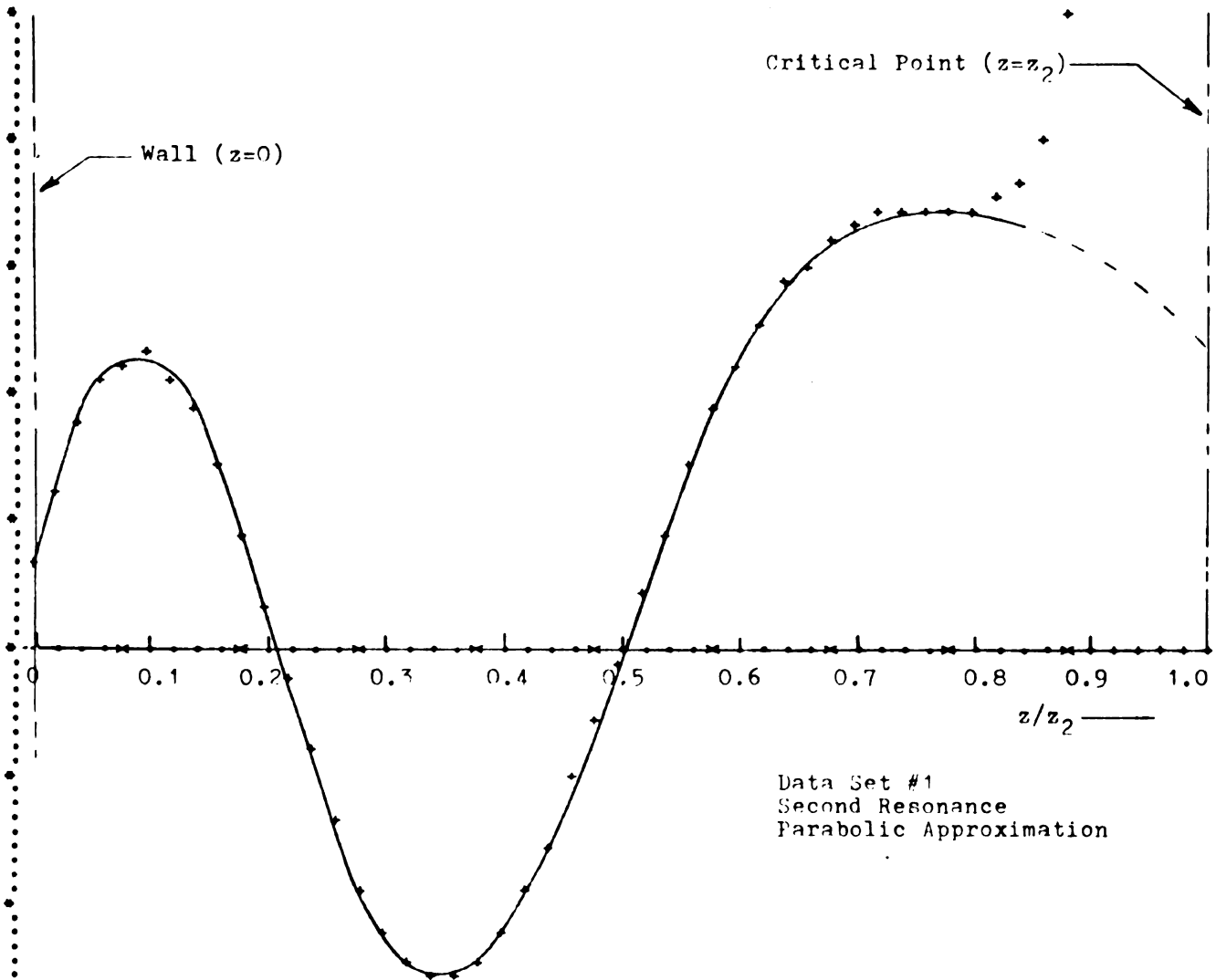


Fig. 4.4.2 Second thermal resonance for data set #1 based on a WKB formulation using the parabolic electron density profile.

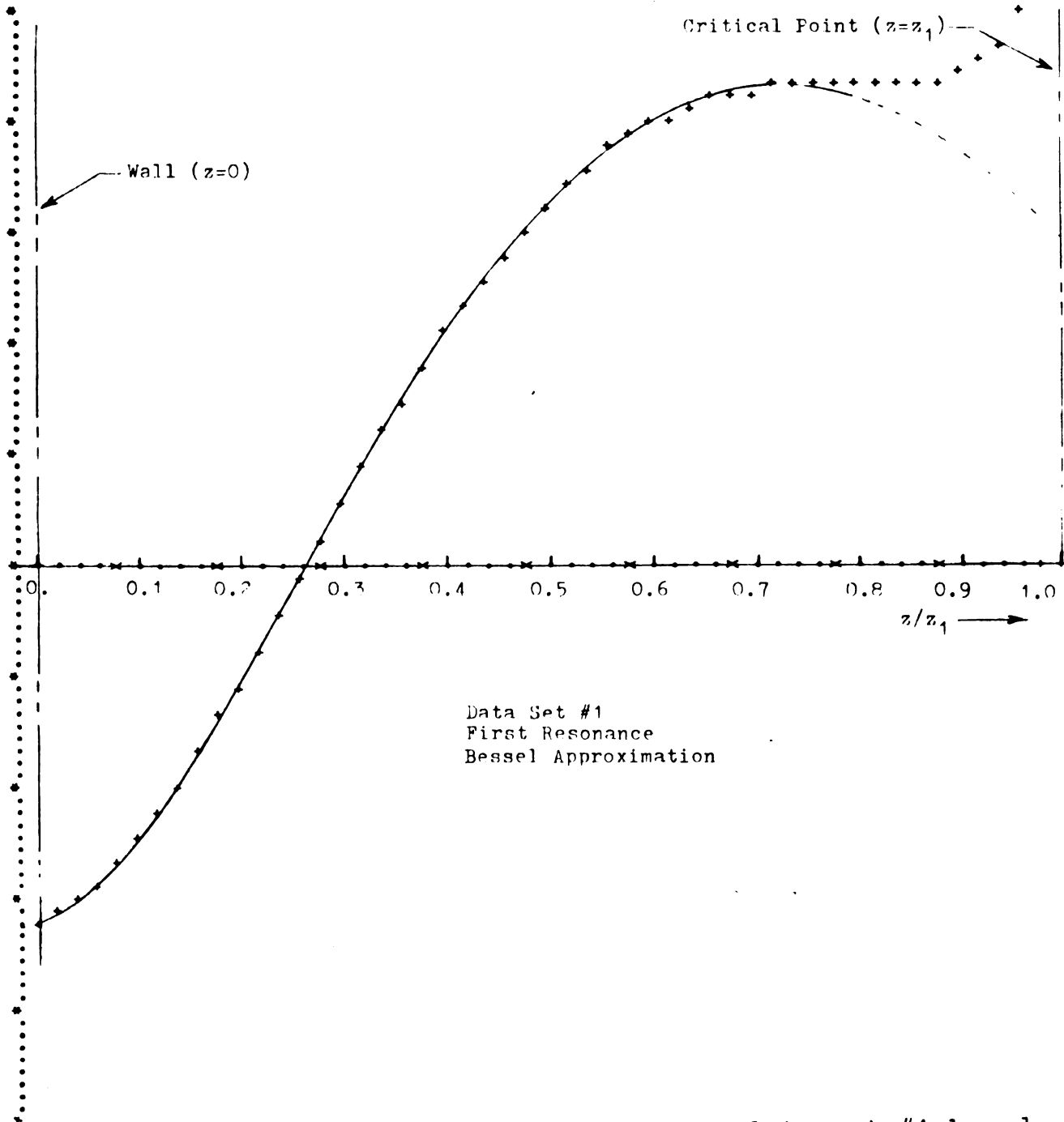


Fig. 4.4.3 First thermal resonance for data set #1 based on a WKB formulation using the Bessel series electron density profile.

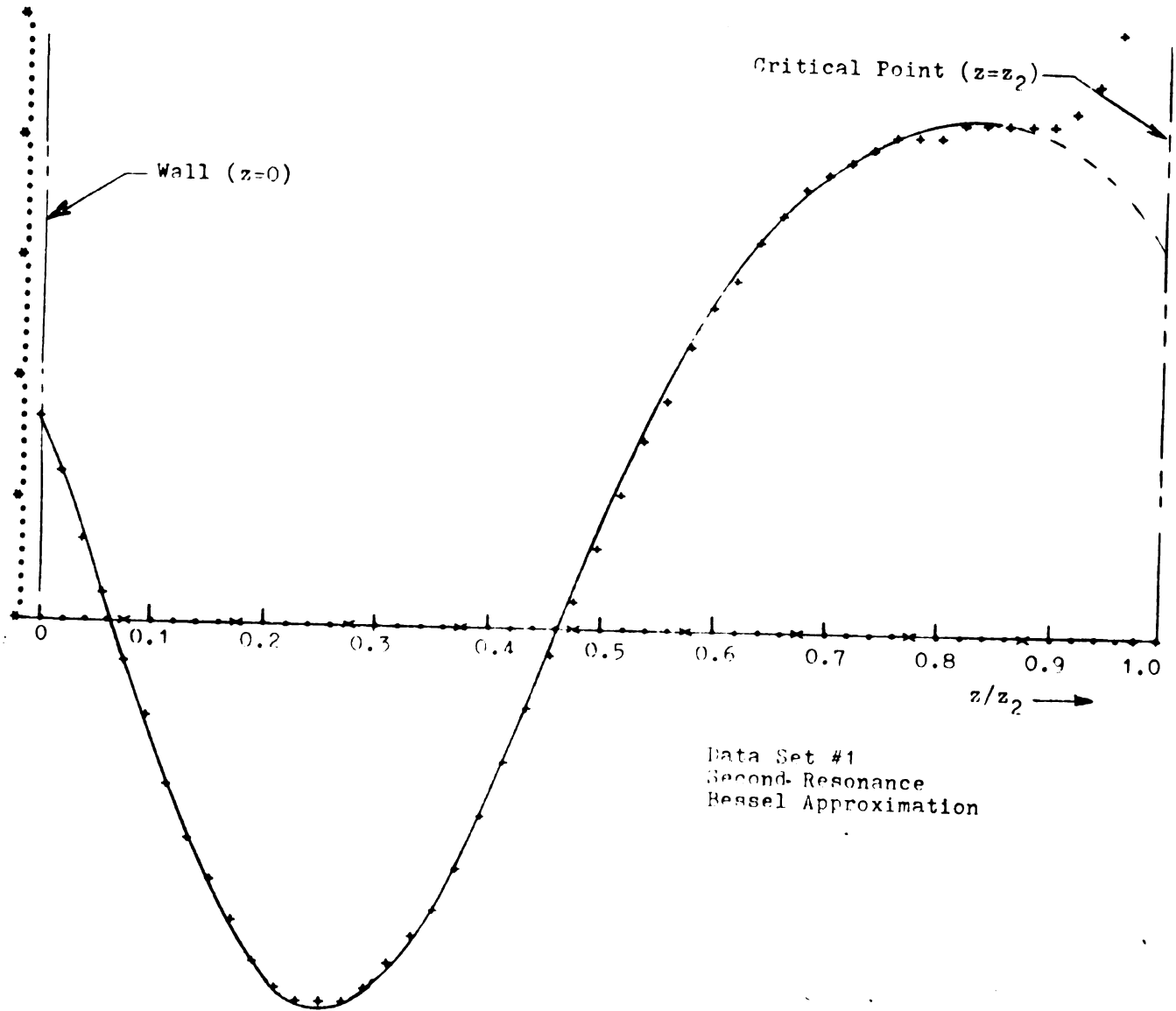


Fig. 4.4.4 Second thermal resonance for data set #1 based on a WKB formulation using the Bessel series electron density profile.

unreasonably long computer run times in view of the large number of parameters determined simultaneously.

Figures 4.4.1 through 4.4.4 do show that, as expected, the phase constant decreases and the magnitude of $n_{1_m}(x)$ increases as x goes from $x = 0$ to $x = x_m$.

APPENDIX A

NUMERICAL COMPUTER READOUTS AND
ADDITIONAL COMPUTER GRAPHS

NUMBER OF DATA SET = 1

THIS IS AN ANALYSIS OF THE ELECTRON DENSITY
IN A CYLINDRICAL PLASMA COLUMN BASED ON A
PARABOLIC DENSITY PROFILE APPROXIMATION
USING RESONANCES 1 AND 2

THE PHASE FOR RESONANCE 1 IS PI TIMES 1.25
THE PHASE FOR RESONANCE 2 IS PI TIMES 2.25

THE SQUARE OF WPOVER W IS EQUAL TO 2.60

ID	=	0.2700E 00
I1	=	0.1850E 00
I2	=	0.1500E 00
W	=	0.1267E 11
BETA=ATOR	=	0.1000E 01
RADIUS	=	0.7000E-02

ALFA	=	0.3259E 00
------	---	------------

R1	=	0.6160E-02
R2	=	0.5787E-02
Z1	=	0.8400E-03
Z2	=	0.1213E-02
NO DIPOLE	=	0.2233E 18
NO 1 RESONANCE	=	0.1530E 18
NO 2 RESONANCE	=	0.1241E 18
Z2 TO Z1	=	0.1444E 01
PEAK TO AVERAGE	=	0.1703E 01
V WALL	=	-0.2210E 01
ETA=VW TO KTTGQ	=	-0.1748E 01
ELECTRON TEMP	=	0.1467E 05

7
8
9
10
11
12
13
14
15
16
17
18
19
20
21
22
23
24
25
26
27
28
29
30
31
32
33
34
35
36
37
38
39
40
41
42
43
44
45
46
47
48
49
50
51

NUMBER OF DATA SET = 1

THIS IS AN ANALYSIS OF THE ELECTRON DENSITY
IN A CYLINDRICAL PLASMA COLUMN BASED ON A
PARABOLIC DENSITY PROFILE APPROXIMATION
USING RESONANCES 1 AND 3

THE PHASE FOR RESONANCE 1 IS PI TIMES 1.25
THE PHASE FOR RESONANCE 2 IS PI TIMES 3.25

THE SQUARE OF ω OVER ω IS EQUAL TO 2.60

ID	=	0.2700E 00
I1	=	0.1850E 00
I2	=	0.1250E 00
W	=	0.1267E 11
BETA=ATJR	=	0.1000E 01
RADIUS	=	0.7000E-02

ALFA	=	0.8259E 00
------	---	------------

R1	=	0.6160E-02
R2	=	0.5366E-02
Z1	=	0.8400E-03
Z2	=	0.1634E-02
NO DIPOLE	=	0.2233E 18
NO 1 RESONANCE	=	0.1530E 18
NO 2 RESONANCE	=	0.1034E 18
Z2 TC Z1	=	0.1945E 01
PEAK TO AVERAGE	=	0.1703E 01
V WALL	=	-0.2210E 01
ETA=VW TO KTTOQ	=	-0.1748E 01
ELECTRON TEMP	=	0.1467E 05

```

1  NUMBER OF DATA SET      =    2
2
3
4
5
6
7
8
9
10
11  THIS IS AN ANALYSIS OF THE ELECTRON DENSITY
12  IN A CYLINDRICAL PLASMA COLUMN BASED ON A
13  PARABOLIC DENSITY PROFILE APPROXIMATION
14  USING RESONANCES 1 AND 2
15
16  THE PHASE FOR RESONANCE 1 IS PI TIMES 1.25
17  THE PHASE FOR RESONANCE 2 IS PI TIMES 2.25
18
19  THE SQUARE OF WPOVER W IS EQUAL TO 2.60
20
21
22
23  ID          =      0.2900E 00
24  I1          =      0.1900E 00
25  I2          =      0.1500E 00
26  W           =      0.1319E 11
27  BETA=ATDR  =      0.1000E 01
28  RADIUS      =      0.7000E-02
29
30
31
32  ALFA        =      0.8218E 00
33
34
35
36  R1          =      0.6090E-02
37  R2          =      0.5633E-02
38  Z1          =      0.9100E-03
39  Z2          =      0.1367E-02
40  NO DIPOLE   =      0.2412E 18
41  NO 1 RESONANCE =      0.1580E 18
42  NO 2 RESONANCE =      0.1248E 18
43  Z2 TO Z1    =      0.1502E 01
44  PEAK TO AVERAGE =      0.1697E 01
45  V WALL      =      -0.2965E 01
46  ETA=VW TO KTDO =      -0.1725E 01
47  ELECTRON TEMP =      0.1996E 05
48
49
50
51

```

NUMBER OF DATA SET = 2

THIS IS AN ANALYSIS OF THE ELECTRON DENSITY
IN A CYLINDRICAL PLASMA COLUMN BASED ON A
PARABOLIC DENSITY PROFILE APPROXIMATION
USING RESONANCES 1 AND 3

THE PHASE FOR RESONANCE 1 IS PI TIMES 1.25
THE PHASE FOR RESONANCE 2 IS PI TIMES 3.25

THE SQUARE OF ω OVER ω IS EQUAL TO 2.60

ID	=	0.2900E 00
I1	=	0.1900E 00
I2	=	0.1200E 00
W	=	0.1319E 11
BETA=ATOR	=	0.1000E 01
RADIUS	=	0.7000E-02

ALFA	=	0.8511E 00
------	---	------------

R1	=	0.6020E-02
R2	=	0.5023E-02
Z1	=	0.9800E-03
Z2	=	0.1977E-02
NO DIPOLE	=	0.2474E 18
NO 1 RESONANCE	=	0.1621E 18
NO 2 RESONANCE	=	0.1024E 18
Z2 TO Z1	=	0.2018E 01
PEAK TO AVERAGE	=	0.1741E 01
V WALL	=	-0.5189E 01
ETA=VW TO KTTQ	=	-0.1904E 01
ELECTRON TEMP	=	0.3163E 05

7
8
9
10
11 NUMBER OF DATA SET = 3

12 THIS IS AN ANALYSIS OF THE ELECTRON DENSITY
13 IN A CYLINDRICAL PLASMA COLUMN BASED ON A
14 PARABOLIC DENSITY PROFILE APPROXIMATION
15 USING RESONANCES 1 AND 2

16 THE PHASE FOR RESONANCE 1 IS PI TIMES 1.25
17 THE PHASE FOR RESONANCE 2 IS PI TIMES 2.25

18
19 THE SQUARE OF WPOVER W IS EQUAL TO 2.60
20
21

22 ID = 0.3400E 00
23 I1 = 0.2350E 00
24 I2 = 0.1850E 00
25 W = 0.1401E 11
26 BETA=ATOR = 0.1000E 01
27 RADIUS = 0.7000E-02
28
29

30
31 ALFA = 0.8317E 00
32
33

34
35 R1 = 0.6160E-02
36 R2 = 0.5735E-02
37 Z1 = 0.8400E-03
38 Z2 = 0.1265E-02
39 NO DIPOLE = 0.2745E 18
40 NO 1 RESONANCE = 0.1897E 18
41 NO 2 RESONANCE = 0.1493E 18
42 Z2 TO Z1 = 0.1506E 01
43 PEAK TO AVERAGE = 0.1712E 01
44 V WALL = -0.2909E 01
45 ETA=VW TO KTTOQ = -0.1782E 01
46 ELECTRON TEMP = 0.1895E 05
47
48
49
50
51

7
8
9
10
11 NUMBER OF DATA SET = 3

12 THIS IS AN ANALYSIS OF THE ELECTRON DENSITY
13 IN A CYLINDRICAL PLASMA COLUMN BASED ON A
14 PARABOLIC DENSITY PROFILE APPROXIMATION
15 USING RESONANCES 1 AND 3

16 THE PHASE FOR RESONANCE 1 IS PI TIMES 1.25
17 THE PHASE FOR RESONANCE 2 IS PI TIMES 3.25

18 THE SQUARE OF WPOVER W IS EQUAL TO 2.60

19
20
21
22
23 ID = 0.3400E 00
24 I1 = 0.2350E 00
25 I2 = 0.1600E 00
26 W = 0.1401E 11
27 BETA=ATOR = 0.1000E 01
28 RADIUS = 0.7000E-02

29
30
31 ALFA = 0.8317E 00

32
33
34 R1 = 0.6160E-02
35 R2 = 0.5403E-02
36 Z1 = 0.8400E-03
37 Z2 = 0.1597E-02
38 NO DIPOLE = 0.2745E 18
39 NO 1 RESONANCE = 0.1897E 18
40 NO 2 RESONANCE = 0.1292E 18
41 Z2 TO Z1 = 0.1901E 01
42 PEAK TO AVERAGE = 0.1712E 01
43 V WALL = -0.2909E 01
44 ETA=VW TO KTTQ = -0.1782E 01
45 ELECTRON TEMP = 0.1895E 05
46
47
48
49
50
51

7
8
9
10
11
12
13
14
15
16
17
18
19
20
21
22
23
24
25
26
27
28
29
30
31
32
33
34
35
36
37
38
39
40
41
42
43
44
45
46
47
48
49
50
51

NUMBER OF DATA SET = 4

THIS IS AN ANALYSIS OF THE ELECTRON DENSITY
IN A CYLINDRICAL PLASMA COLUMN BASED ON A
PARABOLIC DENSITY PROFILE APPROXIMATION
USING RESONANCES 1 AND 2

THE PHASE FOR RESONANCE 1 IS PI TIMES 1.25
THE PHASE FOR RESONANCE 2 IS PI TIMES 2.25

THE SQUARE OF WPOVER W IS EQUAL TO 2.60

ID	=	0.3550E 00
I1	=	0.2450E 00
I2	=	0.2000E 00
W	=	0.1458E 11
BETA=ATOR	=	0.1000E 01
RADIUS	=	0.7000E-02

ALFA	=	0.8040E 00
------	---	------------

R1	=	0.6230E-02
R2	=	0.5861E-02
Z1	=	0.7700E-03
Z2	=	0.1139E-02
NO DIPOLE	=	0.2904E 18
NO 1 RESONANCE	=	0.2004E 18
NO 2 RESONANCE	=	0.1636E 18
Z2 TO Z1	=	0.1479E 01
PEAK TO AVERAGE	=	0.1672E 01
V WALL	=	-0.1627E 01
ETA=VW TO KTTQ	=	-0.1630E 01
ELECTRON TEMP	=	0.1159E 05

```

NUMBER OF DATA SET      =    4

THIS IS AN ANALYSIS OF THE ELECTRON DENSITY
IN A CYLINDRICAL PLASMA COLUMN BASED ON A
PARABOLIC DENSITY PROFILE APPROXIMATION
USING RESONANCES 1 AND 3

THE PHASE FOR RESONANCE 1 IS PI TIMES 1.25
THE PHASE FOR RESONANCE 2 IS PI TIMES 3.25

THE SQUARE OF WPOVER W IS EQUAL TO 2.60

ID          =      0.3550E 00
I1          =      0.2450E 00
I2          =      0.1550E 00
W           =      0.1458E 11
BETA=ATOR  =      0.1000E 01
RADIUS     =      0.7000E-02

ALFA       =      0.8589E 00

R1         =      0.6090E-02
R2         =      0.5179E-02
Z1         =      0.9100E-03
Z2         =      0.1821E-02
NO DIPOLE  =      0.3043E 18
NO 1 RESONANCE =      0.2100E 18
NO 2 RESONANCE =      0.1329E 18
Z2 TO Z1   =      0.2001E 01
PEAK TO AVERAGE =      0.1753E 01
V WALL     =      -0.5579E 01
ETA=VW TO KTTQ =      -0.1959E 01
ELECTRON TEMP =      0.3307E 05

```

7
8
9
10
11
12
13
14
15
16
17
18
19
20
21
22
23
24
25
26
27
28
29
30
31
32
33
34
35
36
37
38
39
40
41
42
43
44
45
46
47
48
49
50
51

NUMBER OF DATA SET = 5

THIS IS AN ANALYSIS OF THE ELECTRON DENSITY
IN A CYLINDRICAL PLASMA COLUMN BASED ON A
PARABOLIC DENSITY PROFILE APPROXIMATION
USING RESONANCES 1 AND 2

THE PHASE FOR RESONANCE 1 IS PI TIMES 1.25
THE PHASE FOR RESONANCE 2 IS PI TIMES 2.25

THE SQUARE OF $w_{\text{POVER W}}$ IS EQUAL TO 2.60

ID	=	0.2700E 00
I1	=	0.1800E 00
I2	=	0.1350E 00
W	=	0.1204E 11
BETA=ATOR	=	0.1000E 01
RADIUS	=	0.7000E-02

ALFA	=	0.8641E 00
------	---	------------

R1	=	0.6020E-02
R2	=	0.5496E-02
Z1	=	0.9800E-03
Z2	=	0.1504E-02
NO DIPOLE	=	0.2085E 18
NO 1 RESONANCE	=	0.1390E 18
NO 2 RESONANCE	=	0.1042E 18
Z2 TO Z1	=	0.1534E 01
PEAK TO AVERAGE	=	0.1761E 01
V WALL	=	-0.4987E 01
ETA=VW TO KTTQ	=	-0.1996E 01
ELECTRON TEMP	=	0.2900E 05

7
8
9
10
11
12
13
14
15
16
17
18
19
20
21
22
23
24
25
26
27
28
29
30
31
32
33
34
35
36
37
38
39
40
41
42
43
44
45
46
47
48
49
50
51

NUMBER OF DATA SET = 5

THIS IS AN ANALYSIS OF THE ELECTRON DENSITY
IN A CYLINDRICAL PLASMA COLUMN BASED ON A
PARABOLIC DENSITY PROFILE APPROXIMATION
USING RESONANCES 1 AND 3

THE PHASE FOR RESONANCE 1 IS PI TIMES 1.25
THE PHASE FOR RESONANCE 2 IS PI TIMES 3.25

THE SQUARE OF WPOVER W IS EQUAL TO 2.60

ID	=	0.2700E 00
I1	=	0.1800E 00
I2	=	0.1100E 00
W	=	0.1204E 11
BETA=ATOR	=	0.1000E 01
RADIUS	=	0.7000E-02

ALFA	=	0.8641E 00
------	---	------------

R1	=	0.6020E-02
R2	=	0.4974E-02
Z1	=	0.9800E-03
Z2	=	0.2026E-02
NO DIPOLE	=	0.2085E 18
NO 1 RESONANCE	=	0.1390E 18
NO 2 RESONANCE	=	0.8494E 17
Z2 TO Z1	=	0.2067E 01
PEAK TO AVERAGE	=	0.1761E 01
V WALL	=	-0.4987E 01
ETA=VW TO KTTQ	=	-0.1996E 01
ELECTRON TEMP	=	0.2900E 05

NUMBER OF DATA SET = 6

THIS IS AN ANALYSIS OF THE ELECTRON DENSITY
 IN A CYLINDRICAL PLASMA COLUMN BASED ON A
 PARABOLIC DENSITY PROFILE APPROXIMATION
 USING RESONANCES 1 AND 2

THE PHASE FOR RESONANCE 1 IS PI TIMES 1.25
 THE PHASE FOR RESONANCE 2 IS PI TIMES 2.25

THE SQUARE OF ω OVER ω IS EQUAL TO 2.60

ID	=	0.2850E 00
I1	=	0.1900E 00
I2	=	0.1500E 00
W	=	0.1267E 11
BETA=ATOR	=	0.1000E 01
RADIUS	=	0.7000E-02

ALFA	=	0.8346E 00
------	---	------------

R1	=	0.6090E-02
R2	=	0.5653E-02
Z1	=	0.9100E-03
Z2	=	0.1347E-02
NO DIPOLE	=	0.2250E 18
NO 1 RESONANCE	=	0.1500E 18
NO 2 RESONANCE	=	0.1184E 18
Z2 TO Z1	=	0.1480E 01
PEAK TO AVERAGE	=	0.1716E 01
V WALL	=	-0.3176E 01
ETA=VW TO KTT00	=	-0.1800E 01
ELECTRON TEMP	=	0.2048E 05

7
8
9
10
11 NUMBER OF DATA SET = 6

12 THIS IS AN ANALYSIS OF THE ELECTRON DENSITY
13 IN A CYLINDRICAL PLASMA COLUMN BASED ON A
14 PARABOLIC DENSITY PROFILE APPROXIMATION
15 USING RESONANCES 1 AND 3

16 THE PHASE FOR RESONANCE 1 IS PI TIMES 1.25
17 THE PHASE FOR RESONANCE 2 IS PI TIMES 3.25

18
19 THE SQUARE OF WPOVER W IS EQUAL TO 2.60
20
21

22 ID = 0.2850E 00
23 I1 = 0.1900E 00
24 I2 = 0.1200E 00
25 W = 0.1267E 11
26 BETA=ATOR = 0.1C00E 01
27 RADIUS = 0.7C00E-02
28
29
30

31
32 ALFA = 0.8346E 00
33
34

35 R1 = 0.6090E-02
36 R2 = 0.5087E-02
37 Z1 = 0.9100E-03
38 Z2 = 0.1913E-02
39 NO DIPOLE = 0.2250E 18
40 NO 1 RESONANCE = 0.1500E 18
41 NO 2 RESONANCE = 0.9475E 17
42 Z2 TO Z1 = 0.2102E 01
43 PEAK TO AVERAGE = 0.1716E 01
44 V WALL = -0.3176E 01
45 ETA=VW TO KTT00 = -0.1800E 01
46 ELECTRON TEMP = 0.2048E 05
47
48
49
50
51

8 NUMBER OF DATA SET = 7

11 THIS IS AN ANALYSIS OF THE ELECTRON DENSITY
 12 IN A CYLINDRICAL PLASMA COLUMN BASED ON A
 13 PARABOLIC DENSITY PROFILE APPROXIMATION
 14 USING RESONANCES 1 AND 2

16 THE PHASE FOR RESONANCE 1 IS PI TIMES 1.25
 17 THE PHASE FOR RESONANCE 2 IS PI TIMES 2.25

19 THE SQUARE OF WPOVER W IS EQUAL TO 2.60

22 ID = 0.2900E 00
 23 I1 = 0.1950E 00
 24 I2 = 0.1500E 00
 25 W = 0.1429E 11
 26 BETA=ATJR = 0.1000E 01
 27 RADIUS = 0.7000E-02

30 ALFA = 0.8408E 00

33 R1 = 0.6090E-02
 34 R2 = 0.5607E-02
 35 Z1 = 0.9100E-03
 36 Z2 = 0.1393E-02
 37 NO DIPOLE = 0.2678E 18
 38 NO 1 RESONANCE = 0.1935E 18
 39 NO 2 RESONANCE = 0.1488E 18
 40 Z2 TO Z1 = 0.1531E 01
 41 PEAK TO AVERAGE = 0.1725E 01
 42 V WALL = -0.4333E 01
 43 ETA=VW TO KTTOQ = -0.1836E 01
 44 ELECTRON TEMP = 0.2737E 05

NUMBER OF DATA SET = 7

THIS IS AN ANALYSIS OF THE ELECTRON DENSITY
IN A CYLINDRICAL PLASMA COLUMN BASED ON A
PARABOLIC DENSITY PROFILE APPROXIMATION
USING RESONANCES 1 AND 3

THE PHASE FOR RESONANCE 1 IS PI TIMES 1.25
THE PHASE FOR RESONANCE 2 IS PI TIMES 3.25

THE SQUARE OF WPOVER W IS EQUAL TO 2.60

ID	=	0.2900E 00
I1	=	0.1950E 00
I2	=	0.1200E 00
W	=	0.1429E 11
BETA=ATOR	=	0.1000E 01
RADIUS	=	0.7000E-02

ALFA	=	0.8704E 00
------	---	------------

R1	=	0.6020E-02
R2	=	0.5018E-02
Z1	=	0.9800E-03
Z2	=	0.1982E-02
NO DIPOLE	=	0.2953E 18
NO 1 RESONANCE	=	0.1986E 18
NO 2 RESONANCE	=	0.1222E 18
Z2 TO Z1	=	0.2022E 01
PEAK TO AVERAGE	=	0.1771E 01
V WALL	=	-0.7536E C1
ETA=VW TO KTTD	=	-0.2043E 01
ELECTRON TEMP	=	0.4282E 05

```

1  NUMBER OF DATA SET      =      8
2
3
4
5  THIS IS AN ANALYSIS OF THE ELECTRON DENSITY
6  IN A CYLINDRICAL PLASMA COLUMN BASED ON A
7  PARABOLIC DENSITY PROFILE APPROXIMATION
8  USING RESONANCES 1 AND 2
9
10 THE PHASE FOR RESONANCE 1 IS PI TIMES 1.25
11 THE PHASE FOR RESONANCE 2 IS PI TIMES 2.25
12
13 THE SQUARE OF WPOVER W IS EQUAL TO 2.60
14
15
16
17
18
19
20
21
22
23  ID          =      0.3200E 00
24  I1          =      0.2100E 00
25  I2          =      0.1600E 00
26  W           =      0.1459E 11
27  BETA=ATOR  =      0.1000E 01
28  RADIUS      =      0.7000E-02
29
30
31
32  ALFA        =      0.8523E 00
33
34
35
36  R1          =      0.6020E-02
37  R2          =      0.5510E-02
38  Z1          =      0.9800E-03
39  Z2          =      0.1490E-02
40  NO DIPOLE   =      0.3030E 18
41  NO 1 RESONANCE =      0.1988E 18
42  NO 2 RESONANCE =      0.1515E 18
43  Z2 TO Z1    =      0.1521E 01
44  PEAK TO AVERAGE =      0.1743E 01
45  V WALL      =      -0.6436E 01
46  ETA=VW TO KTTOQ =      -0.1913E 01
47  ELECTRON TEMP =      0.3906E 05
48
49
50
51

```

NUMBER OF DATA SET = 8

THIS IS AN ANALYSIS OF THE ELECTRON DENSITY
IN A CYLINDRICAL PLASMA COLUMN BASED ON A
PARABOLIC DENSITY PROFILE APPROXIMATION
USING RESONANCES 1 AND 3

THE PHASE FOR RESONANCE 1 IS PI TIMES 1.25
THE PHASE FOR RESONANCE 2 IS PI TIMES 3.25

THE SQUARE OF WPOVER W IS EQUAL TO 2.60

ID	=	0.3200E 00
I1	=	0.2100E 00
I2	=	0.1300E 00
W	=	0.1459E 11
BETA=ATOR	=	0.1000E 01
RADIUS	=	0.7000E-02

ALFA	=	0.8523E 00
------	---	------------

R1	=	0.6020E-02
R2	=	0.4967E-02
Z1	=	0.9800E-03
Z2	=	0.2033E-02
NO DIPOLE	=	0.3030E 18
NO 1 RESONANCE	=	0.1988E 18
NO 2 RESONANCE	=	0.1231E 18
Z2 TO Z1	=	0.2074E 01
PEAK TO AVERAGE	=	0.1743E 01
V WALL	=	-0.6436E 01
ETA=VW TO KTTOQ	=	-0.1913E 01
ELECTRON TEMP	=	0.3906E 05

```

7
8
9 NUMBER OF DATA SET      = 1
10
11 THIS IS AN ANALYSIS OF THE ELECTRON DENSITY
12 IN A CYLINDRICAL PLASMA COLUMN BASED ON A
13 BESSEL FUNCTION PROFILE APPROXIMATION
14 USING THERMAL RESONANCES 1 AND 2
15
16 TOTAL PHASE FOR FIRST RES IS PI TIMES 1.25
17 TOTAL PHASE FOR SEC RES IS PI TIMES 2.25
18
19 THE SQUARE OF WP OVER W      = 2.60
20
21
22
23 LOWER INT. LIMIT           = C.000E 00
24 INITIAL INCR. IN Z1       = C.1000E 00
25 NUMBER OF INTEGR. STEPS   = 20
26 VALUE OF W1                = C.1267E 11
27 VALUE OF W2                = C.1267E 11
28 DIPOLE CURRENT AT W1      = C.2700E 00
29 CURRENT AT W1              = C.1850E 00
30 CURRENT AT W2              = C.1500E 00
31 NUMBER T. D. RESONANCE 2ND W = 2
32
33 COEFF PEAK TC AVG EL DENS = 0.1986E 01
34 GAMMA                      = C.3268E 03
35 ETA = VWALL TC KT CVER Q   = -0.1804E 01
36 GAMMA TIMES Z1             = C.3100E 00
37 GAMMA TIMES Z2             = C.4619E 00
38 Z2 TC Z1                   = C.1490E 01
39 WP1                         = C.2356E 11
40 WP2                         = C.2122E 11
41 NO1                         = C.1744E 18
42 NO2                         = C.1414E 18
43 A1 = WP1 CVER W1 SQUARED   = C.3459E 01
44 A2 = WP2 CVER W2 SQUARED   = C.2804E 01
45 Z1                          = C.9485E-03
46 Z2                          = C.1413E-02
47 VWALL                       = -C.7363E 01
48 ELECTRON TEMPERATURE       = C.4738E 05
49
50
51
52
53
54

```

```

01
02 NUMBER OF DATA SET = 1
03
04
05
06 THIS IS AN ANALYSIS OF THE ELECTRON DENSITY
07 IN A CYLINDRICAL PLASMA COLUMN BASED ON A
08 BESSEL FUNCTION PROFILE APPROXIMATION
09 USING THERMAL RESONANCES 1 AND 3
10
11 TOTAL PHASE FOR FIRST RES IS PI TIMES 1.25
12 TOTAL PHASE FOR SEC RES IS PI TIMES 3.25
13
14 THE SQUARE OF WP OVER W = 2.60
15
16
17
18 LOWER INT. LIMIT = C.000CE CC
19 INITIAL INCR. IN Z1 = C.100CE CC
20 NUMBER OF INTEGR. STEPS = 20
21 VALUE OF W1 = 0.1267E 11
22 VALUE OF W2 = 0.1267E 11
23 DIPGLE CURRENT AT W1 = C.270CE CC
24 CURRENT AT W1 = C.185CE CC
25 CURRENT AT W2 = C.130CE CC
26 NUMBER T. C. RESONANCE 2ND W = 3
27
28
29 COEFF PEAK TO AVG EL DENS = 0.1937E 01
30 GAMMA = 0.3207E 03
31 ETA = VWALL TO KT OVER Q = -0.1717E 01
32 GAMMA TIMES Z1 = 0.250CE CC
33 GAMMA TIMES Z2 = 0.5050E CC
34 Z2 TO Z1 = C.2020E C1
35 WP1 = 0.2392E 11
36 WP2 = 0.2005E 11
37 NO1 = 0.1797E 18
38 NO2 = C.1263E 18
39 A1 = WP1 OVER W1 SQUARED = C.3563E 01
40 A2 = WP2 OVER W2 SQUARED = C.2504E 01
41 Z1 = 0.7795E-03
42 Z2 = 0.1575E-02
43 VWALL = -0.4523E C1
44 ELECTRON TEMPERATURE = 0.3058E 05
45
46
47
48
49
50
51
52
53
54
55

```

NUMBER OF DATA SET = 2

THIS IS AN ANALYSIS OF THE ELECTRON DENSITY
IN A CYLINDRICAL PLASMA COLUMN, BASED ON A
BESSEL FUNCTION PROFILE APPROXIMATION
USING THERMAL RESONANCES 1 AND 2

TOTAL PHASE FOR FIRST RES IS PI TIMES 1.25
TOTAL PHASE FOR SEC RES IS PI TIMES 2.25

THE SQUARE OF WP OVER W = 2.60

LOWER INT. LIMIT	=	C.0000E	CO
INITIAL INCR. IN Z1	=	C.1000E	CO
NUMBER OF INTEGR. STEPS	=		20
VALUE OF W1	=	C.1319E	11
VALUE OF W2	=	C.1319E	11
DIPOLE CURRENT AT W1	=	C.2900E	CC
CURRENT AT W1	=	C.1900E	CC
CURRENT AT W2	=	C.1500E	CC
NUMBER T. D. RESONANCE 2ND W	=		2
Coeff PEAK TO AVG EL DENS	=	0.1975E	C1
GAMMA	=	C.3255E	C3
ETA = VWALL TO KT OVER Q	=	-C.1785E	C1
GAMMA TIMES Z1	=	C.3100E	CO
GAMMA TIMES Z2	=	C.4743E	00
Z2 TO Z1	=	C.1530E	C1
WP1	=	C.2435E	11
WP2	=	C.2163E	11
NO1	=	C.1362E	18
NO2	=	C.1470E	18
A1 = WP1 OVER W1 SQUARED	=	C.3407E	C1
A2 = WP2 OVER W2 SQUARED	=	C.2690E	01
Z1	=	C.9524E-03	
Z2	=	C.1457E-02	
VWALL	=	-C.1287E	C2
ELECTRON TEMPERATURE	=	C.8369E	C5

```

1  NUMBER OF DATA SET      =      2
2
3
4
5  THIS IS AN ANALYSIS OF THE ELECTRON DENSITY
6  IN A CYLINDRICAL PLASMA COLUMN BASED ON A
7  BESSEL FUNCTION PROFILE APPROXIMATION
8  USING THERMAL RESONANCES 1 AND 3
9
10 TOTAL PHASE FOR FIRST RES IS PI TIMES 1.25
11 TOTAL PHASE FOR SEC RES IS PI TIMES 3.25
12
13 THE SQUARE OF WP OVER W      =      2.60
14
15
16
17
18 LOWER INT. LIMIT           =      C.000CE C0
19 INITIAL INCR. IN Z1       =      C.100CE C0
20 NUMBER OF INTEGR. STEPS   =      20
21 VALUE OF W1                =      C.1319E 11
22 VALUE OF W2                =      C.1319E 11
23 DIPOLE CURRENT AT W1      =      C.290CE C0
24 CURRENT AT W1              =      C.190CE C0
25 CURRENT AT W2              =      C.120CE C0
26 NUMBER T. C. RESONANCE 2ND W =      3
27
28 COEFF PEAK TO AVG EL DENS =      0.1926E 01
29 GAMMA                       =      0.3193E 03
30 ETA = VWALL TO KT OVER Q    =      -C.1697E C1
31 GAMMA TIMES Z1              =      C.2680E C0
32 GAMMA TIMES Z2              =      C.5950E C0
33 Z2 TO Z1                    =      C.2220E C1
34 WP1                          =      C.2435E 11
35 WP2                          =      C.1935E 11
36 NO1                          =      C.1862E 18
37 NC2                          =      C.1176E 18
38 A1 = WP1 OVER W1 SQUARED    =      C.3407E C1
39 A2 = WP2 OVER W2 SQUARED    =      C.2152E 01
40 Z1                           =      C.8393E-03
41 Z2                           =      0.1863E-02
42 VWALL                        =      -C.1095E C2
43 ELECTRON TEMPERATURE        =      G.7486E C5
44
45
46
47
48
49
50
51
52
53
54
55

```

```

1  NUMBER OF DATA SET      = 3
2
3
4  THIS IS AN ANALYSIS OF THE ELECTRON DENSITY
5  IN A CYLINDRICAL PLASMA COLUMN BASED ON A
6  BESSEL FUNCTION PROFILE APPROXIMATION
7  USING THERMAL RESONANCES 1 AND 2
8
9  TOTAL PHASE FOR FIRST RES IS PI TIMES 1.25
10 TOTAL PHASE FOR SEC RES IS PI TIMES 2.25
11
12 THE SQUARE OF WP OVER W      = 2.60
13
14
15
16
17 LOWER INT. LIMIT           = C.0000E C0
18 INITIAL INCR. IN Z1       = C.1000E C0
19 NUMBER OF INTEGR. STEPS   = 20
20 VALUE OF W1                = C.1401E 11
21 VALUE OF W2                = C.1401E 11
22 DIPOLE CURRENT AT W1     = C.3400E C0
23 CURRENT AT W1             = C.2350E C0
24 CURRENT AT W2             = C.1850E C0
25 NUMBER T. C. RESONANCE 2ND W = 2
26
27
28 COEFF PEAK TO AVG EL DENS  = C.1956E C1
29 GAMMA                     = 0.3231E 03
30 ETA = VWALL TO KT OVER Q  = -C.1751E C1
31 GAMMA TIMES Z1           = C.2600E C0
32 GAMMA TIMES Z2           = C.4160E C0
33 Z2 TO Z1                 = C.1600E C1
34 WP1                       = C.2656E 11
35 WP2                       = C.2357E 11
36 NO1                       = C.2216E 18
37 NO2                       = 0.1745E 18
38 A1 = WP1 OVER W1 SQUARED  = C.3594E C1
39 A2 = WP2 OVER W2 SQUARED  = 0.2829E C1
40 Z1                         = C.8046E-C3
41 Z2                         = 0.1287E-C2
42 VWALL                     = -C.1018E C2
43 ELECTRON TEMPERATURE     = C.6747E C5
44
45
46
47
48
49
50
51
52
53
54
55
56
57
58
59
60
61
62
63
64
65
66
67
68
69
70
71
72
73
74
75
76
77
78
79
80
81
82
83
84
85
86
87
88
89
90
91
92
93
94
95
96
97
98
99

```

```

"
"
" NUMBER OF DATA SET      =      3
"
"
" THIS IS AN ANALYSIS OF THE ELECTRON DENSITY
" IN A CYLINDRICAL PLASMA COLUMN BASED ON A
" BESSEL FUNCTION PROFILE APPROXIMATION
" USING THERMAL RESONANCES 1 AND 3
"
" TOTAL PHASE FOR FIRST RES IS PI TIMES 1.25
" TOTAL PHASE FOR SEC RES IS PI TIMES 3.25
"
" THE SQUARE OF WP OVER W      = 2.60
"
"
"
" LOWER INT. LIMIT           =      C.600E CC
" INITIAL INCR. IN Z1       =      0.1000E 00
" NUMBER OF INTEGR. STEPS   =      20
" VALUE OF W1                =      C.1401E 11
" VALUE OF W2                =      C.1401E 11
" DIPOLE CURRENT AT W1      =      C.340CE CC
" CURRENT AT W1              =      C.235CE CC
" CURRENT AT W2              =      C.160CE CC
" NUMBER T. G. RESONANCE 2ND W =      3
"
"
" COEFF PEAK TC AVG EL DENS =      C.1993E C1
" GAMMA                      =      C.3277E 03
" ETA = VWALL TO KT OVER Q   =     -C.1817E C1
" GAMMA TIMES Z1             =      C.3100E 00
" GAMMA TIMES Z2             =      C.6014E C0
" Z2 TC Z1                   =      C.1940E 01
" WP1                        =      C.2617E 11
" WP2                        =      C.2159E 11
" NC1                        =      C.2151E 18
" NC2                        =      C.1465E 18
" A1 = WP1 OVER W1 SQUARED   =      C.3489E C1
" A2 = WP2 OVER W2 SQUARED   =      C.2375E 01
" Z1                          =      C.5459E-C3
" Z2                          =      0.1835E-C2
" VWALL                       =     -C.8931E C1
" ELECTRON TEMPERATURE       =      C.5706E C5
"
"
"
"
"

```

```

1  NUMBER OF DATA SET      =    4
2
3
4
5
6
7
8
9
10
11  THIS IS AN ANALYSIS OF THE ELECTRON DENSITY
12  IN A CYLINDRICAL PLASMA COLUMN BASED ON A
13  BESSEL FUNCTION PROFILE APPROXIMATION
14  USING THERMAL RESONANCES 1 AND 2
15
16  TOTAL PHASE FOR FIRST RES IS PI TIMES 1.25
17  TOTAL PHASE FOR SEC RES IS PI TIMES 2.25
18
19  THE SQUARE OF WP OVER W      = 2.60
20
21
22
23
24  LOWER INT. LIMIT          =    C.000E CC
25  INITIAL INCR. IN Z1      =    C.100E CC
26  NUMBER OF INTEGR. STEPS  =    20
27  VALUE OF W1              =    C.1458E 11
28  VALUE OF W2              =    C.1458E 11
29  DIPOLE CURRENT AT W1     =    C.355CE CC
30  CURRENT AT W1            =    C.245CE CC
31  CURRENT AT W2            =    C.200CE CC
32  NUMBER T. O. RESONANCE 2ND W =    2
33
34  COEFF PEAK TO AVG EL DENS =    C.2011E C1
35  GAMMA                    =    C.3299E 03
36  ETA = VWALL TO KT OVER Q =   -C.1850E 01
37  GAMMA TIMES Z1          =    C.310CE CC
38  GAMMA TIMES Z2          =    0.4557E C0
39  Z2 TO Z1                =    C.147CE C1
40  WP1                      =    C.2762E 11
41  WP2                      =    0.2496E 11
42  NC1                      =    C.2397E 18
43  NC2                      =    0.1956E 18
44  A1 = WP1 OVER W1 SQUARED =    C.3589E 01
45  A2 = WP2 OVER W2 SQUARED =    0.2930E 01
46  Z1                      =    C.9396E-C3
47  Z2                      =    C.1381E-C2
48  VWALL                   =   -C.7640E. C1
49  ELECTRON TEMPERATURE    =    C.4795E 05
50
51
52
53
54
55

```

NUMBER OF DATA SET = 4

THIS IS AN ANALYSIS OF THE ELECTRON DENSITY
IN A CYLINDRICAL PLASMA COLUMN BASED ON A
BESSEL FUNCTION PROFILE APPROXIMATION
USING THERMAL RESONANCES 1 AND 3

TOTAL PHASE FOR FIRST RES IS PI TIMES 1.25
TOTAL PHASE FOR SEC RES IS PI TIMES 3.25

THE SQUARE OF WP OVER W = 2.60

LOWER INT. LIMIT	=	C.0000E CC
INITIAL INCR. IN Z1	=	C.1000E CC
NUMBER OF INTEGR. STEPS	=	20
VALUE OF W1	=	C.1458E 11
VALUE OF W2	=	C.1458E 11
DIPOLE CURRENT AT W1	=	C.3550E CO
CURRENT AT W1	=	C.2450E CC
CURRENT AT W2	=	C.1550E CO
NUMBER T. C. RESONANCE 2ND W	=	3
COEFF PEAK TO AVG EL DENS	=	C.1999E C1
GAMMA	=	0.3284E 03
ETA = VWALL TO KT OVER Q	=	-0.1828E C1
GAMMA TIMES Z1	=	G.2780E CO
GAMMA TIMES Z2	=	C.5977E CO
Z2 TO Z1	=	C.2150E 0J
WP1	=	C.2809E 11
WP2	=	0.2234E 11
NO1	=	C.2479E 18
NO2	=	C.1568E 18
A1 = WP1 OVER W1 SQUARED	=	C.3712E C1
A2 = WP2 OVER W2 SQUARED	=	C.2348E C1
Z1	=	C.8464E-03
Z2	=	0.1820E-02
VWALL	=	-0.1223E C2
ELECTRON TEMPERATURE	=	C.7770E 05

```

 9 NUMBER OF DATA SET = 5
10
11
12 THIS IS AN ANALYSIS OF THE ELECTRON DENSITY
13 IN A CYLINDRICAL PLASMA COLUMN BASED ON A
14 BESSEL FUNCTION PROFILE APPROXIMATION
15 USING THERMAL RESONANCES 1 AND 2
16
17 TOTAL PHASE FOR FIRST RES IS PI TIMES 1.25
18 TOTAL PHASE FOR SEC RES IS PI TIMES 2.25
19
20 THE SQUARE OF WP OVER W = 2.60
21
22
23
24 LOWER INT. LIMIT = C.CCOCE CO
25 INITIAL INCR. IN Z1 = C.100CE CO
26 NUMBER OF INTEGR. STEPS = 20
27 VALUE OF W1 = C.1204E 11
28 VALUE OF W2 = C.1204E 11
29 DIPOLE CURRENT AT W1 = C.270CE CO
30 CURRENT AT W1 = C.180CE CO
31 CURRENT AT W2 = C.135CE CO
32 NUMBER T. G. RESCANCE 2ND W = 2
33
34 COEFF PEAK TO AVG EL DENS = 0.1986E 01
35 GAMMA = C.3268E C3
36 ETA = VWALL TC KT OVER Q = -C.18C4E C1
37 GAMMA TIMES Z1 = C.31C0E CO
38 GAMMA TIMES Z2 = 0.4929E CO
39 Z2 TC Z1 = C.1590E C1
40 WP1 = C.2242E 11
41 WP2 = C.1941E 11
42 NO1 = 0.1579E 18
43 NO2 = C.1184E 18
44 A1 = WP1 OVER W1 SQUARED = C.3467E 01
45 A2 = WP2 OVER W2 SQUARED = C.26C0E 01
46 Z1 = 0.9485E-03
47 Z2 = C.15C8E-C2
48 VWALL = -C.16C9E C2
49 ELECTRON TEMPERATURE = C.1035E C6
50
51
52
53
54

```

```

0
1 NUMBER OF DATA SET = 5
2
3
4
5
6
7
8
9
10
11 THIS IS AN ANALYSIS OF THE ELECTRON DENSITY
12 IN A CYLINDRICAL PLASMA COLUMN BASED ON A
13 BESSEL FUNCTION PROFILE APPROXIMATION
14 USING THERMAL RESONANCES 1 AND 3
15
16
17 TOTAL PHASE FOR FIRST RES IS PI TIMES 1.25
18 TOTAL PHASE FOR SEC RES IS PI TIMES 3.25
19
20 THE SQUARE OF WP OVER W = 2.60
21
22
23
24 LOWER INT. LIMIT = C.0000E C0
25 INITIAL INCR. IN Z1 = 0.1000E C0
26 NUMBER OF INTEGR. STEPS = 20
27 VALUE OF W1 = 0.1204E 11
28 VALUE OF W2 = C.1204E 11
29 DIPOLE CURRENT AT W1 = C.2700E CC
30 CURRENT AT W1 = C.1800E CC
31 CURRENT AT W2 = C.1100E 00
32 NUMBER T. D. RESONANCE 2ND W = 3
33
34 COEFF PEAK TC AVG EL DENS = C.1986E C1
35 GAMMA = C.3268E 03
36 ETA = VWALL TC KT OVER Q = -C.1804E 01
37 GAMMA TIMES Z1 = C.3100E C0
38 GAMMA TIMES Z2 = C.6448E CC
39 Z2 TO Z1 = C.2080E 01
40 WP1 = C.2242E 11
41 WP2 = C.1752E 11
42 NO1 = C.1579E 18
43 NO2 = C.9648E 17
44 A1 = WP1 OVER W1 SQUARED = C.3467E C1
45 A2 = WP2 OVER W2 SQUARED = 0.2119E 01
46 Z1 = 0.9485E-C3
47 Z2 = 0.1973E-02
48 VWALL = -C.1609E 02
49 ELECTRON TEMPERATURE = C.1035E 06
50
51
52
53
54
55

```

1
 2
 3
 4
 5
 6
 7
 8
 9
 10
 11
 12
 13
 14
 15
 16
 17
 18
 19
 20
 21
 22
 23
 24
 25
 26
 27
 28
 29
 30
 31
 32
 33
 34
 35
 36
 37
 38
 39
 40
 41
 42
 43
 44
 45
 46
 47
 48
 49
 50
 51
 52
 53
 54
 55
 56
 57
 58
 59
 60

NUMBER OF DATA SET = 6

THIS IS AN ANALYSIS OF THE ELECTRON DENSITY
 IN A CYLINDRICAL PLASMA COLUMN BASED ON A
 BESSEL FUNCTION PROFILE APPROXIMATION
 USING THERMAL RESONANCES 1 AND 2

TOTAL PHASE FOR FIRST RES IS PI TIMES 1.25
 TOTAL PHASE FOR SEC RES IS PI TIMES 2.25

THE SQUARE OF WP OVER W = 2.60

LOWER INT. LIMIT	=	C.0000E C0
INITIAL INCR. IN Z1	=	0.1000E C0
NUMBER OF INTEGR. STEPS	=	20
VALUE OF W1	=	C.1267E 11
VALUE OF W2	=	C.1267E 11
DIPOLE CURRENT AT W1	=	0.2850E C0
CURRENT AT W1	=	C.190CE C0
CURRENT AT W2	=	C.150CE C0
NUMBER T. C. RESONANCE 2ND W	=	2
COEFF PEAK TC AVG EL DENS	=	C.1986E C1
GAMMA	=	C.3268E C3
ETA = VWALL TO KT OVER Q	=	-C.18C4E C1
GAMMA TIMES Z1	=	0.31C0E C0
GAMMA TIMES Z2	=	C.4743E C0
Z2 TC Z1	=	C.1530E C1
WP1	=	C.2359E 11
WP2	=	C.2096E 11
NC1	=	0.1748E 18
NC2	=	C.1380E 18
A1 = WP1 OVER W1 SQUARED	=	C.3467E C1
A2 = WP2 OVER W2 SQUARED	=	0.2737E 01
Z1	=	C.9485E-C3
Z2	=	0.1451E-C2
VWALL	=	-C.1113E C2
ELECTRON TEMPERATURE	=	C.7163E C5

8
 9
 10
 11
 12
 13
 14
 15
 16
 17
 18
 19
 20
 21
 22
 23
 24
 25
 26
 27
 28
 29
 30
 31
 32
 33
 34
 35
 36
 37
 38
 39
 40
 41
 42
 43
 44
 45
 46
 47
 48
 49
 50
 51
 52
 53
 54
 55

NUMBER OF DATA SET = 6

THIS IS AN ANALYSIS OF THE ELECTRON DENSITY
 IN A CYLINDRICAL PLASMA COLUMN BASED ON A
 BESSEL FUNCTION PROFILE APPROXIMATION
 USING THERMAL RESONANCES 1 AND 3

TOTAL PHASE FOR FIRST RES IS PI TIMES 1.25
 TOTAL PHASE FOR SEC RES IS PI TIMES 3.25

THE SQUARE OF WP OVER W = 2.60

LOWER INT. LIMIT	=	C.0000E C0
INITIAL INCR. IN Z1	=	C.1000E C0
NUMBER OF INTEGR. STEPS	=	2C
VALUE OF W1	=	0.1267E 11
VALUE OF W2	=	C.1267E 11
DIPOLE CURRENT AT W1	=	C.2850E CC
CURRENT AT W1	=	C.1900E CC
CURRENT AT W2	=	0.1200E 00
NUMBER T. C. RESONANCE 2ND W	=	3
COEFF PEAK TO AVG EL DENS	=	C.1948E C1
GAMMA	=	C.3221E 03
ETA = VWALL TO KT OVER Q	=	-C.1737E 01
GAMMA TIMES Z1	=	0.2770E 00
GAMMA TIMES Z2	=	C.6066E C0
Z2 TO Z1	=	0.2190E 01
WP1	=	C.2359E 11
WP2	=	0.1875E 11
NO1	=	C.1748E 18
NO2	=	C.1104E 18
A1 = WP1 OVER W1 SQUARED	=	C.3467E 01
A2 = WP2 OVER W2 SQUARED	=	C.2189E 01
Z1	=	C.8599E-03
Z2	=	0.1883E-02
VWALL	=	-C.1000E C2
ELECTRON TEMPERATURE	=	C.6690E C5

1
2
3
4
5
6
7
8
9
10
11
12
13
14
15
16
17
18
19
20
21
22
23
24
25
26
27
28
29
30
31
32
33
34
35
36
37
38
39
40
41
42
43
44
45
46
47
48
49
50
51
52
53
54
55
56

NUMBER OF DATA SET = 7

THIS IS AN ANALYSIS OF THE ELECTRON DENSITY
IN A CYLINDRICAL PLASMA COLUMN BASED ON A
BESSEL FUNCTION PROFILE APPROXIMATION
USING THERMAL RESONANCES 1 AND 2

TOTAL PHASE FOR FIRST RES IS PI TIMES 1.25
TOTAL PHASE FOR SEC RES IS PI TIMES 2.25

THE SQUARE OF WP OVER W = 2.60

LOWER INT. LIMIT = C.000CE C0
INITIAL INCR. IN Z1 = C.100CE CC
NUMBER OF INTEGR. STEPS = 20
VALUE OF W1 = 0.1429E 11
VALUE OF W2 = C.1429E 11
DIPOLE CURRENT AT W1 = C.290CE C0
CURRENT AT W1 = C.195CE CC
CURRENT AT W2 = C.150CE CC
NUMBER T. D. RESONANCE 2ND W = 2

COEFF PEAK TC AVG EL DENS = C.1993E C1
GAMMA = 0.3277E C3
ETA = VWALL TC KT OVER Q = -C.1817E C1
GAMMA TIMES Z1 = 0.310CE C0
GAMMA TIMES Z2 = C.4743E 0C
Z2 TC Z1 = C.1530E C1
WP1 = C.2672E 11
WP2 = C.2344E 11
ND1 = C.2243E 18
NC2 = C.1725E 18
A1 = WP1 OVER W1 SQUARED = C.3497E C1
A2 = WP2 OVER W2 SQUARED = 0.2690E 01
Z1 = C.9459E-C3
Z2 = 0.1447E-C2
VWALL = -C.2254E C2
ELECTRON TEMPERATURE = C.1440E C6

NUMBER OF DATA SET = 7

THIS IS AN ANALYSIS OF THE ELECTRON DENSITY
IN A CYLINDRICAL PLASMA COLUMN BASED ON A
BESSEL FUNCTION PROFILE APPROXIMATION
USING THERMAL RESONANCES 1 AND 3

TOTAL PHASE FOR FIRST RES IS PI TIMES 1.25
TOTAL PHASE FOR SEC RES IS PI TIMES 3.25

THE SQUARE OF WP OVER W = 2.60

LOWER INT. LIMIT	=	C.000CE	C0
INITIAL INCR. IN Z1	=	C.100CE	CC
NUMBER OF INTEGR. STEPS	=		20
VALUE OF W1	=	C.1429E	11
VALUE OF W2	=	C.1429E	11
DIPGLE CURRENT AT W1	=	C.290CE	CC
CURRENT AT W1	=	C.195CE	C0
CURRENT AT W2	=	C.120CE	CC
NUMBER T. O. RESONANCE 2ND W	=		3
Coeff PEAK TC AVG EL DENS	=	0.1993E	C1
GAMMA	=	C.3277E	C3
ETA = VWALL TC KT OVER Q	=	-C.1817E	C1
GAMMA TIMES Z1	=	C.310CE	C0
GAMMA TIMES Z2	=	0.6386E	00
Z2 TC Z1	=	C.2060E	G1
WP1	=	0.2672E	11
WP2	=	C.2096E	11
ND1	=	0.2243E	18
NC2	=	C.1380E	18
A1 = WP1 OVER W1 SQUARED	=	0.3497E	01
A2 = WP2 OVER W2 SQUARED	=	0.2152E	01
Z1	=	C.9459E	-C3
Z2	=	C.1949E	-C2
VWALL	=	-C.2254E	C2
ELECTRON TEMPERATURE	=	0.1440E	06

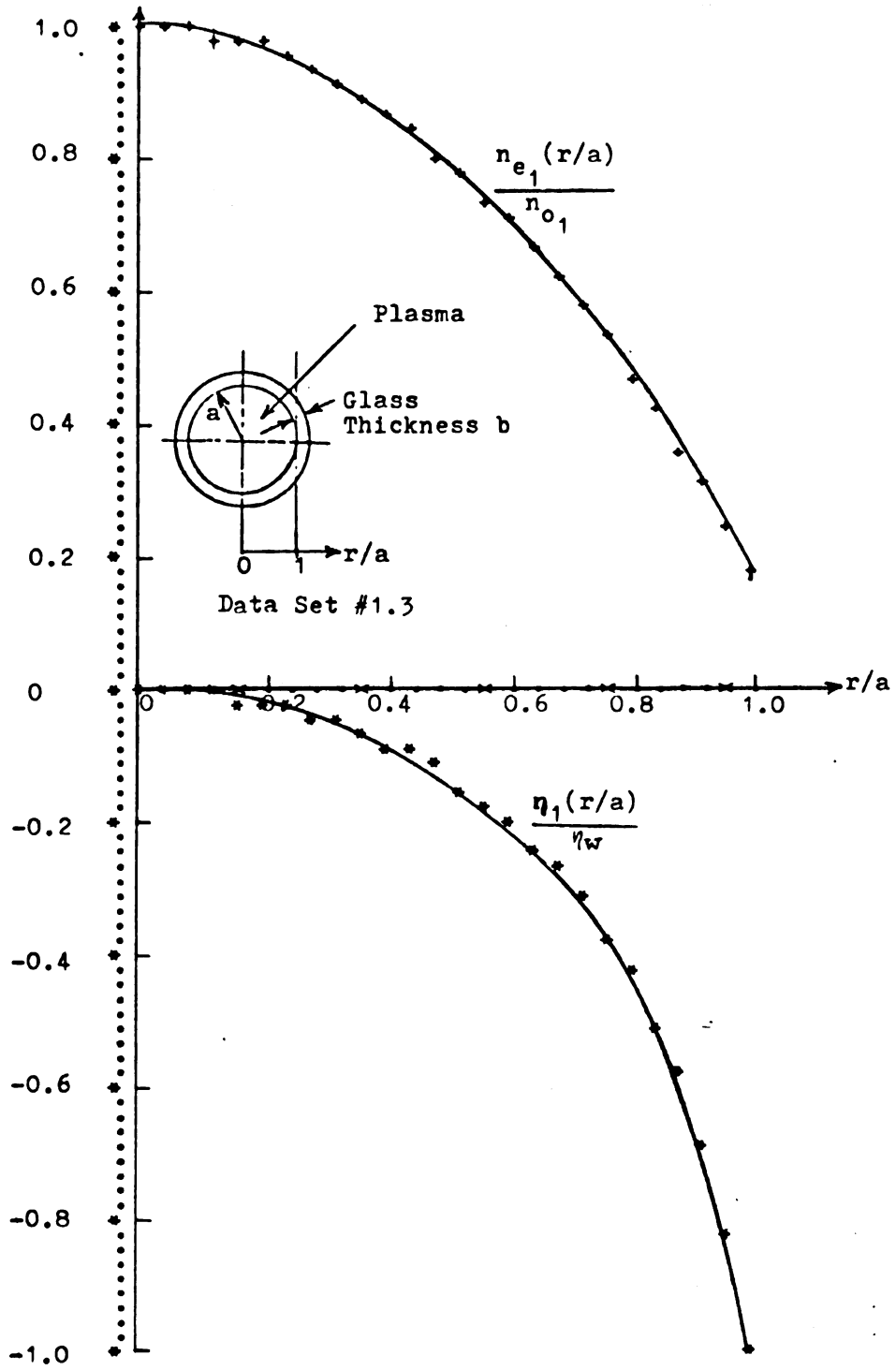
NUMBER OF DATA SET = 8

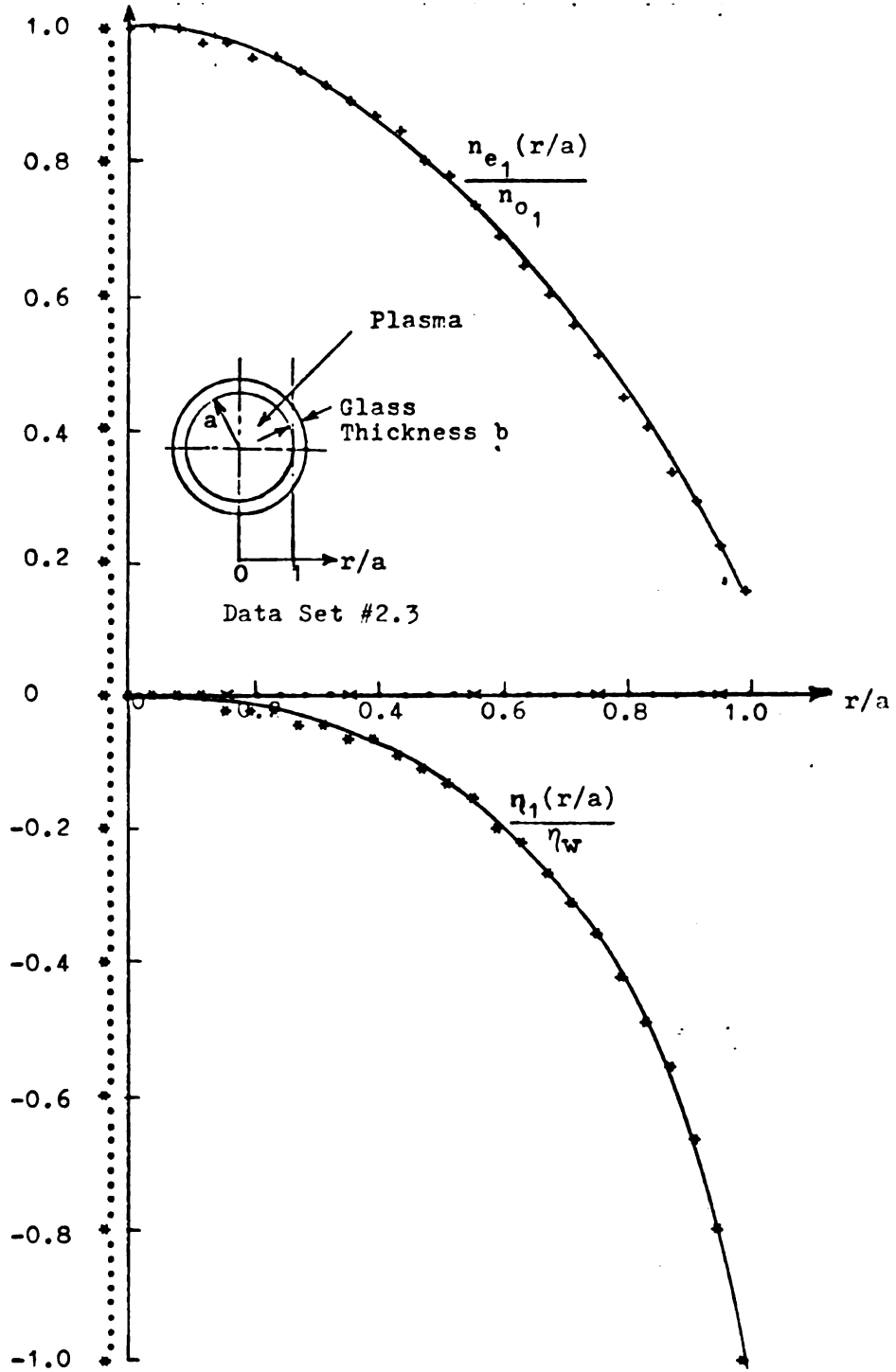
THIS IS AN ANALYSIS OF THE ELECTRON DENSITY
IN A CYLINDRICAL PLASMA COLUMN BASED ON A
BESSEL FUNCTION PROFILE APPROXIMATION
USING THERMAL RESONANCES 1 AND 2

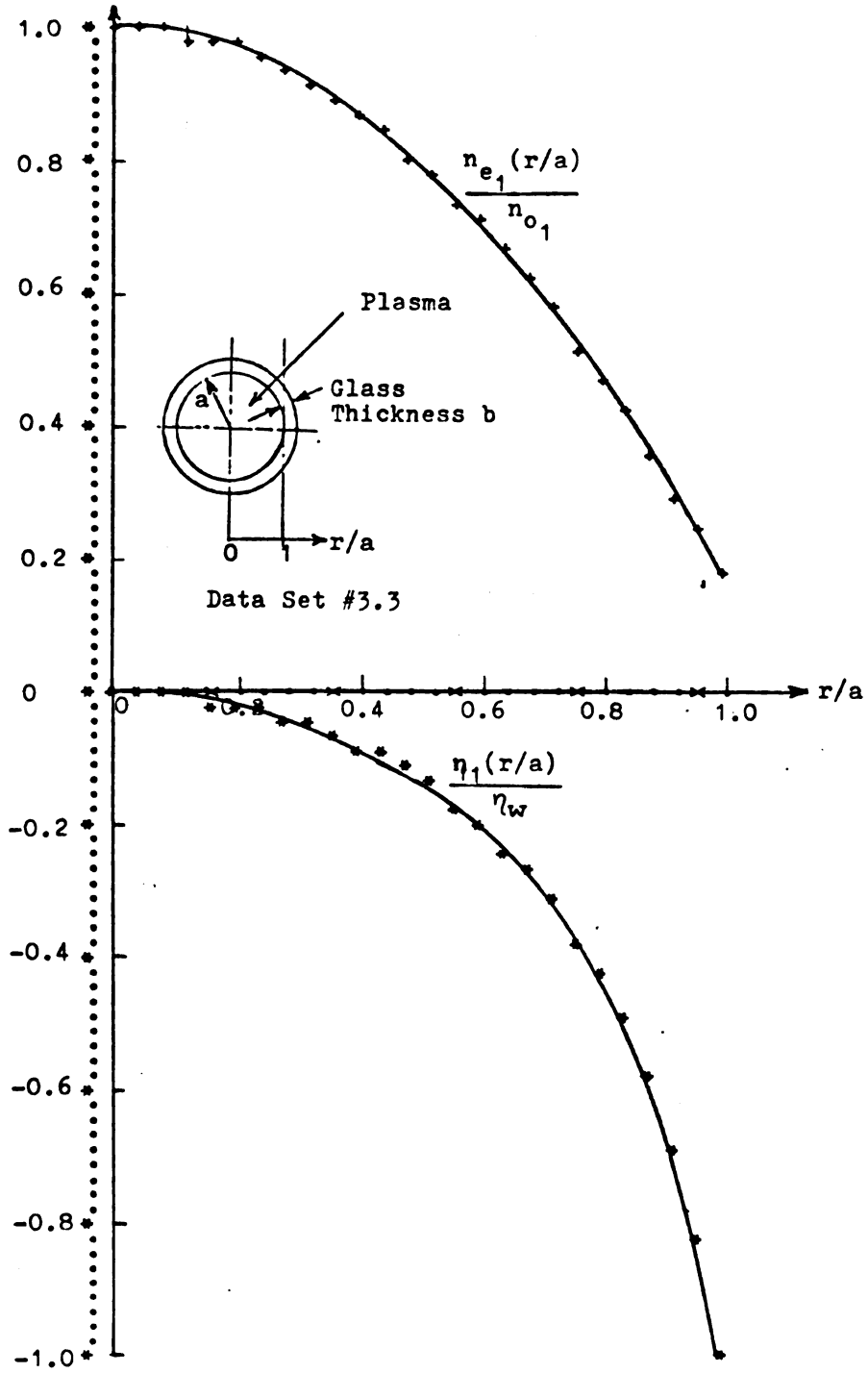
TOTAL PHASE FOR FIRST RES IS PI TIMES 1.25
TOTAL PHASE FOR SEC RES IS PI TIMES 2.25

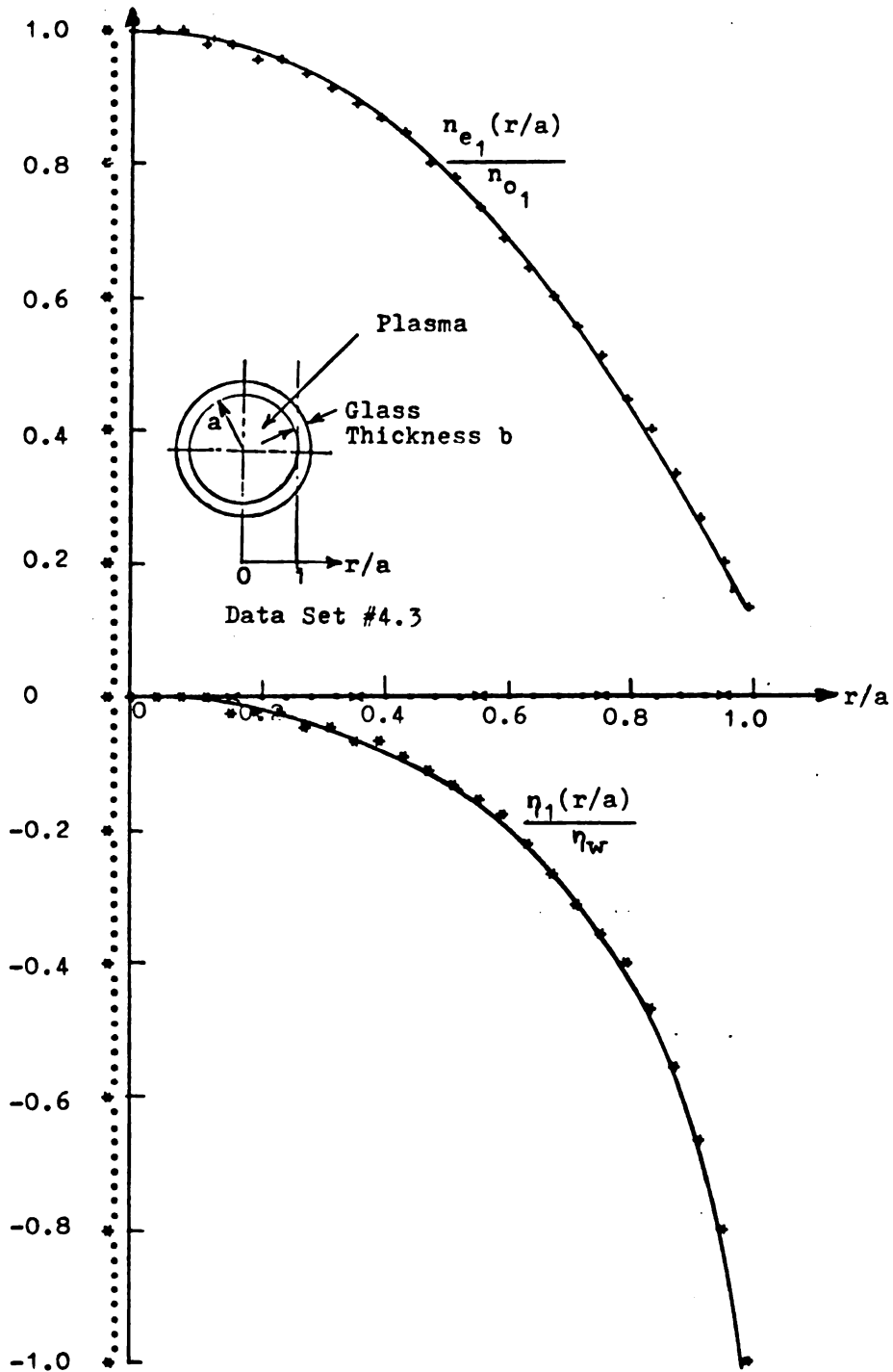
THE SQUARE OF WP OVER W = 2.60

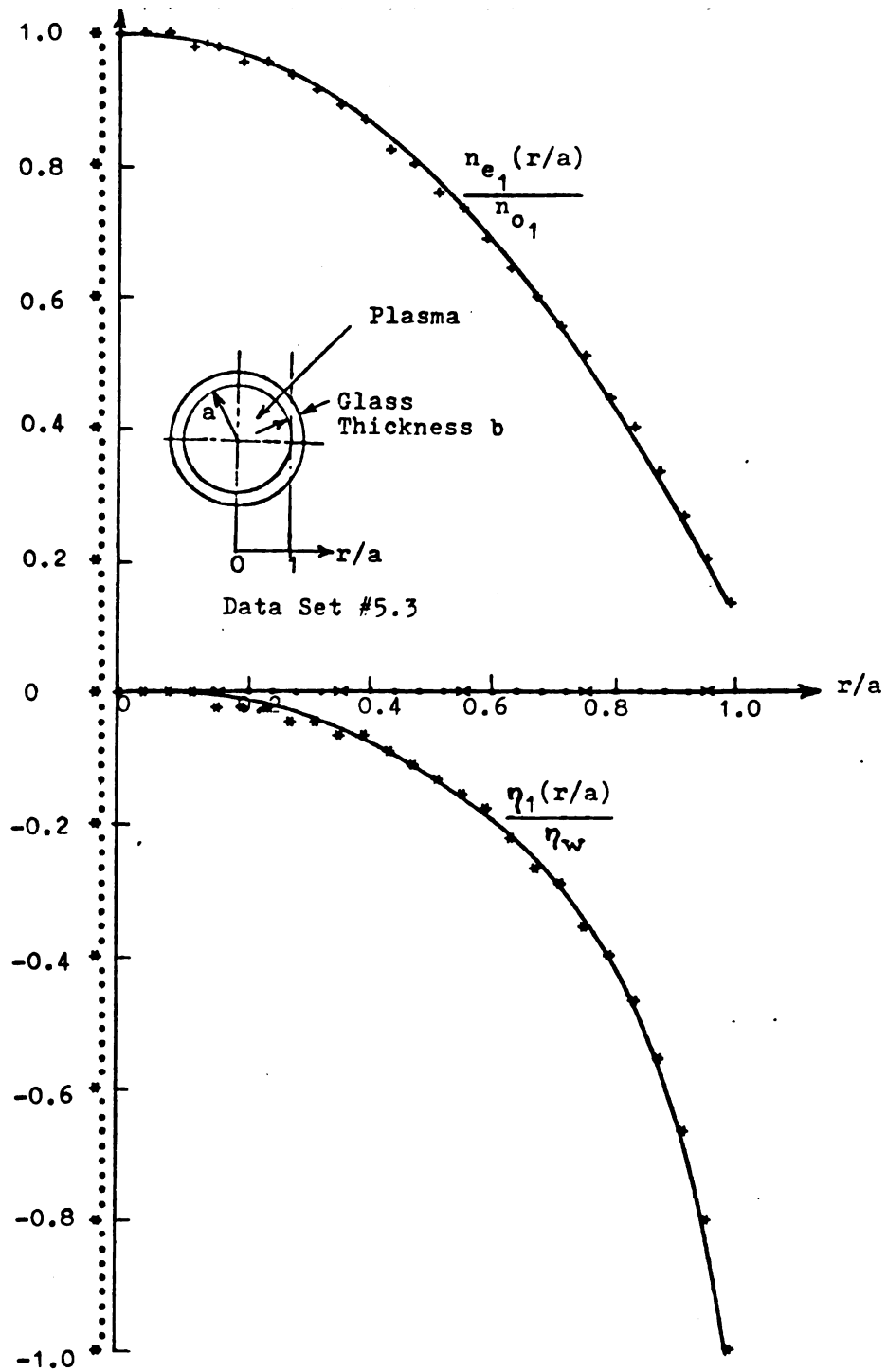
LOWER INT. LIMIT	=	C.000CE	CO
INITIAL INCR. IN Z1	=	C.100CE	CO
NUMBER OF INTEGR. STEPS	=		20
VALUE OF W1	=	C.1459E	11
VALUE OF W2	=	C.1459E	11
DIPOLE CURRENT AT W1	=	C.320CE	CO
CURRENT AT W1	=	C.210CE	CO
CURRENT AT W2	=	C.160CE	CO
NUMBER T. D. RESONANCE 2ND W	=		2
Coeff PEAK TO AVG EL DENS	=	G.2020E	C1
GAMMA	=	C.3310E	O3
ETA = VWALL TO KT OVER Q	=	-C.1866E	O1
GAMMA TIMES Z1	=	O.350E	O0
GAMMA TIMES Z2	=	C.5495E	CO
Z2 TO Z1	=	O.1570E	O1
WP1	=	C.2695E	11
WP2	=	C.2353E	11
NO1	=	C.2282E	18
NO2	=	C.1739E	18
A1 = WP1 OVER W1 SQUARED	=	C.3412E	C1
A2 = WP2 OVER W2 SQUARED	=	O.2600E	O1
Z1	=	C.1057E	-O2
Z2	=	C.1660E	-O2
VWALL	=	-C.1639E	C2
ELECTRON TEMPERATURE	=	C.1020E	O6

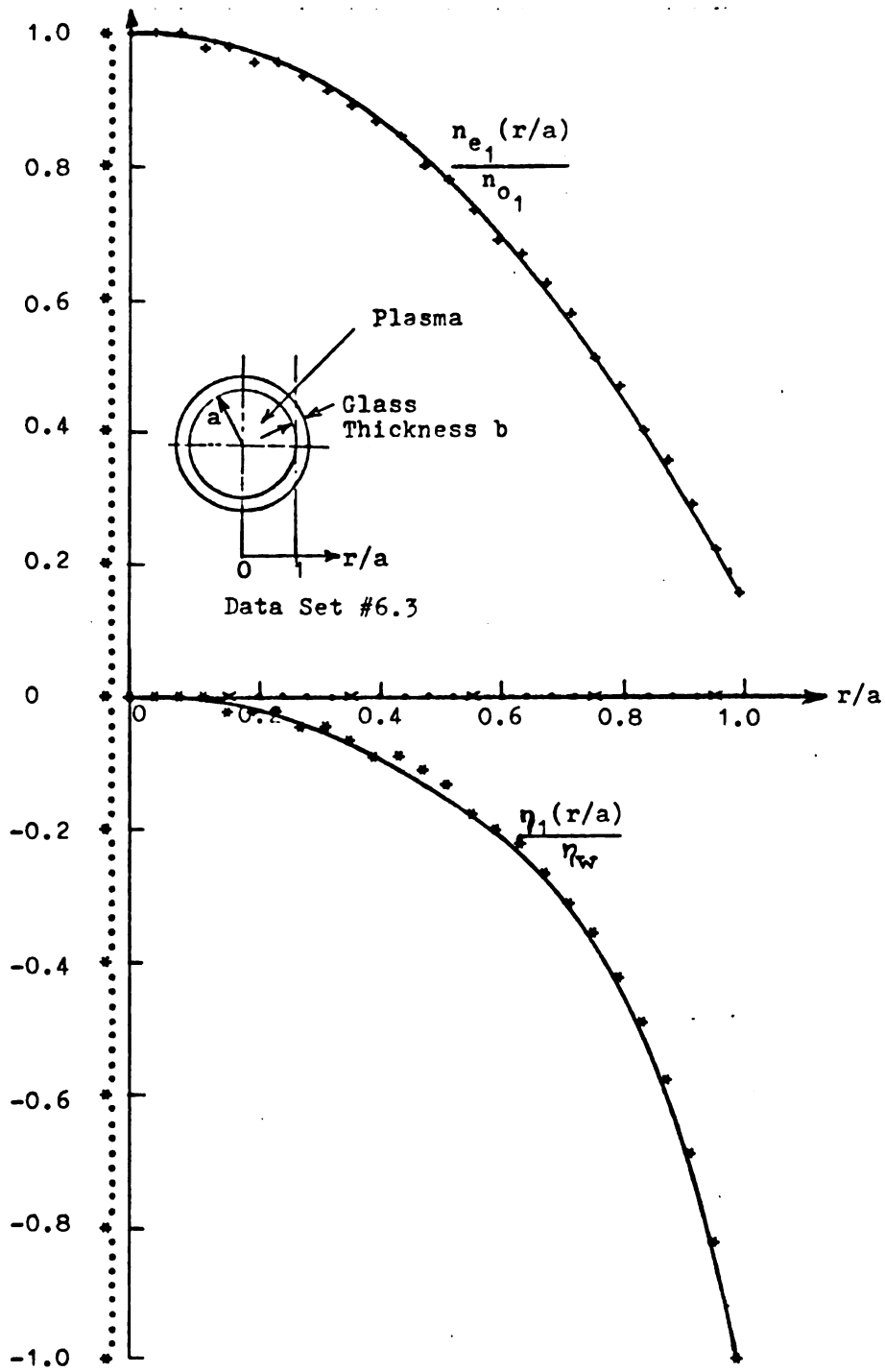


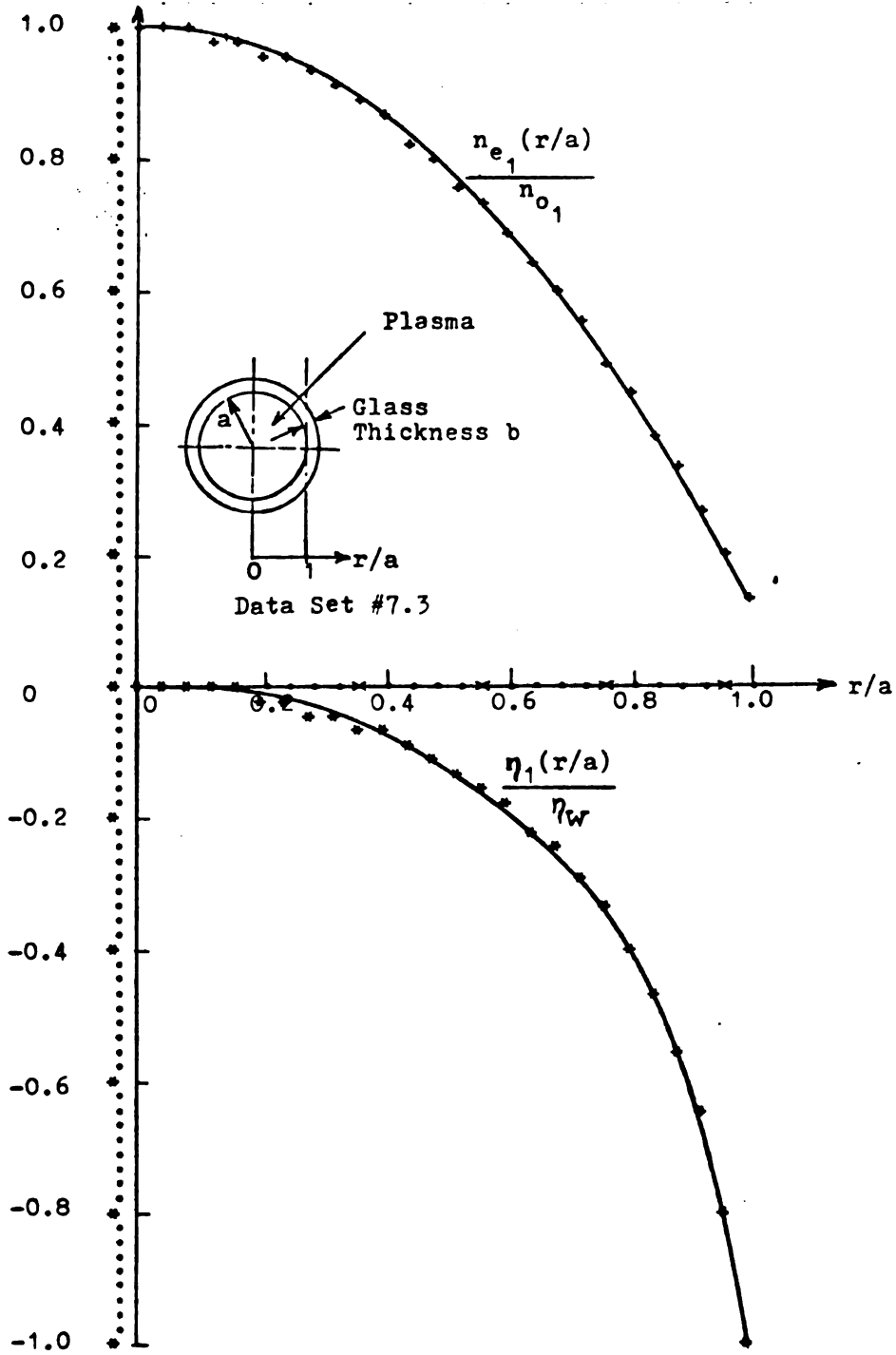


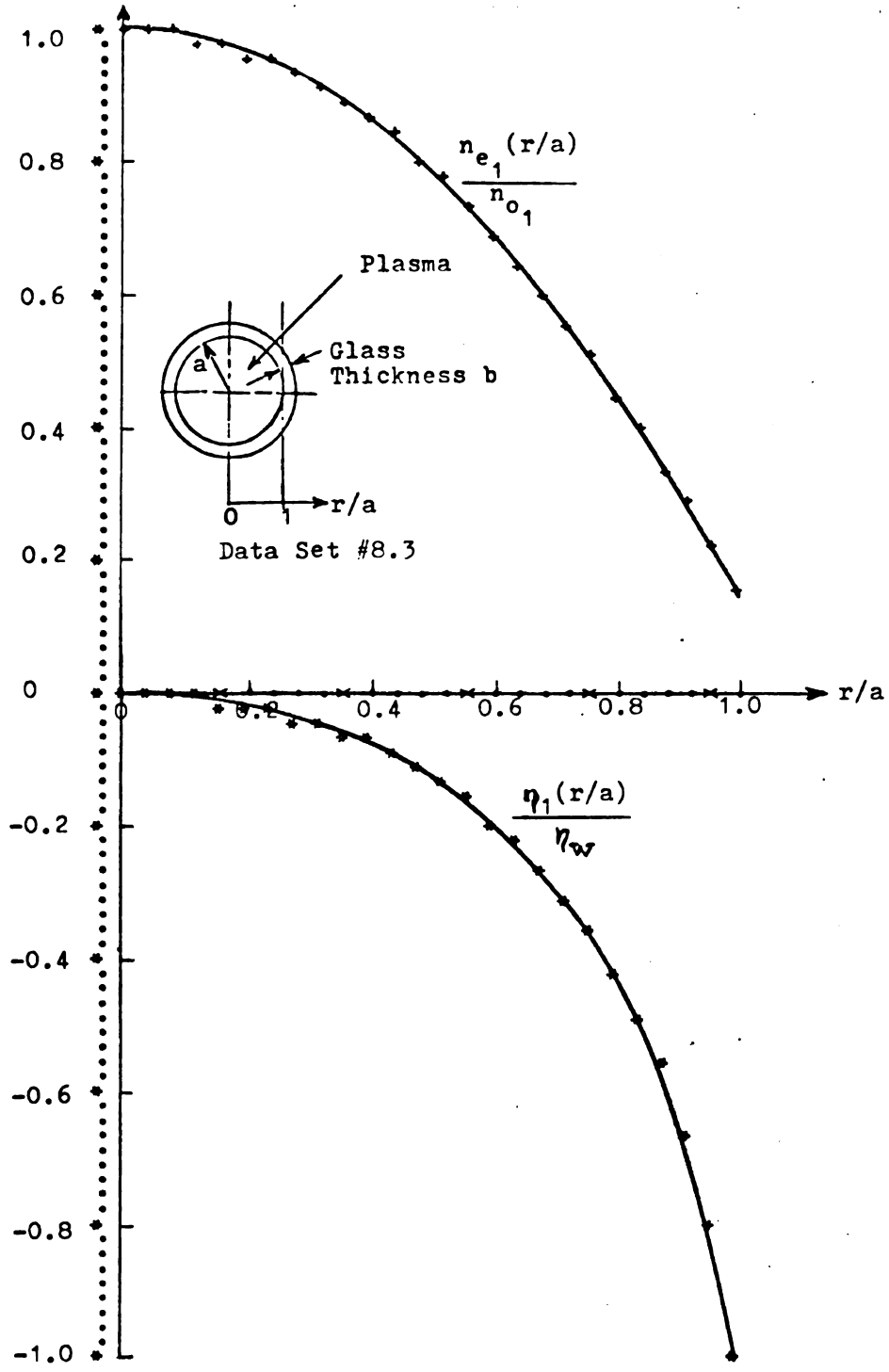


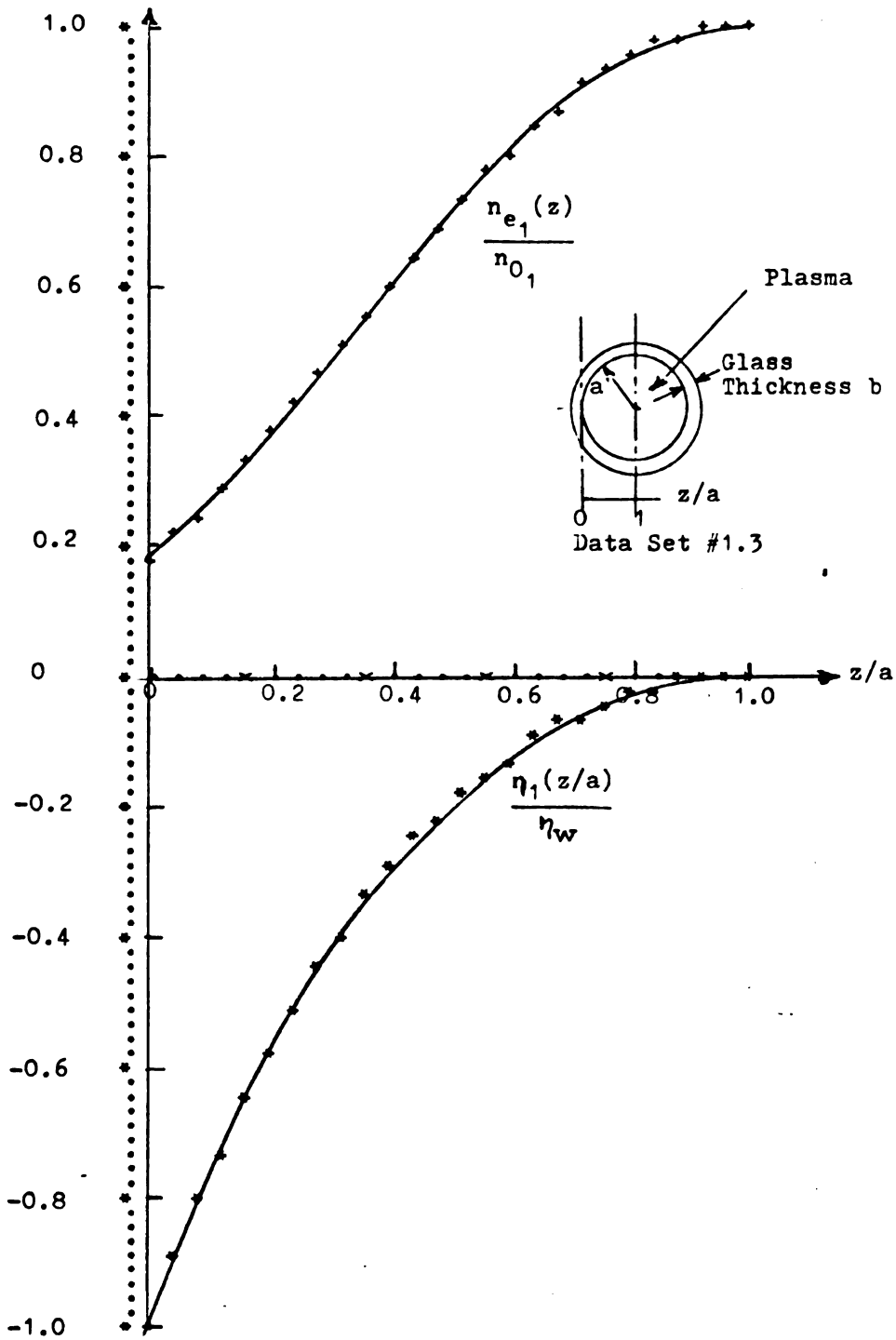


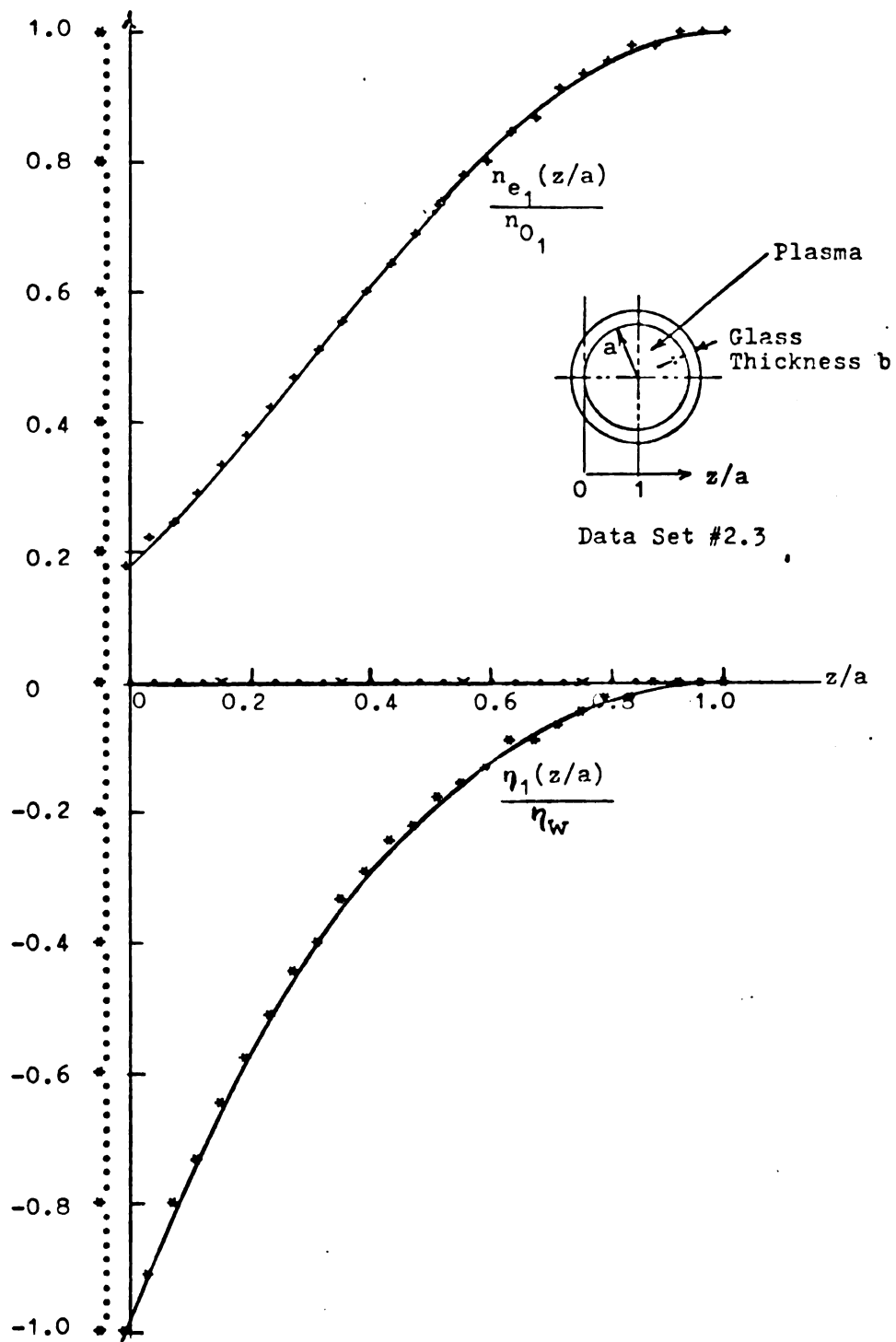


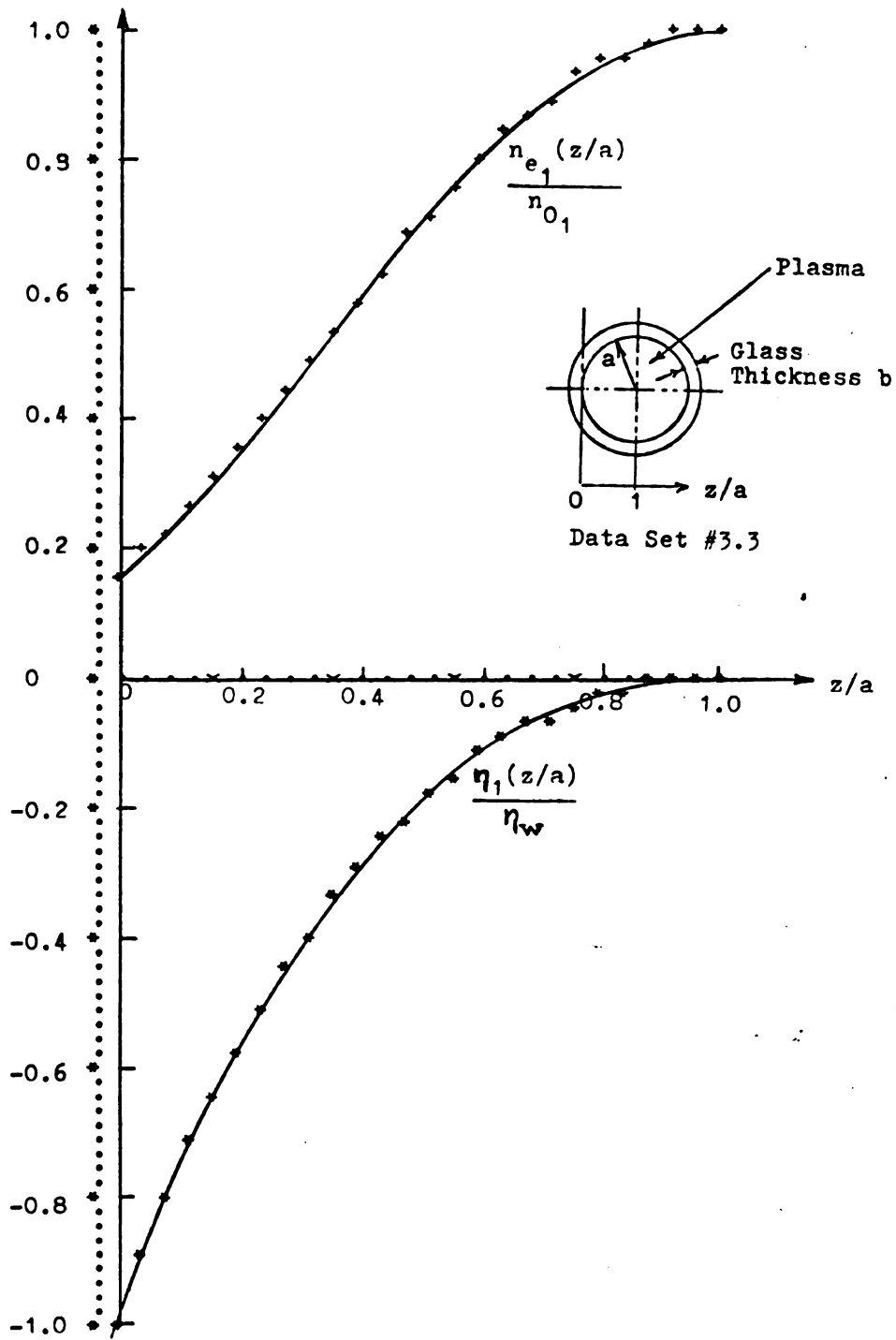


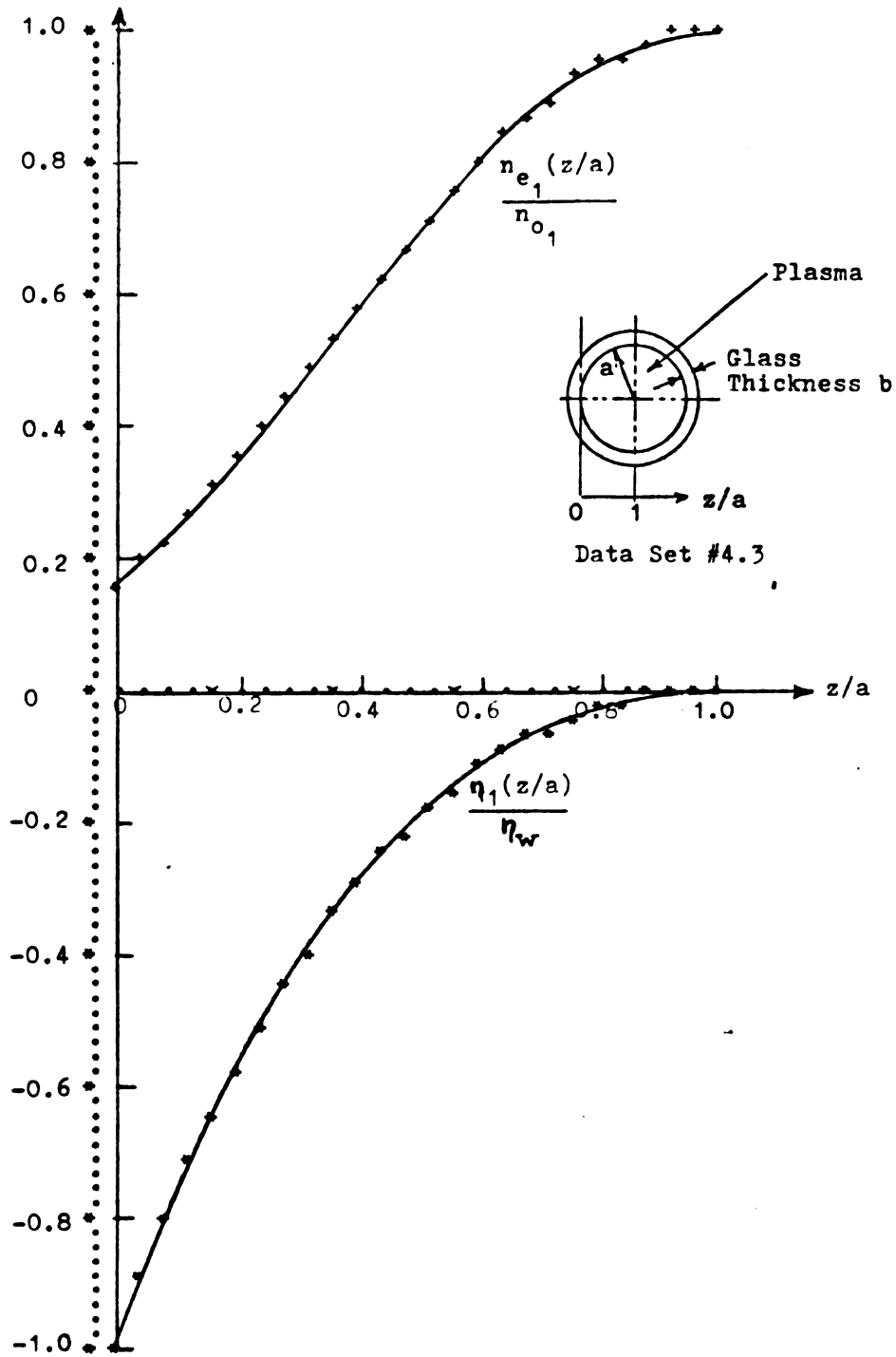


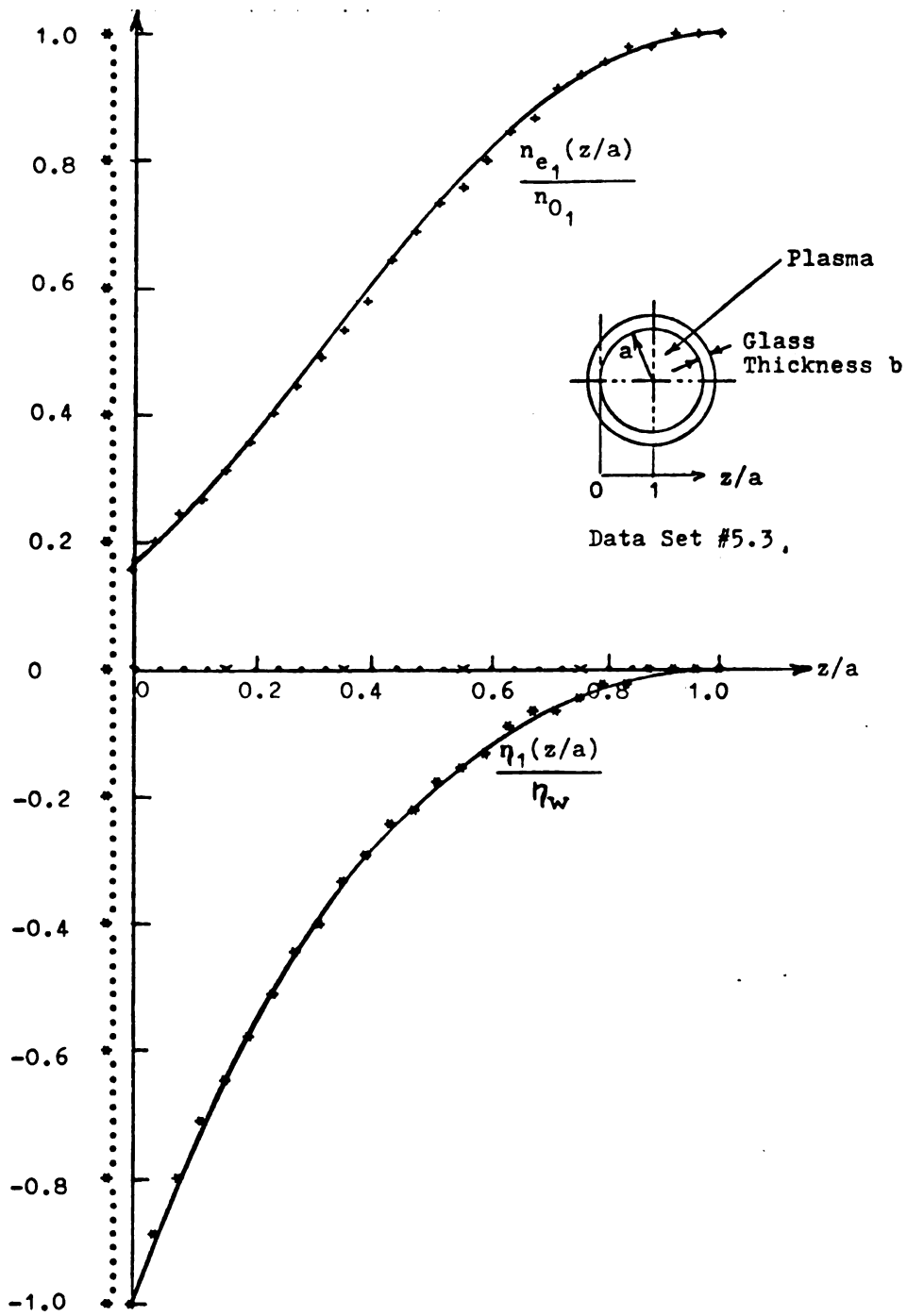


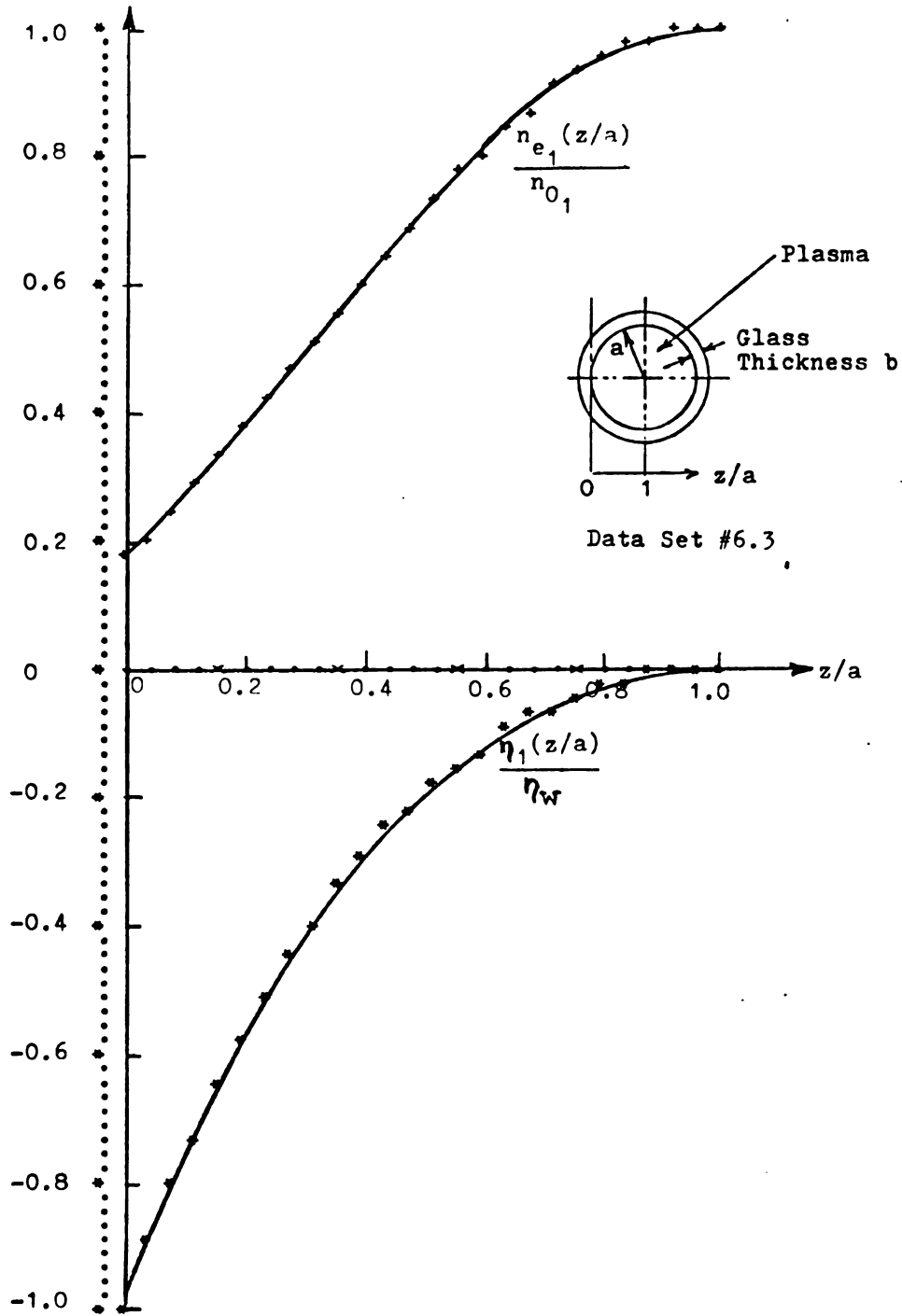


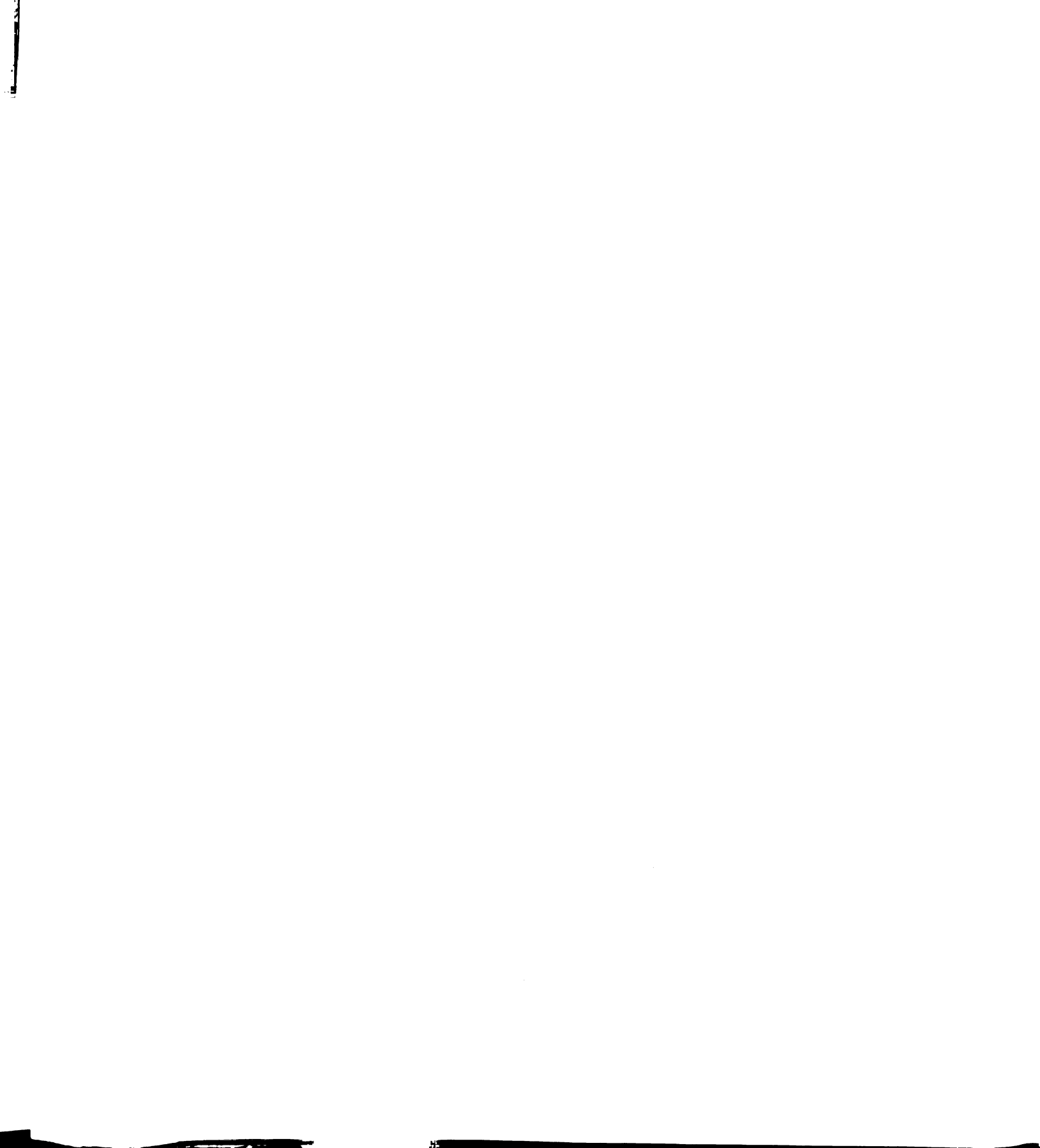


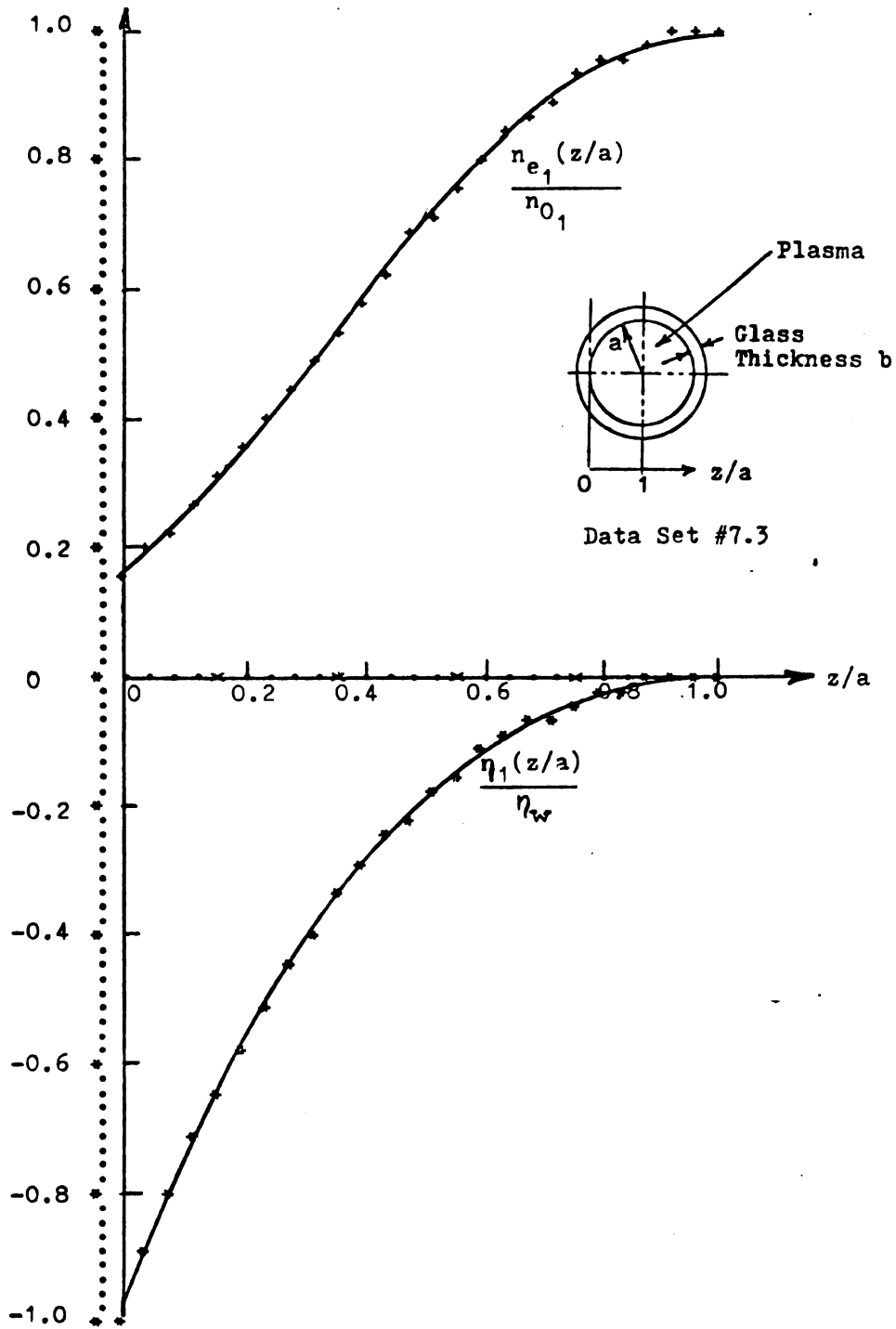




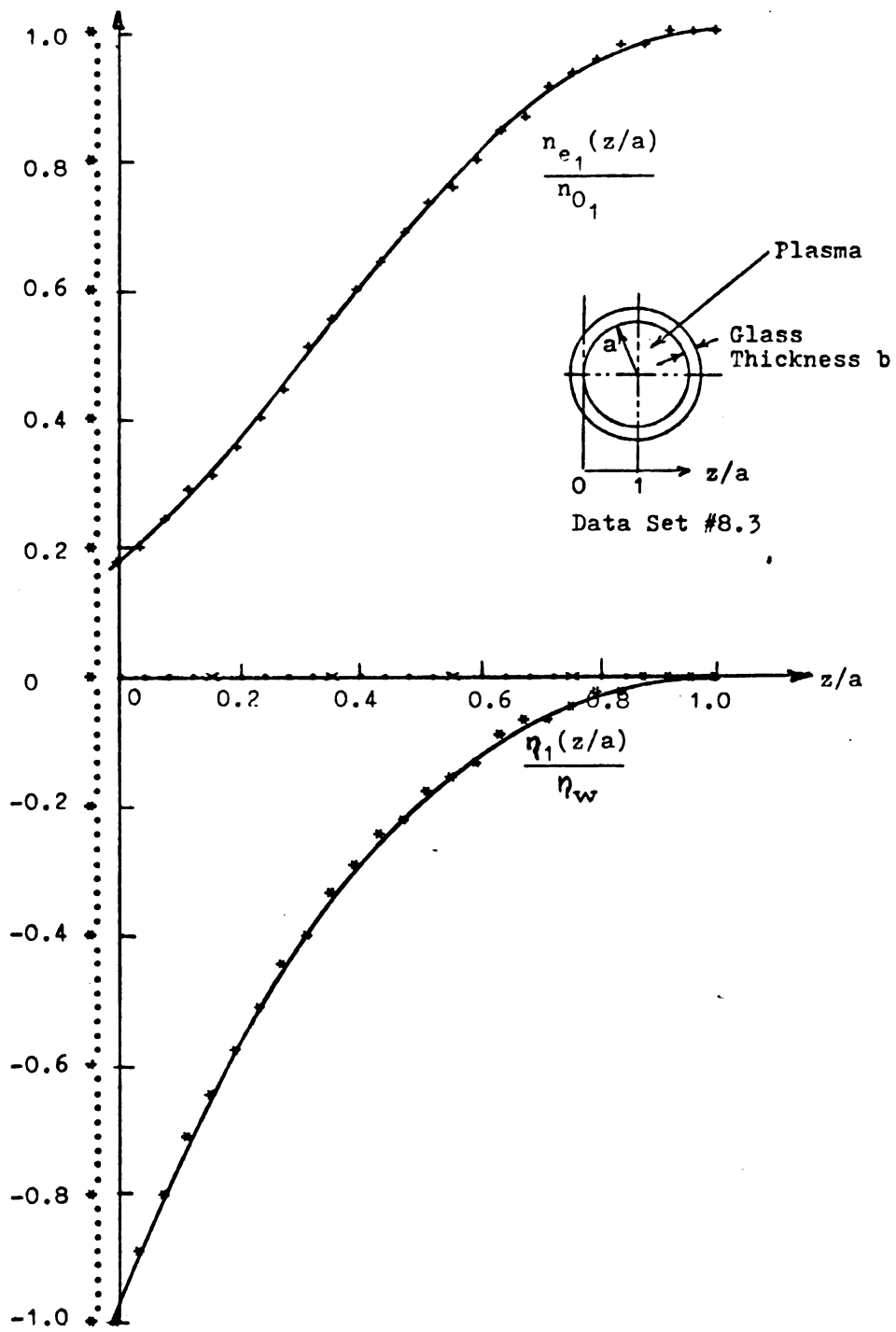






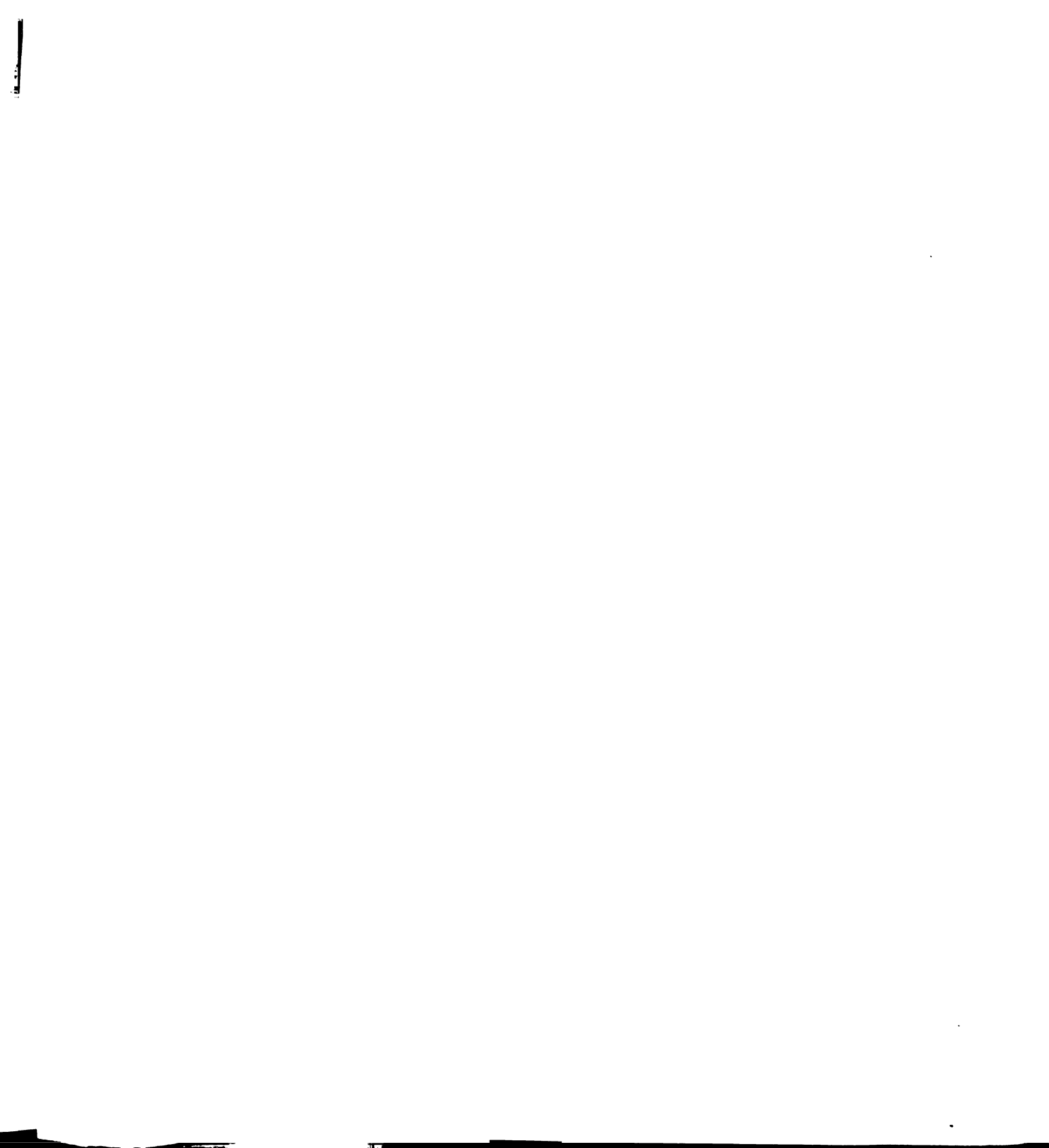






SUMMARY OF RES OF PAR ANALYSIS

NC	ALFA	W	TEMP	Z CRIT.	ETA
DATA SET NC 1		RESONANCE NO 1			
0.153E 18	0.826E 00	0.127E 11	0.142E 05	0.840E-03	-0.175E 01
DATA SET NC 1		RESONANCE NO 2			
0.124E 18	0.826E 00	0.127E 11	0.147E 05	0.121E-02	-0.175E 01
DATA SET NC 1		RESONANCE NO 3			
0.103E 18	0.826E 00	0.127E 11	0.147E 05	0.163E-02	-0.175E 01
DATA SET NC 2		RESONANCE NO 1			
0.156E 18	0.822E 00	0.132E 11	0.200E 05	0.137E-02	-0.173E 01
DATA SET NC 2		RESONANCE NO 2			
0.125E 18	0.822E 00	0.132E 11	0.200E 05	0.137E-02	-0.173E 01
DATA SET NC 2		RESONANCE NO 3			
0.102E 18	0.821E 00	0.132E 11	0.316E 05	0.193E-02	-0.190E 01
DATA SET NC 3		RESONANCE NO 1			
0.190E 18	0.832E 00	0.140E 11	0.190E 05	0.840E-03	-0.178E 01
DATA SET NC 3		RESONANCE NO 2			
0.149E 18	0.832E 00	0.140E 11	0.190E 05	0.127E-02	-0.178E 01
DATA SET NC 3		RESONANCE NO 3			
0.129E 18	0.832E 00	0.140E 11	0.190E 05	0.160E-02	-0.178E 01
DATA SET NC 4		RESONANCE NO 1			
0.200E 18	0.804E 00	0.146E 11	0.116E 05	0.770E-03	-0.163E 01
DATA SET NC 4		RESONANCE NO 2			
0.164E 18	0.804E 00	0.146E 11	0.116E 05	0.114E-02	-0.163E 01
DATA SET NC 4		RESONANCE NO 3			
0.133E 18	0.859E 00	0.146E 11	0.116E 05	0.182E-02	-0.196E 01
DATA SET NC 5		RESONANCE NO 1			
0.139E 18	0.864E 00	0.120E 11	0.290E 05	0.980E 03	-0.200E 01
DATA SET NC 5		RESONANCE NO 2			
0.104E 18	0.864E 00	0.120E 11	0.290E 05	0.150E-02	-0.200E 01
DATA SET NC 5		RESONANCE NO 3			
0.849E 17	0.864E 00	0.120E 11	0.290E 05	0.203E-02	-0.200E 01



U

```

1 DATA SET NO 6 RESONANCE NO 1
2 0.150E 18 0.835E 00 0.127E 11 0.205E 05 0.910E-03 -0.180E 01
3
4 DATA SET NO 6 RESONANCE NO 2
5 0.118E 18 0.835E 00 0.127E 11 0.205E 05 0.135E-02 -0.180E 01
6
7 DATA SET NO 6 RESONANCE NO 3
8 0.948E 17 0.835E 00 0.127E 11 0.205E 05 0.191E-02 -0.180E 01
9
10 DATA SET NO 7 RESONANCE NO 1
11 0.194E 18 0.841E 00 0.143E 11 0.274E 05 0.910E-03 -0.184E 01
12
13 DATA SET NO 7 RESONANCE NO 2
14 0.149E 18 0.841E 00 0.143E 11 0.274E 05 0.139E-02 -0.184E 01
15
16 DATA SET NO 7 RESONANCE NO 3
17 0.122E 18 0.870E 00 0.143E 11 0.428E 05 0.198E-02 -0.204E 01
18
19 DATA SET NO 8 RESONANCE NO 1
20 0.199E 18 0.852E 00 0.146E 11 0.391E 05 0.980E-03 -0.191E 01
21
22 DATA SET NO 8 RESONANCE NO 2
23 0.151E 18 0.852E 00 0.146E 11 0.391E 05 0.149E-02 -0.191E 01
24
25 DATA SET NO 8 RESONANCE NO 3
26 0.123E 18 0.852E 00 0.146E 11 0.391E 05 0.203E-02 -0.191E 01
27

```

SUMMARY OF RES OF BESSEL ANALYSIS

NO	GAMMA	W	TEMP	Z CRIT.	ETA
DATA SET NO 1		RESONANCE NO 1			
0.174E 18	0.327E 03	0.127E 11	0.474E 05	0.948E-03	-0.18CE C1
DATA SET NO 1		RESONANCE NO 2			
0.141E 18	0.327E 03	0.127E 11	0.474E 05	0.141E-02	-0.18CE C1
DATA SET NO 1		RESONANCE NO 3			
0.126E 18	0.321E 03	0.127E 11	0.306E 05	0.157E-02	-0.172E C1
DATA SET NO 2		RESONANCE NO 1			
0.186E 18	0.326E 03	0.132E 11	0.837E 05	0.952E-03	-0.178E C1
DATA SET NO 2		RESONANCE NO 2			
0.147E 18	0.326E 03	0.132E 11	0.837E 05	0.146E-02	-0.178E C1
DATA SET NO 2		RESONANCE NO 3			
0.118E 18	0.319E 03	0.132E 11	0.749E 05	0.186E-02	-0.170E C1
DATA SET NO 3		RESONANCE NO 1			
0.222E 18	0.323E 03	0.140E 11	0.675E 05	0.805E-03	-0.175E C1
DATA SET NO 3		RESONANCE NO 2			
0.174E 18	0.323E 03	0.140E 11	0.675E 05	0.129E-02	-0.175E C1
DATA SET NO 3		RESONANCE NO 3			
0.147E 18	0.328E 03	0.140E 11	0.310E 03	0.184E-02	-0.182E C1
DATA SET NO 4		RESONANCE NO 1			
0.240E 18	0.330E 03	0.146E 11	0.480E 05	0.940E-03	-0.185E C1
DATA SET NO 4		RESONANCE NO 2			
0.196E 18	0.330E 03	0.146E 11	0.480E 05	0.138E-02	-0.185E C1
DATA SET NO 4		RESONANCE NO 3			
0.157E 18	0.328E 03	0.146E 11	0.777E 05	0.182E-02	-0.183E C1
DATA SET NO 5		RESONANCE NO 1			
0.158E 18	0.327E 03	0.120E 11	0.104E 06	0.948E-03	-0.180E C1
DATA SET NO 5		RESONANCE NO 2			
0.118E 18	0.327E 03	0.120E 11	0.104E 06	0.151E-02	-0.180E C1
DATA SET NO 5		RESONANCE NO 3			
0.965E 17	0.327E 03	0.120E 11	0.104E 06	0.197E-02	-0.18CE C1

```

1 DATA SET NO 6 RESONANCE NO 1
2 0.175E 18 0.327E 03 0.127E 11 0.716E 05 0.948E-03 -0.180E 01
3
4 DATA SET NO 6 RESONANCE NO 2
5 0.138E 18 0.327E 03 0.127E 11 0.716E 05 0.145E-02 -0.180E 01
6
7 DATA SET NO 6 RESONANCE NO 3
8 0.110E 18 0.322E 03 0.127E 11 0.669E 05 0.198E-02 -0.174E 01
9
10 DATA SET NO 7 RESONANCE NO 1
11 0.224E 18 0.328E 03 0.143E 11 0.144E 06 0.946E-03 -0.182E 01
12
13 DATA SET NO 7 RESONANCE NO 2
14 0.172E 18 0.328E 03 0.143E 11 0.144E 06 0.145E-02 -0.182E 01
15
16 DATA SET NO 7 RESONANCE NO 3
17 0.138E 18 0.328E 03 0.143E 11 0.144E 06 0.195E-02 -0.182E 01
18
19 DATA SET NO 8 RESONANCE NO 1
20 0.228E 18 0.331E 03 0.146E 11 0.102E 06 0.106E-02 -0.187E 01
21
22 DATA SET NO 8 RESONANCE NO 2
23 0.174E 18 0.331E 03 0.146E 11 0.102E 06 0.166E-02 -0.187E 01
24
25 DATA SET NO 8 RESONANCE NO 3
26 0.141E 18 0.325E 03 0.146E 11 0.101E 06 0.204E-02 -0.177E 01
27

```

APPENDIX B

**FORTRAN COMPUTER PROGRAMS WRITTEN SPECIFICALLY FOR
THE NUMERICAL ANALYSIS IN THIS RESEARCH PROJECT**

```

/SYS TIME=10
/LOAD WATFIV
/OPT NOSOURCE
*****THIS PROGRAM IS DESIGNED TO DETERMINE THE PARAMETERS
*****OF A BESSEL SERIES ELECTRON SENSITIVITY PROFILE BASED ON
*****THERMAL RESONANCE DATA OBTAINED WITH AN ELECTROACOUSTIC PROCBE.
      FUNCTION FIO(X)
      IF(X-.01) 1,1,2
1      FIO=1.+X**2/2.**2
      GO TO 3C
2      IF(X-5)1C,20,20
2C     FIC=EXP(X)/SQRT(2.*3.14159*X)*(1.+1./8./X)
      GO TO 3C
1C     FIC=1.+X**2/2.**2
1       +X**4/(2.**4*2.**2)
2       +X**6/(2.**6*(3.**2)**2)
3       +X**8/(2.**8*(4.**3.**2)**2)
4       +X**10/(2.**10*(5.**4.**3.**2)**2)
5       +X**12/(2.**12*(6.**5.**4.**3.**2)**2)
6       +X**14/(2.**14*(7.**6.**5.**4.**3.**2)**2)
30     RETURN
      END
C      GO CN
      FUNCTION F(GZ1,IWITCH,GZ,A1,A2,W1,W2,
1WPL,W2,GZDIFF)
      COMMON AGAMMA
      COMMON MTEST
      Y1=AGAMMA-GZ
13     IF(IWITCH) 13,13,15
      D=1.-A2*EXP(1.-FIC(Y1))
      IF(D) 18,18,23
23     F=SQRT(D)
      GO TO 16
15     D=1.-A1*EXP(1.-FIC(Y1))
      IF(D) 18,18,25
25     F=SQRT(D)
      GO TO 16
18     F=C.
16     RETURN
      END
      FUNCTION FINT(X,GAMMA,ETA)
      Y1=GAMMA+.007-GAMMA*X
      FINT=EXP(1.-FIO(Y1))*(.007-X)
      RETURN
      END
C      SINGLE PRECISIONPROGRAM
      COMMON AGAMMA
      COMMON MTEST
      DIMENSION AN2(100)
      DIMENSION DIFF(2)
      DIMENSION V(150),AN(150)
      READ(5,*) NSET
      READ(5,*) NU,W1,W2,DIP11,W1I,W2I,NHARM
      READ(5,*) AGAMMA,COEFF
      READ(5,*) PH1,PH2,WPTMS
      GZ11=C.
      OGZ1F=.C1

```

```

WRITE(6,949) NSET
949 FORMAT(/,2X,'NUMBER OF DATA SET FOR BIC = ',I3,/)
WRITE(6,950) NHARM,PH1,PH2,WPTWS
950 FORMAT(2X,'THIS IS AN ANALYSIS OF THE ELECTRON DENSITY',/,
1      2X,'IN A CYLINDRICAL PLASMA COLUMN BASED ON A',/,
2      2X,'BESSEL FUNCTION PROFILE APPROXIMATION',/,
3      2X,'USING THERMAL RESONANCES 1 AND ',I3,/,
4      2X,'TOTAL PHASE FOR FIRST RES IS PI TIMES ',F4.2,/,
5      2X,'TOTAL PHASE FOR SEC RES IS PI TIMES ',F4.2,/,
6      2X,'THE SQUARE OF WP OVER W = ',F4.2,/)
WRITE(6,930) GZ1,DGZ1F,NU,W1,W2,DIP11,W11,W21,NHARM
930 FORMAT(2X,'LOWER INT. LIMIT =',E15.4,/,
1      2X,'INITIAL INCR. IN Z1 =',E15.4,/,
2      2X,'NUMBER OF INTEGR. STEPS =',I15,/,
3      2X,'VALUE OF W1 =',E15.4,/,
4      2X,'VALUE OF W2 =',E15.4,/,
5      2X,'DIPOLE CURRENT AT W1 =',E15.4,/,
6      2X,'CURRENT AT W1 =',E15.4,/,
7      2X,'CURRENT AT W2 =',E15.4,/,
8      2X,'NUMBER T. D. RESONANCE 2ND W =',I15,/)
73C AG=AGAMMA
72 DGZ1F=.G1
GAMA=AGAMMA/.007
EM=9.11E-31
EPS=.0.85E-12
Q=1.6C2E-19
ANC1=3.*W1**2*EM*EPS/Q**2*W11/DIP11
1 /3.*WPTWS
ANC1=ANC1*CCEFF
ANC2=3.*W1**2*EM*EPS/Q**2*W21/DIP11
1 /3.*WPTWS
AND2=ANC2*CCEFF
WP1=SQRT(C**2*ANC1/EM/EPS)
WP2=SQRT(C**2*AND2/EM/EPS)
A1=WP1**2/W1**2
A2=WP2**2/W2**2
GZ1=-CGZ1F/2.
M=1
3C DO 1C I=M,2
GZ1=GZ1+CGZ1F
DGZ=GZ1/1C.
GZ2=GZ1
7C1 GZ2=GZ2+DGZ
Y1=AGAMMA-GZ1
Y2=AGAMMA-GZ2
DGZT=A1*EXP(1.-F10(Y1))-A2*EXP(1.-F1C(Y2))
IF(DGZT)700,702,701
700 IF(DGZ-GZ1/90.) 702,702,703
7C3 GZ2=GZ2-DGZ
DGZ=DGZ/1C.
GO TC 7C1
702 CONTINUE
IWITCH=-1
UL=GZ2
CALL INT(GZ1,NU,UL,AINT,GZ1,W1,W2,WP1,WP2,A1,A2,IWITCH,GZ1FF)
AINT1=AINT
IWITCH=1
UL=GZ1

```

```

CALL INT(GZ11,NU,UL,AINT,GZ1,W1,W2,WP1,WP2,A1,A2,IWITCH,GZDIFF)
AINT2=AINT
1C DIFF(1)=AINT1-W1/W2*AINT2*
1 PH2/PH1
IF(GZ1-4.) 60,60,61
e1 WRITE(6,759) GAMA,COEFF
759 FORMAT(2X,'FOR GAMA = ',E15.4,/,
1 2X,'AND COEFF = ',E15.4,/,
2 2X,'THE DIFFERENCE DIVERGES FOR ALL POSITIVE GZ1',/)
eC IF(DIFF(1)*DIFF(2)) 40,20,2C
2C ERR=GZ1
M=2
DIFF(1)=DIFF(2)
GO TO 30
4C IF(DGZ1F-.01) 100,90,9C
5C GZ1=GZ1-DGZ1F
DGZ1F=DGZ1F/1C.
GO TO 30
100 CONTINUE
GAT=-GZ1+.0COC1
DGAT=GZ1
710 GAT=GAT+DGAT
Y3=GAT-GZ1
Z1=FIC(Y3)-(1.-ALOG(1./A1))
IF(Z1) 71C,711,712
712 IF(DGAT-GZ1/9.) 711,711,713
713 GAT=GAT-DGAT
DGAT=DGAT/1C.
GO TO 71C
711 CONTINUE
IF(ABS(GAT-AGAMMA)-ABS(GAT/5C.)) 720,72C,721
721 AGAMMA=(AGAMMA+GAT)/2.
GO TO 73C
720 CONTINUE
BCCNST=L.38E-23
YY=AGAMMA-GZ1
ETA=L.-FIC(AGAMMA)
B2=A2
B1=A1
Z2TOZ1=GZ2/GZ1
TE=W1**2+EM*AINT2**2/GAMA**2/3.14159**2/3./BCCNST
VWALL=ETA*BCCNST*TE/Q
Z11=GZ1/GAMA
Z22=GZ2/GAMA
CALL INTE(ETA,GAMA,S)
COEFFT=.0C7**2/2./S
IF(ABS(COEFF-COEFFT)-ABS(COEFF/2C.)) 74C,74C,741
741 COEFF=(COEFF+COEFFT)/2.
GO TO 72
74C CONTINUE
WRITE(6,879) COEFFT,GAMA,ETA,GZ1,GZ2,Z2TCZ1,WP1,WP2,ANCL,ANC2,
1 A1,A2,Z11,Z22,VWALL,TE
879 FORMAT(2X,'COEFF PEAK TO AVG EL DENS = ',E15.4,/,
1 2X,'GAMMA = ',E15.4,/,
2 2X,'ETA = VWALL TO KT CVER Q = ',E15.4,/,
3 2X,'GAMMA TIMES Z1 = ',E15.4,/,
4 2X,'GAMMA TIMES Z2 = ',E15.4,/,
5 2X,'Z2 TO Z1 = ',E15.4,/)

```

```

6      2X,'WP1          = ',E15.4//,
7      2X,'WP2          = ',E15.4//,
8      2X,'NO1          = ',E15.4//,
1      2X,'NO2          = ',E15.4//,
2      2X,'A1 = WP1 OVER W1 SQUARED = ',E15.4//,
3      2X,'A2 = WP2 OVER W2 SQUARED = ',E15.4//,
4      2X,'Z1          = ',E15.4//,
5      2X,'Z2          = ',E15.4//,
6      2X,'VWALL        = ',E15.4//,
7      2X,'ELECTRON TEMPERATURE = ',E15.4//,
8      /// )
DZ=.CC7/29.
Z=-DZ
DO 80C I=1,26
Z=Z+CZ
R1=AGAMMA-GAMA*Z
V(I)=1.-F10(R1)
ANZ(I)=AN02*EXP(V(I))
ECC AN(I)=AN01*EXP(V(I))
CALL PLOT4(V,AN,26)
CALL PLGT2(AN,AN2,26)
777 STOP
END
SUBROUTINE INT(XI,N,XF,S,GZ1,W1,W2,WP1,WP2,A1,A2,IWITCH,GZDIFF)
DIMENSION X(3)
COMMON AGAMMA
COMMON MTEST
N=N/2*2+1
XN=N
DX=(XF-XI)/(XN-1.)
NCCUNT=C
X(1)=XI-2.*DX
X(2)=XI-DX
X(3)=XI
S=C.
DO 10 I=3,N,2
X(1)=X(1)+2.*DX
X(2)=X(2)+2.*DX
X(3)=X(3)+2.*DX
DS=F(GZ1,IWITCH,X(1),A1,A2,W1,W2,WP1,WP2,GZDIFF)
1+4.*F(GZ1,IWITCH,X(2),A1,A2,W1,W2,WP1,WP2,GZDIFF)
2+F(GZ1,IWITCH,X(3),A1,A2,W1,W2,WP1,WP2,GZDIFF)
1C S=S+DX/3.*DS
4C RETURN
END
SUBROUTINE INTE(ETA,GAMMA,S)
DIMENSION X(3)
N=20
N=N/2*2+1
XN=N
XI=0.
XF=.7CE-2
DX=(XF-XI)/(XN-1.)
NCCUNT=C
X(1)=XI-2.*DX
X(2)=XI-DX
X(3)=XI
S=C.

```

```
DO 1C I=3,N,2
X(1)=X(1)+2.*DX
X(2)=X(2)+2.*DX
X(3)=X(3)+2.*DX
DS=FINT(X(1),GAMMA,ETA)+4.*FINT(X(2),
1 GAMMA,ETA) +FINT(X(3),GAMMA,ETA)
1C S=S+DX/3.*DS
4C RETURN
END
```

```

**** PIC    JACK GLIN    BSSR
/LCAD WATFIV
/CPT NOSOURCE
*****THIS PROGRAM IS DESIGNED TO DETERMINE THE PARAMETERS
*****OF A PARABOLIC ELECTRON DENSITY PROFILE BASED ON THERMAL
*****RESONANCE DATA OBTAINED WITH AN ELECTROACOUSTIC PROBE.
      FUNCTION FINT(RTA)
      COMMON MT
      COMMON AIC,AI1,AI2,RITA
      COMMON ALFA,BETA
      COMMON A
      IF(MT) 15,15,13
13      D=1.-AI1/AID*3./(1.-.5*ALFA)*(1.-ALFA*RTA**2)/BETA**2
      IF(D) 18,18,23
23      FINT=SQRT(D)
      GO TO 16
15      D=1.-AI2/AID*3./(1.-.5*ALFA)*(1.-ALFA*RTA**2)/BETA**2
      IF(D) 18,18,25
25      FINT=SQRT(D)
      GO TO 16
18      FINT=C.
16      RETURN
      END
C MAIN PROGRAM
      DIMENSION DIFF(2)
      DIMENSION AN(100),ETAR(100)
      COMMON MT
      COMMON AIC,AI1,AI2,RITA
      COMMON ALFA,BETA
      COMMON A
17      CONTINUE
      READ(5,*) NSET
      READ(5,*) AID,AI1,AI2,W,RADIUS,NHARM
      READ(5,*) DRITA,RITAI,BETA
      READ(5,*) PH1,PH2,WPTWS
      WRITE(6,949) NSET
949      FORMAT(//,2X,'NUMBER OF DATA SET      = ',I3,/)
      WRITE(6,950) NHARM,PH1,PH2,WPTWS
950      FORMAT(2X,'THIS IS AN ANALYSIS OF THE ELECTRON DENSITY ',/,
1          2X,' IN A CYLINDRICAL PLASMA COLUMN BASED ON A ',/,
2          2X,' PARABOLIC DENSITY PROFILE APPROXIMATION ',/,
3          2X,' USING RESONANCES 1 AND ',I3,/,
4          /,
5          2X,' THE PHASE FOR RESONANCE 1 IS PI TIMES ',F4.2,/,
6          2X,' THE PHASE FOR RESONANCE 2 IS PI TIMES ',F4.2,/,
7          /,
8          2X,' THE SQUARE OF WPCVER W IS EQUAL TO ',F4.2,/)
      WRITE(6,970) AID,AI1,AI2,W,BETA,RADIUS
970      FORMAT(2X,' ID          = ',E15.4,/,
1          2X,' I1          = ',E15.4,/,
2          2X,' I2          = ',E15.4,/,
3          2X,' W          = ',E15.4,/,
4          2X,' BETA=ATOR    = ',E15.4,/,
5          2X,' RADIUS      = ',E15.4,/)
      A=BETA*RADIUS
      RITA=RITAI
      M=1
20      DO 10 I=M,2

```

```

1      RITA=RITA+DRITA
      ALFA=(1.-AID/WPTWS/A11*BETA**2)/(RITA**2-AID/6./A11*BETA**2)
      AD1=1./ALFA-(1./ALFA-.5)/WPTWS*AID/A12*BETA**2
      AD2=1./ALFA-(1./ALFA-.5)/WPTWS*AID/A11*BETA**2
      IF(AD1) 1,1,2
2      IF(AD2) 1,1,3
3      DRTA=SQRT(AD1)-SQRT(AD2)
      MT=-1
      UL=DRTA+RITA
      CALL INT(UL,AINT)
      AINT1=AINT
      MT=1
      UL=RITA
      CALL INT(UL,AINT)
      AINT2=AINT
1C     DIFF(1)=AINT1-AINT2*PH2/PH1
      IF(RITA-2.) 5C,51,51
51     WRITE(6,980)
98C    FORMAT(2X,'DIFFERENCE DIVERGES',//)
      GO TO 52
5C     IF(DIFF(1)*DIFF(2)) 4C,20,2C
20     ERR=RITA
      DIFF(1)=DIFF(2)
      M=2
      GO TO 3C
40     IF(ABS(RITA-ERR)-.01) 100,9C,9C
9C     RITA=RITA-DRITA
      DRITA=DRITA/10.
      GO TO 3C
10C    R1=RITA*A+(1./BETA-1.)*A
      R2=R1+DRTA*A+A*(1./BETA-1.)
      Z1=A-R1
      Z2=A-R2
      ANCD=bPTWS/(1.-.5*ALFA)*8.85E-12*9.11E-31/1.602E-19**2
1      *W**2
      ANO1=ANCD/AID*A11
      ANO2=ANCD/AID*A12
      ETEMP=9.11E-31/3./1.38E-23*W**2/3.14159**2
1      *(AINT2*A)**2
985   WRITE(6,985) ALFA
      FORMAT(2X,'ALFA' = ',E15.4,//)
      COEFF =1./((1.-ALFA/2.)
      Z2TCZ1=Z2/Z1
      ETA=ALOG(1.-ALFA)
      VWALL=ETA*1.38E-23*ETEMP/1.602E-19
      WRITE(6,960) R1,R2,Z1,Z2,ANCD,ANO1,ANO2,Z2TCZ1,COEFF,VWALL,
1      ETA,ETEMP
960   FORMAT(2X,'R1' = ',E15.4,/,
1      1 2X,'R2' = ',E15.4,/,
2      2 2X,'Z1' = ',E15.4,/,
3      3 2X,'Z2' = ',E15.4,/,
4      4 2X,'NO DIPOLE' = ',E15.4,/,
5      5 2X,'NO 1 RESONANCE' = ',E15.4,/,
7      7 2X,'NO 2 RESONANCE' = ',E15.4,/,
8      8 2X,'Z2 TC Z1' = ',E15.4,/,
9      9 2X,'PEAK TO AVERAGE' = ',E15.4,/,
9      9 2X,'V WALL' = ',E15.4,/,
9      9 2X,'ETA=VW TO KTTQ' = ',E15.4,/,

```



```

**** FOZGRF JACK GLIN BSSR
/LOAD WATFIV
C      THIS SUBROUTINE PLOTS TWO VARIABLES ON THE SAME PLOT
C      WITH THE ZERO AXIS AS THE CENTER -MAX VALUES ARE
C      CALCULATED AUTOMATICALLY FOR Y - ZMAX = YMAX
C      SUBROUTINE FLGT2(Y,Z,N)
C      DIMENSION CCL(102),Y(100),Z(100)
C      INTEGER STAR, DOT, BLANK, COL, PLUS
C      STAR='*'
C      STAR=          1547714624
C      DOT='.'
C      DOT=          1262501952
C      BLANK=' '
C      BLANK=        1077952576
C      PLUS='+'
C      PLUS=         1312833600
C      XXXXX='X'
C      XXXXX=        -415219648
C      YMAX=C.CC
C      ZMAX=C.CC
50     DO 95 K=1,N
C      X=ABS(Y(K))-ABS(YMAX)
C      IF(X) 92,95,92
53     YMAX=Y(K)
55     CONTINUE
C      YMAX=ABS(YMAX)
56     DO 100 L=1,N
C      Q=ABS(Z(L))-ABS(ZMAX)
C      IF(Q) 100,100,99
59     ZMAX=Z(L)
100    CONTINUE
C      ZMAX=ABS(ZMAX)
C      WRITE(6,200) YMAX,ZMAX
C      IF(ZMAX-YMAX) 70,71,71
71     YMAX=ZMAX
70     ZMAX=YMAX
200    FORMAT(///,18X,'*XMAX =',E14.6,5X,'+YMAX =',E14.6,43X,'X',10X,'Y')
C      WRITE(6,400)
400    FORMAT('1')
C      WRITE(6,2)
2      FORMAT('*.....*.....*.....*.....*.....*.....*')
1      '
1 '*.....*.....*.....*.....*.....*.....*')
3     DO 3 I=1,101
C      COL(I) = BLANK
C      COL(51)=DOT
C      II=4
C      DO 4 I=1,N
C      J=50.*(Y(I)/YMAX+1.)+1.5
C      K=50.*(Z(I)/ZMAX+1.)+1.5
32    COL(J) = STAR
35    COL(K)=PLUS
36    WRITE(6,5)(COL(IJ),IJ=1,101),Y(I),Z(I)
5     FORMAT(1X,101A1,1P2E9.1)
42    COL(J)=BLANK
45    COL(K)=BLANK
C      IF(I-II) 250,300,300
200    COL(51)=XXXXX

```

```
42 COL(J)=BLANK
45 COL(K)=BLANK
   IF(I-II) 250,300,300
300 COL(46)=XXXXX
   II=II+5
   GO TC 4
250 COL(46)=DCT
4   CONTINUE
   WRITE(6,990)
990 FORMAT(//////////)
   RETURN
   END
```

```

**** F02GRF JACK GLIN BSSR
/LCAD WATFIV
C      THIS SUBROUTINE PLOTS TWO VARIABLES ON THE SAME PLCT
C      WITH THE ZERO AXIS AS THE CENTER -MAX VALUES ARE
C      CALCULATED AUTOMATICALLY FOR Y - ZMAX = YMAX
SUBROUTINE FLGT2(Y,Z,N)
DIMENSION CCL(102),Y(100),Z(100)
INTEGER STAR,DOT,BLANK,COL,PLUS
C      STAR='*'
C      STAR=          1547714624
C      DOT='.'
C      DOT=          1262501952
C      BLANK=' '
C      BLANK=        1077952576
C      PLUS='+ '
C      PLUS=         1312833600
C      XXXXX='X '
C      XXXXX=        -415219648
YMAX=C.CC
ZMAX=C.CC
DO 95 K=1,N
X=ABS(Y(K))-ABS(YMAX)
IF(X) 95,95,92
93 YMAX=Y(K)
95 CONTINUE
YMAX=ABS(YMAX)
DO 100 L=1,N
Q=ABS(Z(L))-ABS(ZMAX)
IF(Q) 100,100,99
99 ZMAX=Z(L)
100 CONTINUE
ZMAX=ABS(ZMAX)
WRITE(6,200) YMAX,ZMAX
IF(ZMAX-YMAX) 70,71,71
71 YMAX=ZMAX
70 ZMAX=YMAX
200 FORMAT(///,18X,'*XMAX =',E14.6,5X,'+YMAX =',E14.6,43X,'X',10X,'Y')
WRITE(6,400)
400 FORMAT('1')
WRITE(6,2)
2   FORMAT('*.....*.....*.....*.....*.....*.....*')
1   '
1 '*.....*.....*.....*.....*.....*.....*')
DO 3 I=1,101
3   COL(I) = BLANK
   COL(51)=DOT
   II=4
   DO 4 J=1,N
   J=50.*(Y(I)/YMAX+1.)+1.5
   K=50.*(Z(I)/ZMAX+1.)+1.5
32  COL(J) = STAR
35  COL(K)=PLUS
36  WRITE(6,5)(COL(IJ),IJ=1,101),Y(I),Z(I)
5   FORMAT(1X,101A1,1P2E9.1)
42  COL(J)=BLANK
45  COL(K)=BLANK
   IF(I-II) 250,300,300
300 COL(51)=XXXXX

```

```
      II=II+5  
      GO TO 4  
250   COL(51)=DCT  
      CONTINUE  
      WRITE(6,977)  
577   FORMAT(//////////)  
      RETURN  
      END
```

```

**** WKB      JACK OLIN   BSSR
/SYS TIME=10
/LCAD WATFIV
/GPT NOSOURCE
*****THIS PROGRAM PLOTS THERMAL RESONANCES BASED ON A WKB
*****APPROXIMATION AWAY FROM THE CRITICAL POINT FOR A GIVEN
*****BESSEL SERIES ELECTRON DENSITY PROFILE
      FUNCTION FIC(X)
      IF(X-.01) 1,1,?
1      FIC=1.+X**2/2.**2
      GO TO 30
2      IF(X-5)10,20,20
20     FIC=EXP(X)/SQRT(2.*3.14159*X)*(1.+1./8./X)
      GO TO 30
10     FIC=1.+X**2/2.**2
      1 +X**4/(2.**4*2.**2)
      2 +X**6/(2.**6*(3.**2)**2)
      3 +X**8/(2.**8*(4.**3.**2)**2)
      4 +X**10/(2.**10*(5.**4.**3.**2)**2)
      5 +X**12/(2.**12*(6.**5.**4.**3.**2)**2)
      6 +X**14/(2.**14*(7.**6.**5.**4.**3.**2)**2)
20     RETURN
      END
      FUNCTION F(X)
      COMMON ANC,GAMMA,A,W,TEMP,EM,EPS,C,BCONST
      Y= A*GAMMA-GAMMA*X
      D=1.-1./W**2*C**2/EM/EPS*ANG*EXP(1.-FIO(Y))
      IF(D) 18,18,23
23     F=SQRT(D)*W/SQRT(3.*BCONST*TEMP/EM)
      GO TO 16
18     F=C.
16     RETURN
      END
*****MAIN PROGRAM
      DIMENSION BETAP(100),ANI(100)
      COMMON ANC,GAMMA,A,W,TEMP,EM,EPS,C,BCONST
      READ(5,*) NSET,NRES,ANG,GAMMA,W,TEMP,ZP
      READ(5,*) A,N,M
      READ(5,*) TEST
      WRITE(6,996) NSET,NRES
996   FORMAT(//,2X,'SET NUMBER IS ',I3,/,
1      2X,'RES NUMBER IS ',I3,/)
      WRITE(6,997) ANG,GAMMA,A,W,TEMP,ZP,NSET
997   FORMAT(2X,'NO           = ',E15.4,/,
1      2X,'GAMMA           = ',E15.4,/,
2      2X,'RADIUS          = ',E15.4,/,
3      2X,'RADIAN FREQUENCY = ',E15.4,/,
4      2X,'TEMPERATURE      = ',E15.4,/,
5      2X,'Z CRITICAL      = ',E15.4,/,
6      2X,'NUMBER OF DATA SET = ',I3,/,
7      //)
      WRITE(6,998)
998   FORMAT(2X,'DISTANCE FROM WALL',3X,'PERTURBED ELECTR DENSITY',/)
      EM=9.11E-31
      EPS=8.85E-12
      Q=1.602E-19
      BCONST=1.38E-23
      XNN=N

```

```

DZ=ZM/(XN-1.)
Z=-DZ
DO 1C I=1,N
Z=Z+DZ
CALL INT(Z,ZM,S,M)
Y=A*GAMMA-GAMMA*Z
D=1.-1./h**2*Q**2/EM/EPS*ANC*EXP(1.-F10(Y))
IF(D) 4C,40,41
4C BETAP(I)=C.
GO TO 5C
41 BETAP(I)=SQRT(D)*W/SQRT(3.*BCCNST*TEMP/EM)
5C IF(BETAP(I)-TEST)60,6C,61
6C ANI(I)=C.
GO TO 62
61 ANI(I)=1./SQRT(BETAP(I))*SIN(3.14159/4.*S)
62 WRITE(6,999) Z,ANI(I)
999 FORMAT(2X,E15.6,6X,E15.6)
1C CONTINUE
CALL PLGT4(ANI,ANI,N)
STOP
END
SUBROUTINE INT(XI,XF,S,N)
DIMENSION X(3)
COMMON ANC,GAMMA,A,W,TEMP,EM,EPS,C,BCCNST
N=2C
N=N/2*2+1
XN=N
DX=(XF-XI)/(XN-1.)
NCCUNT=C
5 X(1)=XI-2.*DX
X(2)=XI-CX
X(3)=XI
S=C.
DO 10 I=3,N,2
X(1)=X(1)+2.*DX
X(2)=X(2)+2.*DX
X(3)=X(3)+2.*DX
10 DS=F(X(1))+4.*F(X(2))+F(X(3))
S=S+DX/3.*DS
4C RETURN
END

```

```

**** WKBPAR JACK OLIN BSSR
/SYS TIME=10
/LOAD WATFIV
/CPT NOSOURCE
C*****THIS PROGRAM PLOTS THERMAL RESONANCES BASED ON A WKB
C*****APPROXIMATION AWAY FROM THE CRITICAL POINT FOR A GIVEN
C*****PARABOLIC ELECTRON DENSITY PROFILE
FUNCTION F(X)
COMMON ANC,ALFA,A,W,TEMP,EM,EPS,Q,BCONST
Z=X
D=1.-1./W**2+C**2/EM/EPS*ANC*(1.-ALFA*(1.-Z/A)**2)
IF(D) 18,18,23
23 F=SQRT(D)*W/SQRT(3.*BCONST*TEMP/EM)
GO TO 16
18 F=C.
16 RETURN
END
C*****MAIN PROGRAM
DIMENSION BETAP(100),ANI(100)
COMMON ANC,ALFA,A,W,TEMP,EM,EPS,Q,BCONST
READ(5,*) NSET,NRES,ANC,ALFA,h,TEMP,ZM
READ(5,*) A,N,M.
READ(5,*) TEST
WRITE(6,996) NSET,NRES
996 FORMAT(//,2X,'SET NUMBER IS ',I3,/,
1 2X,'RES NUMBER IS ',I3,/,
2 2X,'PARABOLIC APPROXIMATION OF PROFILE',//)
WRITE(6,997) ANC,ALFA,A,W,TEMP,ZM,NSET
997 FORMAT(2X,'NO = ',E15.4,/,
1 2X,'ALFA = ',E15.4,/,
2 2X,'RADIUS = ',E15.4,/,
3 2X,'RADIAN FREQUENCY = ',E15.4,/,
4 2X,'TEMPERATURE = ',E15.4,/,
5 2X,'Z CRITICAL = ',E15.4,/,
6 2X,'NUMBER OF DATA SET = ',I3,/,
7 //)
WRITE(6,998)
998 FORMAT(2X,'DISTANCE FROM WALL',3X,'PERTURBED ELECTR DENSITY',//)
EM=9.11E-31
EPS=8.85E-12
Q=1.602E-19
BCONST=1.38E-23
XNN=N
DZ=ZM/(XNN-1.)
Z=-DZ
DO 10 I=1,N
Z=Z+DZ
CALL INT(Z,ZM,S,M)
D=1.-1./W**2+Q**2/EM/EPS*ANC*(1.-ALFA*(1.-Z/A)**2)
IF(D) 40,40,41
40 BETAP(I)=C.
GO TO 50
41 BETAP(I)=SQRT(D)*W/SQRT(3.*BCONST*TEMP/EM)
50 IF(BETAP(I)-TEST)60,60,61
60 ANI(I)=C.
GO TO 62
61 ANI(I)=1./SQRT(BETAP(I))*SIN(3.14159/4.*S)
62 WRITE(6,999) Z,ANI(I)

```

```

999  FORMAT(2X,E15.6,6X,E15.6)
10   CONTINUE
     CALL PLOT4(ANI,ANI,N)
     STOP
     END
     SUBROUTINE INT(XI,XF,S,N)
     DIMENSION X(3)
     COMMON  AND,ALFA,A,W,TEMP,EM,EPG,C,RCENST
     N=20
     N=N/2*2+1
     XN=N
     DX=(XF-XI)/(XN-1.)
     NCCUNT=C
5     X(1)=XI-2.*DX
     X(2)=XI-DX
     X(3)=XI
     S=0.
     DO 10 I=3,N,2
     X(1)=X(1)+2.*DX
     X(2)=X(2)+2.*DX
     X(3)=X(3)+2.*DX
     DS=F(X(1))+4.*F(X(2))+F(X(3))
10    S=S+DX/3.*DS
40    RETURN
     END

```

REFERENCES

REFERENCES

- 1 B. S. Tanenbaum, "Plasma Physics", McGraw - Hill Co., N. Y., 1967.
- 2 A. Dattner, "Plasma Resonance," Ericsson Tech., Vol. 3, No. 2, pp. 309-350, 1957.
- 3 "Resonances Oscillations in a Hot Nonuniform Plasma", The Physics of Fluids, Vol. 7, No. 9, pp. 1489-1500, Sep. 1964.
- 4 P. E. Vandenplas, "Electron Waves and Resonances in Bounded Plasma", Interscience Publishers, N. Y., 1968.
- 5 F. W. Crawford and G. S. Kino, "The Mechanism of Tonks-Dattner Resonances of a Discharge Column", Proc. of the Sixth International Conference on Ionization Phenomena in Gases, Paris, July 1963.
- 6 B. Ho and K. M. Chen, "Electroacoustic Resonance in Plasma Layer Surrounding a Metallic Cylinder", Proc. of IEEE, Vol. 56, No. 9, pp. 1600-1602, Sept. 1968.
- 7 P. D. Golden and E. J. Yadlowsky, "Plasma Resonance and Standing Longitudinal Electron Waves", The Physics of Fluids, Vol. 14, No. 9, pp. 1990-1996, Sept. 1971.
- 8 A. W. Baird III, "Determination of Electron Density Profiles from Tonks-Dattner Resonance Data in Plasmas", J. of Appl. Phys., Vol. 42, No. 13, pp. 5358-5361, Apr. 1971.
- 9 J. V. Parker, "Collisionless Plasma Sheath in Cylindrical Geometry", The Physics of Fluids, Vol. 6, Research Notes, pp. 1657-1658, Nov. 1963.
- 10 F. W. Crawford, G. S. Kino, and A. B. Cannara, "Dipole Resonances of a Plasma in a Magnetic Field", J. of Appl. Phys., Vol. 34, No. 11, pp. 3168-3175, Nov. 1963.
- 11 J. L. Powell, and B. Crasemann, "Quantum Mechanics", Addison Wesley Publ. Co., Inc., Reading, Mass., 1961.
- 12 C. Y. Lee, "Electromagnetic Scattering from a Plasma-Coated Cylinder", Ph.D. Thesis, M.S.U., 1971.

- 13 P. E. Vandenplas, "Oscillations de plasmas finis, inhomogenes et de temperature non nulle", Ph. D. Thesis, Universite de Bruxelles, April 1961.
- 14 K. J. Parblakar and Brian C. Gregory, "Direct Measurement of Dipolar Radial Electric Fields in a resonating Plasma Column", The Physics of Fluids, Vol. 14, No. 9, pp. 1984-1989, September 1971.

MICHIGAN STATE UNIVERSITY LIBRARIES



3 1293 03169 2365